OLD DOMINION UNIVERSITY RESEARCH FOUNDATION

DEPARTMENT OF PHYSICS
SCHOOL OF SCIENCES AND HEALTH PROFESSIONS
OLD DOMINION UNIVERSITY
NORFOLK, VIRGINIA

Technical Report PTR-81-7

ANTENNA DESIGN AND DEVELOPMENT FOR THE MICROWAVE SUBSYSTEM EXPERIMENTS FOR THE TERMINAL CONFIGURED VEHICLE PROJECT

By

Jacob Becher

Norman Cohen

and

Jim Rublee

Principal Investigator: Jacob Becher

Final Report
For the period August 1, 1976 - December 31, 1979

Prepared for the
National Aeronautics and Space Administration
Langley Research Center
Hampton, Virginia

Under
Research Grant NSG 1331
Thomas G. Campbell, Technical Monitor
Flight Electronics Division

March 1981

DEPARTMENT OF PHYSICS
SCHOOL OF SCIENCES AND HEALTH PROFESSIONS
OLD DOMINION UNIVERSITY
NORFOLK, VIRGINIA

Technical Report PTR-81-7

ANTENNA DESIGN AND DEVELOPMENT FOR THE MICROWAVE SUBSYSTEM EXPERIMENTS FOR THE TERMINAL CONFIGURED VEHICLE PROJECT

By

Jacob Becher

Norman Cohen

and

Jim Rublee

Principal Investigator: Jacob Becher

Final Report
For the period August 1, 1976 - December 31, 1979

Prepared for the
National Aeronautics and Space Administration
Langley Research Center
Hampton, Virginia 23665

Under
Research Grant NSG 1331
Thomas G. Campbell, Technical Monitor
Flight Electronics Division

Submitted by the
Old Dominion University Research Foundation
P.O. Box 6369
Norfolk, Virginia 23508

March 1981

TABLE OF CONTENTS

LIST OF FIGURES

LIST OF FIGURES (Continued)

ANTENNA DESIGN AND DEVELOPMENT FOR THE MICROWAVE SUBSYSTEM EXPERIMENTS FOR THE TERMINAL CONFIGURED VEHICLE PROJECT

By

Jacob Becher[1], Norman Cohen[2], and Jim Rublee[3]

INTRODUCTION

The increase of airport usage and advances in technology have shown the need to examine new methods for improving aircraft control in the terminal area. New methods of transferring information between ground systems and aircraft are being devised and tested to provide extremely accurate position data and approach control. The Terminal Configured Vehicle Project Office (TCVPO) at NASA/Langley Research Center (LaRC) is presently involved in testing and evaluating some of these systems. Three of these systems are described below:

1. Bendix Microwave Landing System (MLS): The MLS is a nonvisual, precision approach and landing system. One such system will be tested and evaluated by the TCVPO using the NASA/LaRC Boeing 737.

2. Flight Display Research System (FDRS): This is a ground-based system that develops visual indicators and cues which are transmitted to an aircraft via an FM/TV microwave link where the received signals are presented in visual flight displays for the pilot.

3. Transponder Data System (TDS): The TDS is a unified command telemetry and radar system which uses the existing C-band radar link for telecommunication purposes.

To evaluate any air-to-ground communication system, it is essential to examine the multipath effects (refs. 1 - 15).. These effects are the algebraic

---

[1] Associate Professor of Physics, Old Dominion University, Norfolk, VA 23508

[2] Research Associate, Old Dominion University Research Foundation, P.O. Box 6369, Norfolk, VA 23508

[3] Consultant

summation of all the reflected radiation arriving at the antenna which is to be included with the direct ray. These effects can be siginificant depending on the geometry of the reflecting surfaces and the directional gain of the receiver/transmitter antenna. It is important to note that the airport radar antennas are highly directional. The main signal is transmitted and received at substantially higher gains compared to the reflected radiations since the reflected signals generally arrive at angles greater than the acceptance angle of the antenna. The reflected signal arriving within the acceptance angle of the antenna, or any antenna having large side lobes, interferes with the main signal, occasionally producing nulls. For a given aircraft position, the direction of the reflected signal is determined by the location of antenna relative to the neighboring reflecting surfaces. The magnitude of the reflected signal depends largely on the texture of the surfaces, which determines the extent of specular reflection. Thus the relative position of the aircraft to antenna determines the active reflection surface, and the specular contribution is examined by evaluating reflection coefficients and phase shifts. These are determined for a specific transmitting frequency with the aid of surface characteristics such as permittivity and conductivity.

This report examines the feasibility of classifying the terminal area for multipath effects, i.e., fade-out potentials or limits of video resolution. To do this, established transmission links in terminal areas were modeled for landing approaches and overflight patterns. This model was applied to evaluate the signal transmission obtained from a B-737 flight with additional signal strength monitoring equipment. The test was conducted at Wallops Flight Center because of airfield availability, the fact that there are no commercial activities there, and because the terminal area consists mostly of concrete and flat land with only a few potential obstructions in the signal's path.

THEORY

Flat Earth Consideration

The terminal communication system at Wallops Flight Center consists of a highly directional antenna and an omnidirectional antenna on the aircraft. The airport terminal surrounding geography (see fig. 1)

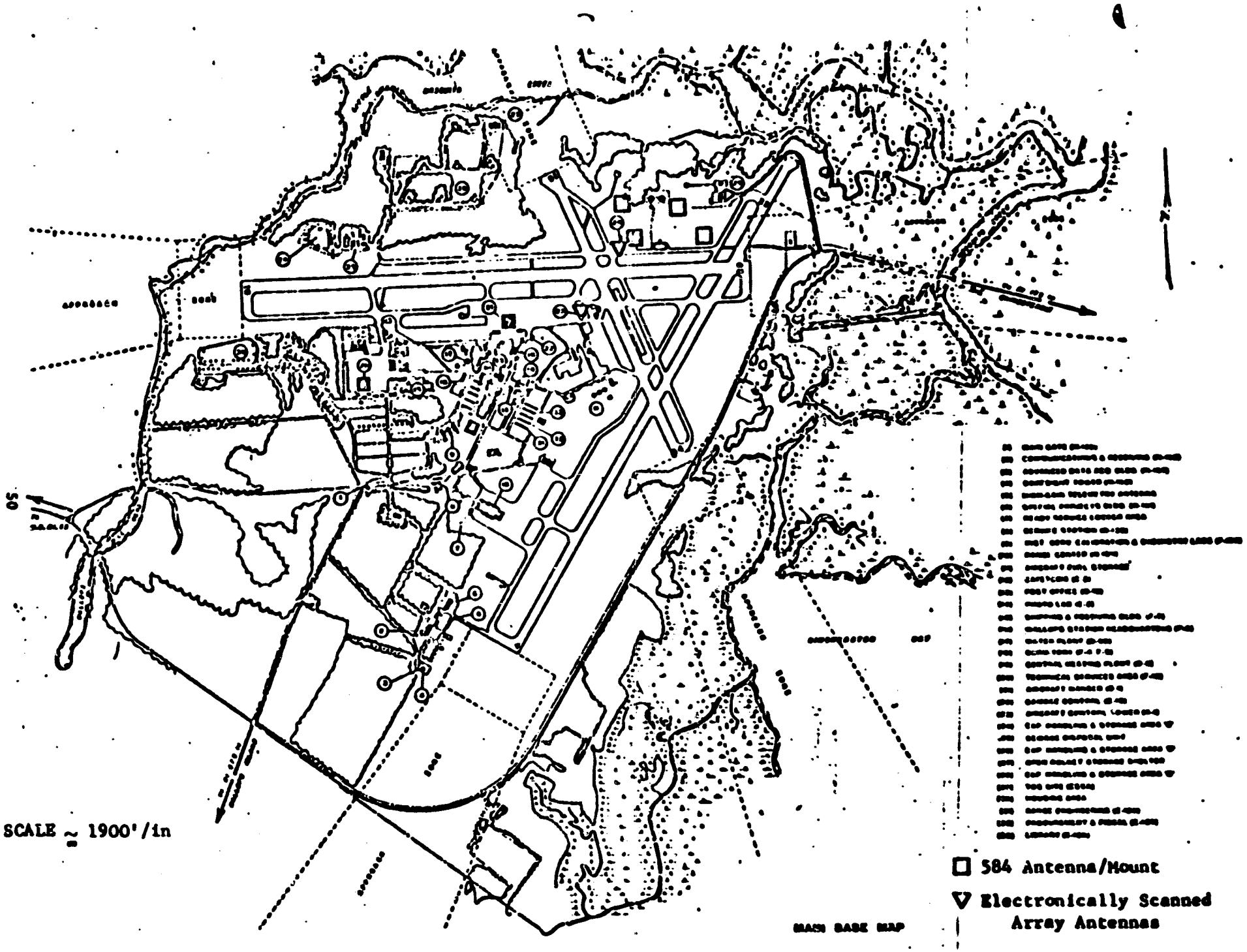

Figure 1. Airport terminal at Wallops Flight Center and surrounding geography.

consists mainly of concrete. The obstructions constitute the problem in simulating the simple surface that is assumed to be completely uniform. Thus, assuming flat and specular reflection and no atmospheric absorptions, the transmission/reception is equated to the Lloyd's mirror interferometer studies in optics. In this case the reflection coefficient depends on transmitting frequency, the angle of incidence, permittivity of the reflecting surface, and ground moisture content. The reflection coefficient and the phase change at the reflection for either a vertically or horizontally polarized electromagnetic field are defined by the following equations, known as Fresnel's Formulas:

$$R_V = \rho_V e^{-i\phi_V} = \frac{y^2 \sin\gamma - \sqrt{y^2 - \cos^2\gamma}}{y^2 \sin\gamma + \sqrt{y^2 - \cos^2\gamma}} \tag{1}$$

$$R_H = \rho_H e^{-i\phi_H} = \frac{\sin\gamma - \sqrt{y^2 - \cos^2\gamma}}{\sin\gamma + \sqrt{y^2 - \cos^2\gamma}} \tag{2}$$

where R_V and R_H are complex reflection coefficients for vertical and horizontal polarizations, respectively; ρ_V and ρ_H are the magnitudes of vertical and horizontal reflection; ϕ_V and ϕ_H are the magnitudes of vertical and horizontal reflection phase shift, γ is the grazing angle, and y is the normalized admittance, defined by

$$y = \sqrt{\frac{\varepsilon_{rc}}{\mu_{rc}}} \tag{3}$$

The Earth's relative complex dielectric constant ε_{rc} characterizes the interface in mks units and is expressed as follows:

$$\varepsilon_{rc} = \frac{\varepsilon}{\varepsilon_o} - (i\ 60\ \lambda\sigma) \tag{4}$$

Where λ is the wavelength in meters, σ is the material's conduction in ohms per meter, and ε is the earth's permittivity. The magnetic permittivity, μ_{rc}, can be set equal to 1 for air-to-ground interface.

Figure 2 illustrates the conditions associated with the direct and reflected waves for the following conditions:

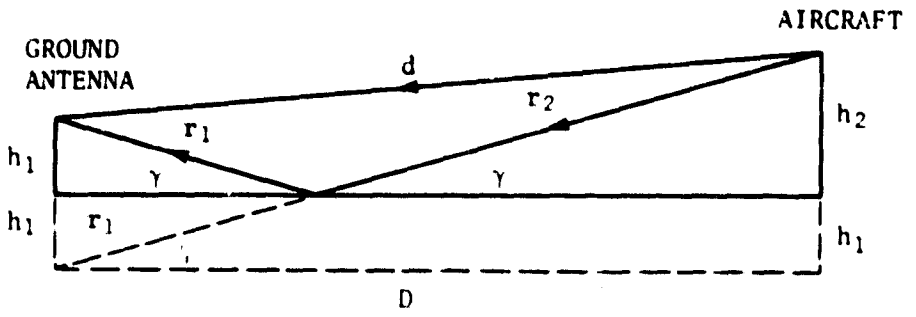

Figure 2. Conditions associated with direct and reflected waves.

$$(r_1 + r_2)^2 = D^2 + (h_1 + h_2)^2 \tag{5}$$

$$d^2 = D^2 + (h_2 - h_1)^2 \tag{6}$$

$$\delta = (r_1 + r_2) - d = \sqrt{D^2 + (h_2 + h_1)^2} - \sqrt{D^2 + (h_2 - h_1)^2} \tag{7}$$

$$\tan \gamma = \left(\frac{h_1 + h_2}{D}\right) \tag{8}$$

Where h_1 is height of the ground antenna, h_2 is the height of the aircraft, and D is the horizontal distance between the aircraft and ground antenna.

Illustrated in figure 3 is the relationship of the direct wave E_o and the reflected wave $|R|E_o$ which results in the vector sum E. The phase shift ψ is the sum of the reflection phase shifts and the phase shift due to path difference $2\pi\delta/\lambda$.

$$D = \sqrt{(x_2 - x_1)^2 + (y_2 - y_1)^2} \tag{9}$$

where (x_1, y_1) and (x_2, y_2) are the positions in the horizontal plane of the antenna and the aircraft, respectively. Then

$$\psi = \frac{2\pi\delta}{\lambda} + \phi \tag{10}$$

Note that for vertical polarization $\phi = \phi_V$ and for horizontal polarization $\phi = \phi_H$. By referring to figure 3 and applying the law of cosines, we find the ratio of E/E_o can be found by

$$E^2 = E_o^2 + E^2|R|^2 - 2E_o^2|R|\cos\psi$$

$$E^2 = E_o^2(1 + |R|^2 - 2|R|\cos\psi)$$

$$\text{with } \cos\frac{\psi}{2} = \sqrt{\frac{1 + \cos\psi}{2}}$$

$$E^2 = E_o^2(1 + |R|^2 - 4|R|\cos^2\frac{\psi}{2} = 2|R|)$$

$$\frac{E}{E_o} = \sqrt{(1 + |R|)^2 - 4|R|\cos^2\frac{1}{2}\psi} \tag{11}$$

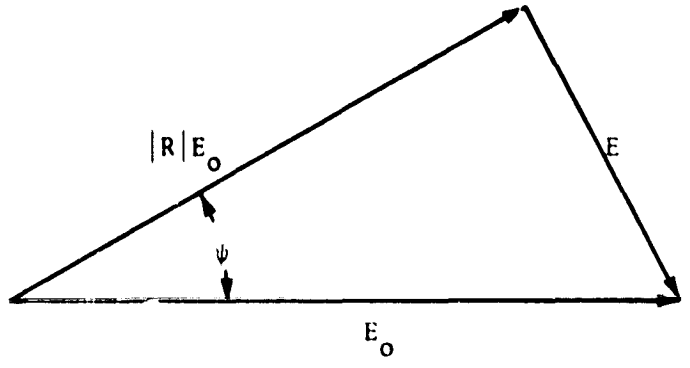

Figure 3. Relationship of the direct wave E_o and the reflected wave $|R|E_o$ which results in the vector sum E.

To present a relative dB value for the resultant amplitude, the transmitted signal (E_o) is assumed to be 1, and the ratio value of E/E_o is expressed as

$$E = 20 \log_{10} \left(\sqrt{(1 + |R|)^2 - 4|R| \cos^2 \frac{\psi}{2}} \right) \tag{12}$$

Irregular Terrain

The divergence of energy upon reflection from a spherical surface has to be included only when a large distance exists between the antenna and aircraft. This divergence reduces the amount of energy seen by the receiver. In more precise terms, the curved surface reflection coefficient R_c is effectively reduced from that of a plane surface by the degree of curvature depicted by a divergence coefficient D_v*:

$$R_c = D_v R_o \tag{13}$$

The resulting formula taken from reference 1

$$D_v = \left[1 + \frac{2r_1 r_2}{a(r_1 + r_2) \sin \gamma} \right]^{-1/2} \left[1 + \frac{2r_1 r_2}{b(r_1 + r_2)} \right]^{-1/2} \tag{14}$$

is general and may be applied to any form of the earth's surface. Figure 4 is provided for correlation of the terms of equation (14); r_1 is the distance from the transmitter T to the point of reflection I; r_2 is the distance from the receiver R to the point of reflection I; γ is the grazing angle of the incident ray, and a and b are the radii of curvature of the intersections of the earth and two vertical planes perpendicular to the direction of propagation. The calculation of the divergence coefficient must be considered separately for either the curved earth or curved terrain. In calculating the model for a curved earth surface, the variables a and b can be considered as constants. The values of the variables r_1 and r_2 are found by equations (15) and (16):

$$r_1 = \frac{\sin \gamma}{h_1} \tag{15}$$

* The derivation of the divergence coefficient D_V is based on the laws of geometrical optics and can be found in chapter 11 of reference 1.

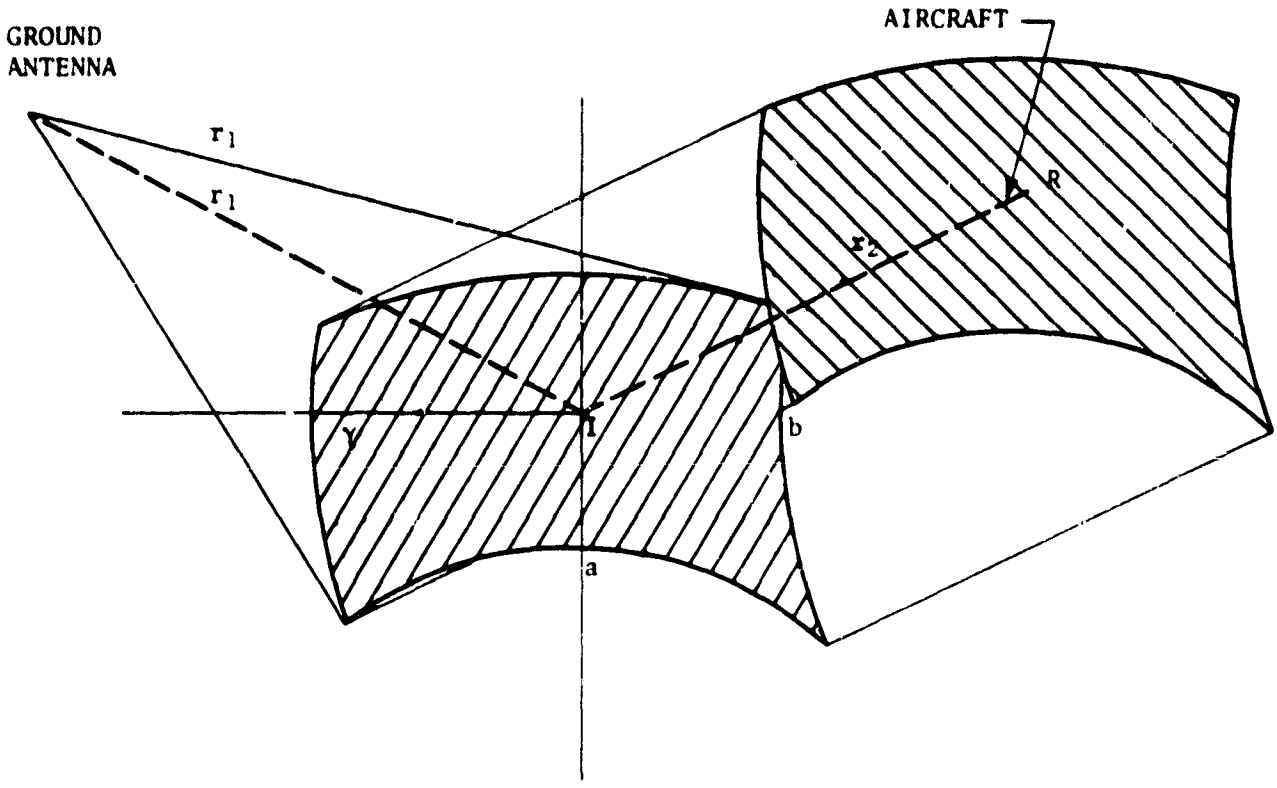

Figure 4. Correlation of the terms of equation (14).

$$r_2 = \frac{\sin \gamma}{h_2} \tag{16}$$

For the case of irregular terrain, the values of a and b are calculated for each transmitter/receiver position and the resulting point of reflection. Points on four sides of the point of reflection and located on the lines of intersection of the surface of the earth and two vertical planes perpendicular to the direction of propagation (as illustrated in fig. 3) are used to determine a and b.

$$a = \frac{y^2 + z^2}{2z} \tag{17}$$

$$b = \frac{x^2 + z^2}{2z} \tag{18}$$

Since our concern centered on communication around the airport, coefficient D_v has been set equal to 1. Therefore, $R_c = R_o$.

Additional Reflecting Objects

The basic reflection model considers the earth as a flat reflector; thus there exists a single reflection path. To consider airport structure, one would have to add mostly vertical surface, which would create additional reflecting paths. Figure 5 illustrates the additional reflection points. A limited number of planes could be introduced to model the terminal area. These additional reflection points would create reflected waves which would have to be incorporated into the calculation of combined signal. Once the geography of the terminal area is approximated by a number of planes, the problem is to determine at what position of the aircraft the planes contribute to the reflected wave. To calculate the contribution one has to consider the plane produced by the antenna position, aircraft position, and the normal to the reflecting plane. Here the reflected wave polarizations have to be incorporated; otherwise the calculation is similar to the reflection from the earth.

Although additional reflections must be given thorough consideration, the influence of those reflections on the received signal has to be determined for each individual case. The ground reflection points during

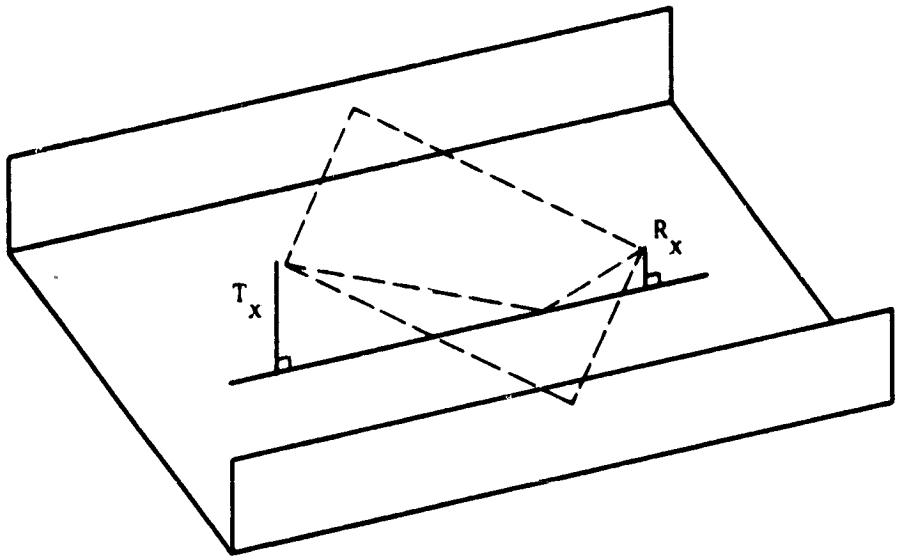

Figure 5. Multiple reflection paths.

an aircraft's landing, based on the fact that the antenna is about 91 m (300 ft) above ground, are found to be between 30 and 610 m (100 and 2000 ft) from the ground antenna. Tall buildings could be much further and still contribute to the reflected signal. Such buildings might therefore necessitate a change in the gain profile of the receiver/transmitter to limit their influence. In this simulation extra structures were not incorporated.

COMPUTER PROGRAM

Description

A computer program was written to obtain signal strength based on a described flight path. The general terminal environment was taken into consideration through parameters such as the surface-to-air permittivity of the landing approach path and the specific antenna pointing position as it tracks the approaching aircraft so as to include the variations in gain.

The program is provided with two options to define the flight path: option I consists of specifying up to 2,000 points with (x,y,z), and option II specifies up to 7 headings and radial distance (r_i, α_i, β_i, γ_i) where r_i stands for the radial distance and the angles (α_i, β_i, γ_i) provide the direction cosines for that heading. Using option II, the program generates up to 2,000 equally spaced points describing the flight path. At this point, the program has been written to adjust the flight path to take into account the antenna position and pointing direction which is tracking the aircraft. Since the antenna position and pointing direction depend on the position of the aircraft, it is necessary to determine the receiver position at each point. For each position the program calculates the direction cosines of the direct and the reflected beams.

For each position, the grazing angle γ is calculated first, followed by R_V, R_H, ϕ_V, and ϕ_H; R_V and R_H are the coefficients for vertical and horizontal polarization, and ϕ_V, ϕ_H are phase shifts introduced due to reflection. At this point the path difference is obtained between the direct and the reflected wave and is used in calculating a phase shift produced between these beams. At this point there

are again two options for selecting the potential antenna: (1) an omnidirectional receiving antenna and (2) a specified gain antenna. In the first option, the previously calculated phase shift and the appropriate reflection coefficients are used to obtain the signal E/E_o at each point on the flight path. The second option takes into account the previously specified gains along the direction. Thus, using the orientation determined earlier in the program, the amplitudes of the direct and the reflected waves are calculated. This information is then used to obtain the addition of the two waves to determine E/E_o, taking into consideration the relative phase shift between the direct and reflected waves and thus obtaining signal strengths at the 2,000 points on the flight.

It was desirable to obtain a method for determining the influences of various parameters in the receiving signal and to determine the accuracy of the program. Therefore the program was designed to provide a number of different displays, plotting the previously calculated parameters as functions of each other. This option was made available through a conversational mode by specifying the names of the variables which were to be exhibited as functions of other variables.

Analyzing and Testing

Testing of the program was performed using special flight approaches and assuming special reflecting surfaces. These tests examined whether the program properly calculates the reflection coefficients for vertical and horizontal polarization. In the first test it is worth noting that, in equations (1) and (2), assuming $\cos^2 \gamma = y^2$, the reflection coefficients should be equal to one. This test was easy to perform by setting the values of σ to 10^{-3} and the permittivity $\varepsilon = 4$. The above parameters yield a value for $\cos \gamma = 1/2$ which produces an approach angle of approximately 80°. The results of this test, shown in figure 6, demonstrate that the reflection coefficients R_V, R_H along the path are in fact equal to one. A second way of determining whether the reflection coefficients R_V and R_H are calculated properly is to set y^2 to infinity in equations (1) and (2). This diminishes the significance of $\cos^2 \gamma$ and thus reduces the expressions for R_H and R_V to 1. This

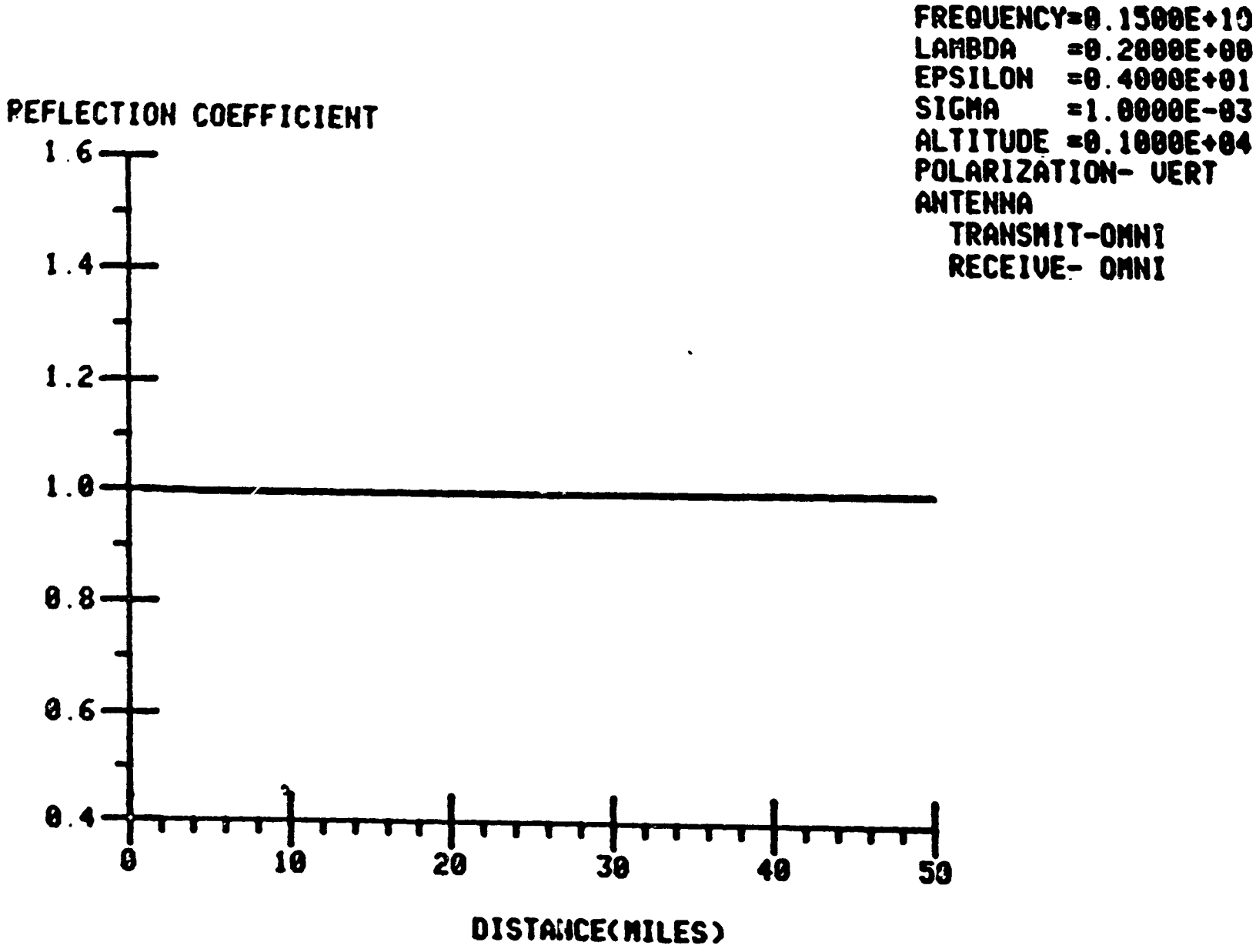

Figure 6. Results of first computer program test, demonstrating that reflection coefficients R_V, R_H = 1, as predicted.

test was performed by setting the permittivity $\epsilon_{rc} = 10^{12}$ and letting the program calculate the reflection coefficients for the total path. The results for this test are shown in figure 7, which again verified the program's calculated values. A third test was performed to determine whether Brewster's angle B, which is defined as the angle of incidence where minimum reflection for vertical polarization occurs accompanied by a phase shift of 90° relative to the phase of the incident wave, was being calculated properly. Note that setting the grazing angle in equation (1) so that

$$\tan \gamma = \frac{1}{y} \tag{16}$$

produces $R_V = 0$. This test was performed setting $\sigma = 0$ while maintaining level flight as the aircraft approached the receiving antenna. Thus the position of Brewster's angle along the approach path was determined:

$$\frac{h_1 + h_2}{D} = \tan B = \frac{1}{y} = \frac{1}{\sqrt{\frac{\epsilon_{rc}}{\epsilon_o}}} \quad \text{or} \quad D = \sqrt{\frac{\epsilon_{rc}}{\epsilon_o}}\,(h_1 + h_2) \tag{17}$$

In fact, the program calculated value was at 9.291 km (5.0168 nmi), compared to 9.257 km (4.99 nmi) obtained from the formula (see fig. 8).

Periodic Structure Analysis

The program was tested to determine if the periodic structure was properly repeating. Examining the optical path difference determined by equation (6),

$$\delta = \left[D^2 + (h_1 + h_2)^2\right]^{1/2} - \left[D^2 + (h_1 - h_2)^2\right]^{1/2} \tag{18}$$

Let $p^2 = h_1^2 + h_2^2 + D^2$, then $\delta = (p^2 + 2h_1h_2)^{1/2} - (p^2 - 2h_1h_2)^{1/2}$.

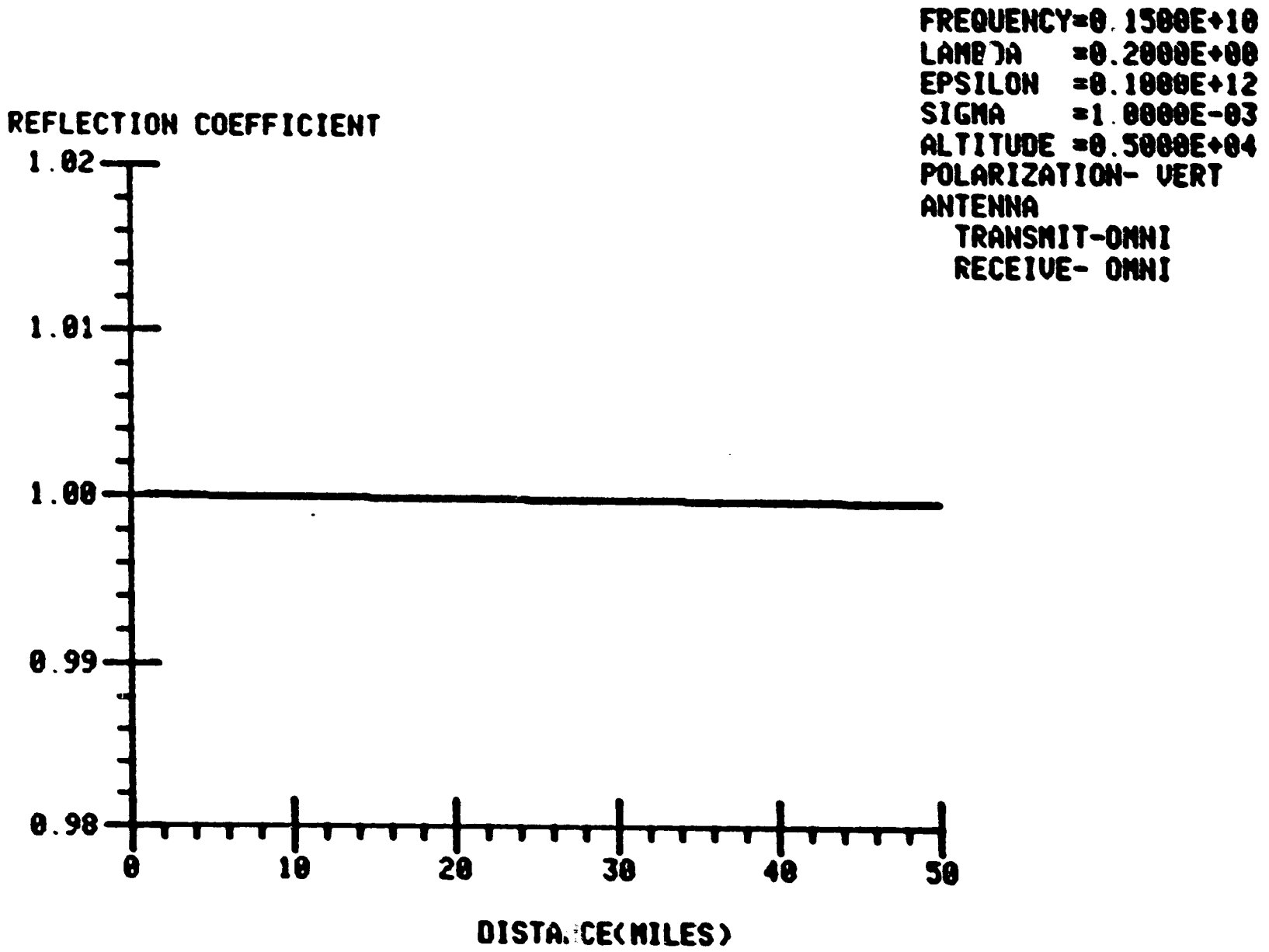

Figure 7. Results of computer program test which set y^2 to infinity in equations (2) and (3) to verify calculation of reflection coefficients R_V and R_H.

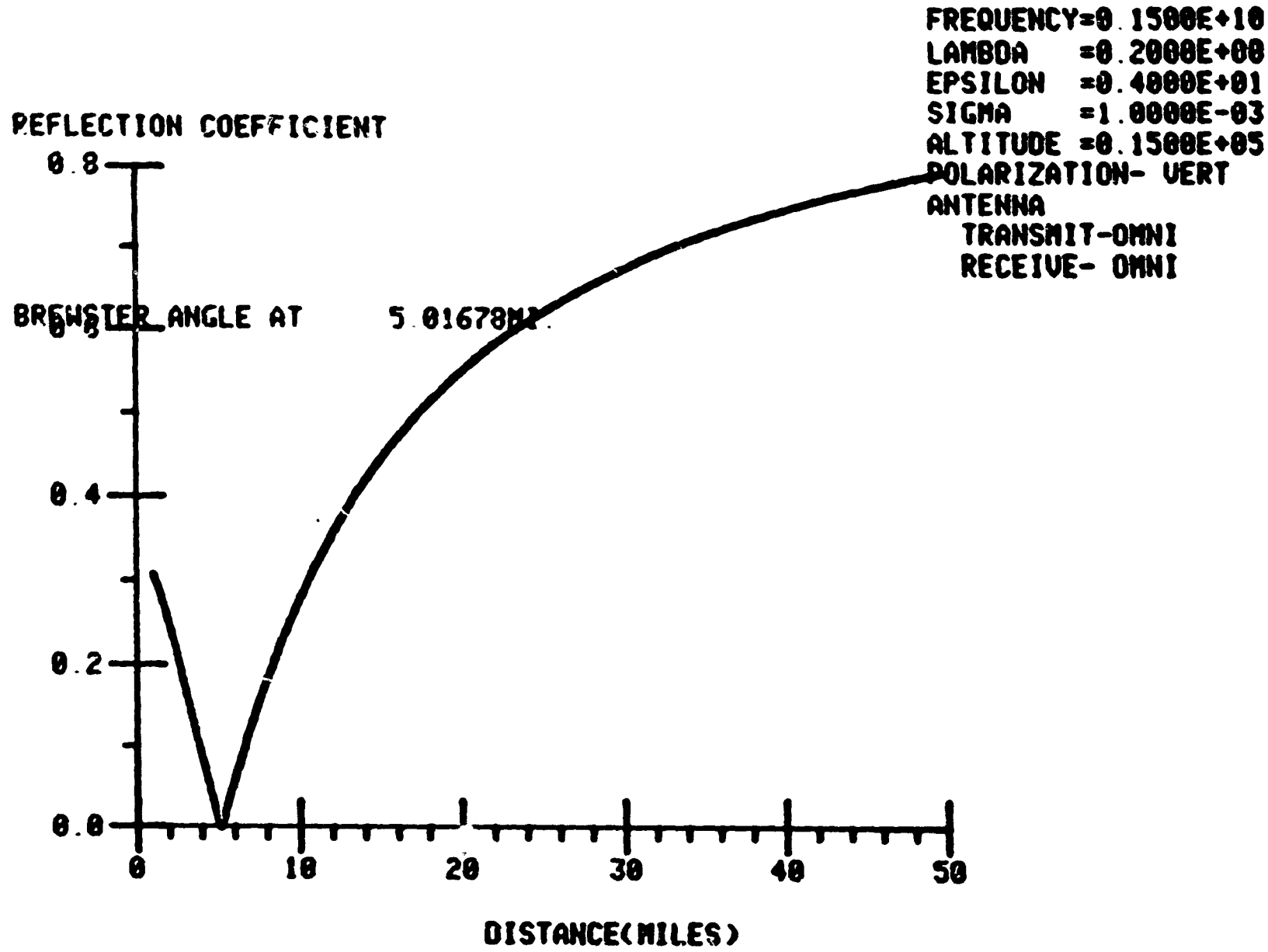

Figure 8. Results of computer program test to verify calculation of Brewster's angle.

Using the binomial expression and assuming $p^2 >> 2h_1h_2$, it follows that

$$\delta = \left(p^2 + \frac{(2h_1h_2)}{2p} + \ldots\right) - \left(p^2 - \frac{(2h_1h_2)}{2p} + \ldots\right)$$

$$\delta = \frac{2h_1h_2}{p} = \frac{2h_1h_2}{(h_1^2 + h_2^2 + D^2)^{1/2}} \tag{19}$$

Taking the derivative of δ with respect to D, we obtain

$$\frac{d\delta}{dD} = -\frac{2h_1h_2D}{(h_1^2 + h_2^2 + D^2)^{3/2}} \tag{20}$$

Noting that $\psi = \frac{2\pi\delta}{\lambda} + \phi$ and assuming that we are in a region where ϕ does not change rapidly, changes in phase would be due to δ. Setting $d\delta = \lambda$ should repeat the phase relation; thus the spacings between minima S is given by

$$S = \frac{(h_1^2 + h_2^2 + D^2)^{3/2}}{2h_1h_2D}\,\lambda \tag{21}$$

Further, assuming $D >> h_2$ and $D >> h_1$, we have

$$S = \frac{D^2}{2h_1h_2}\,\lambda \tag{22}$$

This was tested using the program by examining the spacing at several points along the path, and it was found to be in good agreement with the calculated spacing [eqs. (21) and (22)]. Figure 9 shows an example of the periodic structure.

Analysis of the Variation of Periodic Structure with Approach

Calculation of the variation in periodic structure with the aircraft's approach provided some insight into multipath effects. Setting the flight path level, variations were observed with large distances between the aircraft and ground antenna, and satisfactory agreement was found in comparing the program's spacing and that obtained by calculation [eq. (23)].

Examining the variations of spacing as a function of D, the derivative follows:

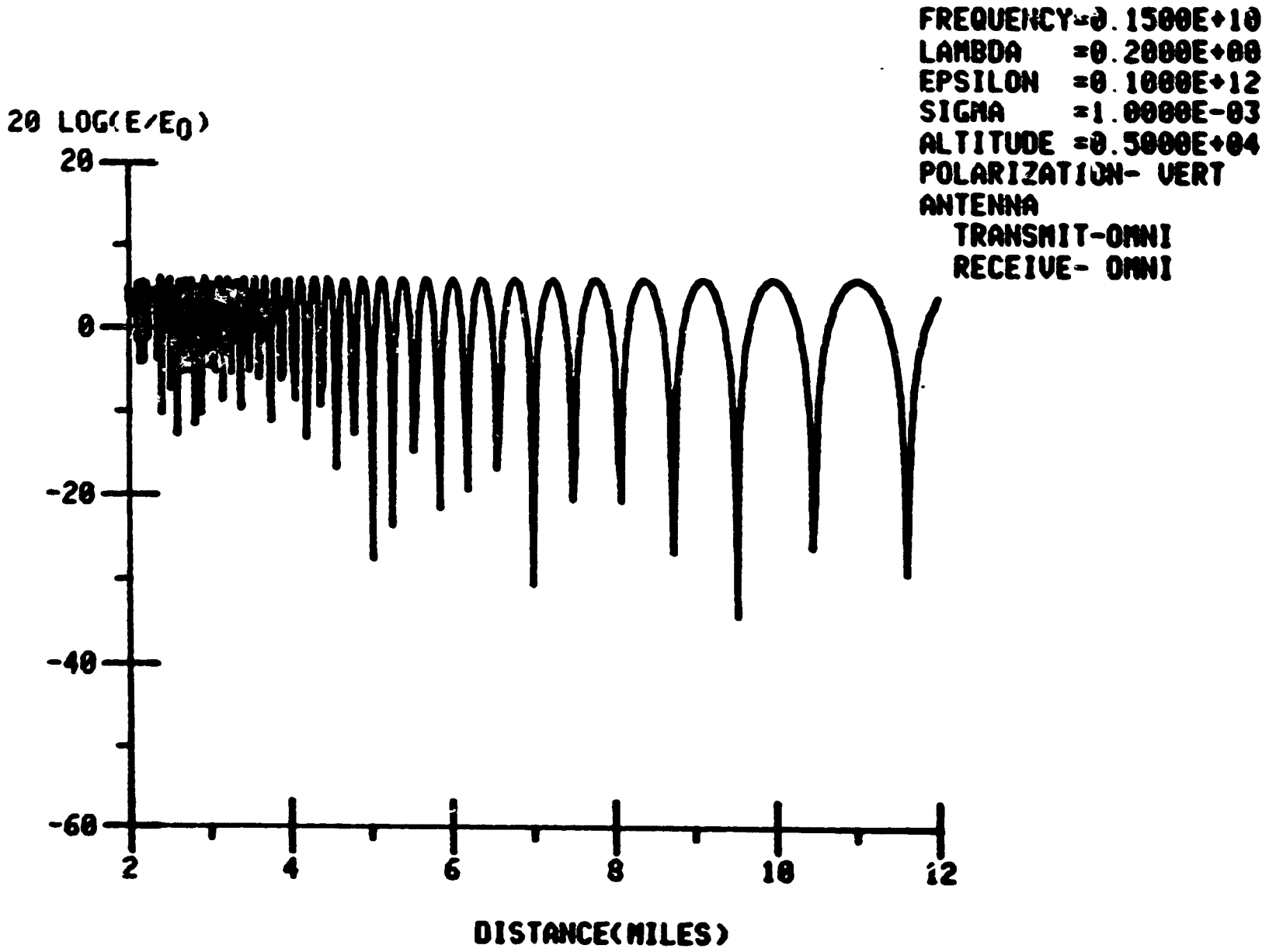

Figure 9. Sample periodic structure.

$$\frac{dS}{dD} = \frac{\frac{3}{2}(h_1^2 + h_2^2 + D^2)^{1/2} 2D}{2h_1h_2D} - \frac{(h_1^2 + h_2^2 + D^2)^{3/2}}{2h_1h_2D^2} \tag{23a}$$

which reduces to

$$\frac{dS}{dD} = \frac{(2D^2 - h_1^2 - h_2^2)(h_1^2 + h_2^2 + D^2)^{\frac{1}{2}}}{2h_1h_2D^2} \tag{23b}$$

Setting the derivative equal to zero, we obtain a minimum spacing between signal maxima.

$$2D^2 - h_1^2 - h_2^2 = 0$$

reducing to

$$D^2 = \frac{h_1^2 + h_2^2}{2} \quad \text{or} \quad D = \sqrt{\frac{h_1^2 + h_2^2}{2}} \tag{24}$$

The observance of the minima was the final test of the program. It was performed by setting the flight path level and examining the signal variations at short distances between the antenna and the aircraft. Here again satisfactory agreement was found between the location of minimum spacing between signal maxima determined by equation (24) and the calculation performed by the program.

OVERFLIGHT CHARACTERISTICS

Predicted Signal Strengths

Introduction.- A series of calculations was performed to evaluate the potential problem areas arising from multipath interference. The parameters used to evaluate signal strength dependence as a function of horizontal distance were reflective surface characteristics, type of polarization, transmitter frequency, and overflight altitude. These calculations were performed for omnidirectional ground antenna and for the directional antenna whose gain is given in figure 10. Since the signal amplitude variations strongly depend on position of the aircraft relative to the ground antenna, the detailed variations could best be brought out by dividing the range 0.8 to 80 km (0.5 - 50 mi) into long distance 19 to 80 km (12 - 50 mi), final approach 3 to 19 km (2 - 12 mi) and short

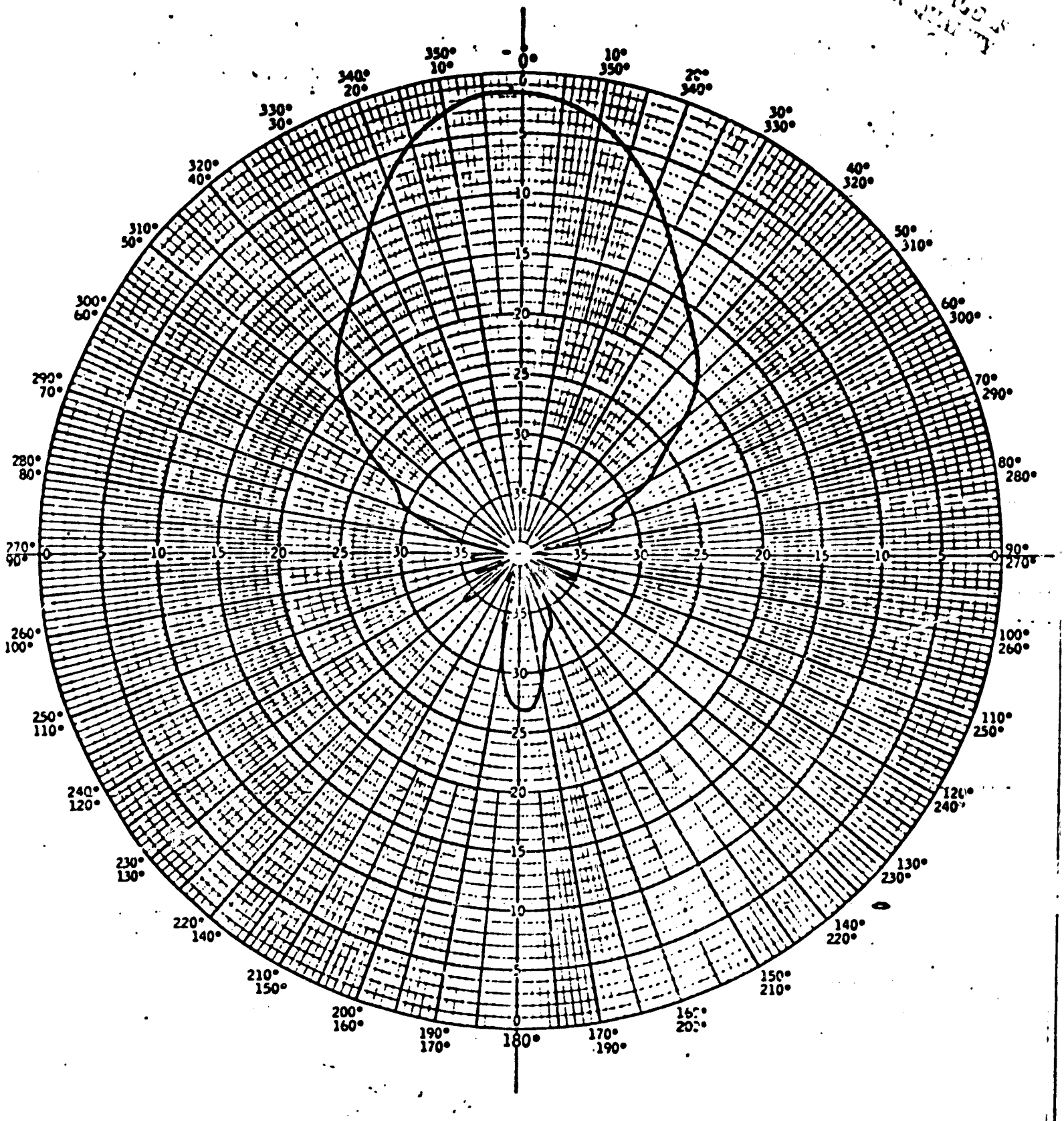

Figure 10. Directional antenna gain.

range 0.8 to 3 km (0.5 - 2 mi). The distance of 80 km (50 mi) is consistent with the transmission horizon that can be evaluated by

$$D = \sqrt{2\,Rh_1} + \sqrt{2\,Rh_2} = \sqrt{2R}\left\{\sqrt{h_1} + \sqrt{h_2}\right\}$$

where D is the distance between the aircraft and ground antenna, R the radius of the earth, h_1 the height of the ground antenna, and h_2 the height of the aircraft. Using the above formula for an aircraft altitude of 396 m (1300 ft) and ground antenna height of 1.5 m (4.8 ft), a transmission horizon of 80 km (50 mi) is obtained.

Communication at 19 to 80 km (12 - 50 mi).- The analysis of signal strength from 19 to 80 km is governed by the fact that the grazing angle is relatively small for considered approaches up to 1524 m (5000 ft) in altitude. This results in a phase shift due to reflection of nearly 180° for both vertical and horizontal polarization. Thus the location of maxima and minima for both polarizations are determined by the optical paths' difference. For small grazing angles the reflection coefficients for horizontal polarization are larger than for vertical polarization; thus the former produces deeper minima and slightly higher maxima. Figures A1 to A6 (see Appendix A) show the reflection coefficient (phase and amplitude) characteristics vs. grazing angle and frequency. Thus, in the region from 19 to 80 km, the relative degree of the variation could be estimated purely by examining the values of the amplitude coefficients. Note the dependence of reflection coefficients and phase lag on polarization and surface conditions. Actual examples of signals for both antennas are presented in figures B1 to B20 and described in table B (see Appendix B).

Communication at 3 to 19 km.- The signal strength in this region is strongly influenced by the rapid variations of reflection coefficients with aircraft position. There is a strong dependence on type of polarization and reflecting surface characteristics. The reflecting phase lag changes dramatically for vertical polarization over a small range of grazing angles; therefore the onset of the phase lag has a significant effect on communication. Up to the point where the phase lag change occurs, the

maxima and minima signal strength coincide in position for various surface characteristics and types of polarization. However, once the phase lag assumes a significant value, the relative positions of the maxima and minima for vertical polarization change relative to horizontal polarization. This is shown in table C and figures C1 to C48 (Appendix C).

Communication at 0.8 to 3 km.- In this region the reflection coefficients as well as the phase lag for vertical polarization vary dramatically. Since the grazing angle increases rapidly, the oscillations of the signal are generally governed by the transmission frequency. The duration of nulls are very low and their repetition can be rather high. This is exhibited in table D and figures D1 to D18 (Appendix D).

EXPERIMENTAL TEST

Description of Aircraft Antenna

Preflight studies for the Terminal Configured Vehicle (TCV) Project were conducted at NASA/Wallops Flight Center, Wallops Island, Virginia. The TCV, a modified Boeing 737 jet, was equipped with highly flexible display and control equipment, an aft flight deck for research purposes, and stacked vertical antennas positioned on the top forward edge of the vertical tail fin assembly (Appendix E). The antennas were stacked to provide omni coverage for each band without shadowing effects. Low loss Andrew's FHJ-50 Heliax cable was installed between the antennas and the receivers to increase the sensitivity for observing multipath fluctuations. This minimized the transmission line loss over that of regular coax by a factor of better than 3 dB. A receiver that has a wide AGC dynamic range was installed in the plane for this flight (fig. 11).

Ground Antenna

The FPS-16 C-band radar complex was used for the prime tracking site of the Microwave Landing System. An S-band parabolic antenna was mounted to the side of the FPS-16 antenna to accommodate the Flight Display Research System (Appendix F). This S-band antenna was designed to provide horizontal, vertical, left-hand circular, and right-hand circular polarizations. A low-loss elliptical waveguide was run from the transmitter to the antenna

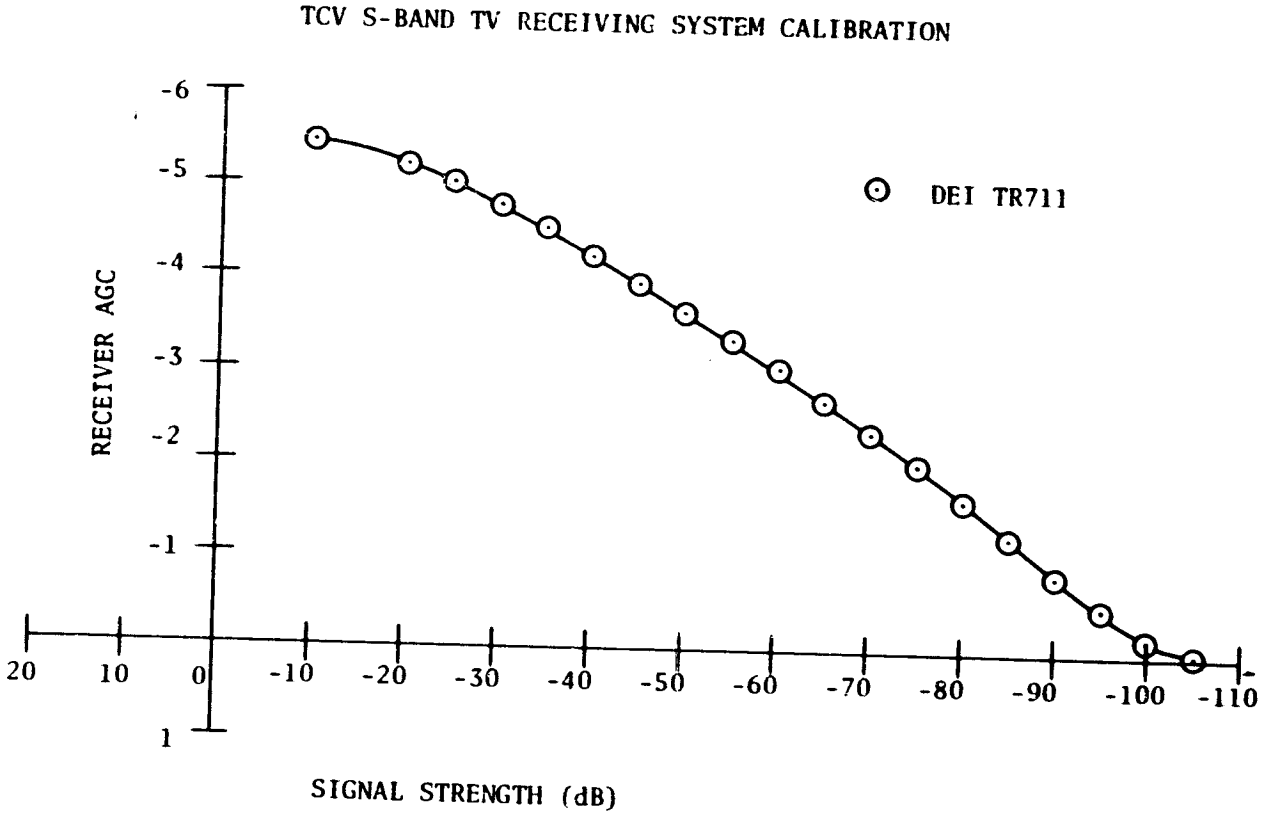

Figure 11. Plot of signal strength for a receiver having a wide AGC dynamic range.

to provide the lowest loss path possible. Figure 12 shows the mounting arrangement of the antennas and the method of tracking the aircraft. The antenna movement changes h_1, the antenna's altitude, as a function of aircraft position. The procedure used to calculate signal strength compensated for the movement.

Flight Test

The inflight tests for the TCV project were conducted at NASA/Wallops Flight Center on May 15, 1979. The modified TCV B-737 was used to fly two paths, which consisted of three segments each. The second flight path was to be a repetition of the first to provide confirmation for comparison. It was desired to maintain constant altitude throughout the flight. The first and fourth segments were to be flown away from the ground antenna. The second and fifth segments were to maintain a fixed distance from the ground antenna, and the third and sixth were to approach the ground antenna. In actuality, only the first flight path and the first two segments of the second were flown. Flight path repetition was not completely achieved; however, some segments were of a sufficient degree of closeness as to allow the desired comparisons. Level flight could not be maintained to the degree desired, but the altitude changes were gradual and therefore were linearly interpolated into the results. Figure 13 shows the actual flight path the aircraft flew as it headed south over water for a distance of approximately 93 km (50 nmi), turned west till it was over land, and then headed back over land to the starting point. Weather conditions changed the flight schedule, allowing one complete flight profile to be conducted in the morning and the first two legs of the profile in the afternoon on the return flight to NASA/LaRC.

TEST ANALYSIS AND RESULTS

Data Analysis

During the flight the received signal strength was monitored and recorded onboard the aircraft every 0.025 sec. Simultaneously, the FPS radar tracked and recorded the aircraft position. Heading velocity information and the FPS 16 data were used in monitoring aircraft positions.

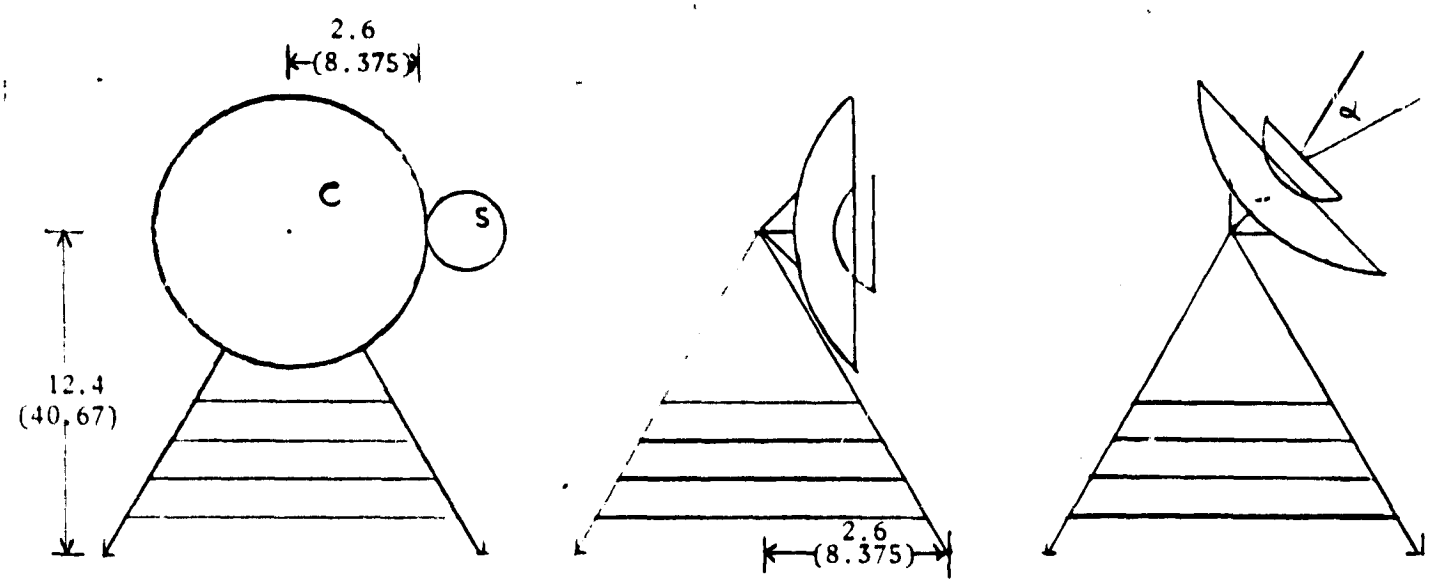

Figure 12. Mounting arrangement of ground antenna and method of tracking aircraft; dimensions are given in meters (feet).

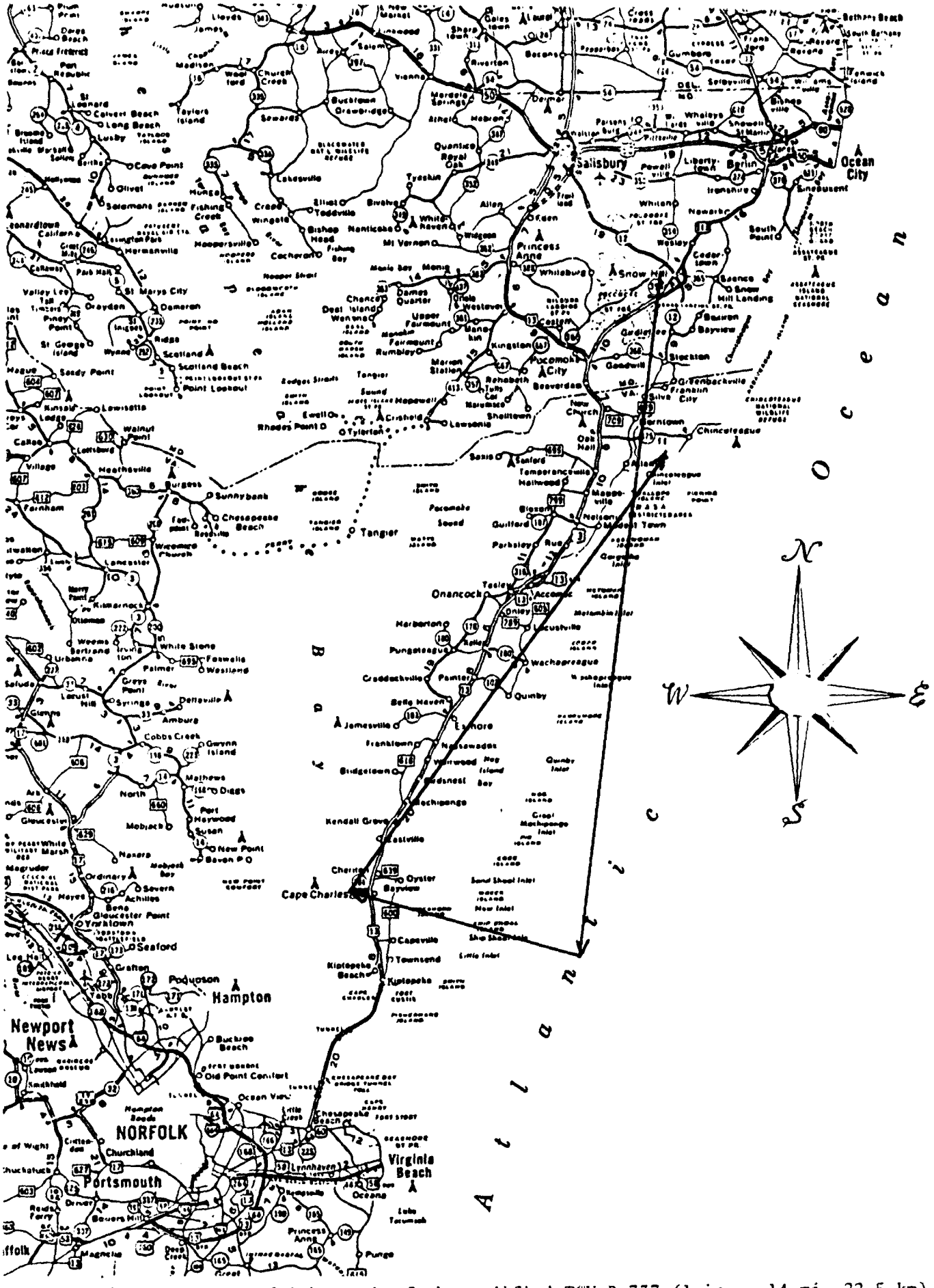

Figure 13. Test flight path of the modified TCV B-737 (1 in. = 14 mi, 22.5 km).

The FPS 16 aircraft position was available in 10-sec increments in the form of an X-Y plot and a time (altitude) plot on plotboard paper. This resulted in significantly more received signal data points (approximately 57,500) than flight aircraft position data points (approximately 114/flight). Thus, the data had to be collated using time as the reference variable. Using time as a common factor, the aircraft position data and signal strengths were incorporated into a set of 2000 points with signal strength and position determined for each point.

Several problems were encountered in utilizing the aircraft position data. The extraction of accurate aircraft position from the plotboard paper was subject to inaccuracies due to scaling and print size. Aircraft horizontal position (X-Y) was scaled at 1,800 m/cm (15,000 ft/in.), and the 10-sec time marks were circular with a diameter of 0.13 cm (0.05 in.) [229 m (750 ft)]. Aircraft altitude (Z) was scaled at 120 m/cm (1000 ft/in.) with the same size time marks, 0.13 cm (0.05 in.) [15.2 m (50 ft)]. The fact that the altitude data marks were folded back on themselves after approximately 9 min of flight made the extraction of data from the presentation very difficult.

Using the previously determined 2000 points along the flight paths, the program was used to calculate predictions for signal strength. It is important to note that we were unable to do good initial referencing, i.e., the variations should be used for comparison rather than as absolute values. To obtain a proper simulation, the input parameters to the program σ and ε had to be selected. The points of reflection along the flight path were calculated to determine the actual reflecting surface. The surface turned out to be solid earth (no reflection from water); therefore a σ-ε combination of 0.00[illegible] was chosen. These values are typical for ground surface, where ε range is 2 to 24 and the σ range is 0.0001 to 0.001 mhos/m depending on how dry or wet the ground is. Calculations indicated the reflection point was in an area composed of very dry and/or hard runway surface. No detailed study was made for individual reflection points. To reduce complication in comparisons, each segment of each flight was considered separately, ignoring the flight position during which major changes in heading occurred. The aircraft position

data from the second segment of the first flight was found to be unreliable due to large breaks in the data; therefore only four segments were prepared for comparison. Initial point-by-point comparison of actual and computed received signals revealed little useful information. A much more suitable method of comparison was made by plotting the two data sets against the horizontal distance between the ground antenna and the aircraft. These plots are presented in figures 14 to 17 for actual recorded signal and 18 to 21 for the theoretically predicted signal strength.

Results

A comparison of the actual and computed received signal shows qualitative agreement. The computed signal had a cleaner appearance with no amplitude distortions; however, several factors which affect amplitude and distortion were not included in the computer simulation, the most significant of these being the inverse square signal dependence and extent of spectral reflection, scattering, absorption, and changes in the index of refraction. Of greater interest is the comparison of the signal oscillations, that is, the frequency of dropouts. The equation for the received signal amplitude suggests the signal should be sinusoidal. The major parameters controlling the frequency of dropouts are the horizontal distance between the ground antenna and the aircraft and the altitude of the aircraft. Comparison of actual and computed received signals show good agreement in frequency of dropouts, particularly at large horizontal distances. In order to understand why this agreement is best at large distances, it is important to remember that, in our method of determining position, the accuracy is fixed and therefore does not have the same relative influence. Aircraft position is ±228.6 m (±750 ft) for horizontal position and ±15.24 m (±50 ft) for altitude. Altitude is the most significant parameter in the calculations. Improved agreement was achieved by recomputing signal strength using horizontal distance and actual altitude obtained from flight data rather than the FPS 16 antenna.

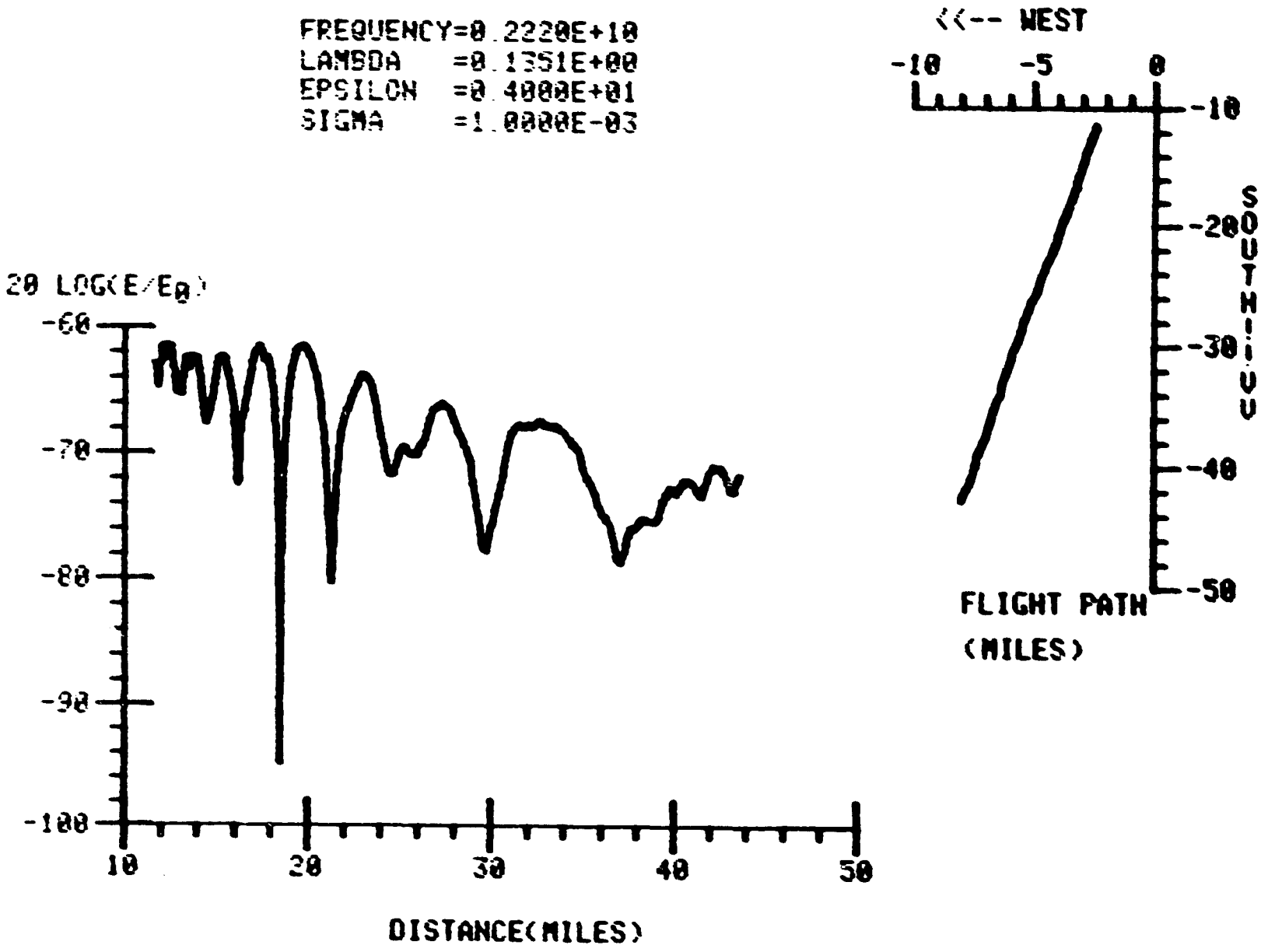

Figure 14. Experimental Flight 1, leg 1.

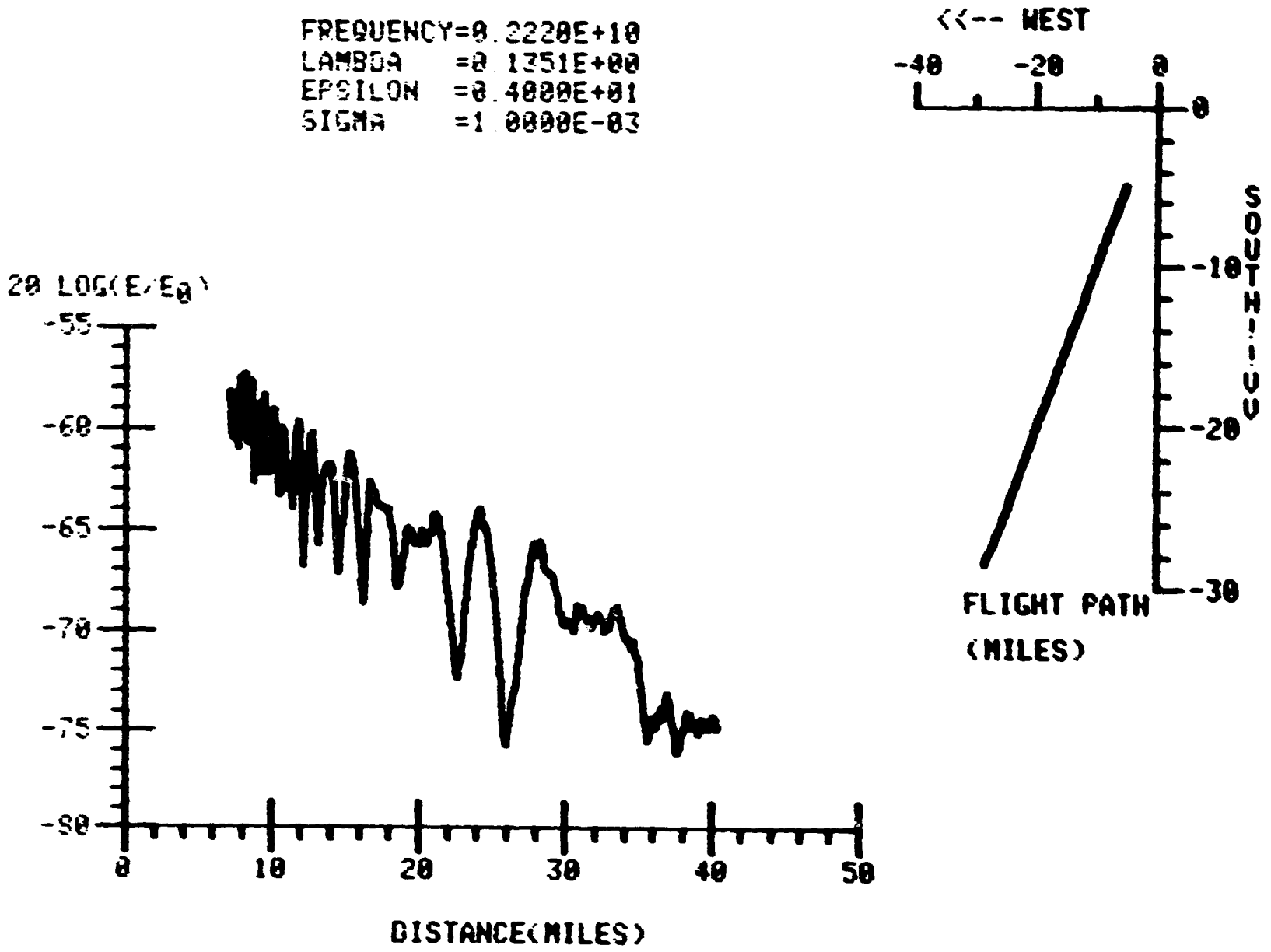

Figure 15. Experimental flight 1, leg 3.

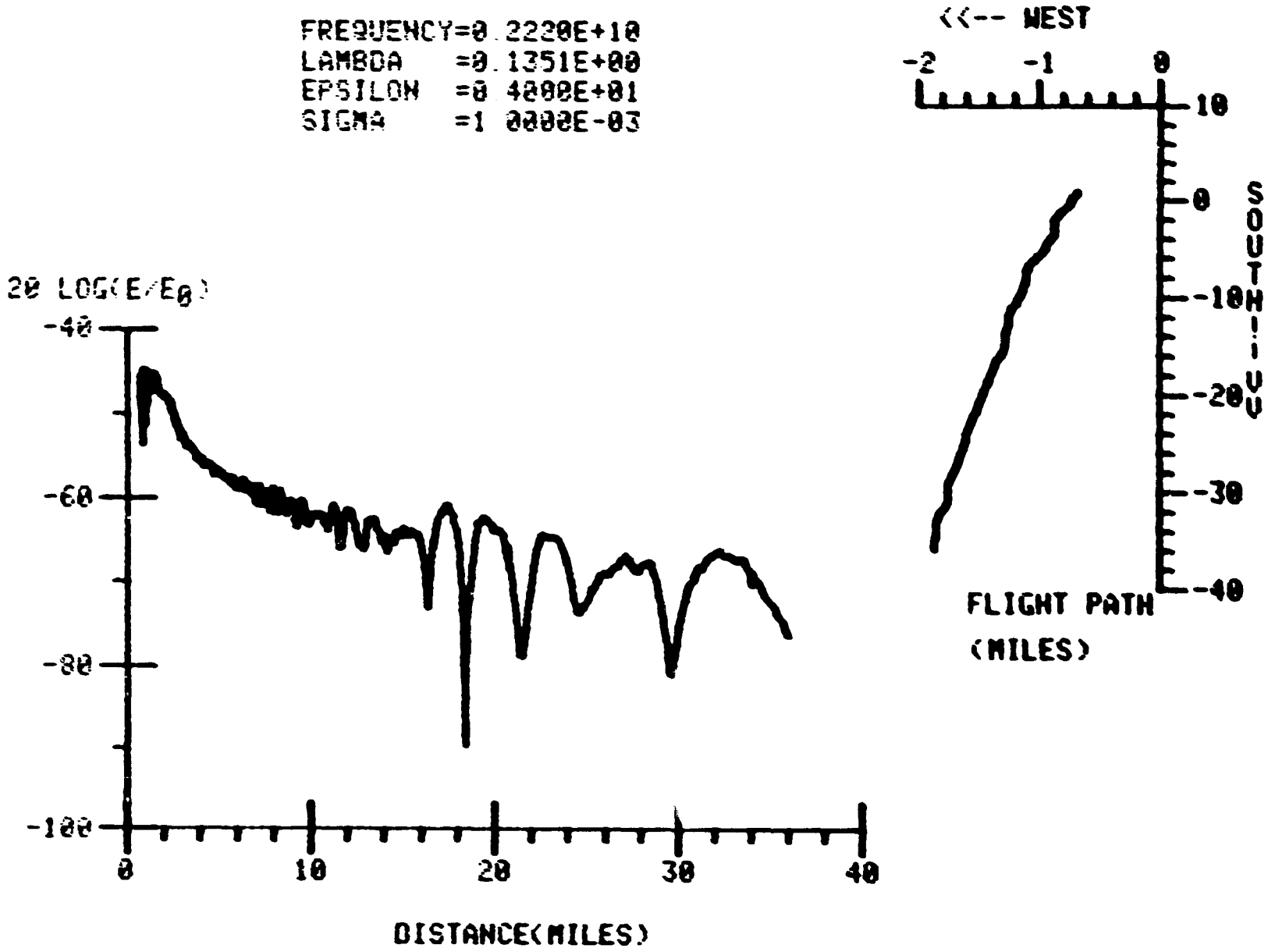

Figure 16. Experimental flight 2, leg 1.

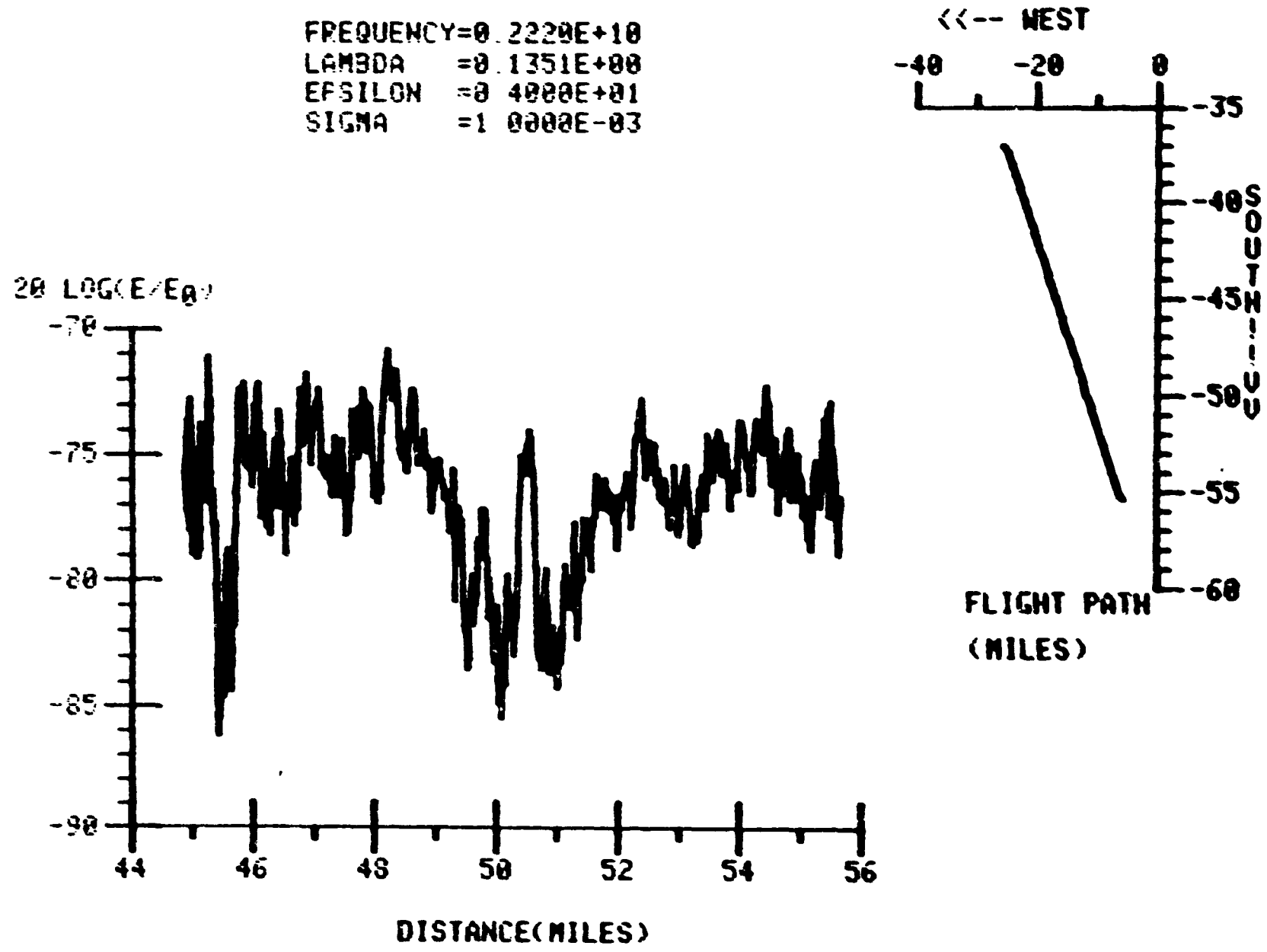

Figure 17. Experimental flight 2, leg 2.

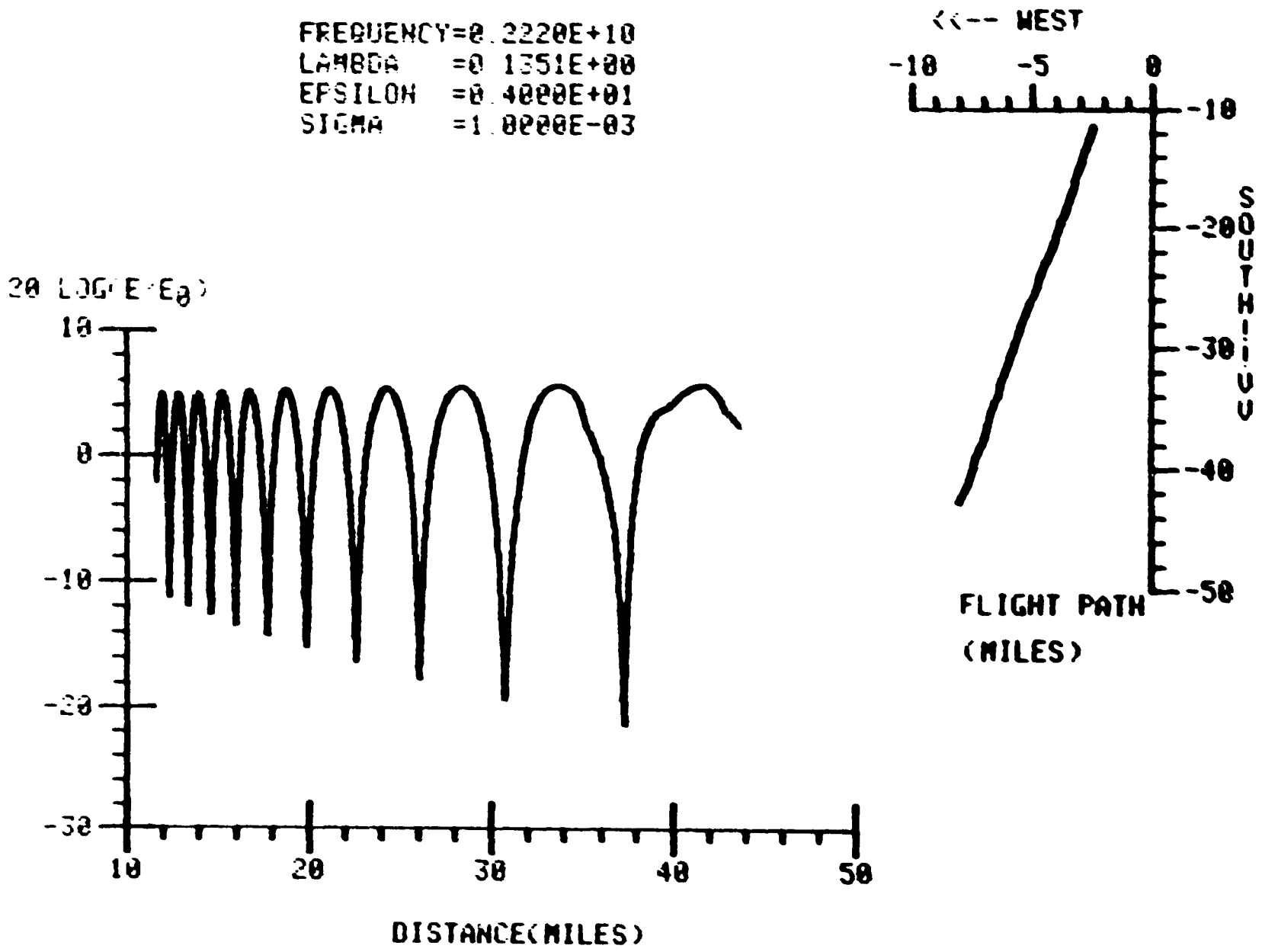

Figure 18. Theoretical flight 1, leg 1.

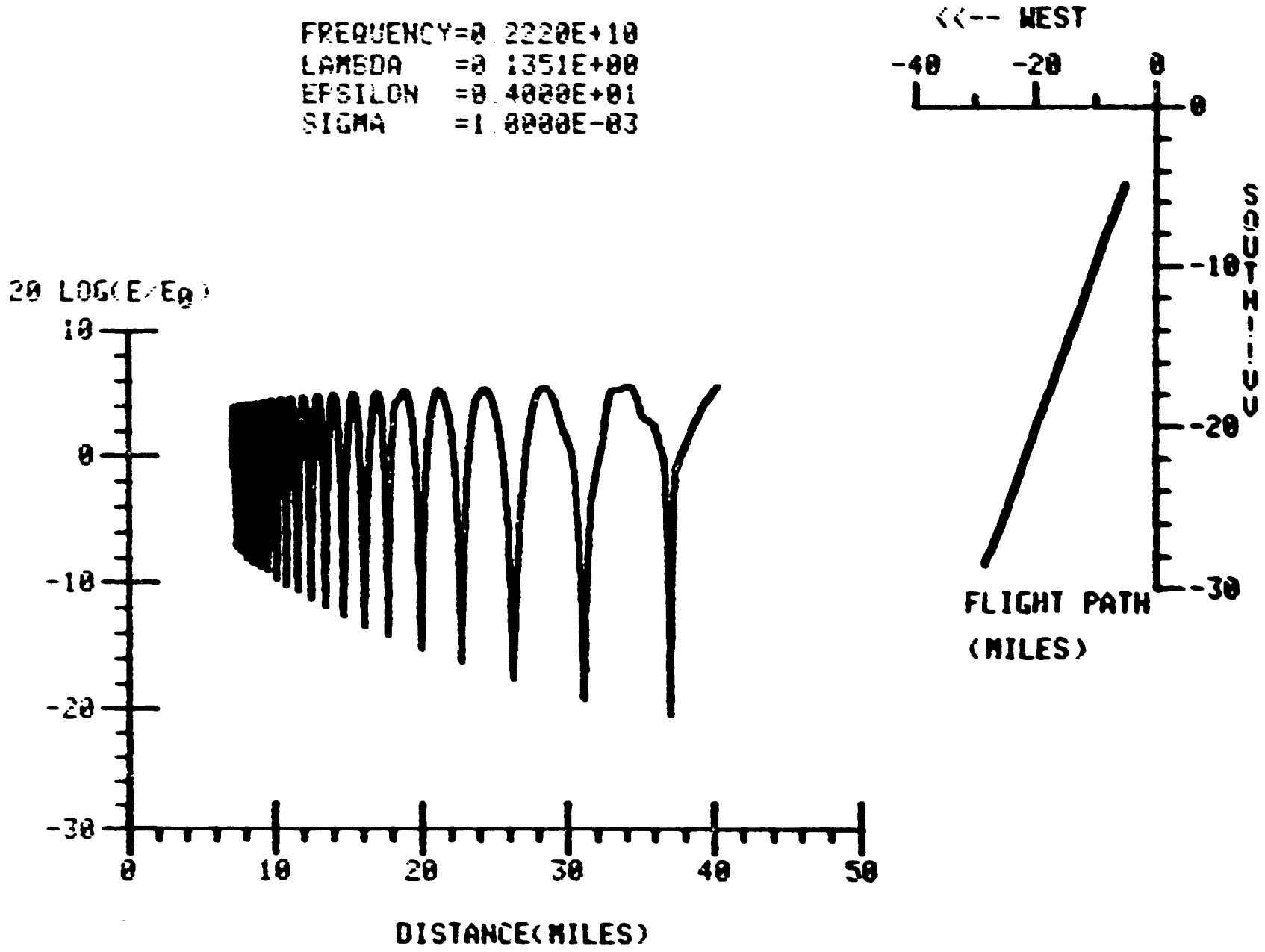

Figure 19. Theoretical flight 1, leg 3.

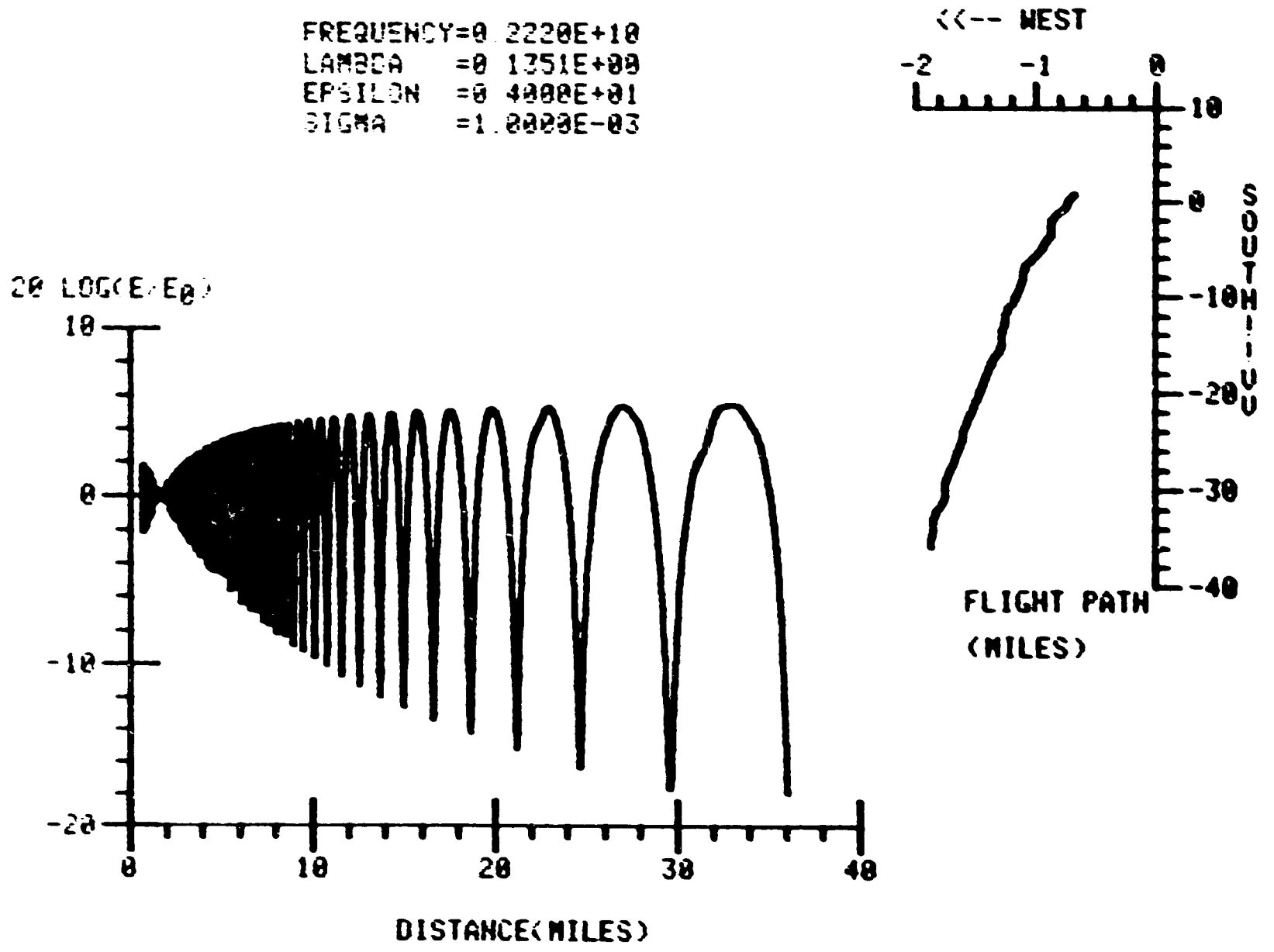

Figure 20. Theoretical flight 2, leg 1.

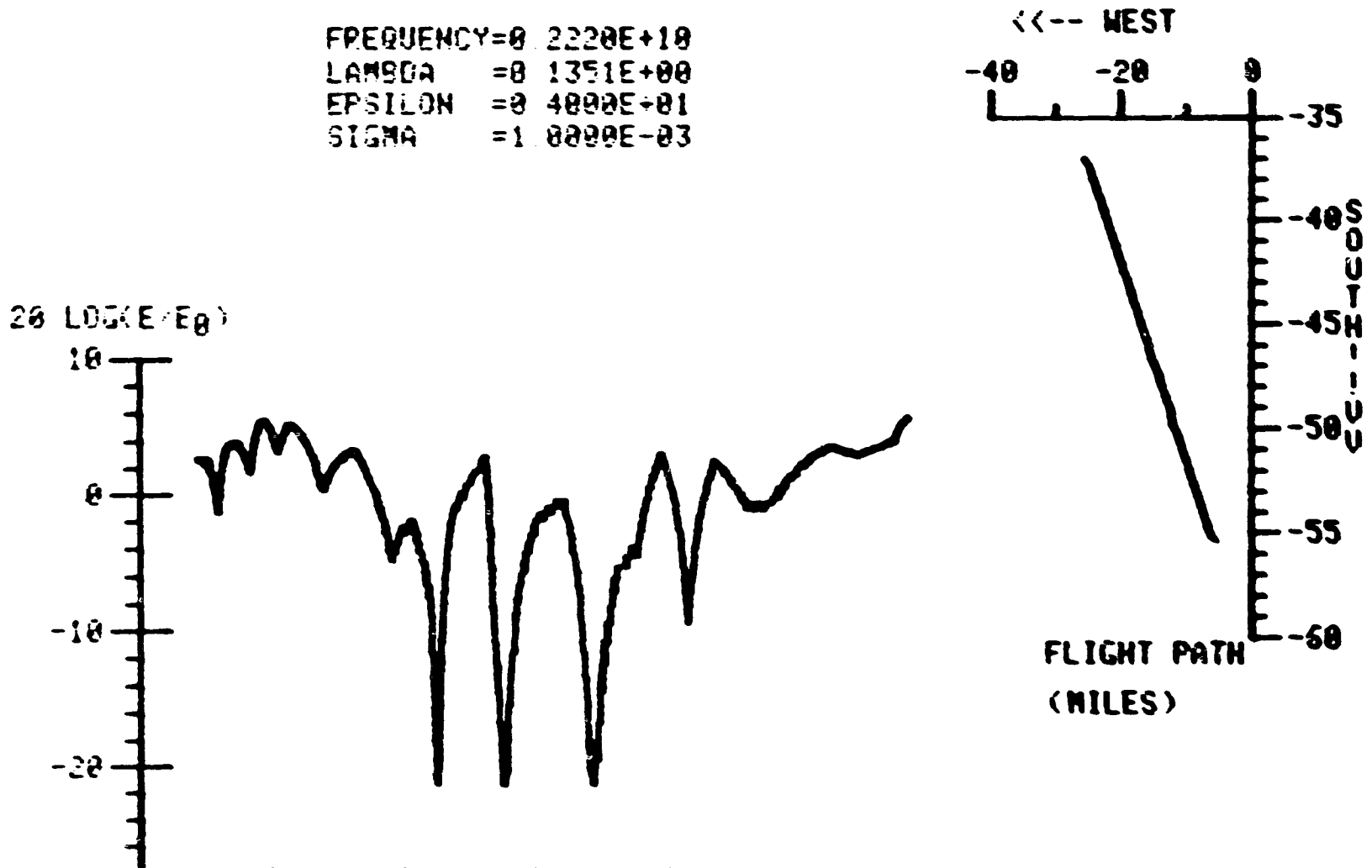

Figure 21. Theoretical Flight 2, leg 2.

FURTHER COMMENTS

An almost infinite number of inflight and ground situations can exist which can affect signal amplitude fluctuations. Only limited variations could be included in one experimental flight. The comparisons made as a result of this flight and the agreement achieved lend confidence and credibility to the simulation program developed. Since the overall system under discussion relates to landing communications, the received signal characteristics which exist during a landing profile are of considerable importance. Results of this investigation using simulated landing flight profiles generated questions which suggest the need for including topography. It appears that the area where reflection occurs is relatively small. This implies that it should be possible to model the reflection surface area effectively. To establish the extent and frequency of dropout, it will be necessary to perform a study which incorporates topographic data about the area surrounding the receiving site.

CONCLUSIONS

1. The agreement achieved between actual and computed received signal indicates that the computer simulation for predicitng signal amplitude fluctuations is highly feasible.

2. The basic mathematical model utilized seems to be a good first approximation. Changes in the simulation to allow inclusion of such parameters as σ and ε as a function of reflection point location, specular reflection, scattering, absorption, and index of refraction will improve predictability of signal strengths.

3. This program, properly modified to consider the topography of a site, could be used in the planning and geographic layout of future airport facilities which plan to use microwave landing systems.

4. Inclusion of antenna signal strength patterns in evaluating the communication link could be very valuable in predicting a degree of dropout.

APPENDIX A

REFLECTION COEFFICIENT (PHASE AND AMPLITUDE) CHARACTERISTICS VS. GRAZING ANGLE AND FREQUENCY

TABLE A

FIGURE	FREQUENCY	REFLECTION COEFFICIENT	REFLECTION PHASE
A1	1500 MHz	✓	
A2	2220 MHz	✓	
A3	5500 MHz	✓	
A4	1500 MHz		✓
A5	2220 MHz		✓
A6	5500 MHz		✓

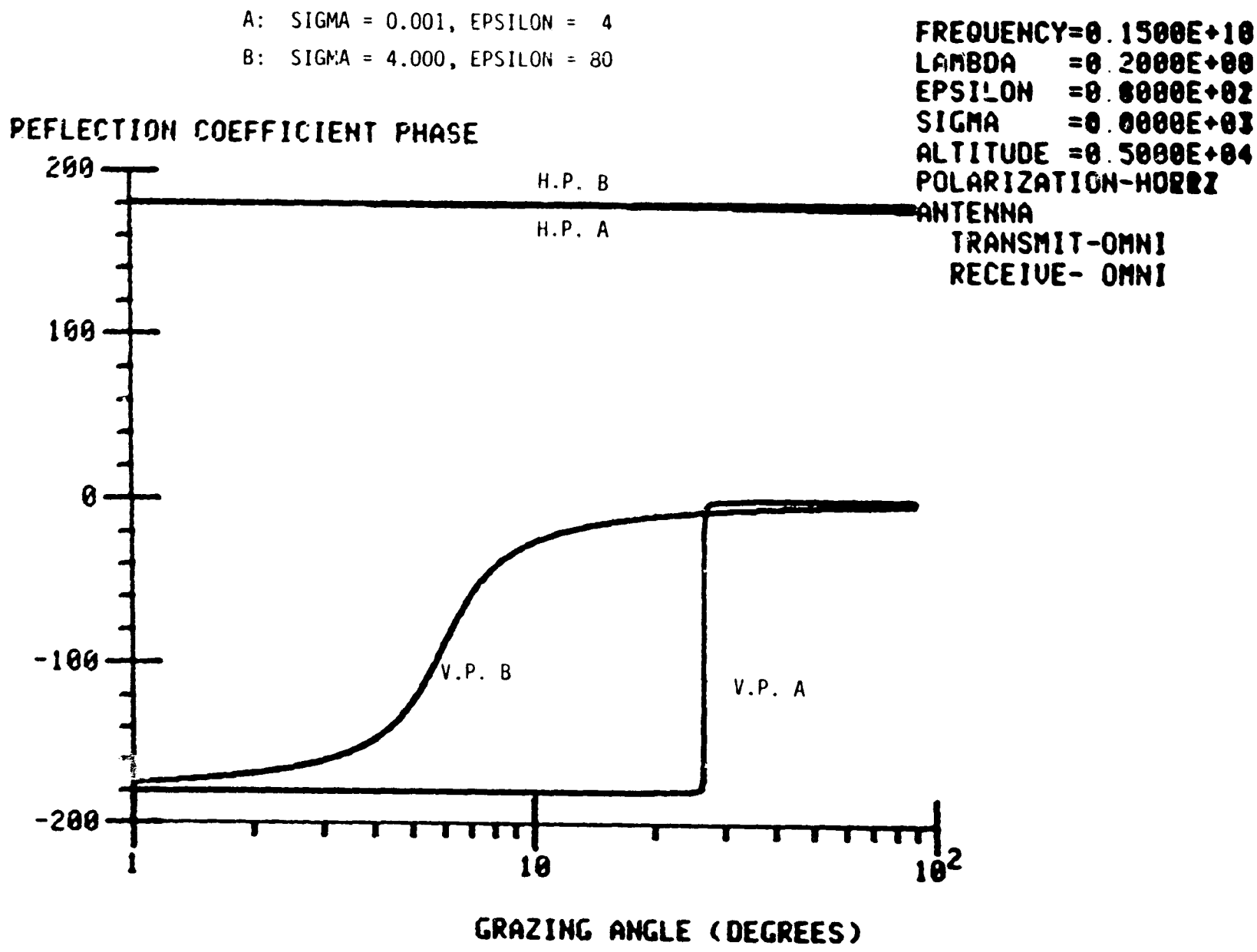

Figure A1. Magnitude of phase shift vs. grazing angle (frequency 1500 MHz).

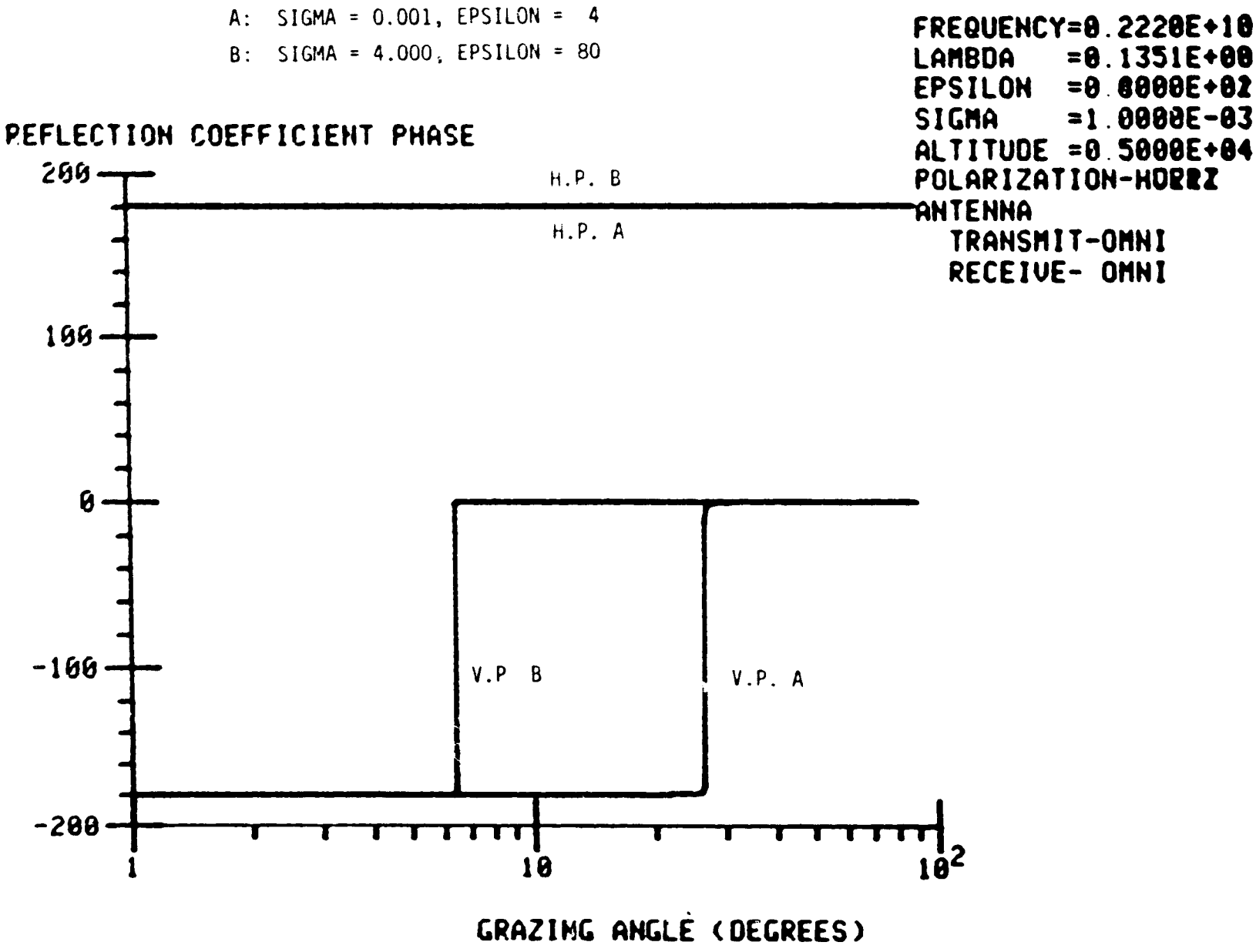

Figure A2. Magnitude of phase shift vs. grazing angle (frequency 2220 MHz).

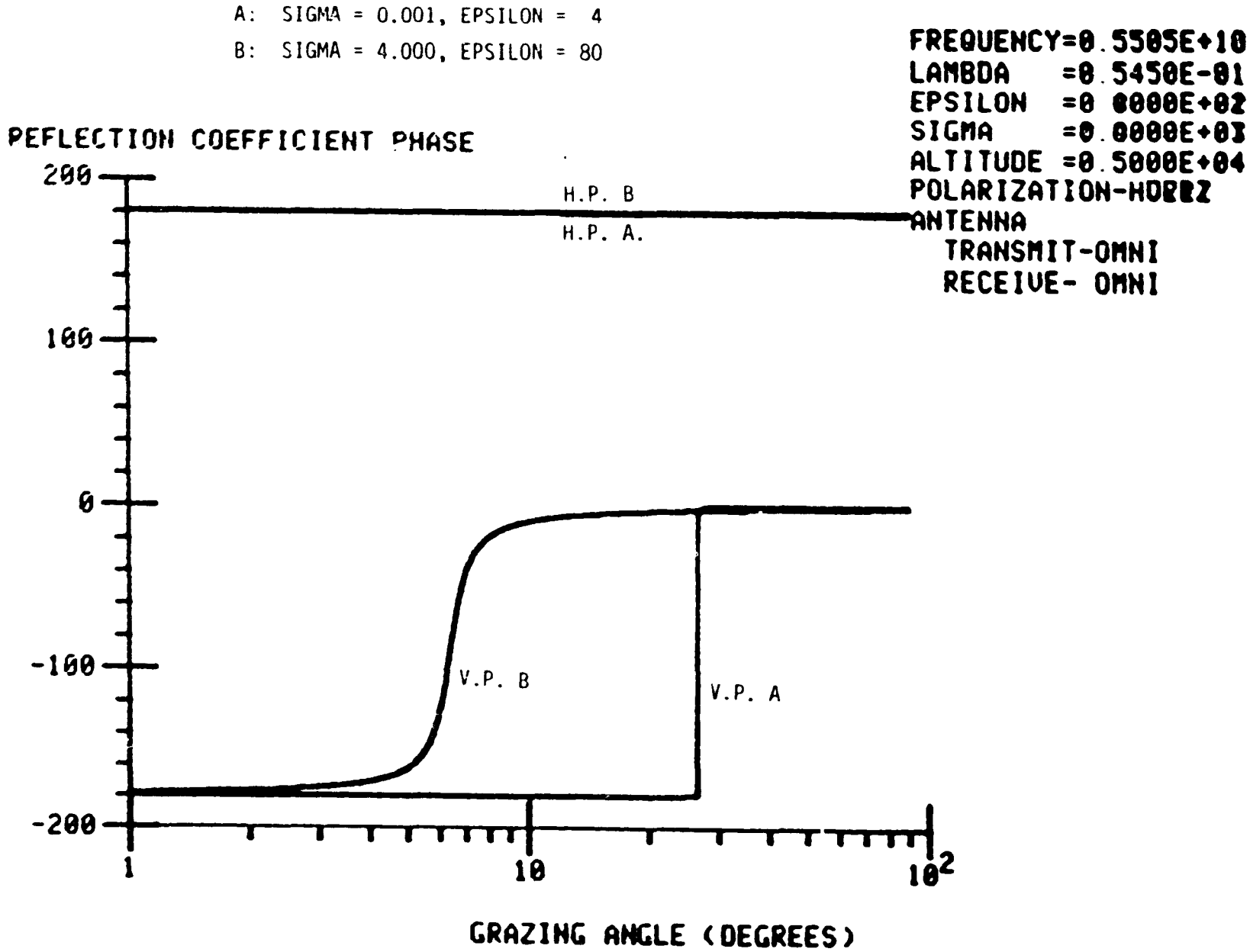

Figure A3. Magnitude of phase shift vs. grazing angle (frequency 5500 MHz).

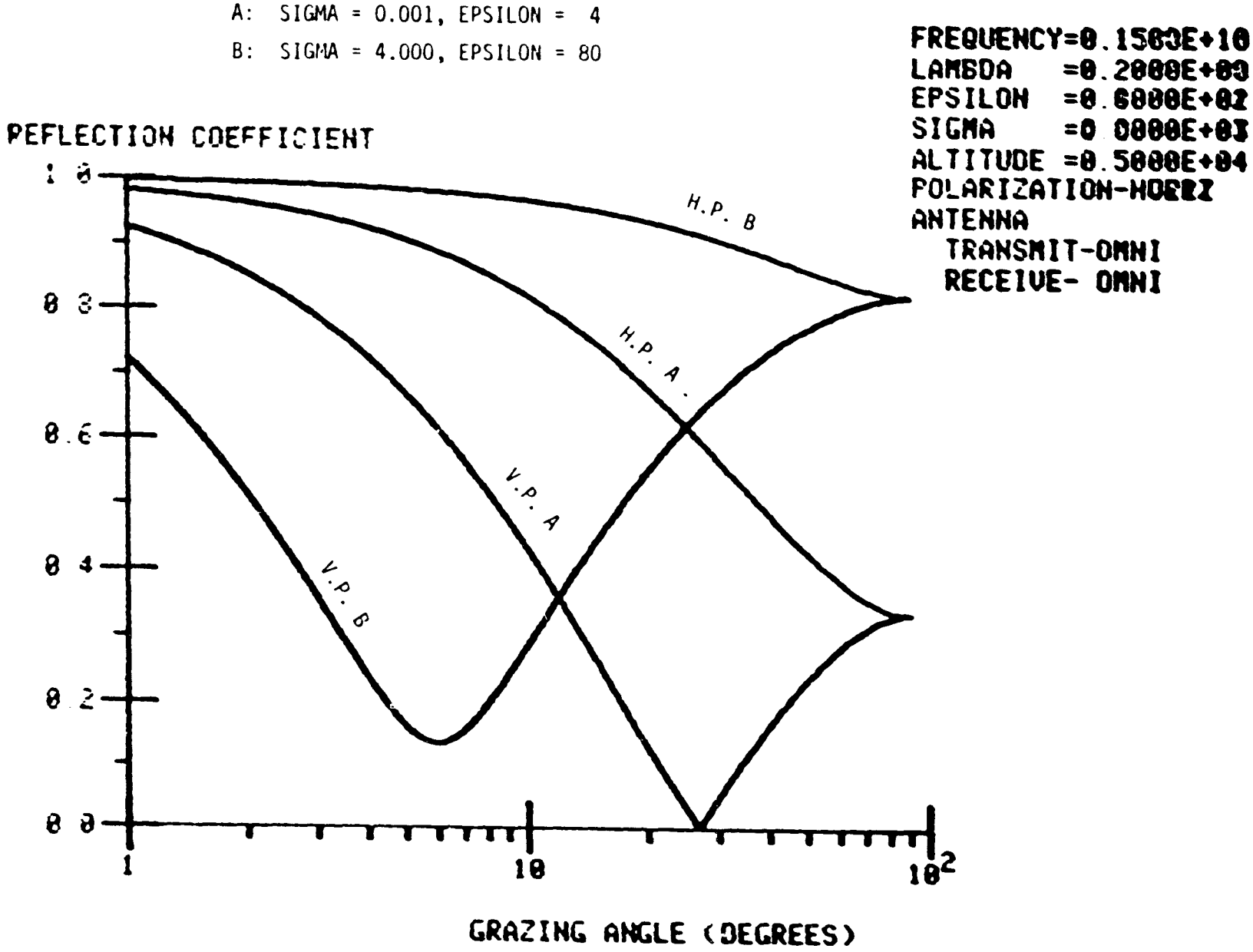

Figure A4. Magnitude of reflection coefficient vs. grazing angle (frequency 1500 MHz).

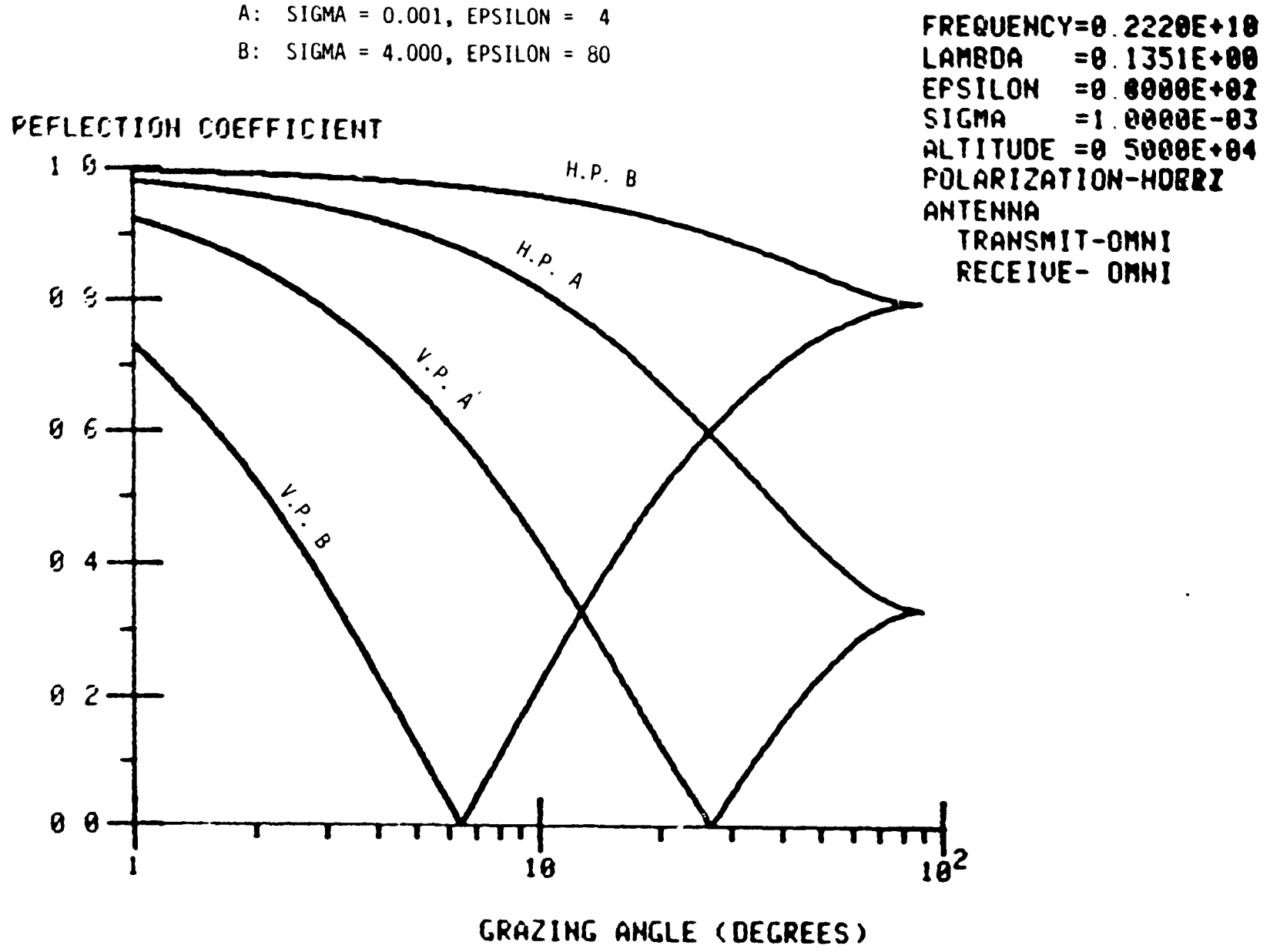

Figure A5. Magnitude of reflection coefficient vs. grazing angle (frequency 2220 MHz).

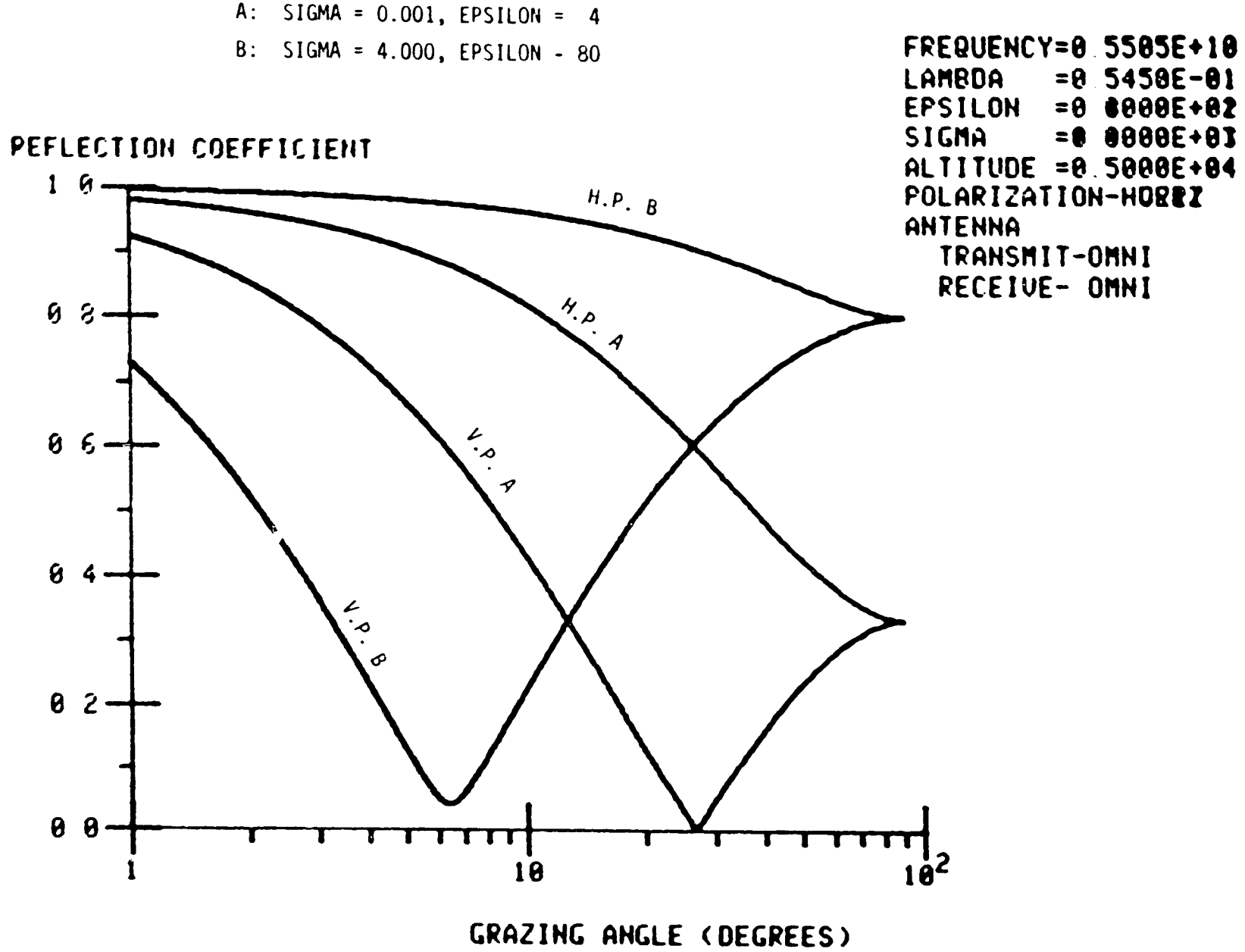

Figure A6. Magnitude of reflection coefficient vs. grazing angle (frequency 5500 MHz).

APPENDIX B

SAMPLE SIGNALS FOR BOTH VERTICAL AND HORIZONTAL POLARIZATIONS IN THE 0.8 TO 80 KM RANGE

TABLE B

0.8 - 80 km Range

FIGURE	LAMBDA	ALTITUDE*	SIGMA	EPSILON	POLARIZATION	GAIN
B1	0.2000	1000 ft	0.001	4	V	no
B2	0.2000	1000 ft	0.001	4	V	yes
B3	0.2000	1000 ft	0.001	4	H	no
B4	0.2000	1000 ft	4.000	80	V	no
B5	0.2000	5000 ft	0.001	4	V	no
B6	0.2000	5000 ft	0.001	4	V	yes
B7	0.2000	5000 ft	0.001	4	H	no
B8	0.2000	5000 ft	4.000	80	V	no
B9	0.1351	1000 ft	0.001	4	V	no
B10	0.1351	1000 ft	0.001	4	H	no
B11	0.1351	1000 ft	4.000	80	V	no
B12	0.1351	1000 ft	0.001	4	V	yes
B13	0.1351	5000 ft	0.001	4	V	no
B14	0.1351	5000 ft	0.001	4	H	no
B15	0.1351	5000 ft	4.000	80	V	no
B16	0.1351	5000 ft	0.001	4	V	yes
B17	0.0545	1000 ft	0.001	4	V	no
B18	0.0545	1000 ft	0.001	4	V	yes
B19	0.0545	5000 ft	0.001	4	V	no
B20	0.0545	5000 ft	0.001	4	V	yes

* 1000 ft = 305 m, 5000 ft = 1524 m

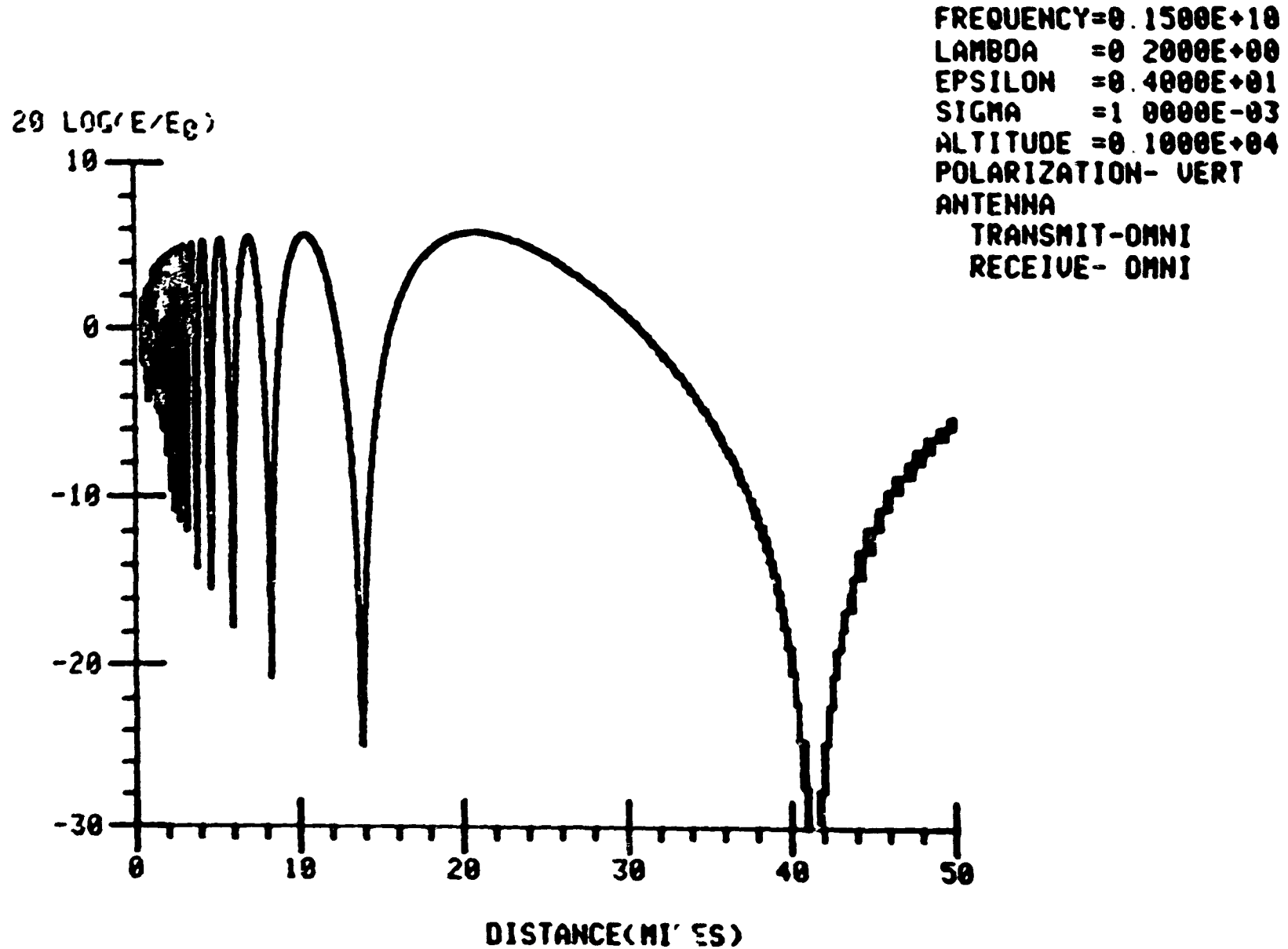
FREQUENCY=0.1500E+10
LAMBDA =0 2000E+00
EPSILON =0.4000E+01
SIGMA =1 0000E-03
ALTITUDE =0.1000E+04
POLARIZATION- VERT
ANTENNA
TRANSMIT-OMNI
RECEIVE- OMNI
20 LOG(E/Eo)
10
0
-10
-20
-30
0
10
20
30
40
50
DISTANCE(MI ES)

Figure B1

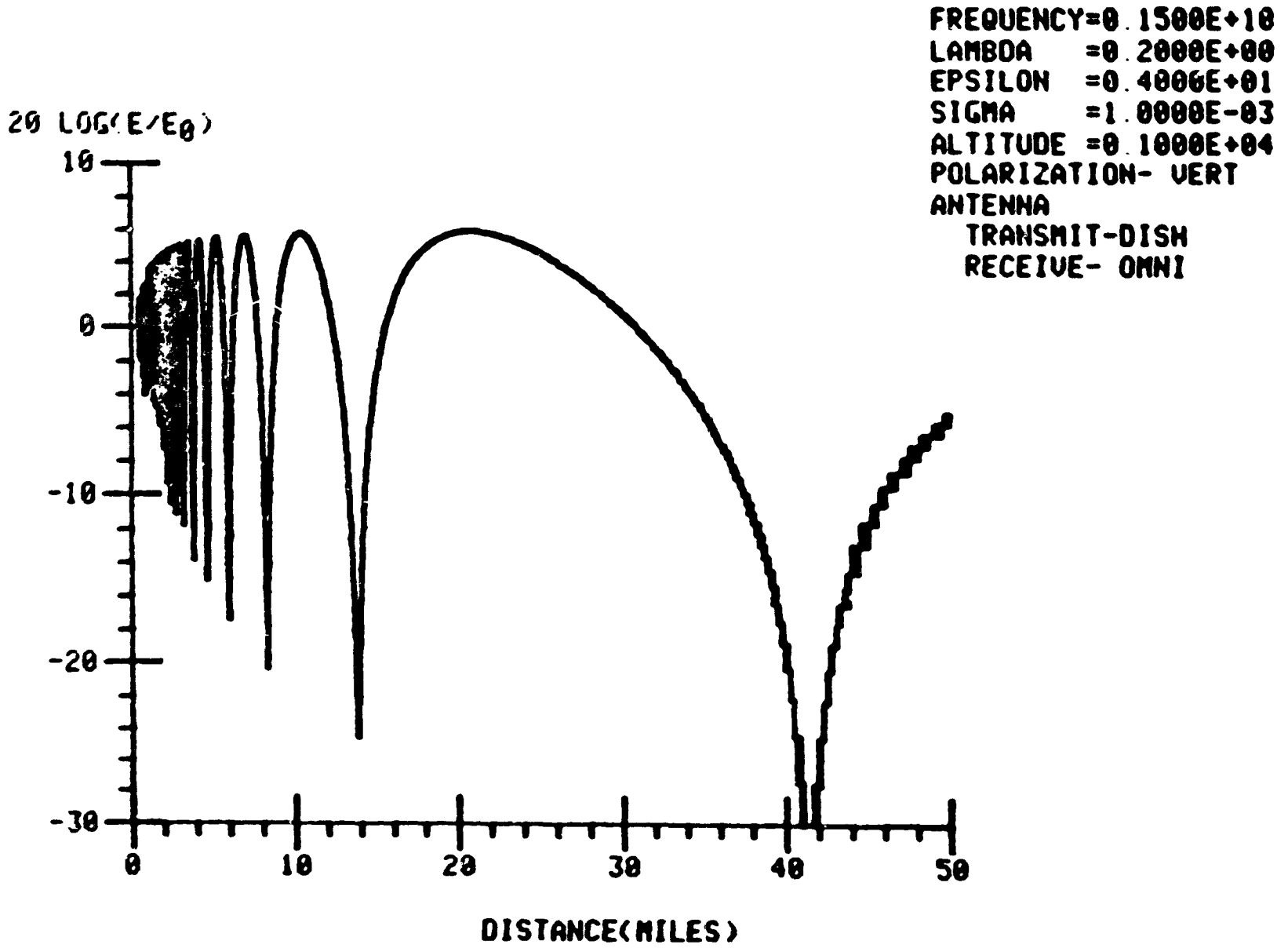
FREQUENCY=0.1500E+10
LAMBDA =0.2000E+00
EPSILON =0.4006E+01
SIGMA =1.0000E-03
ALTITUDE =0.1000E+04
POLARIZATION- VERT
ANTENNA
TRANSMIT-DISH
RECEIVE- OMNI
20 LOG(E/E0)
10
0
-10
-20
-30
0
10
20
30
40
50
DISTANCE(MILES)

Figure B2

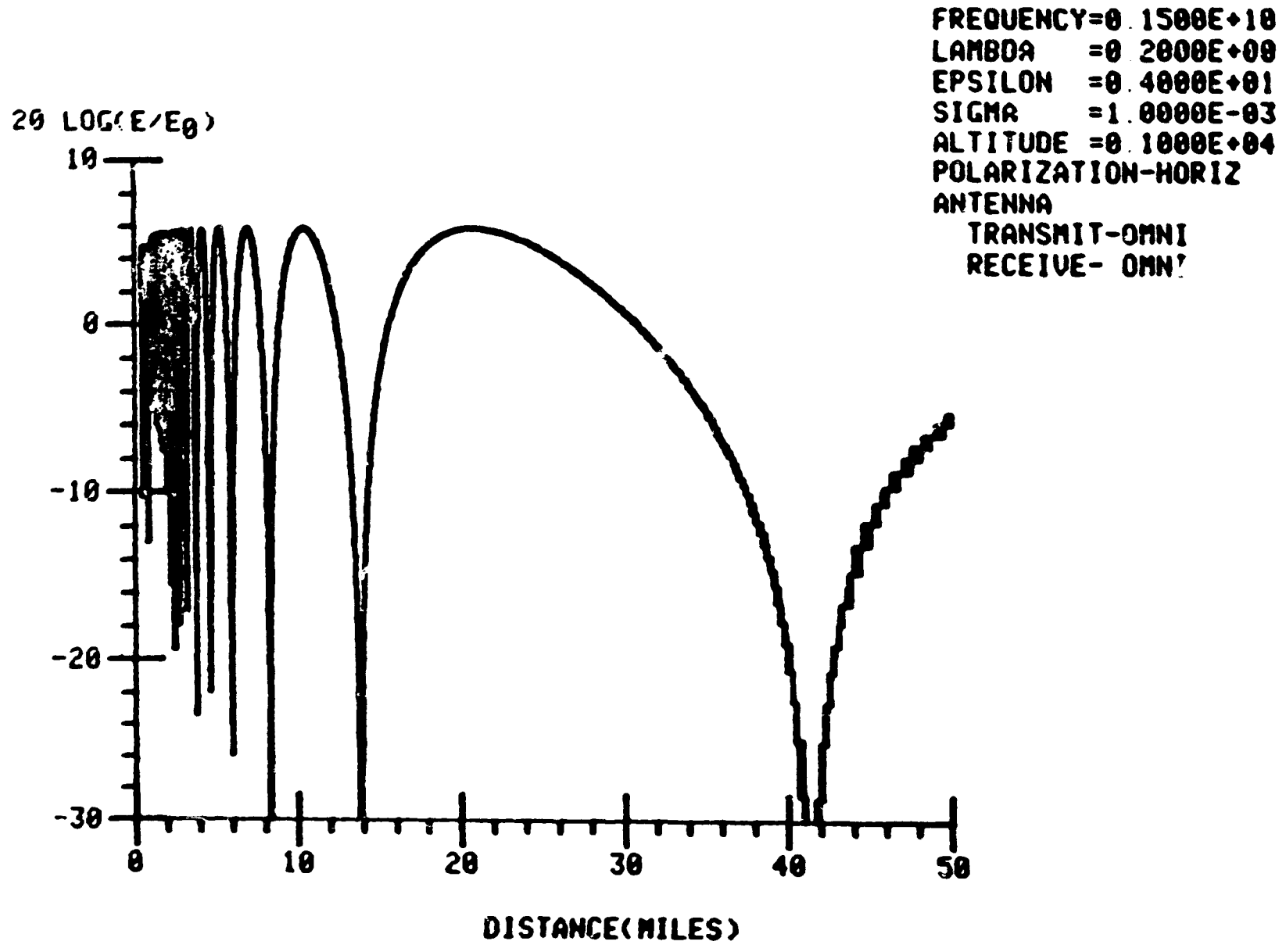
FREQUENCY=0.1500E+10
LAMBDA =0.2000E+00
EPSILON =0.4000E+01
SIGMA =1.0000E-03
ALTITUDE =0.1000E+04
POLARIZATION-HORIZ
ANTENNA
TRANSMIT-OMNI
RECEIVE- OMNI
20 LOG(E/E0)
10
0
-10
-20
-30
0
10
20
30
40
50
DISTANCE(MILES)

Figure B3

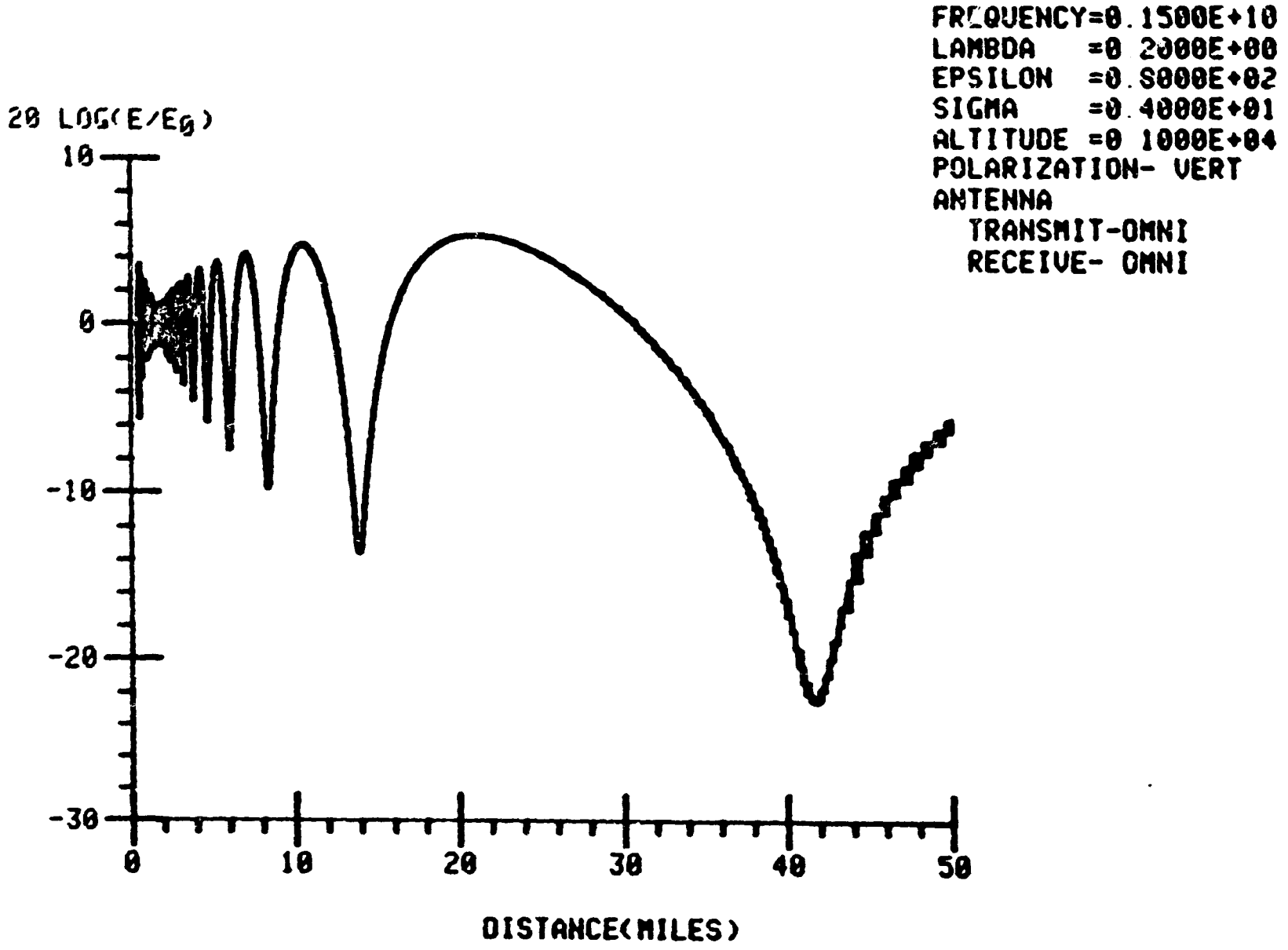
FREQUENCY=0.1500E+10
LAMBDA =0 2000E+00
EPSILON =0.5000E+02
SIGMA =0.4000E+01
ALTITUDE =0 1000E+04
POLARIZATION- VERT
ANTENNA
TRANSMIT-OMNI
RECEIVE- OMNI
20 LOG(E/E0)
10
0
-10
-20
-30
0
10
20
30
40
50
DISTANCE(MILES)

Figure B4

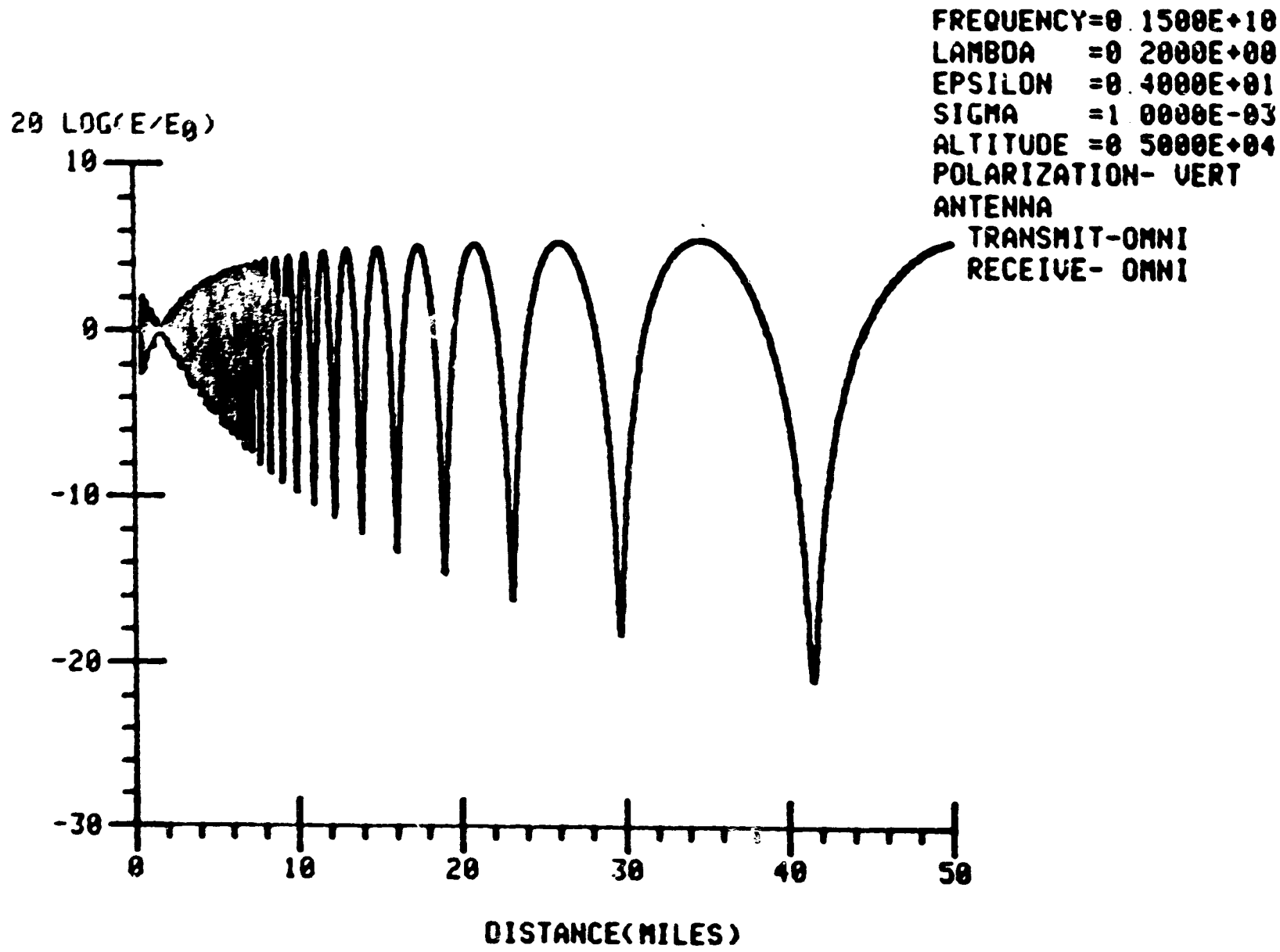
FREQUENCY=0 1500E+10
LAMBDA =0 2000E+00
EPSILON =0 4000E+01
SIGMA =1 0000E-03
ALTITUDE =0 5000E+04
POLARIZATION- VERT
ANTENNA
TRANSMIT-OMNI
RECEIVE- OMNI
20 LOG(E/E0)
10
0
-10
-20
-30
0
10
20
30
40
50
DISTANCE(MILES)

Figure B5

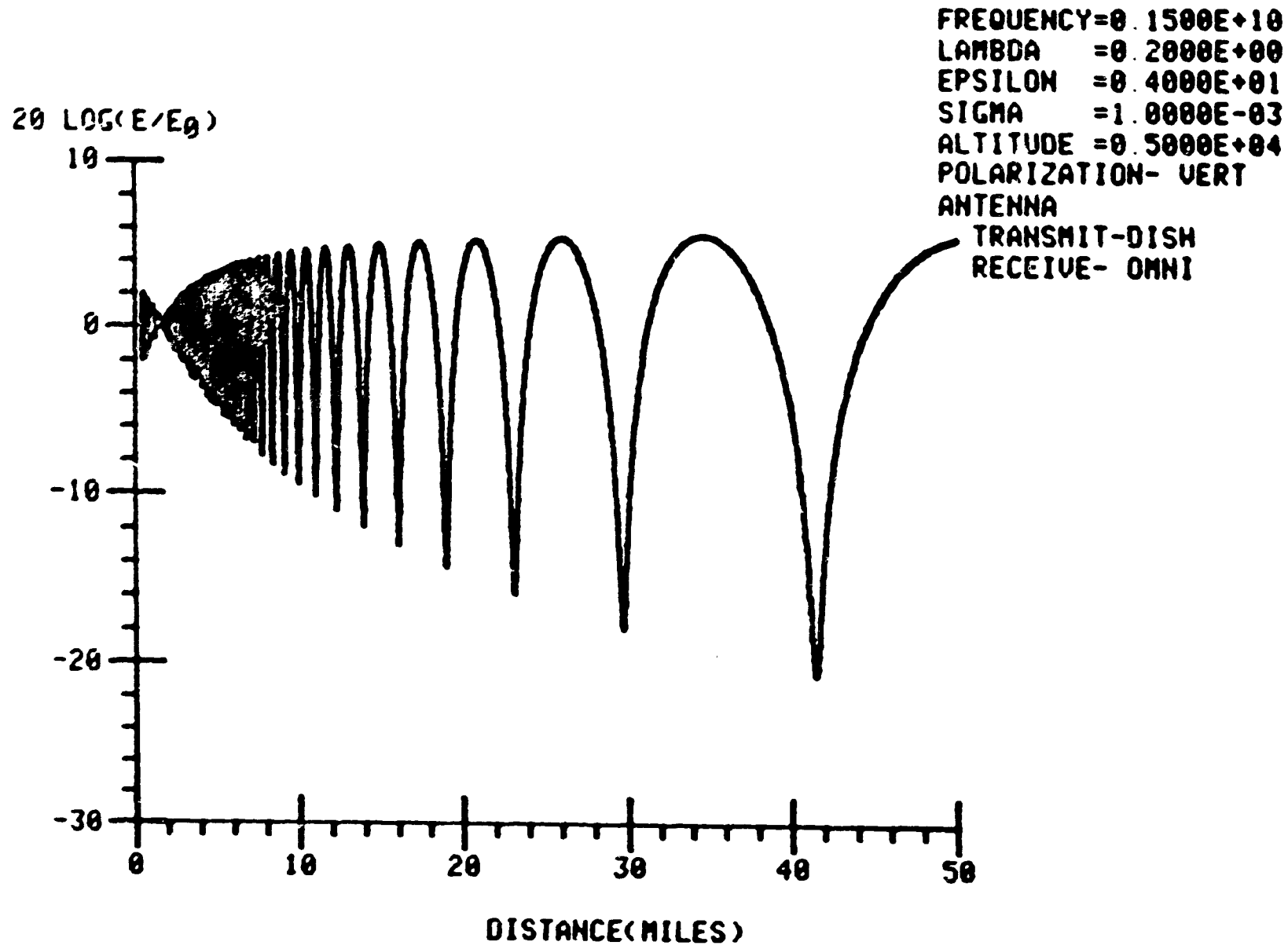
FREQUENCY=0.1500E+10
LAMBDA =0.2000E+00
EPSILON =0.4000E+01
SIGMA =1.0000E-03
ALTITUDE =0.5000E+04
POLARIZATION- VERT
ANTENNA
TRANSMIT-DISH
RECEIVE- OMNI
20 LOG(E/E0)
10
0
-10
-20
-30
0
10
20
30
40
50
DISTANCE(MILES)

Figure B6.

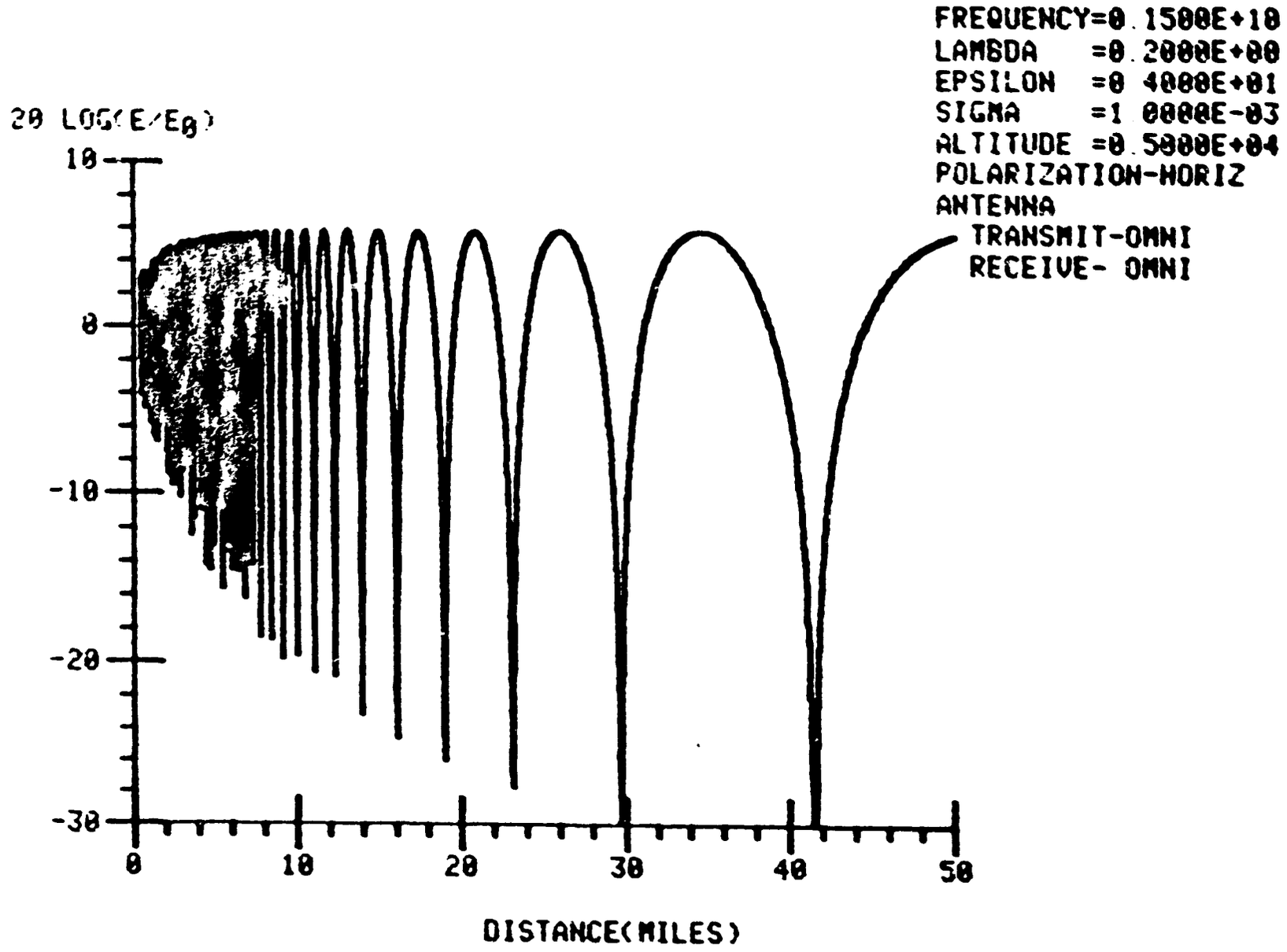
FREQUENCY=0.1500E+10
LAMBDA =0.2000E+00
EPSILON =0.4000E+01
SIGMA =1.0000E-03
ALTITUDE =0.5000E+04
POLARIZATION-HORIZ
ANTENNA
TRANSMIT-OMNI
RECEIVE- OMNI
20 LOG(E/E0)
10
0
-10
-20
-30
0
10
20
30
40
50
DISTANCE(MILES)

Figure B7

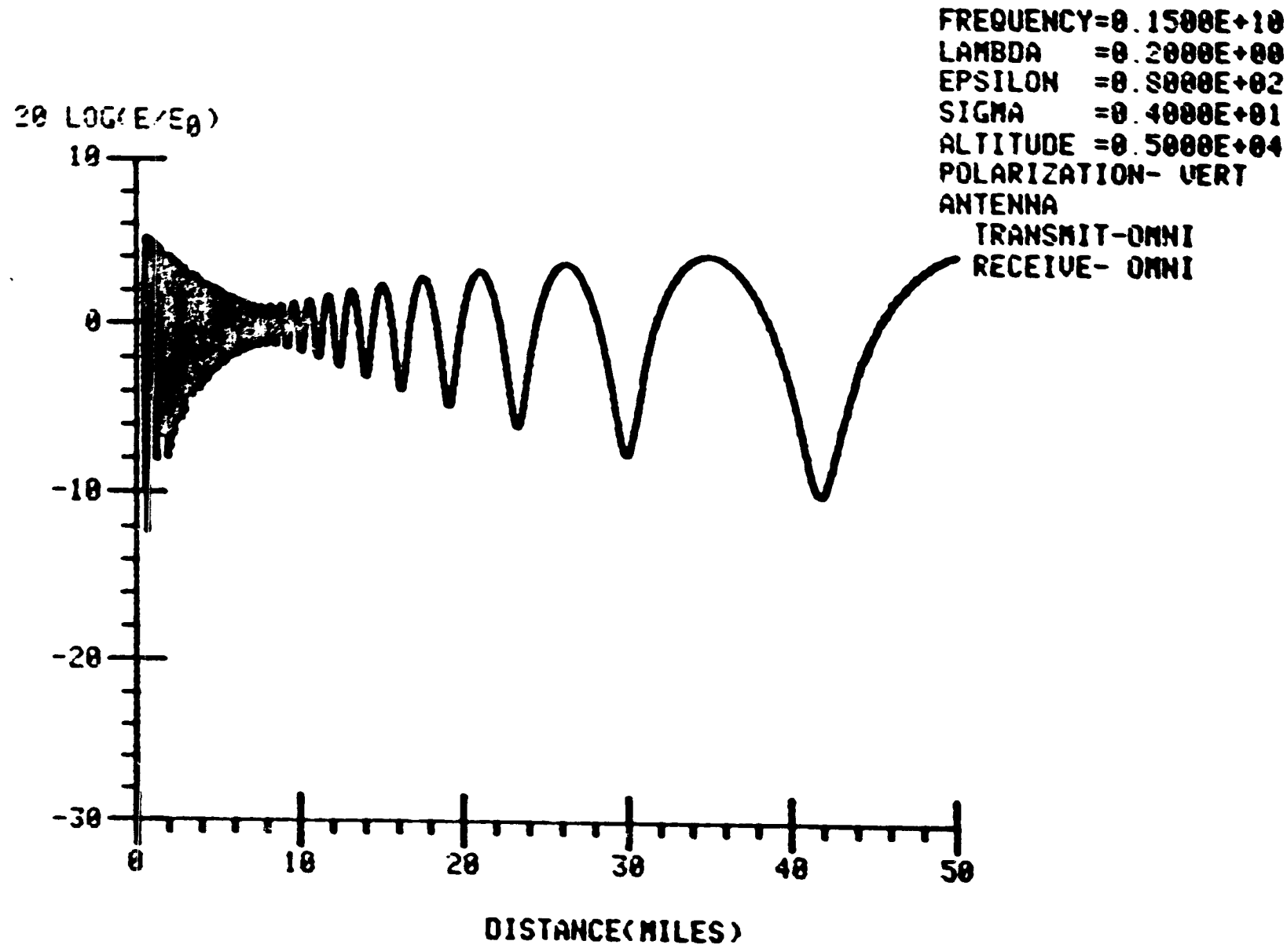
FREQUENCY=0.1500E+10
LAMBDA =0.2000E+00
EPSILON =0.5000E+02
SIGMA =0.4000E+01
ALTITUDE =0.5000E+04
POLARIZATION- VERT
ANTENNA
TRANSMIT-OMNI
RECEIVE- OMNI
20 LOG(E/E0)
10
0
-10
-20
-30
0
10
20
30
40
50
DISTANCE(MILES)

Figure B8

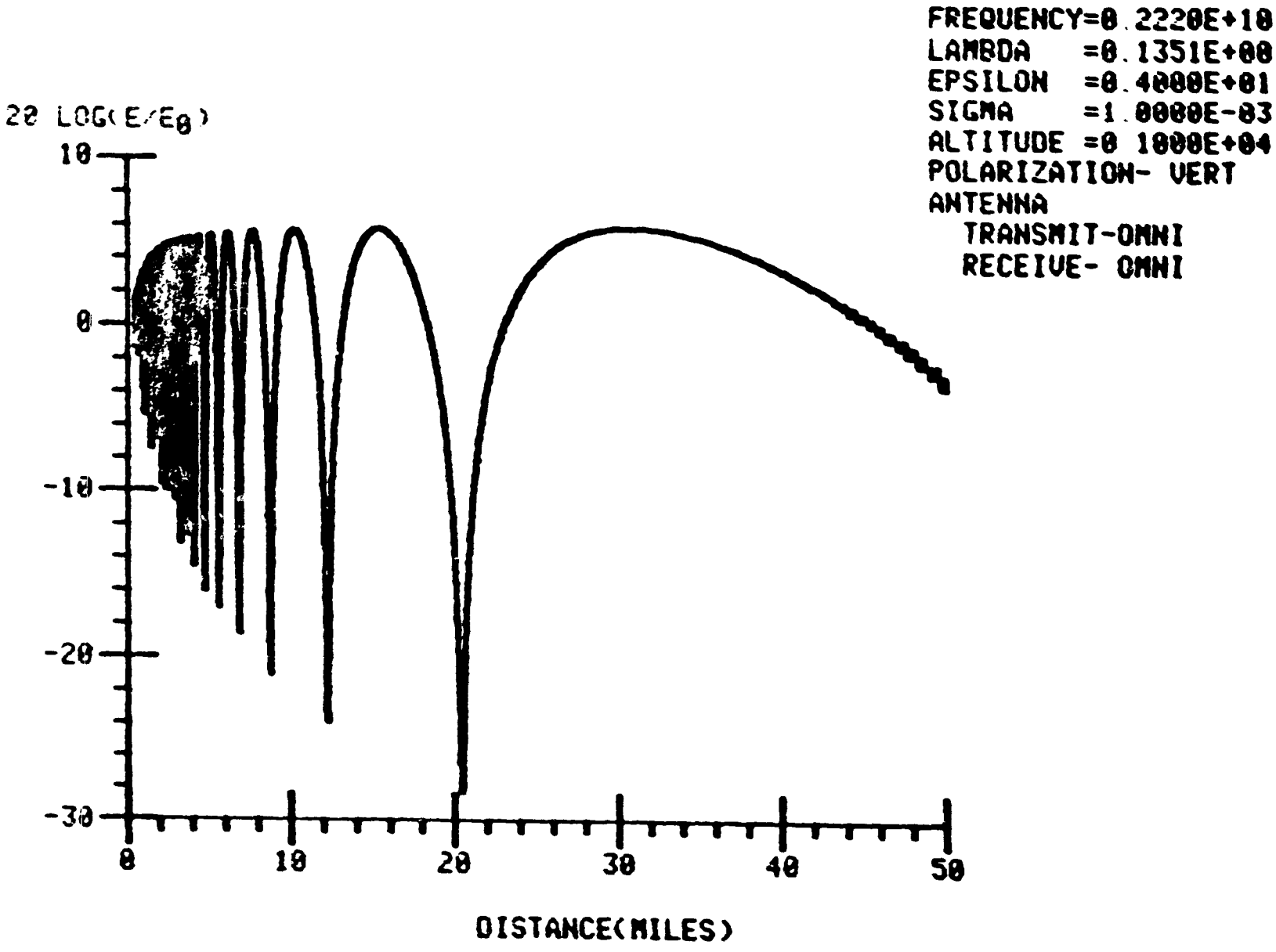
FREQUENCY=0.2220E+10
LAMBDA =0.1351E+00
EPSILON =0.4000E+01
SIGMA =1.0000E-03
ALTITUDE =0.1000E+04
POLARIZATION- VERT
ANTENNA
TRANSMIT-OMNI
RECEIVE- OMNI
20 LOG(E/E0)
10
0
-10
-20
-30
0
10
20
30
40
50
DISTANCE(MILES)

Figure B9

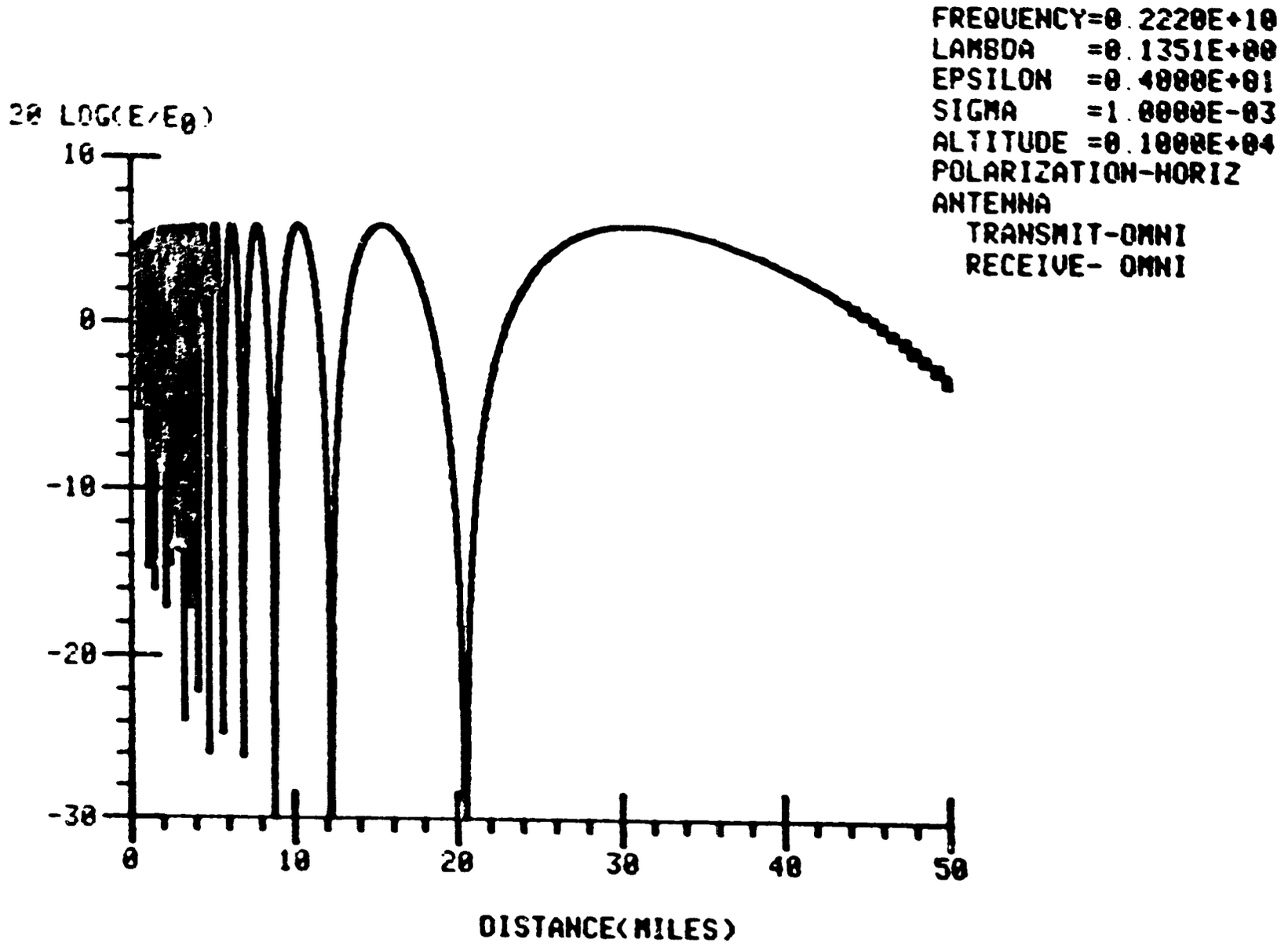
FREQUENCY=0.2220E+10
LAMBDA =0.1351E+00
EPSILON =0.4000E+01
SIGMA =1.0000E-03
ALTITUDE =0.1000E+04
POLARIZATION-HORIZ
ANTENNA
TRANSMIT-OMNI
RECEIVE- OMNI
20 LOG(E/E0)
10
0
-10
-20
-30
0
10
20
30
40
50
DISTANCE(MILES)

Figure B10

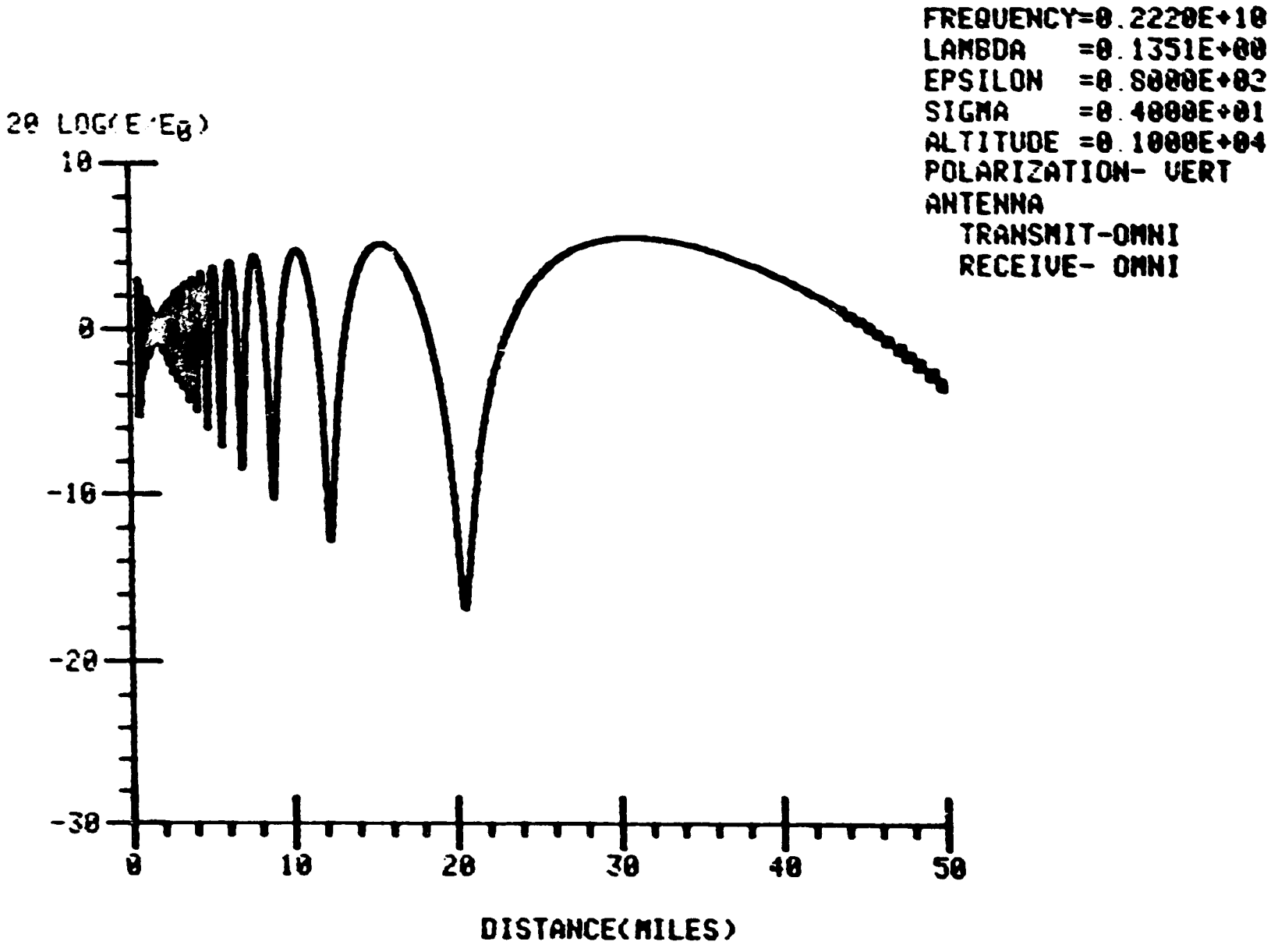
FREQUENCY=0.2220E+10
LAMBDA =0.1351E+00
EPSILON =0.8000E+02
SIGMA =0.4000E+01
ALTITUDE =0.1000E+04
POLARIZATION- VERT
ANTENNA
TRANSMIT-OMNI
RECEIVE- OMNI
20 LOG(E/E0)
10
0
-10
-20
-30
0
10
20
30
40
50
DISTANCE(MILES)

Figure B11

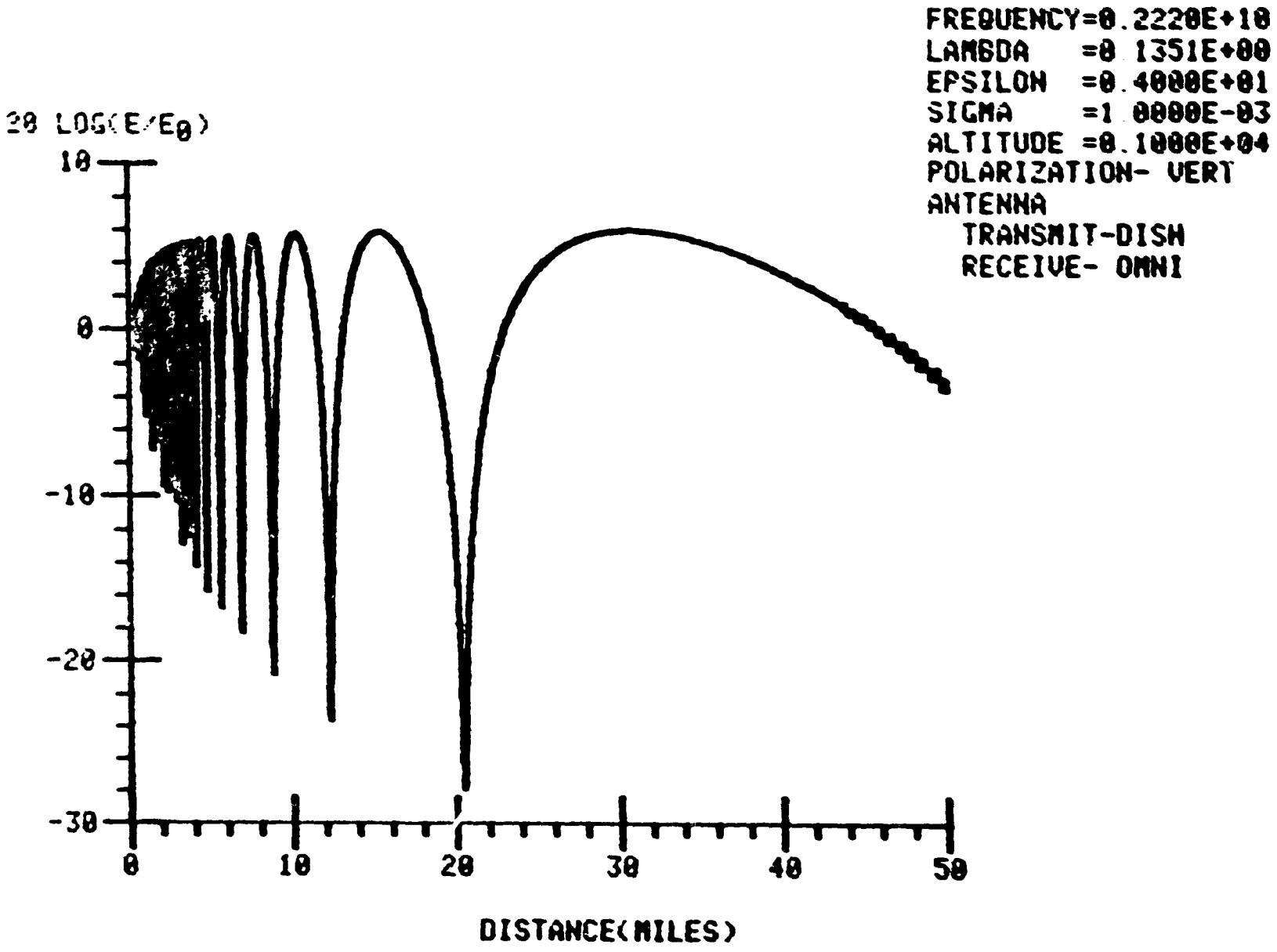
FREQUENCY=0.2220E+10
LAMBDA =0.1351E+00
EPSILON =0.4000E+01
SIGMA =1.0000E-03
ALTITUDE =0.1000E+04
POLARIZATION- VERT
ANTENNA
TRANSMIT-DISH
RECEIVE- OMNI
20 LOG(E/E0)
10
0
-10
-20
-30
0
10
20
30
40
50
DISTANCE(MILES)

Figure B12

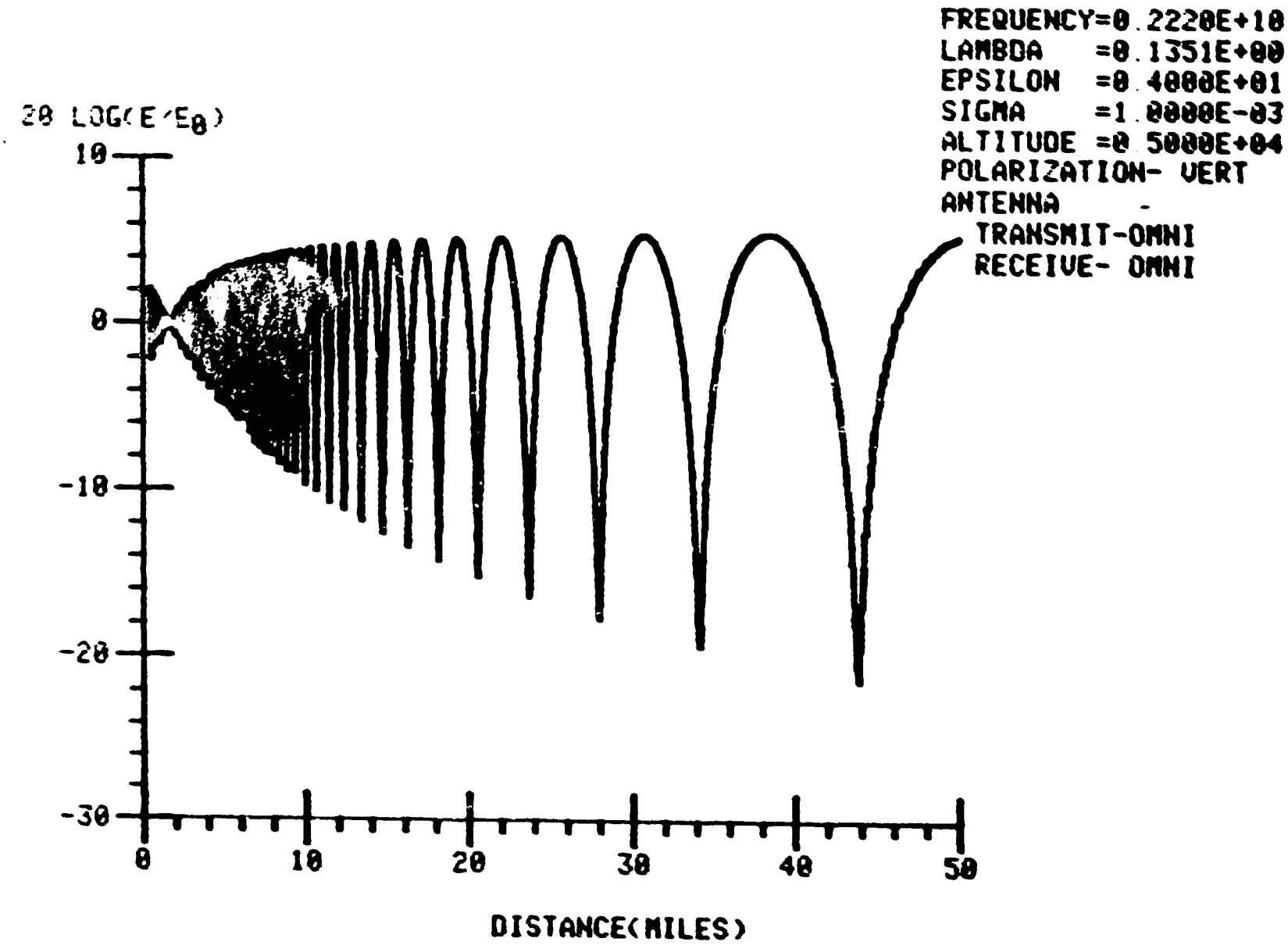
FREQUENCY=0.2220E+10
LAMBDA =0.1351E+00
EPSILON =0.4000E+01
SIGMA =1.0000E-03
ALTITUDE =0.5000E+04
POLARIZATION- VERT
ANTENNA -
TRANSMIT-OMNI
RECEIVE- OMNI
20 LOG(E/E0)
10
0
-10
-20
-30
0
10
20
30
40
50
DISTANCE(MILES)

Figure B13

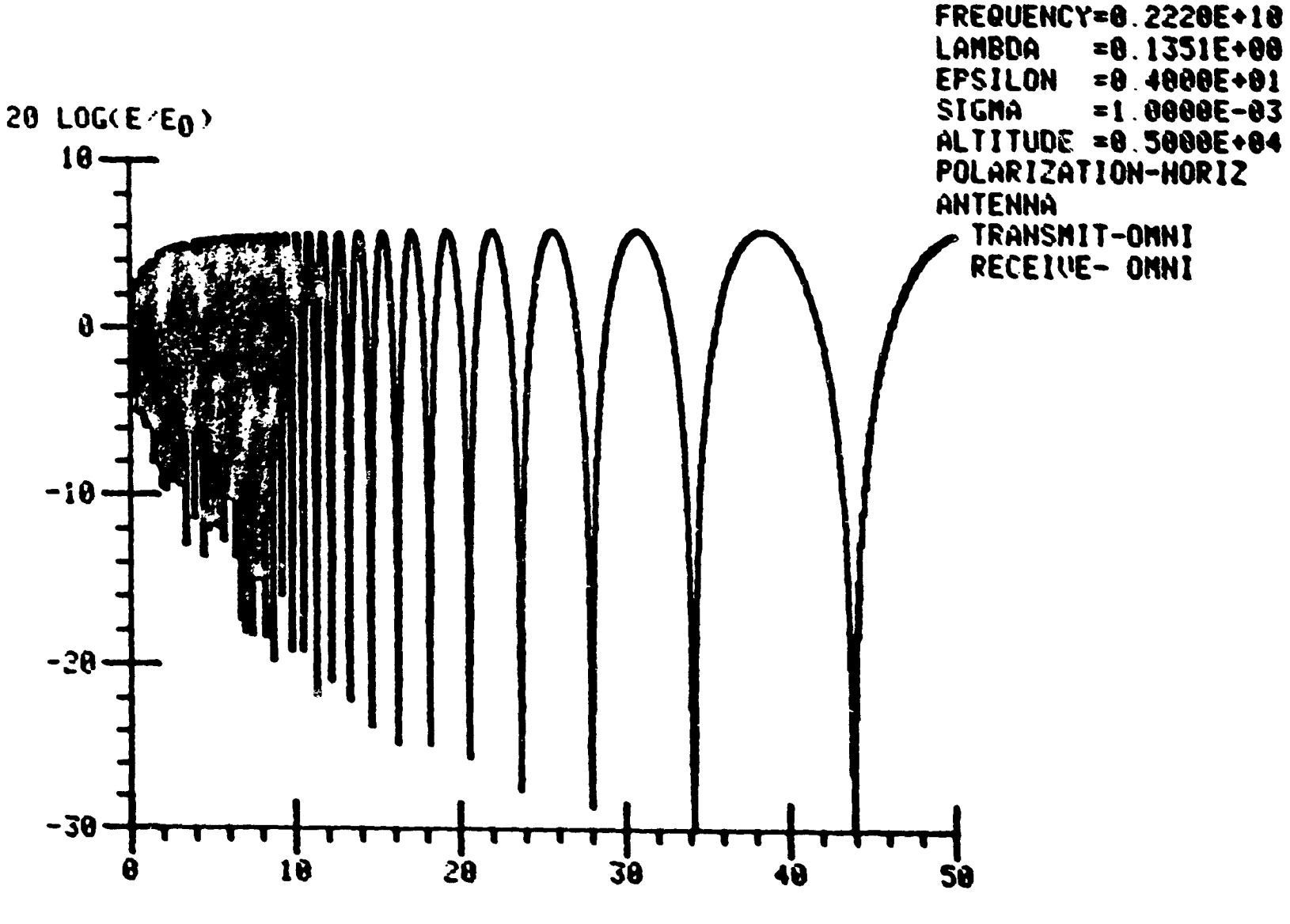
FREQUENCY=0.2220E+10
LAMBDA =0.1351E+00
EPSILON =0.4000E+01
SIGMA =1.0000E-03
ALTITUDE =0.5000E+04
POLARIZATION-HORIZ
ANTENNA
TRANSMIT-OMNI
RECEIVE- OMNI
20 LOG(E/E0)
10
0
-10
-20
-30
0
10
20
30
40
50
DISTANCE(MILES)

Figure B14

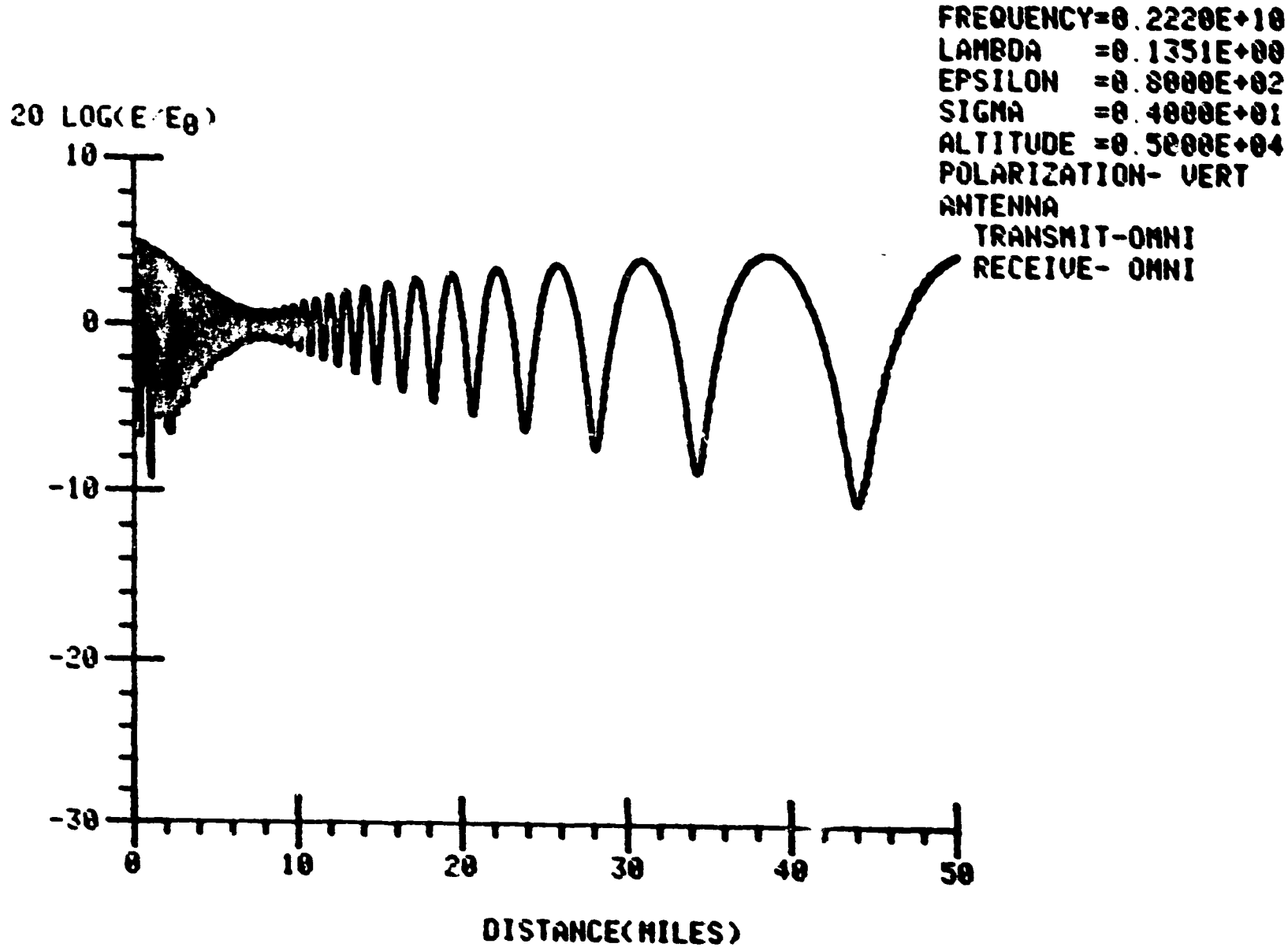
FREQUENCY=0.2220E+10
LAMBDA =0.1351E+00
EPSILON =0.8000E+02
SIGMA =0.4000E+01
ALTITUDE =0.5000E+04
POLARIZATION- VERT
ANTENNA
TRANSMIT-OMNI
RECEIVE- OMNI
20 LOG(E/E0)
10
0
-10
-20
-30
0
10
20
30
40
50
DISTANCE(MILES)

Figure B15

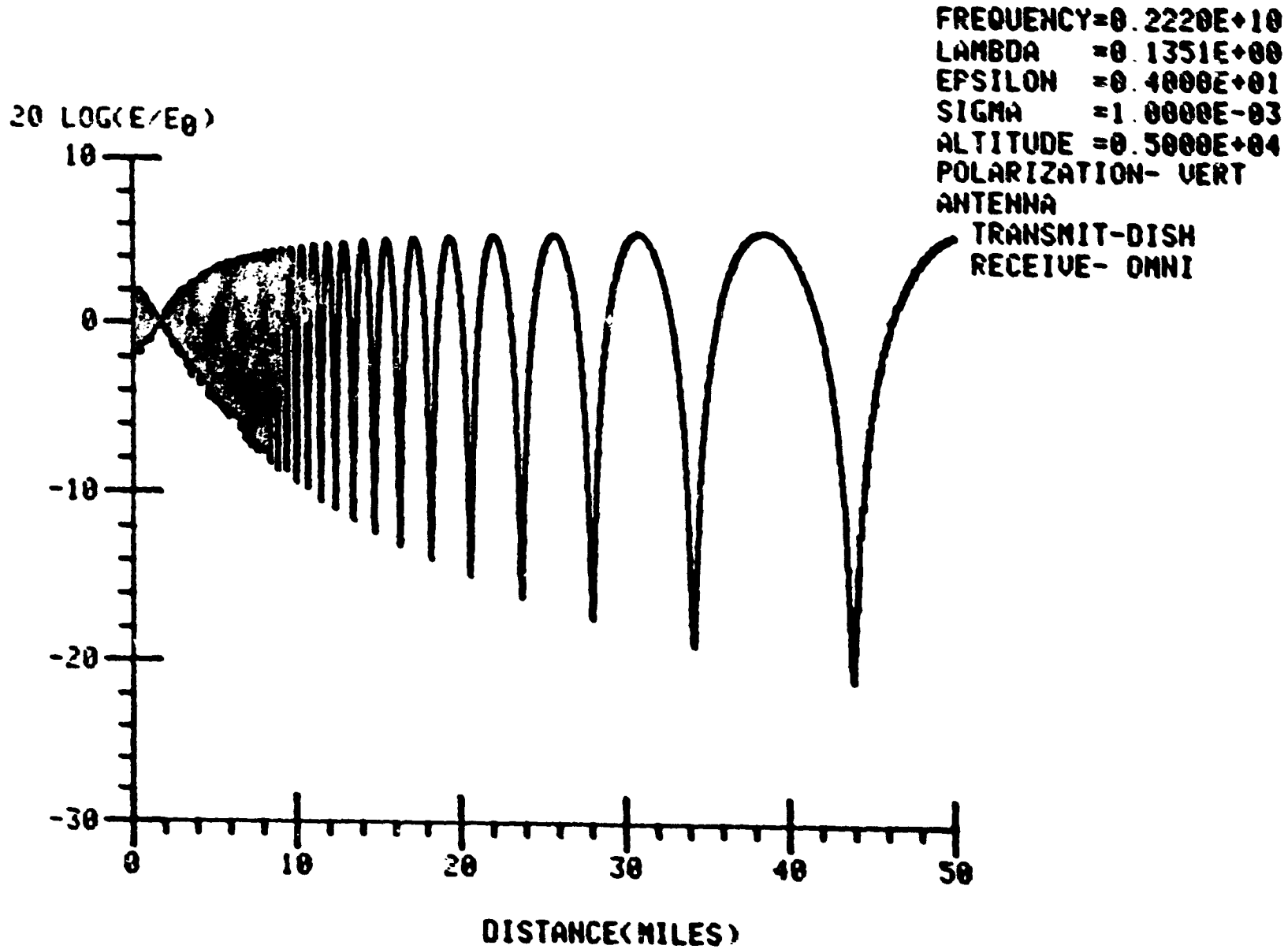
FREQUENCY=0.2220E+10
LAMBDA =0.1351E+00
EPSILON =0.4000E+01
SIGMA =1.0000E-03
ALTITUDE =0.5000E+04
POLARIZATION- VERT
ANTENNA
TRANSMIT-DISH
RECEIVE- OMNI
20 LOG(E/E0)
10
0
-10
-20
-30
0
10
20
30
40
50
DISTANCE(MILES)

Figure B16

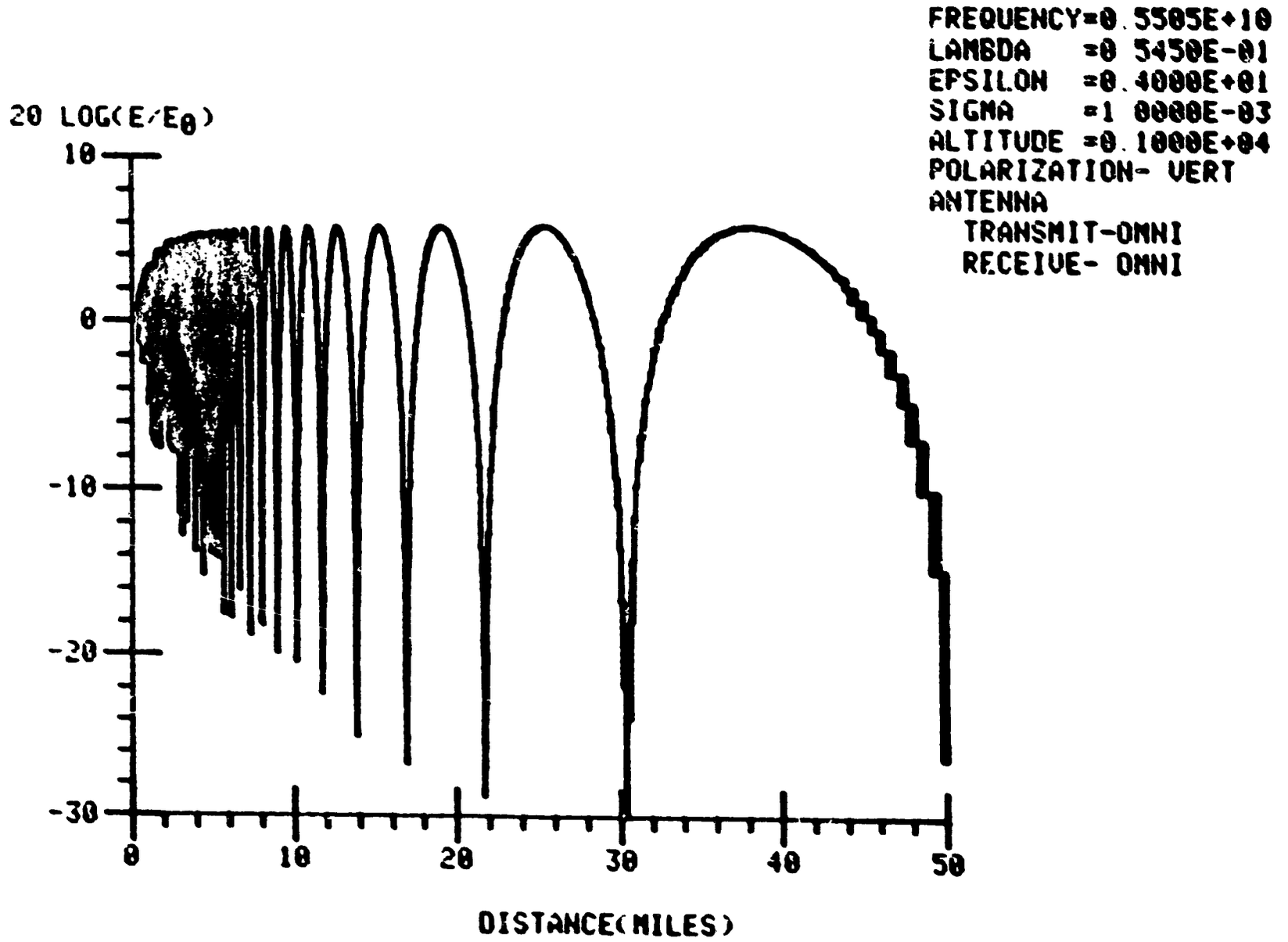
FREQUENCY=0.5505E+10
LAMBDA =0.5450E-01
EPSILON =0.4000E+01
SIGMA =1.0000E-03
ALTITUDE =0.1000E+04
POLARIZATION- VERT
ANTENNA
TRANSMIT-OMNI
RECEIVE- OMNI
20 LOG(E/E0)
10
0
-10
-20
-30
0
10
20
30
40
50
DISTANCE(MILES)

Figure B17

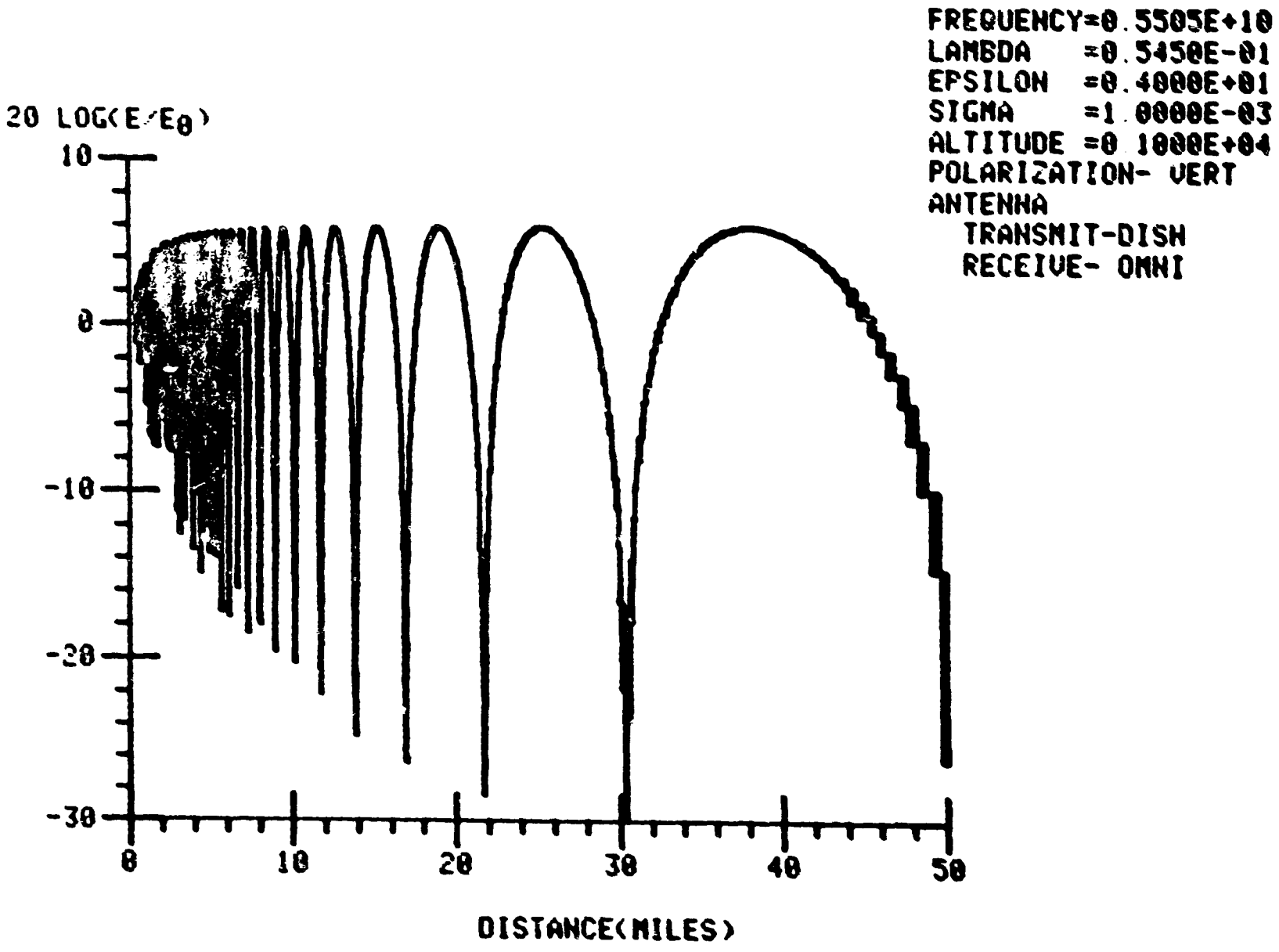
FREQUENCY=0.5505E+10
LAMBDA =0.5450E-01
EPSILON =0.4000E+01
SIGMA =1.0000E-03
ALTITUDE =0.1000E+04
POLARIZATION- VERT
ANTENNA
TRANSMIT-DISH
RECEIVE- OMNI
20 LOG(E/E0)
10
0
-10
-20
-30
0
10
20
30
40
50
DISTANCE(MILES)

Figure B18

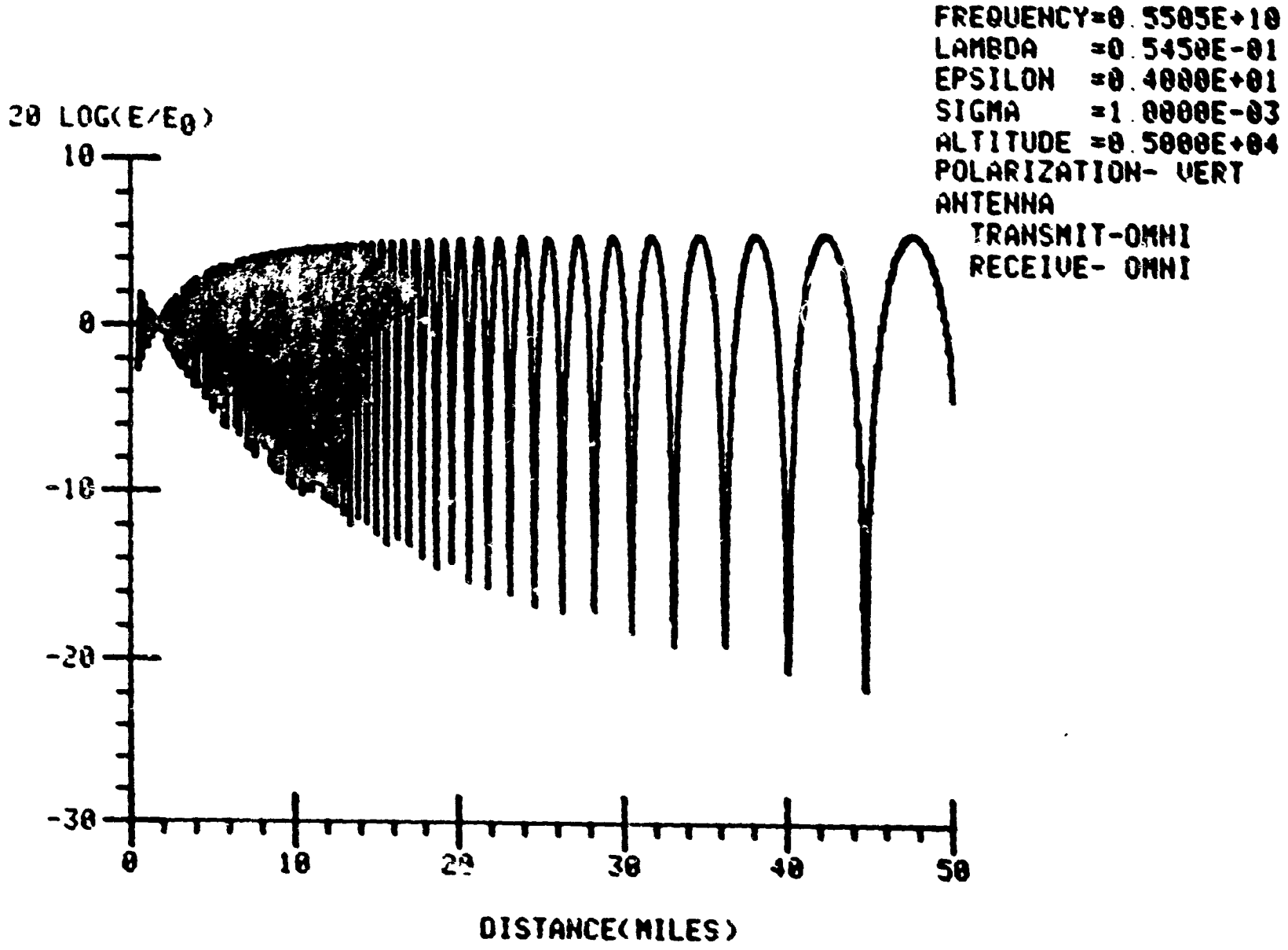
FREQUENCY=0.5505E+10
LAMBDA =0.5450E-01
EPSILON =0.4000E+01
SIGMA =1.0000E-03
ALTITUDE =0.5000E+04
POLARIZATION- VERT
ANTENNA
TRANSMIT-OMNI
RECEIVE- OMNI
20 LOG(E/E0)
10
0
-10
-20
-30
0
10
20
30
40
50
DISTANCE(MILES)

Figure B19

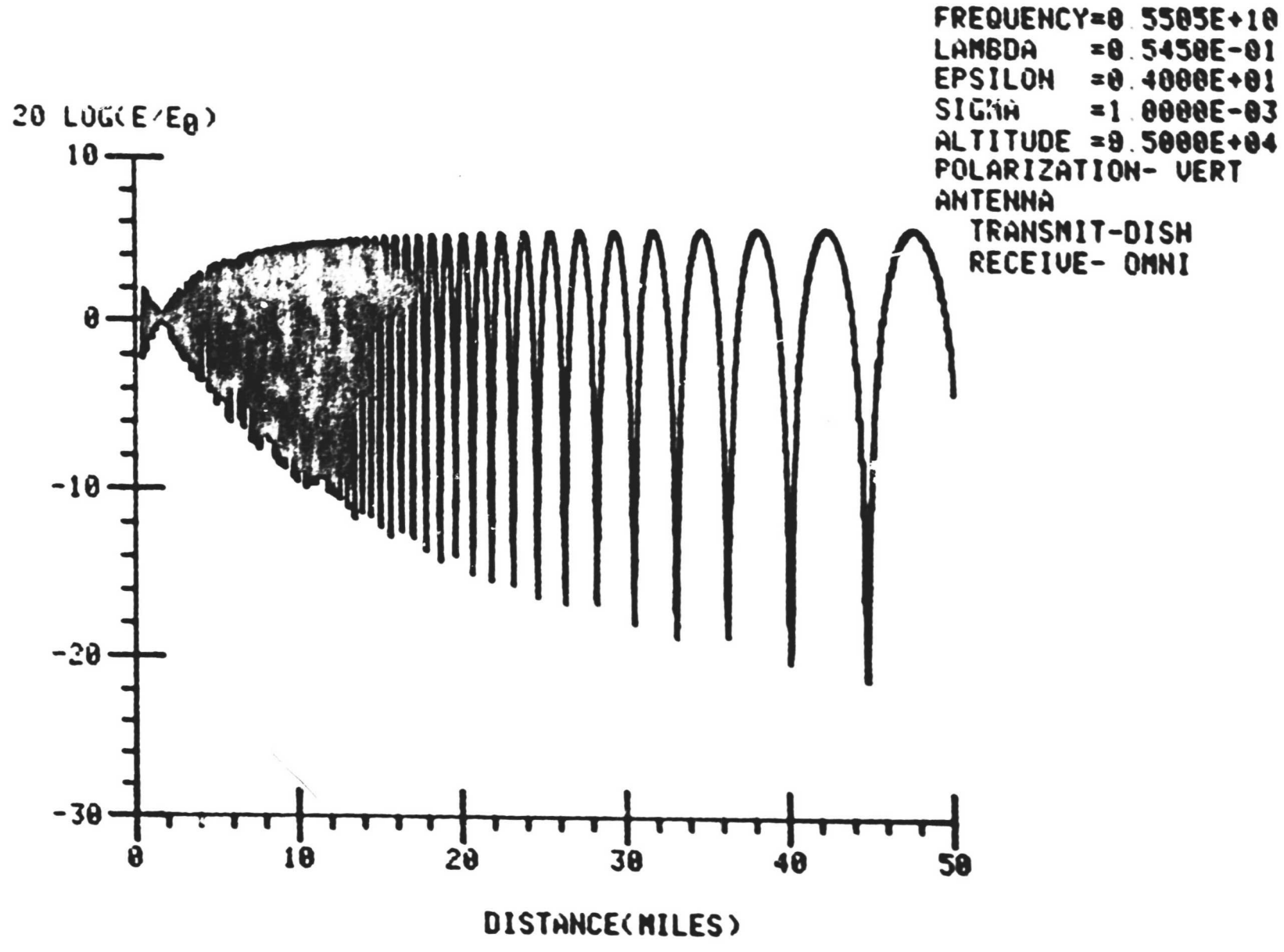
FREQUENCY=0.5505E+10
LAMBDA =0.5450E-01
EPSILON =0.4000E+01
SIGMA =1.0000E-03
ALTITUDE =0.5000E+04
POLARIZATION- VERT
ANTENNA
TRANSMIT-DISH
RECEIVE- OMNI
20 LOG(E/E0)
10
0
-10
-20
-30
0
10
20
30
40
50
DISTANCE(MILES)

Figure B20

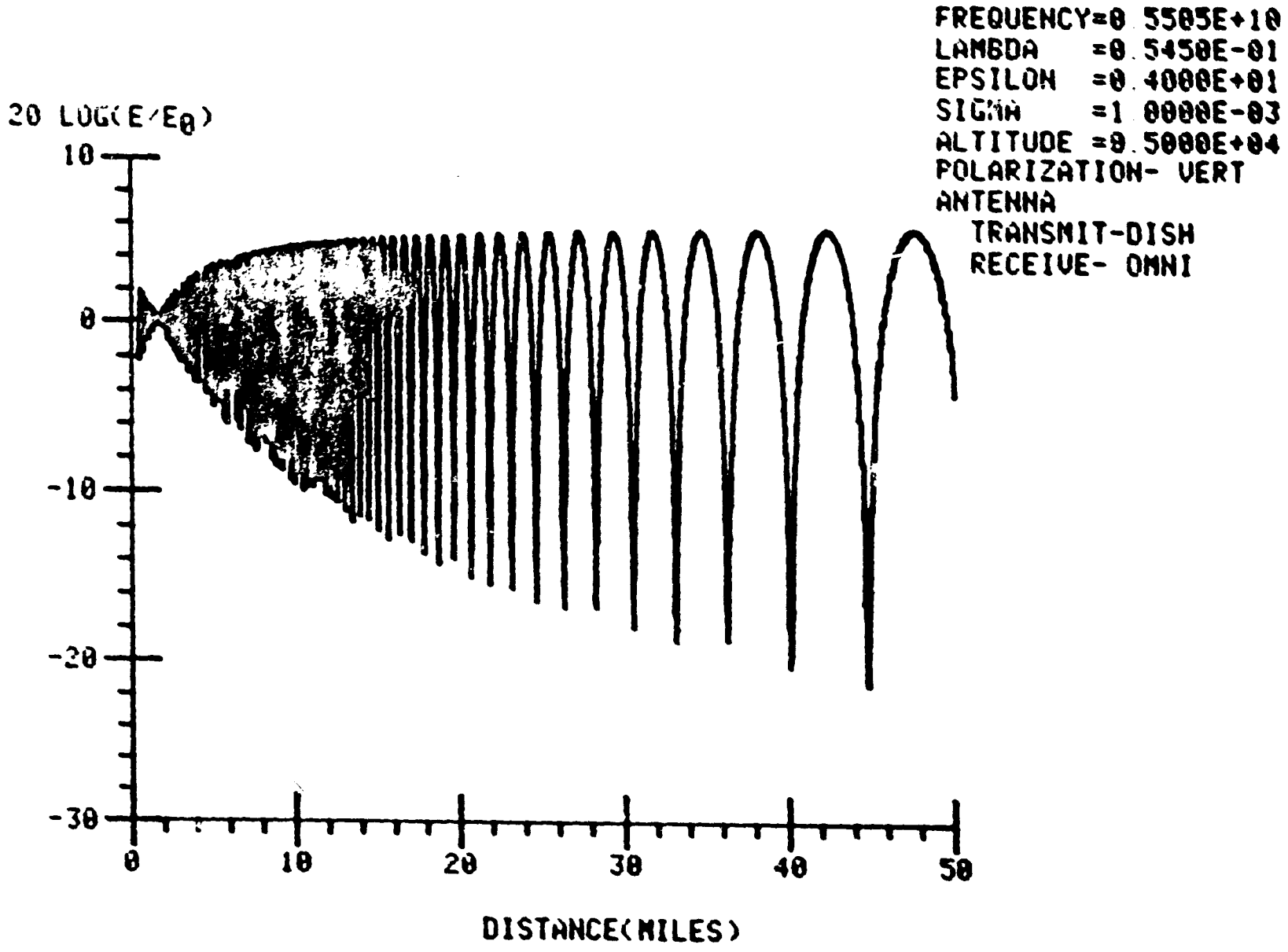
FREQUENCY=0.5505E+10
LAMBDA =0.5450E-01
EPSILON =0.4000E+01
SIGMA =1.0000E-03
ALTITUDE =0.5000E+04
POLARIZATION- VERT
ANTENNA
TRANSMIT-DISH
RECEIVE- OMNI
20 LOG(E/E0)
10
0
-10
-20
-30
0
10
20
30
40
50
DISTANCE(MILES)

Figure B20

APPENDIX C

SAMPLE SIGNALS FOR BOTH VERTICAL AND HORIZONTAL POLARIZATIONS IN THE 3 TO 19 KM RANGE

APPENDIX C

SAMPLE SIGNALS FOR BOTH VERTICAL AND HORIZONTAL POLARIZATIONS IN THE 3 TO 19 KM RANGE

TABLE C

3 - 19 km Range

FIGURE	LAMBDA	ALTITUDE*	SIGMA	EPSILON	POLARIZATION	GAIN
C1	0.2000	1000 ft	0.001	4	V	no
C2	0.2000	1000 ft	0.001	4	H	no
C3	0.2000	1000 ft	0.001	4	V	yes
C4	0.2000	1000 ft	0.001	4	H	yes
C5	0.2000	1000 ft	4.000	80	V	no
C6	0.2000	1000 ft	4.000	80	H	no
C7	0.2000	1000 ft	4.000	80	V	yes
C8	0.2000	1000 ft	4.000	80	H	yes
C9	0.2000	5000 ft	0.001	4	V	no
C10	0.2000	5000 ft	0.001	4	H	no
C11	0.2000	5000 ft	0.001	4	V	yes
C12	0.2000	5000 ft	0.001	4	H	yes
C13	0.2000	5000 ft	4.000	80	V	no
C14	0.2000	5000 ft	4.000	80	H	no
C15	0.2000	5000 ft	4.000	80	V	yes
C16	0.2000	5000 ft	4.000	80	H	yes
C17	0.1351	1000 ft	0.001	4	V	no
C18	0.1351	1000 ft	0.001	4	H	no
C19	0.1351	1000 ft	0.001	4	V	yes
C20	0.1351	1000 ft	0.001	4	H	yes
C21	0.1351	1000 ft	4.000	80	V	no
C22	0.1351	1000 ft	4.000	80	H	no
C23	0.1351	1000 ft	4.000	80	V	yes
C24	0.1351	1000 ft	4.000	80	H	yes
C25	0.1351	5000 ft	0.001	4	V	no
C26	0.1351	5000 ft	0.001	4	H	no
C27	0.1351	5000 ft	0.001	4	V	yes
C28	0.1351	5000 ft	0.001	4	H	yes
C29	0.1351	5000 ft	4.000	80	V	no

* 1000 ft = 305 m, 5000 ft = 1524 m

TABLE C

3 - 19 km Range

FIGURE	LAMBDA	ALTITUDE*	SIGMA	EPSILON	POLARIZATION	GAIN
C1	0.2000	1000 ft	0.001	4	V	no
C2	0.2000	1000 ft	0.001	4	H	no
C3	0.2000	1000 ft	0.001	4	V	yes
C4	0.2000	1000 ft	0.001	4	H	yes
C5	0.2000	1000 ft	4.000	80	V	no
C6	0.2000	1000 ft	4.000	80	H	no
C7	0.2000	1000 ft	4.000	80	V	yes
C8	0.2000	1000 ft	4.000	80	H	yes
C9	0.2000	5000 ft	0.001	4	V	no
C10	0.2000	5000 ft	0.001	4	H	no
C11	0.2000	5000 ft	0.001	4	V	yes
C12	0.2000	5000 ft	0.001	4	H	yes
C13	0.2000	5000 ft	4.000	80	V	no
C14	0.2000	5000 ft	4.000	80	H	no
C15	0.2000	5000 ft	4.000	80	V	yes
C16	0.2000	5000 ft	4.000	80	H	yes
C17	0.1351	1000 ft	0.001	4	V	no
C18	0.1351	1000 ft	0.001	4	H	no
C19	0.1351	1000 ft	0.001	4	V	yes
C20	0.1351	1000 ft	0.001	4	H	yes
C21	0.1351	1000 ft	4.000	80	V	no
C22	0.1351	1000 ft	4.000	80	H	no
C23	0.1351	1000 ft	4.000	80	V	yes
C24	0.1351	1000 ft	4.000	80	H	yes
C25	0.1351	5000 ft	0.001	4	V	no
C26	0.1351	5000 ft	0.001	4	H	no
C27	0.1351	5000 ft	0.001	4	V	yes
C28	0.1351	5000 ft	0.001	4	H	yes
C29	0.1351	5000 ft	4.000	80	V	no

* 1000 ft = 305 m, 5000 ft = 1524 m

FIGURE	LAMBDA	ALTITUDE*	SIGMA	EPSILON	POLARIZATION	GAIN
C30	0.1351	5000 ft	4.000	80	H	no
C31	0.1351	5000 ft	4.000	80	V	yes
C32	0.1351	5000 ft	4.000	80	H	yes
C33	0.0545	1000 ft	0.001	4	V	no
C34	0.0545	1000 ft	0.001	4	H	no
C35	0.0545	1000 ft	0.001	4	V	yes
C36	0.0545	1000 ft	0.001	4	H	yes
C37	0.0545	1000 ft	4.000	80	V	no
C38	0.0545	1000 ft	4.000	80	H	no
C39	0.0545	1000 ft	4.000	80	V	yes
C40	0.0545	1000 ft	4.000	80	H	yes
C41	0.0545	5000 ft	0.001	4	V	no
C42	0.0545	5000 ft	0.001	4	H	no
C43	0.0545	5000 ft	0.001	4	V	yes
C44	0.0545	5000 ft	0.001	4	H	yes
C45	0.0545	5000 ft	4.000	80	V	no
C46	0.0545	5000 ft	4.000	80	H	no
C47	0.0545	5000 ft	4.000	80	V	yes
C48	0.0545	5000 ft	4.000	80	H	yes

* 1000 ft = 305 m, 5000 ft = 1524 m

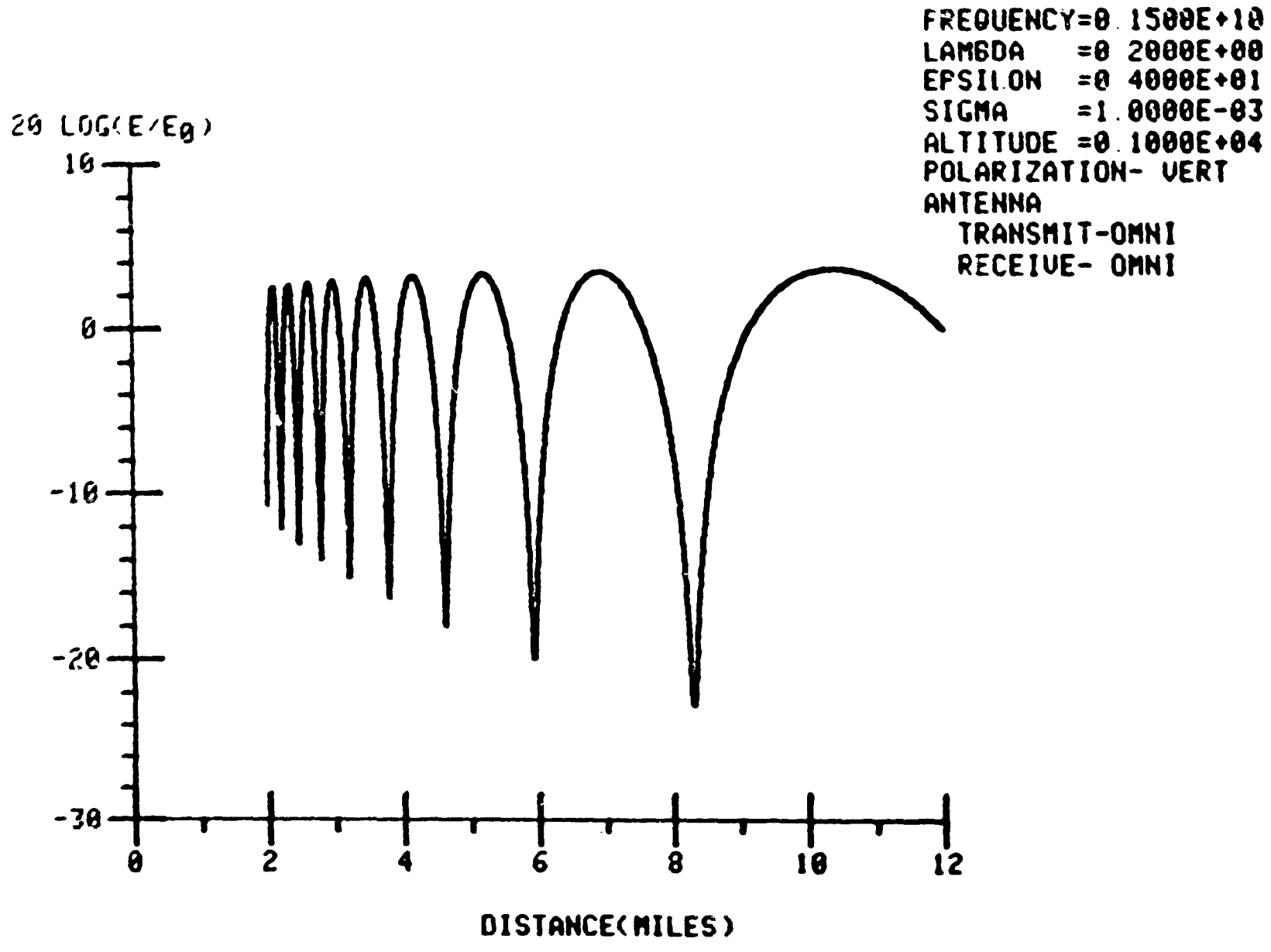
FREQUENCY=0.1500E+10
LAMBDA =0.2000E+00
EPSILON =0.4000E+01
SIGMA =1.0000E-03
ALTITUDE =0.1000E+04
POLARIZATION- VERT
ANTENNA
TRANSMIT-OMNI
RECEIVE- OMNI
20 LOG(E/Eo)
10
0
-10
-20
-30
0
2
4
6
8
10
12
DISTANCE(MILES)

Figure C1

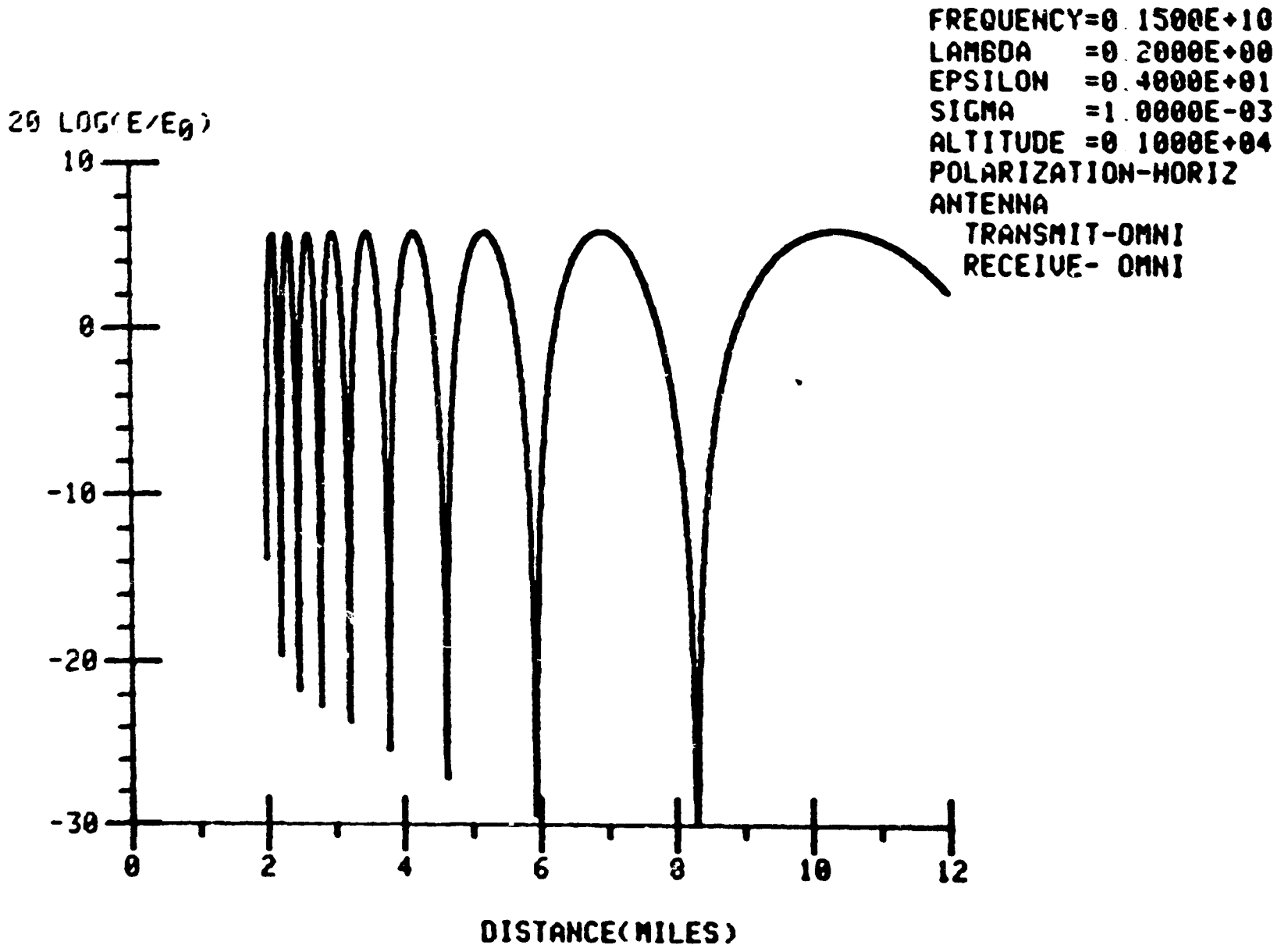
FREQUENCY=0.1500E+10
LAMBDA =0.2000E+00
EPSILON =0.4000E+01
SIGMA =1.0000E-03
ALTITUDE =0.1000E+04
POLARIZATION-HORIZ
ANTENNA
TRANSMIT-OMNI
RECEIVE- OMNI
20 LOG(E/E0)
10
0
-10
-20
-30
0
2
4
6
8
10
12
DISTANCE(MILES)

Figure C2

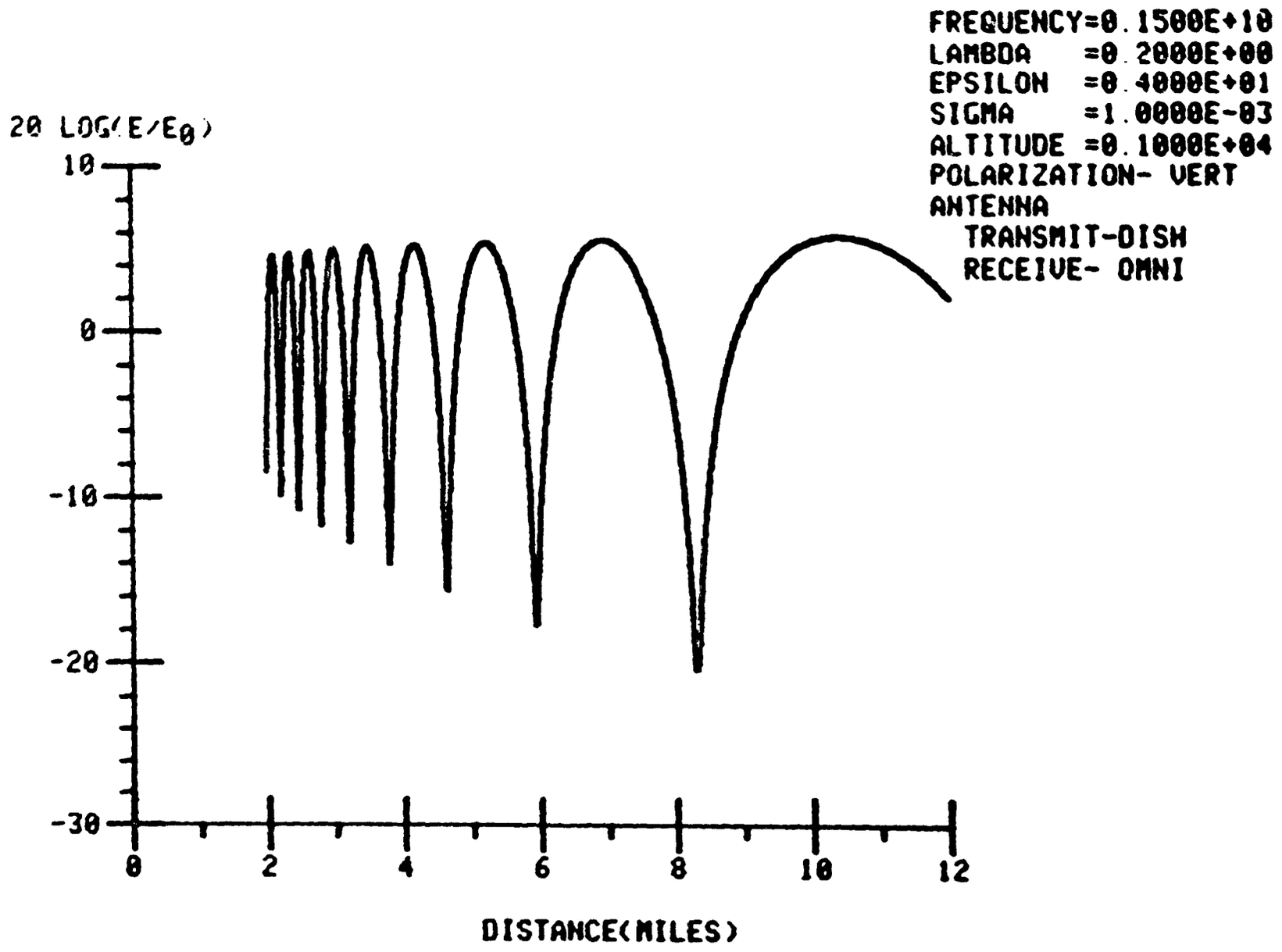
FREQUENCY=0.1500E+10
LAMBDA =0.2000E+00
EPSILON =0.4000E+01
SIGMA =1.0000E-03
ALTITUDE =0.1000E+04
POLARIZATION- VERT
ANTENNA
TRANSMIT-DISH
RECEIVE- OMNI
20 LOG(E/E0)
10
0
-10
-20
-30
0
2
4
6
8
10
12
DISTANCE(MILES)

Figure C3

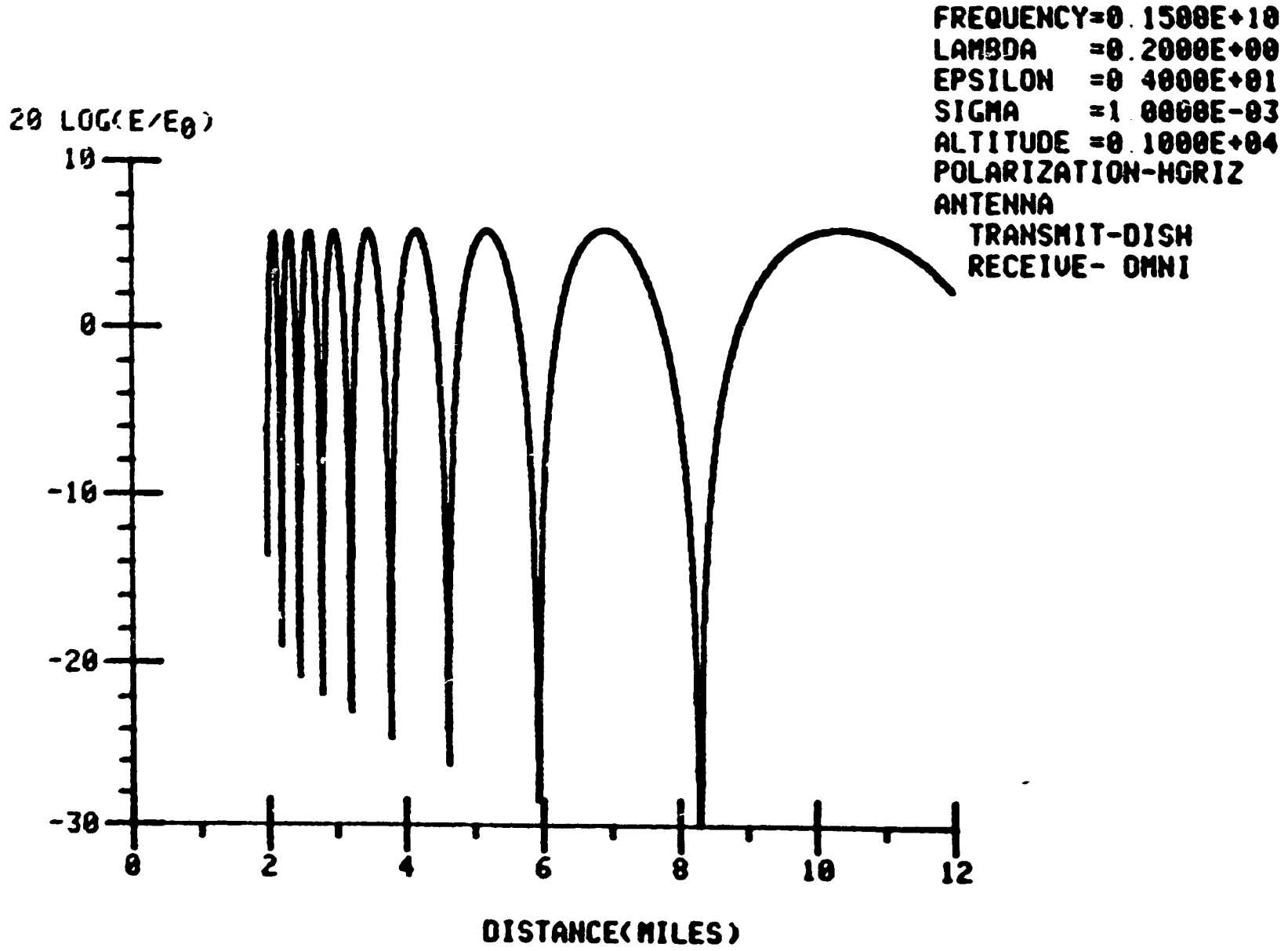
FREQUENCY=0.1500E+10
LAMBDA =0.2000E+00
EPSILON =0.4000E+01
SIGMA =1.0000E-03
ALTITUDE =0.1000E+04
POLARIZATION-HORIZ
ANTENNA
TRANSMIT-DISH
RECEIVE- OMNI
20 LOG(E/E0)
10
0
-10
-20
-30
0
2
4
6
8
10
12
DISTANCE(MILES)

Figure C4

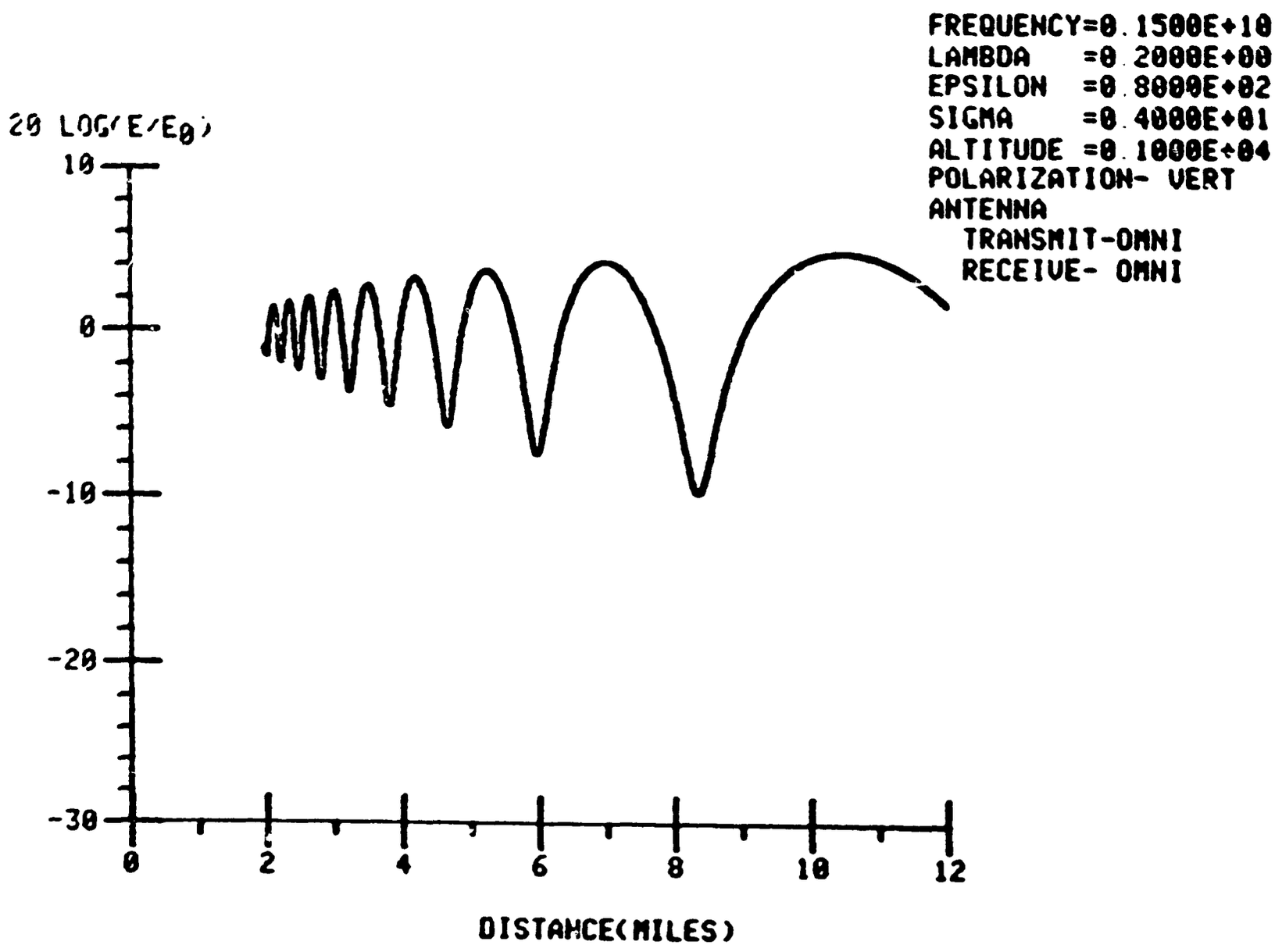
FREQUENCY=0.1500E+10
LAMBDA =0.2000E+00
EPSILON =0.8000E+02
SIGMA =0.4000E+01
ALTITUDE =0.1000E+04
POLARIZATION- VERT
ANTENNA
TRANSMIT-OMNI
RECEIVE- OMNI
20 LOG(E/E0)
10
0
-10
-20
-30
0
2
4
6
8
10
12
DISTANCE(MILES)

Figure C5

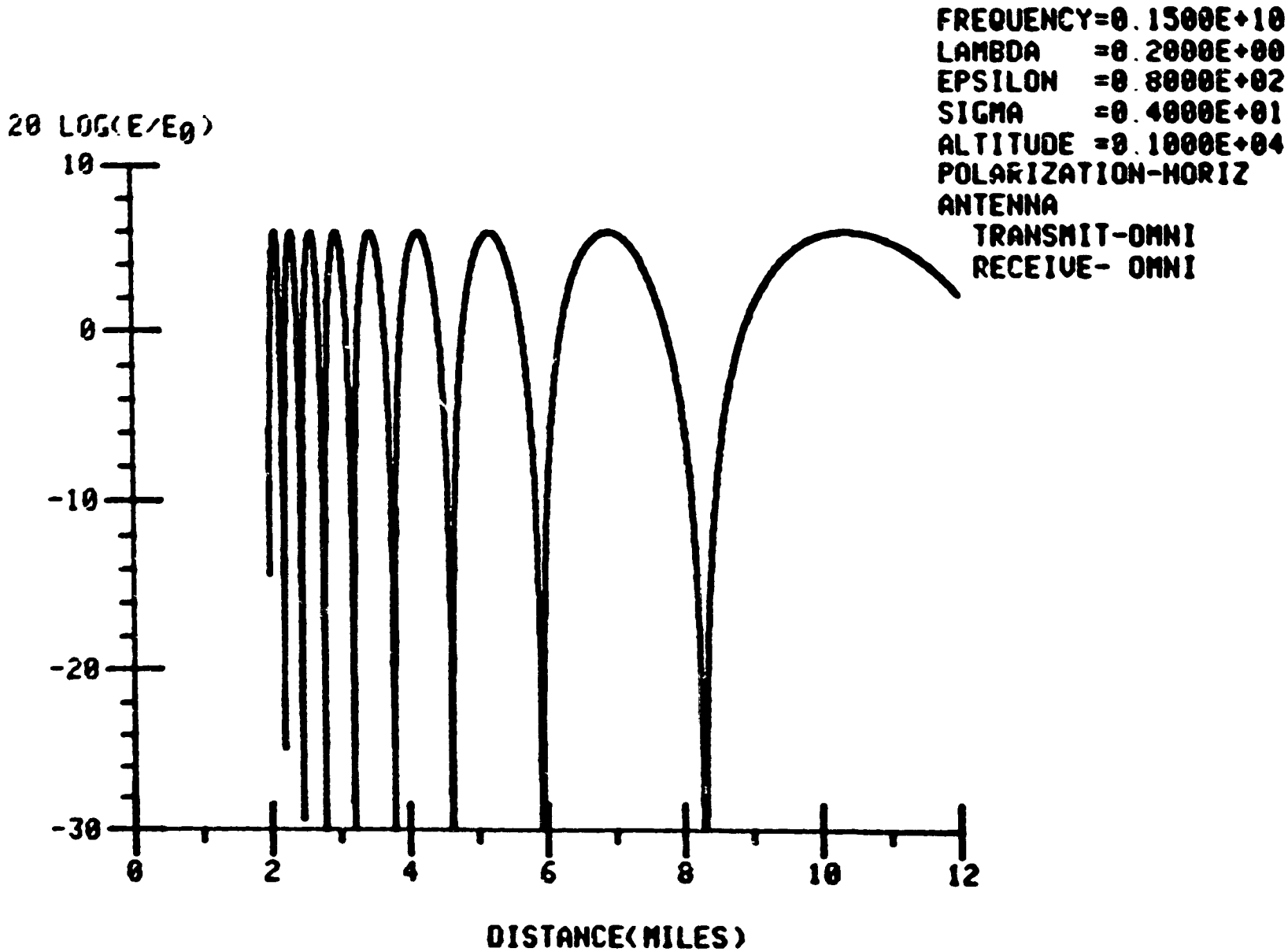
FREQUENCY=0.1500E+10
LAMBDA =0.2000E+00
EPSILON =0.8000E+02
SIGMA =0.4000E+01
ALTITUDE =0.1000E+04
POLARIZATION-HORIZ
ANTENNA
TRANSMIT-OMNI
RECEIVE- OMNI
20 LOG(E/E0)
10
0
-10
-20
-30
0
2
4
6
8
10
12
DISTANCE(MILES)

Figure C6

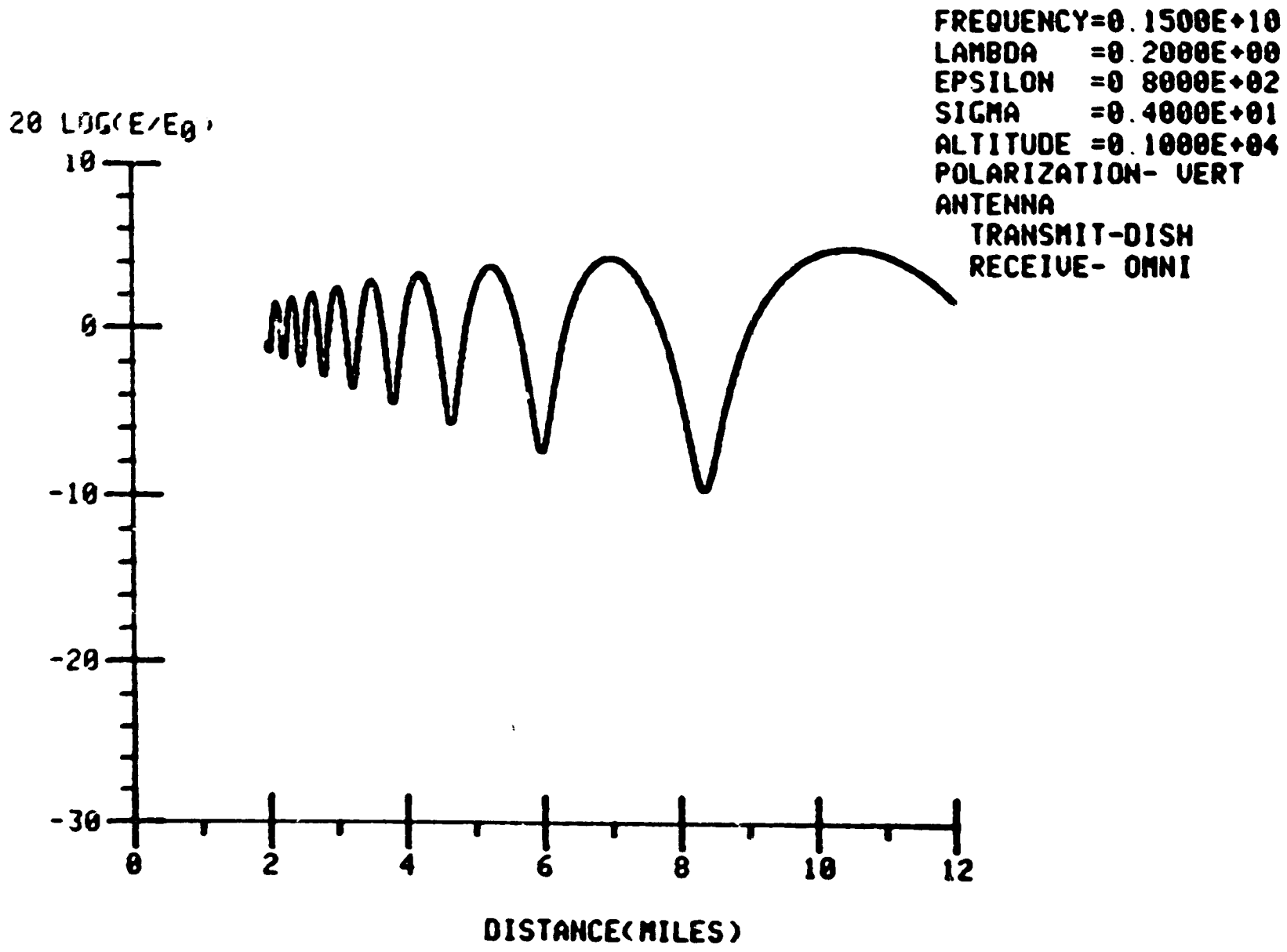
FREQUENCY=0.1500E+10
LAMBDA =0.2000E+00
EPSILON =0 8000E+02
SIGMA =0.4000E+01
ALTITUDE =0.1000E+04
POLARIZATION- VERT
ANTENNA
TRANSMIT-DISH
RECEIVE- OMNI
20 LOG(E/E0)
10
0
-10
-20
-30
0
2
4
6
8
10
12
DISTANCE(MILES)

Figure C7

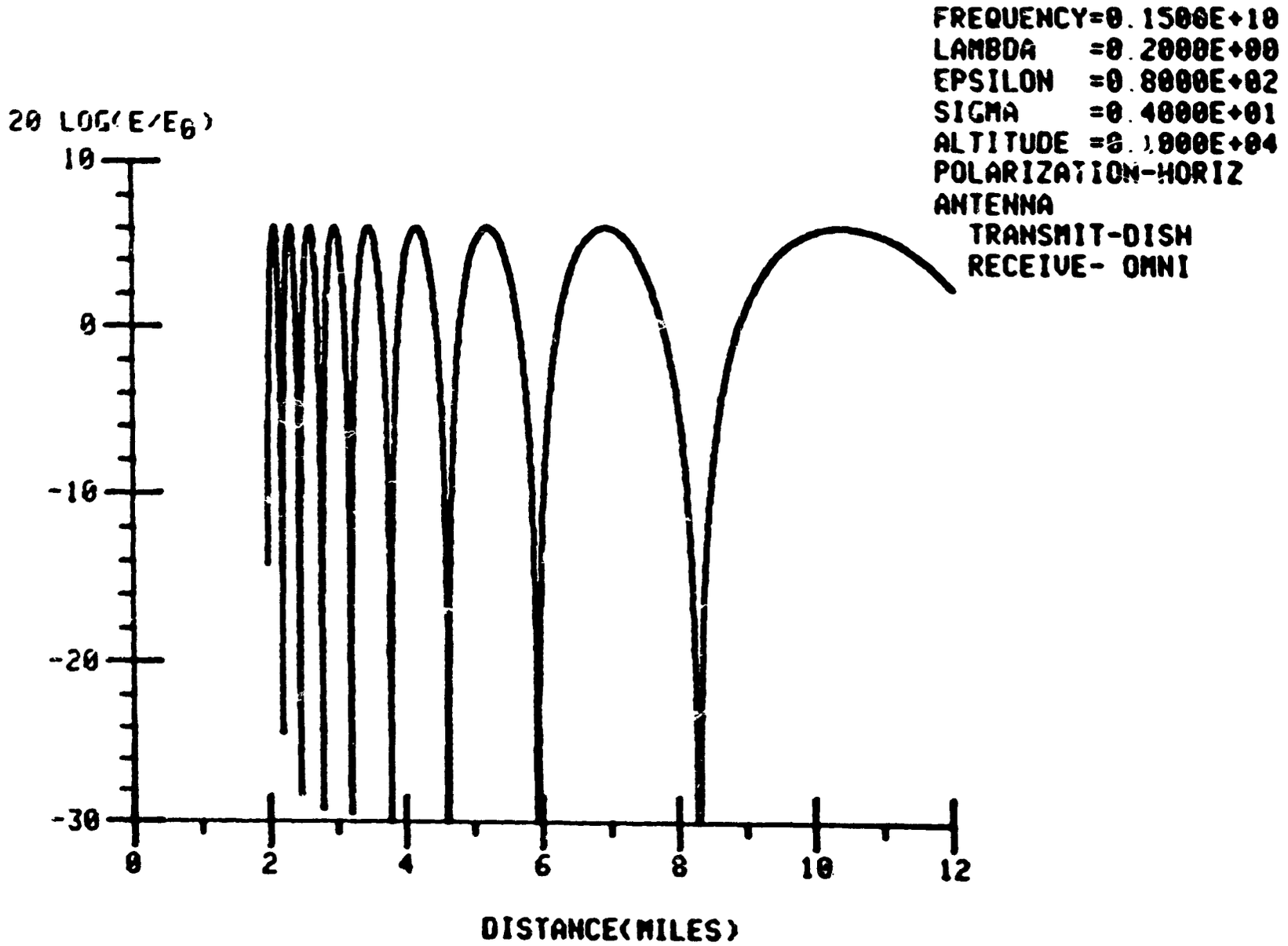
FREQUENCY=0.1500E+10
LAMBDA =0.2000E+00
EPSILON =0.8000E+02
SIGMA =0.4000E+01
ALTITUDE =0.1000E+04
POLARIZATION-HORIZ
ANTENNA
TRANSMIT-DISH
RECEIVE- OMNI
20 LOG(E/E0)
10
0
-10
-20
-30
0
2
4
6
8
10
12
DISTANCE(MILES)

Figure C8

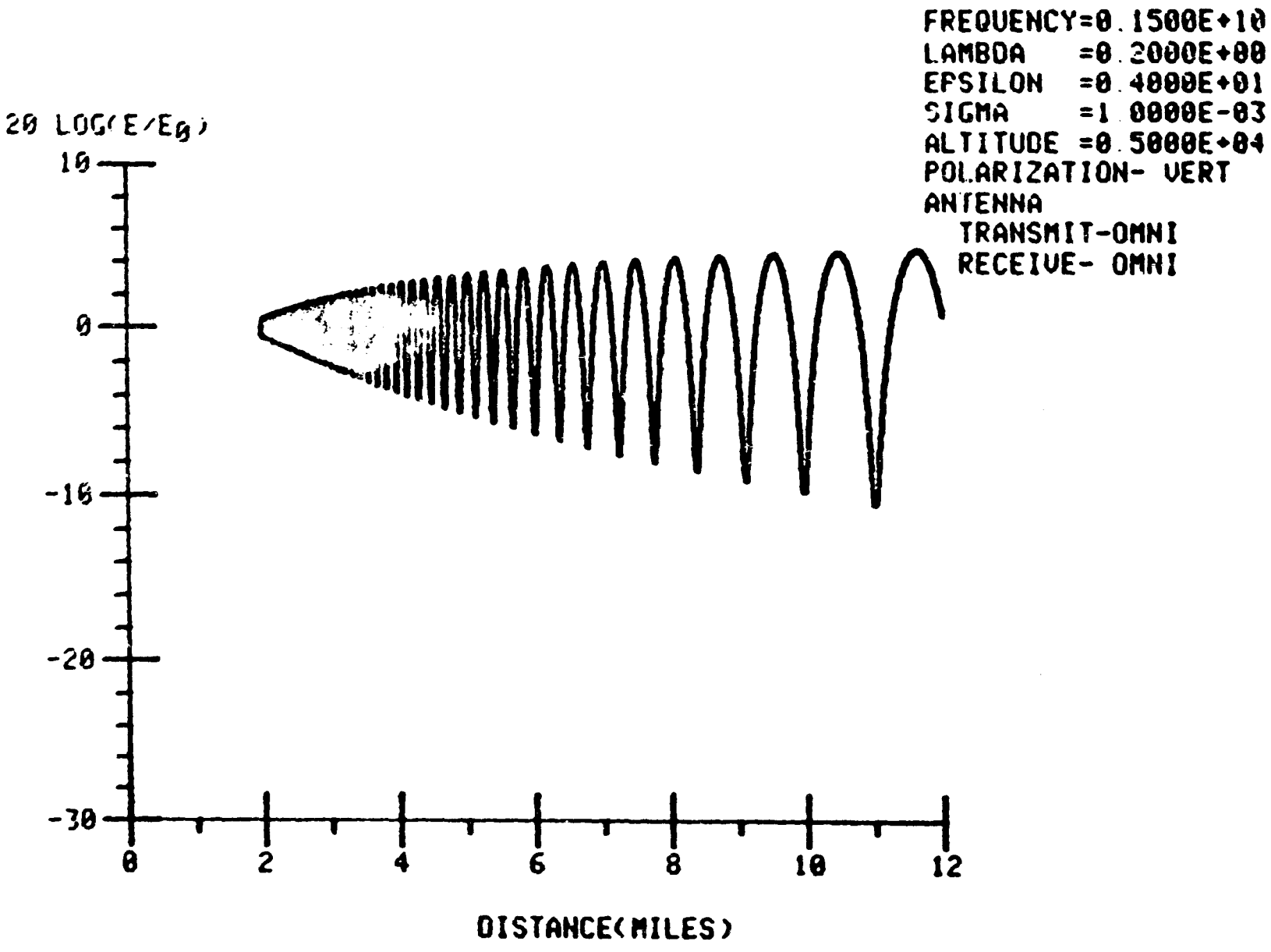
FREQUENCY=0.1500E+10
LAMBDA =0.2000E+00
EPSILON =0.4000E+01
SIGMA =1.0000E-03
ALTITUDE =0.5000E+04
POLARIZATION- VERT
ANTENNA
TRANSMIT-OMNI
RECEIVE- OMNI
20 LOG(E/E0)
10
0
-10
-20
-30
0
2
4
6
8
10
12
DISTANCE(MILES)

Figure C9

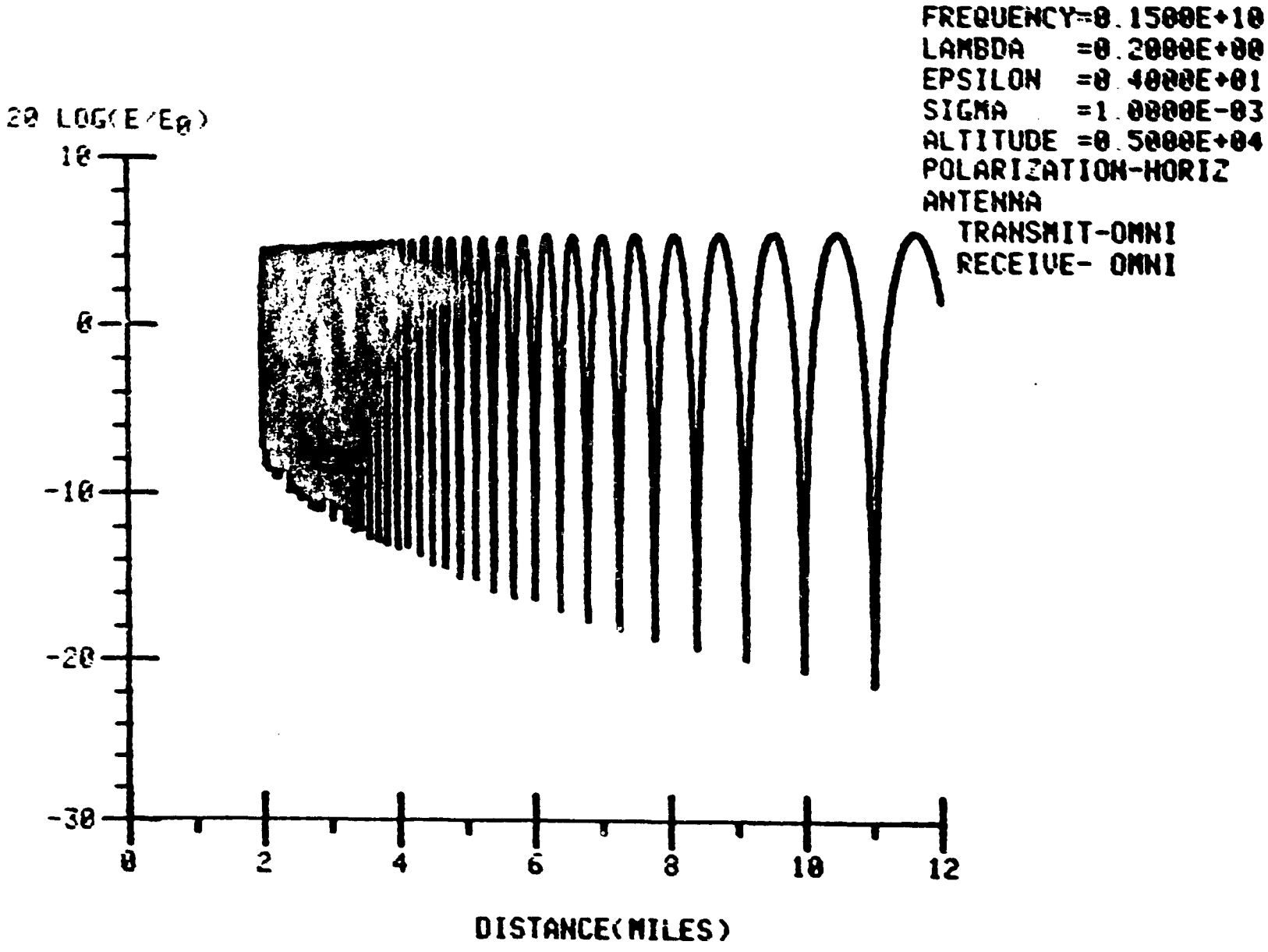
FREQUENCY=0.1500E+10
LAMBDA =0.2000E+00
EPSILON =0.4000E+01
SIGMA =1.0000E-03
ALTITUDE =0.5000E+04
POLARIZATION-HORIZ
ANTENNA
TRANSMIT-OMNI
RECEIVE- OMNI
20 LOG(E/E0)
10
0
-10
-20
-30
0
2
4
6
8
10
12
DISTANCE(MILES)

Figure C10

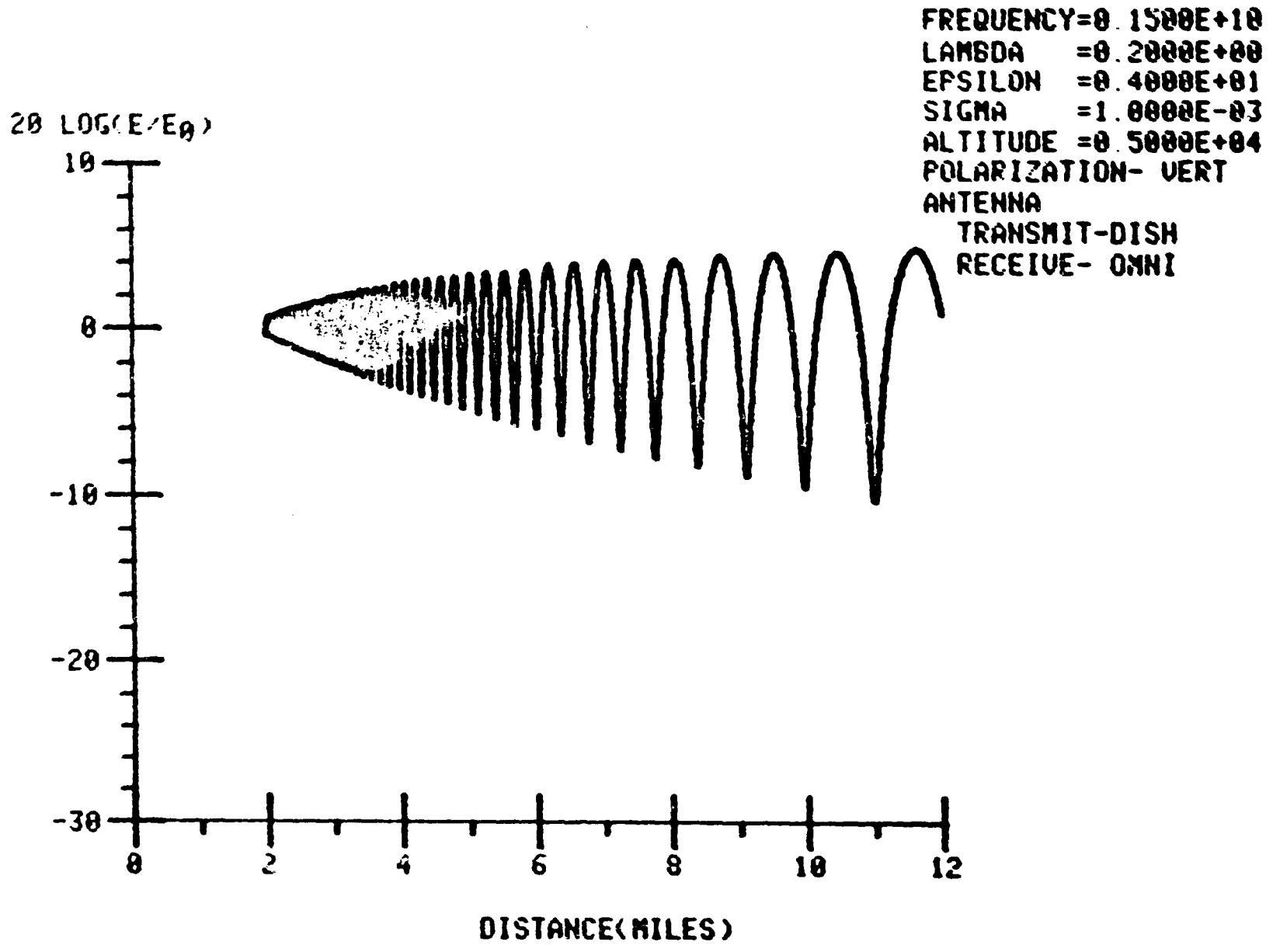
FREQUENCY=0.1500E+10
LAMBDA =0.2000E+00
EPSILON =0.4000E+01
SIGMA =1.0000E-03
ALTITUDE =0.5000E+04
POLARIZATION- VERT
ANTENNA
TRANSMIT-DISH
RECEIVE- OMNI
20 LOG(E/E0)
10
0
-10
-20
-30
0
2
4
6
8
10
12
DISTANCE(MILES)

Figure C11

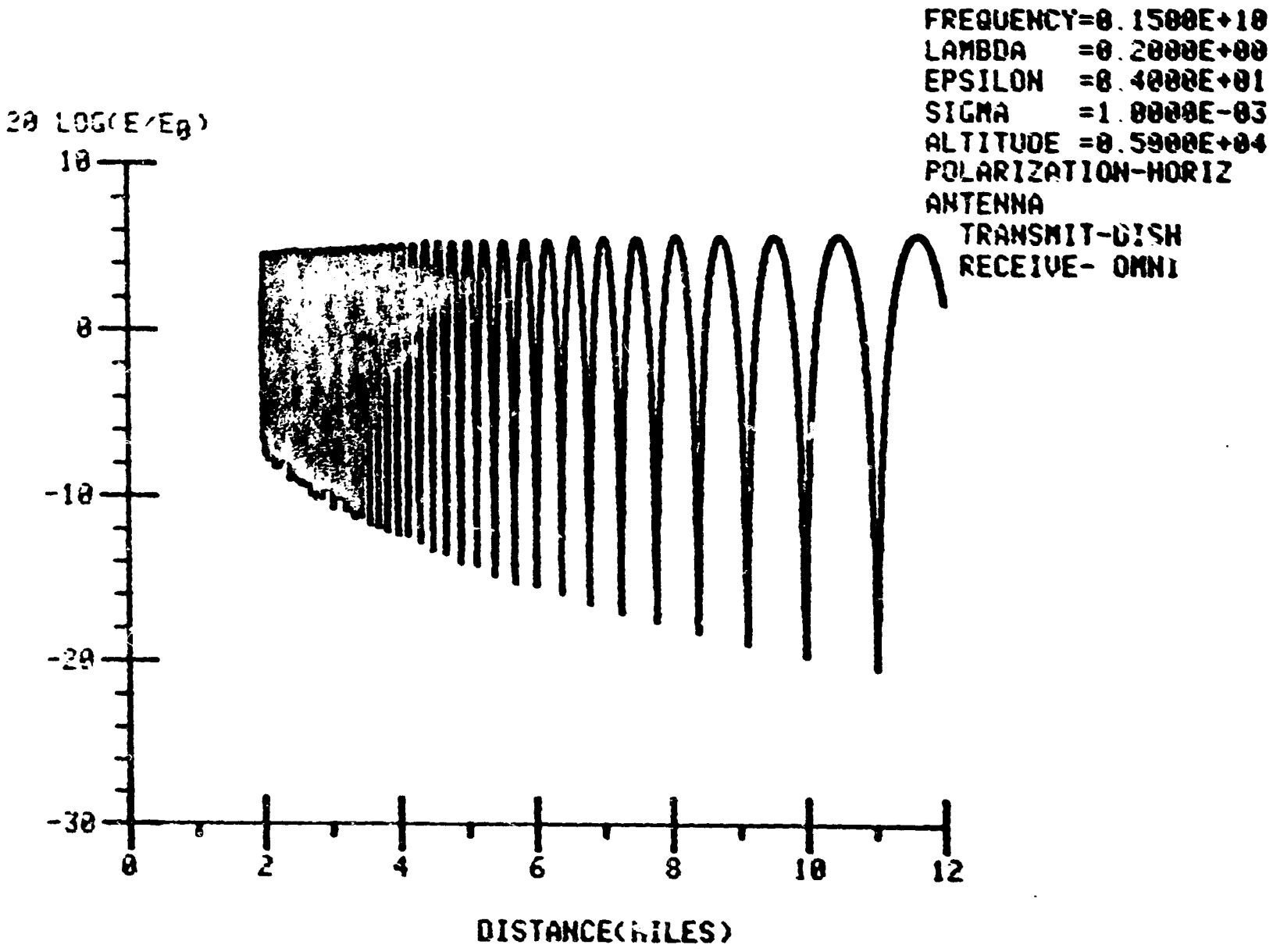
FREQUENCY=0.1500E+10
LAMBDA =0.2000E+00
EPSILON =0.4000E+01
SIGMA =1.0000E-03
ALTITUDE =0.5000E+04
POLARIZATION-HORIZ
ANTENNA
TRANSMIT-DISH
RECEIVE- OMNI
20 LOG(E/E0)
10
0
-10
-20
-30
0
2
4
6
8
10
12
DISTANCE(MILES)

Figure C12

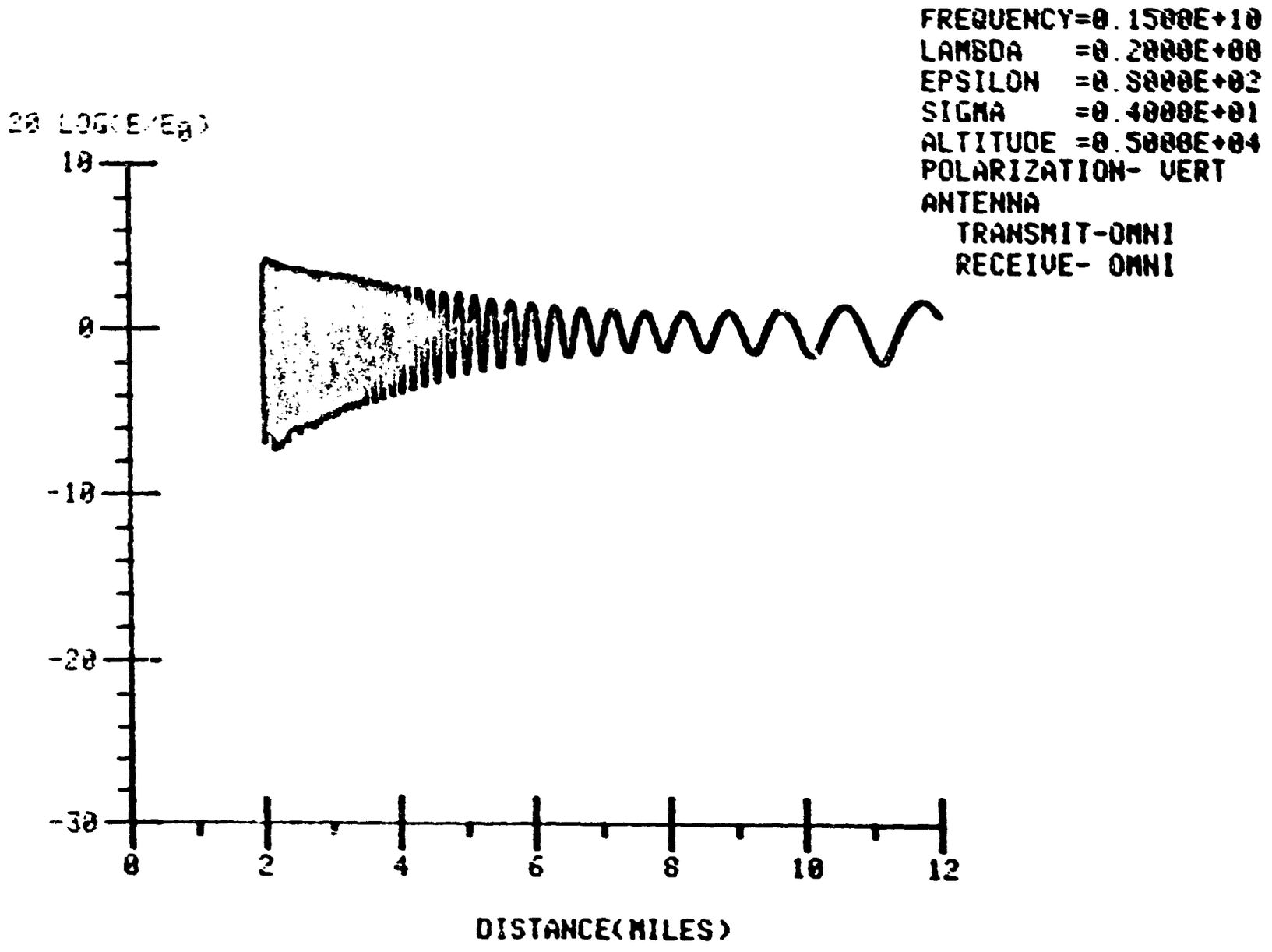
FREQUENCY=0.1500E+10
LAMBDA =0.2000E+00
EPSILON =0.5000E+02
SIGMA =0.4000E+01
ALTITUDE =0.5000E+04
POLARIZATION- VERT
ANTENNA
TRANSMIT-OMNI
RECEIVE- OMNI
20 LOG(E/E0)
10
0
-10
-20
-30
0
2
4
6
8
10
12
DISTANCE(MILES)

Figure C13

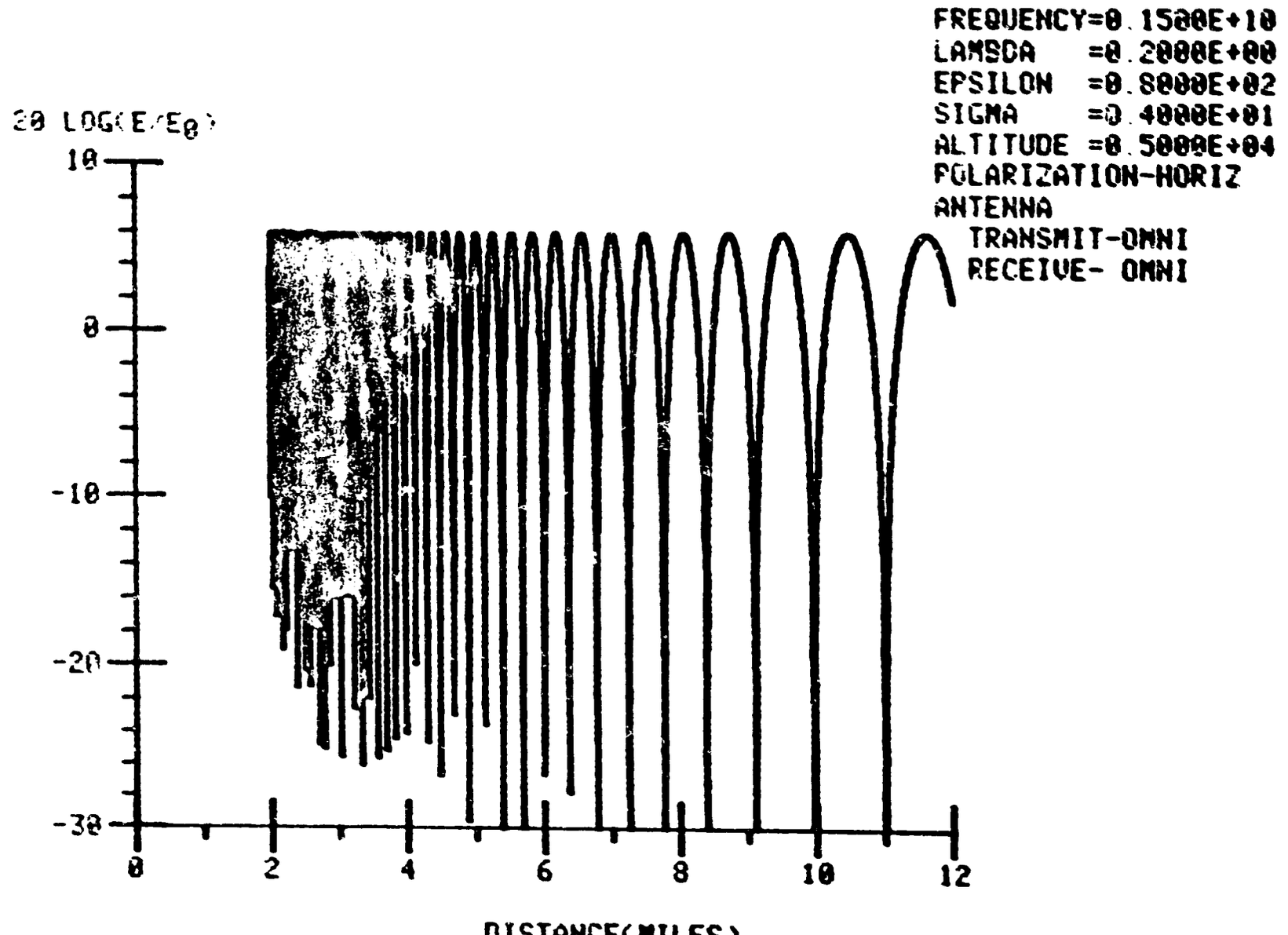
FREQUENCY=0.1500E+10
LAMSDA =0.2000E+00
EPSILON =0.8000E+02
SIGMA =0.4000E+01
ALTITUDE =0.5000E+04
POLARIZATION-HORIZ
ANTENNA
TRANSMIT-OMNI
RECEIVE- OMNI
20 LOG(E/Eθ)
10
0
-10
-20
-30
0
2
4
6
8
10
12
DISTANCE(MILES)

Figure C14

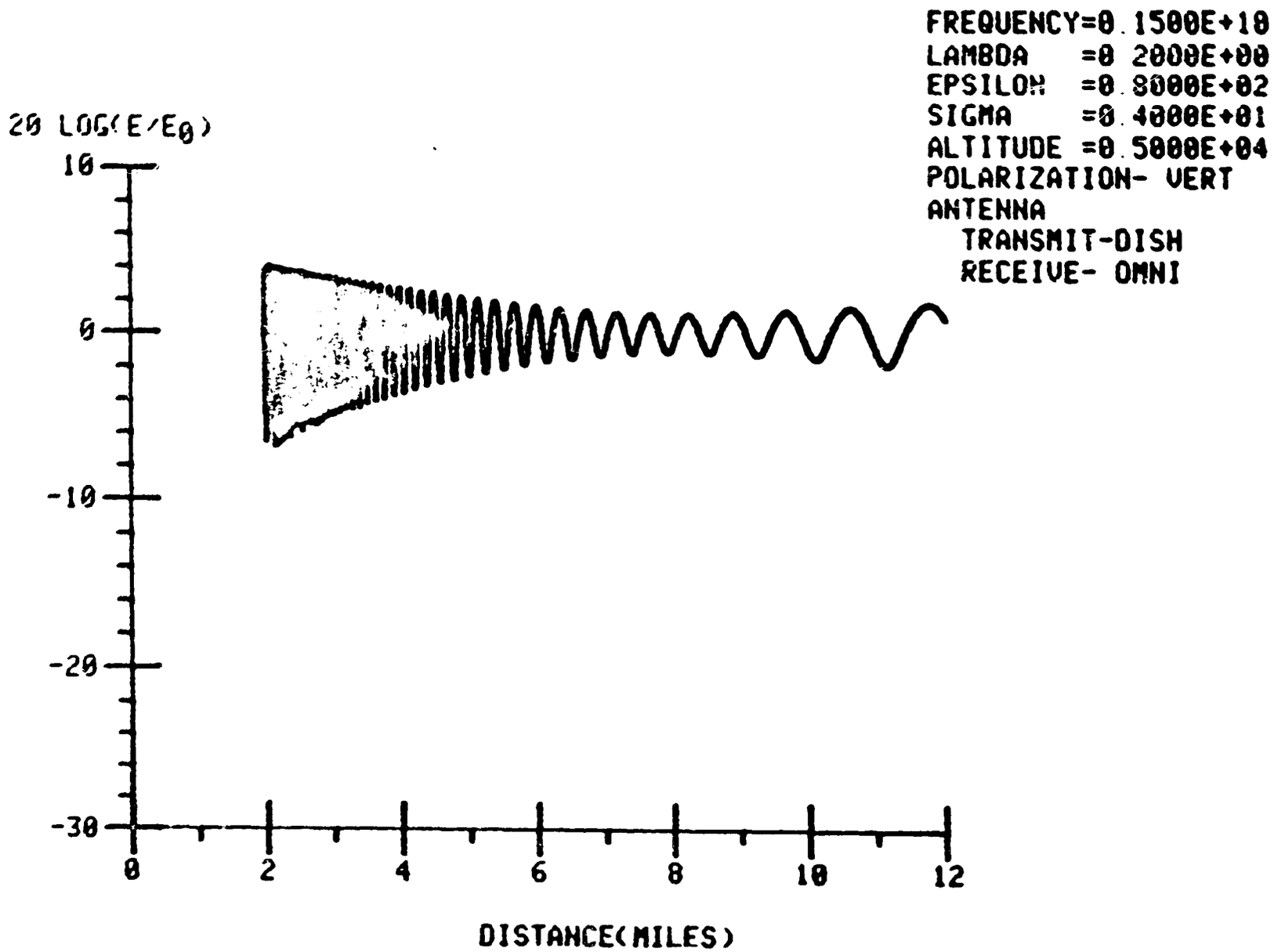
FREQUENCY=0.1500E+10
LAMBDA =0.2000E+00
EPSILON =0.8000E+02
SIGMA =0.4000E+01
ALTITUDE =0.5000E+04
POLARIZATION- VERT
ANTENNA
TRANSMIT-DISH
RECEIVE- OMNI
20 LOG(E/E0)
10
0
-10
-20
-30
0
2
4
6
8
10
12
DISTANCE(MILES)

Figure C15

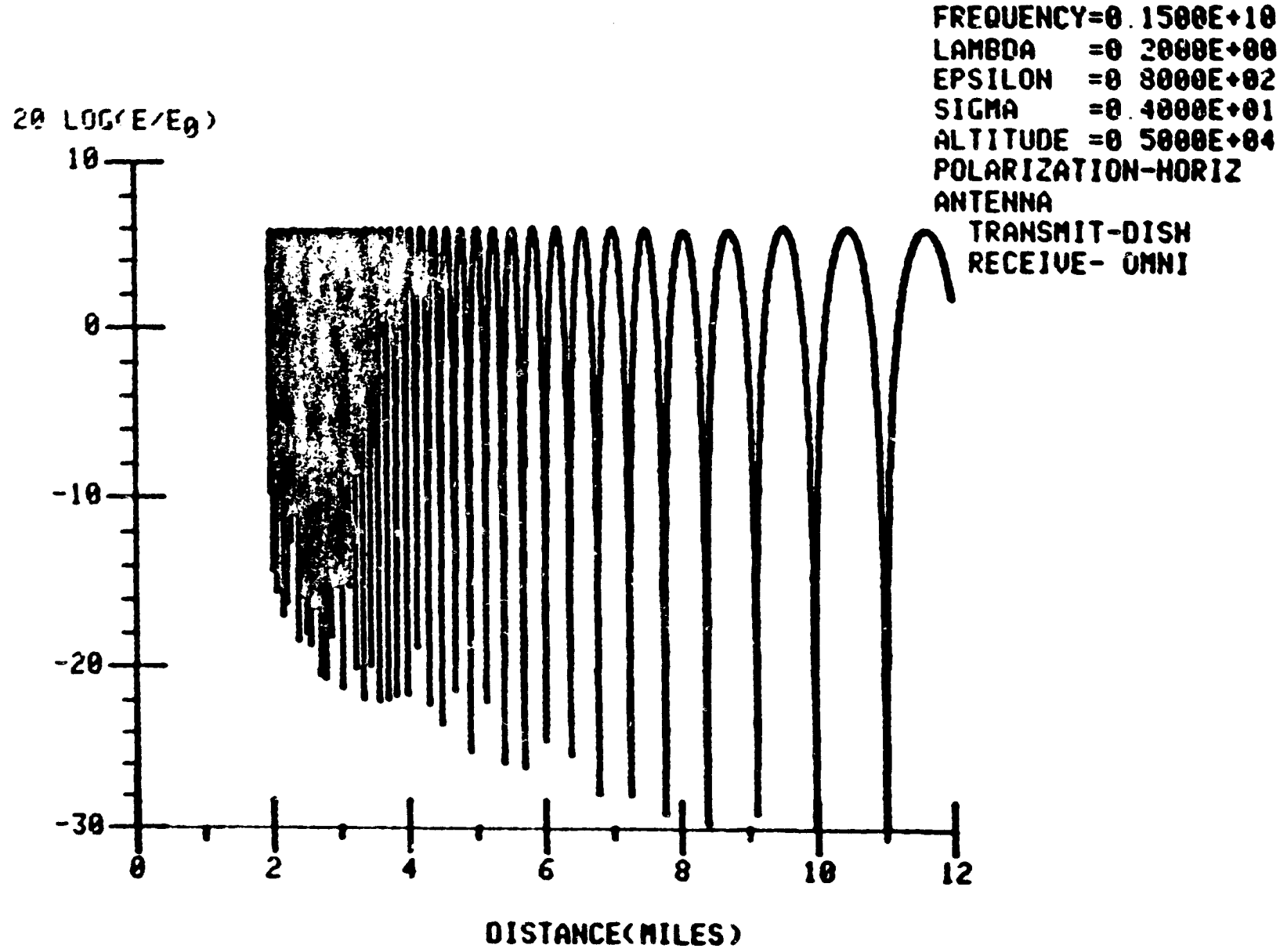
FREQUENCY=0.1500E+10
LAMBDA =0.2000E+00
EPSILON =0.8000E+02
SIGMA =0.4000E+01
ALTITUDE =0.5000E+04
POLARIZATION-HORIZ
ANTENNA
TRANSMIT-DISH
RECEIVE- OMNI
20 LOG(E/E0)
10
0
-10
-20
-30
0
2
4
6
8
10
12
DISTANCE(MILES)

Figure C16

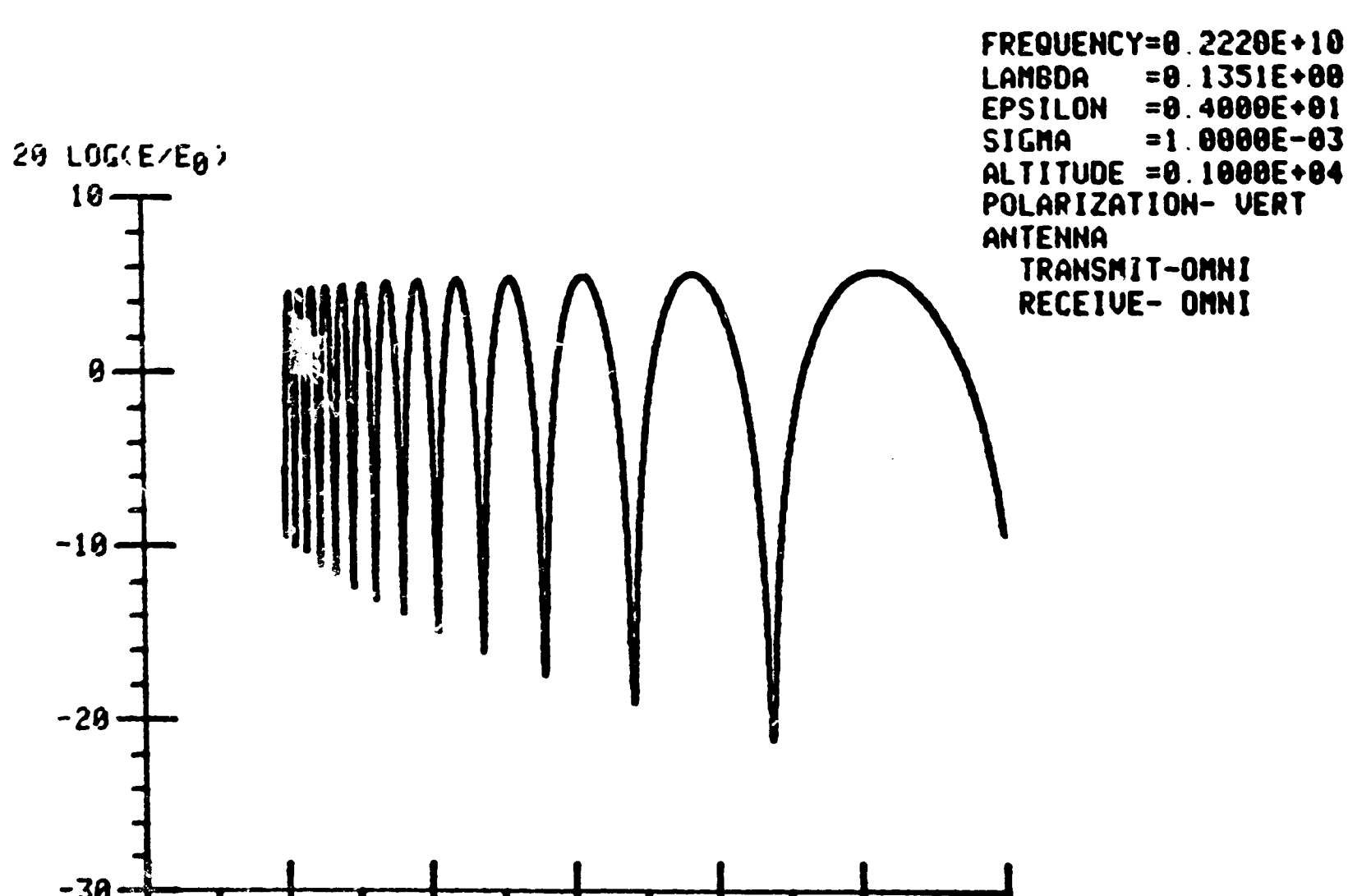
FREQUENCY=0.2220E+10
LAMBDA =0.1351E+00
EPSILON =0.4000E+01
SIGMA =1.0000E-03
ALTITUDE =0.1000E+04
POLARIZATION- VERT
ANTENNA
TRANSMIT-OMNI
RECEIVE- OMNI
20 LOG(E/E0)
10
0
-10
-20
-30
0
2
4
6
8
10
12
DISTANCE(MILES)

Figure C17

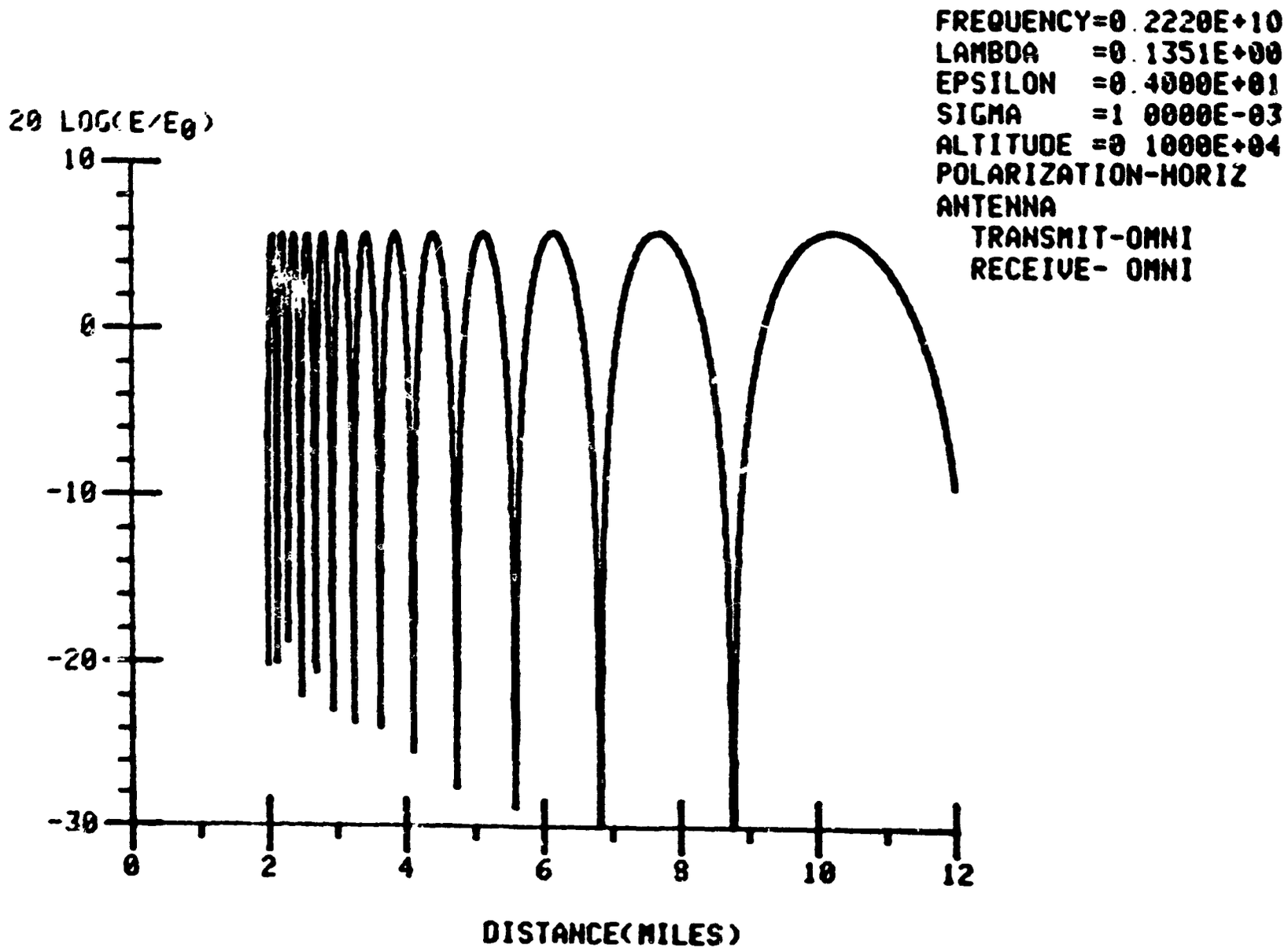
FREQUENCY=0.2220E+10
LAMBDA =0.1351E+00
EPSILON =0.4000E+01
SIGMA =1.0000E-03
ALTITUDE =0.1000E+04
POLARIZATION-HORIZ
ANTENNA
TRANSMIT-OMNI
RECEIVE- OMNI
20 LOG(E/E0)
10
0
-10
-20
-30
0
2
4
6
8
10
12
DISTANCE(MILES)

Figure C18

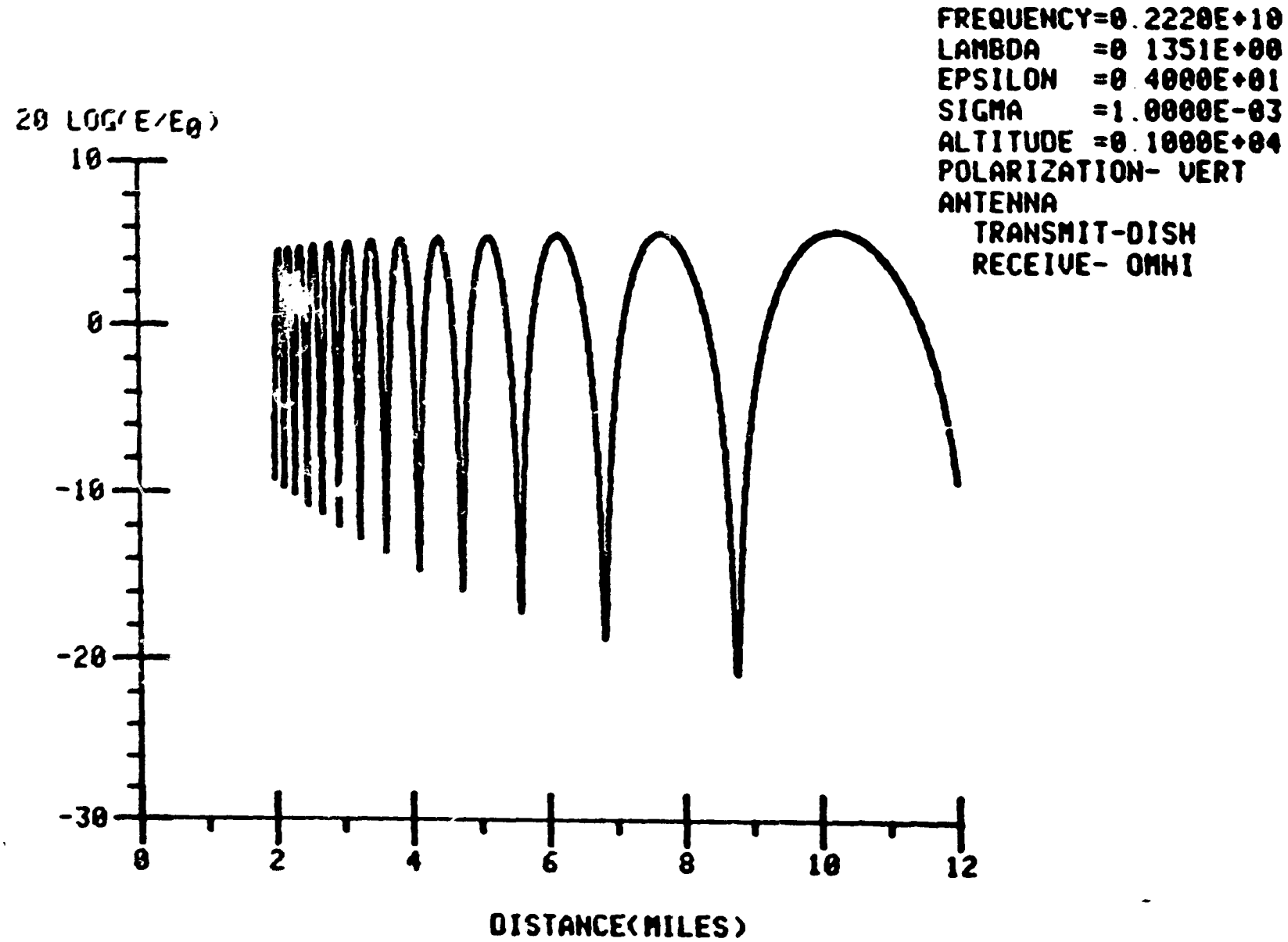
FREQUENCY=0.2220E+10
LAMBDA =0 1351E+00
EPSILON =0 4000E+01
SIGMA =1.0000E-03
ALTITUDE =0 1000E+04
POLARIZATION- VERT
ANTENNA
TRANSMIT-DISH
RECEIVE- OMNI
20 LOG(E/E0)
10
0
-10
-20
-30
0
2
4
6
8
10
12
DISTANCE(MILES)

Figure C19

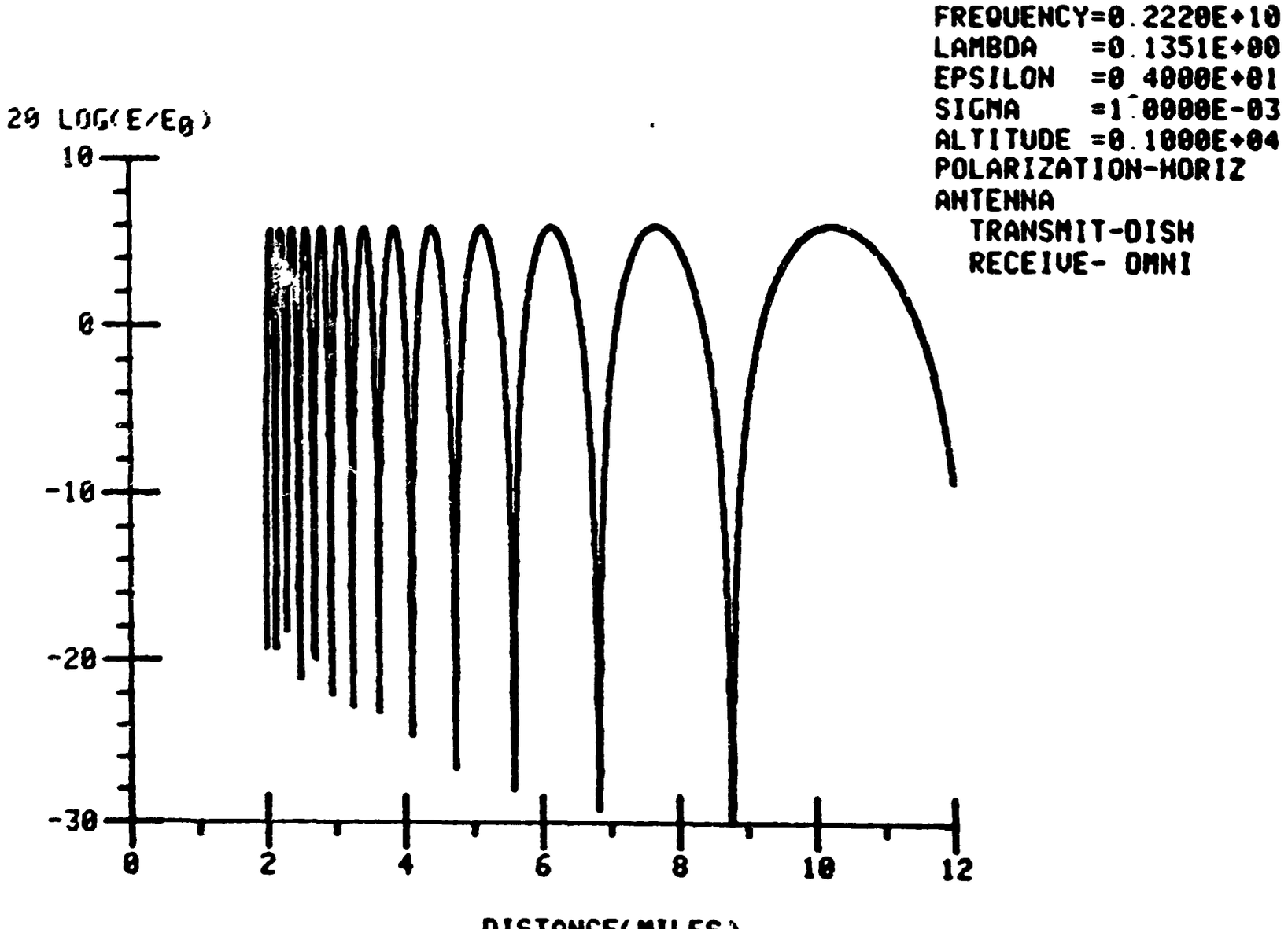
FREQUENCY=0.2220E+10
LAMBDA =0.1351E+00
EPSILON =0.4000E+01
SIGMA =1.0000E-03
ALTITUDE =0.1000E+04
POLARIZATION-HORIZ
ANTENNA
TRANSMIT-DISH
RECEIVE- OMNI
20 LOG(E/E0)
10
0
-10
-20
-30
0
2
4
6
8
10
12
DISTANCE(MILES)

Figure C20

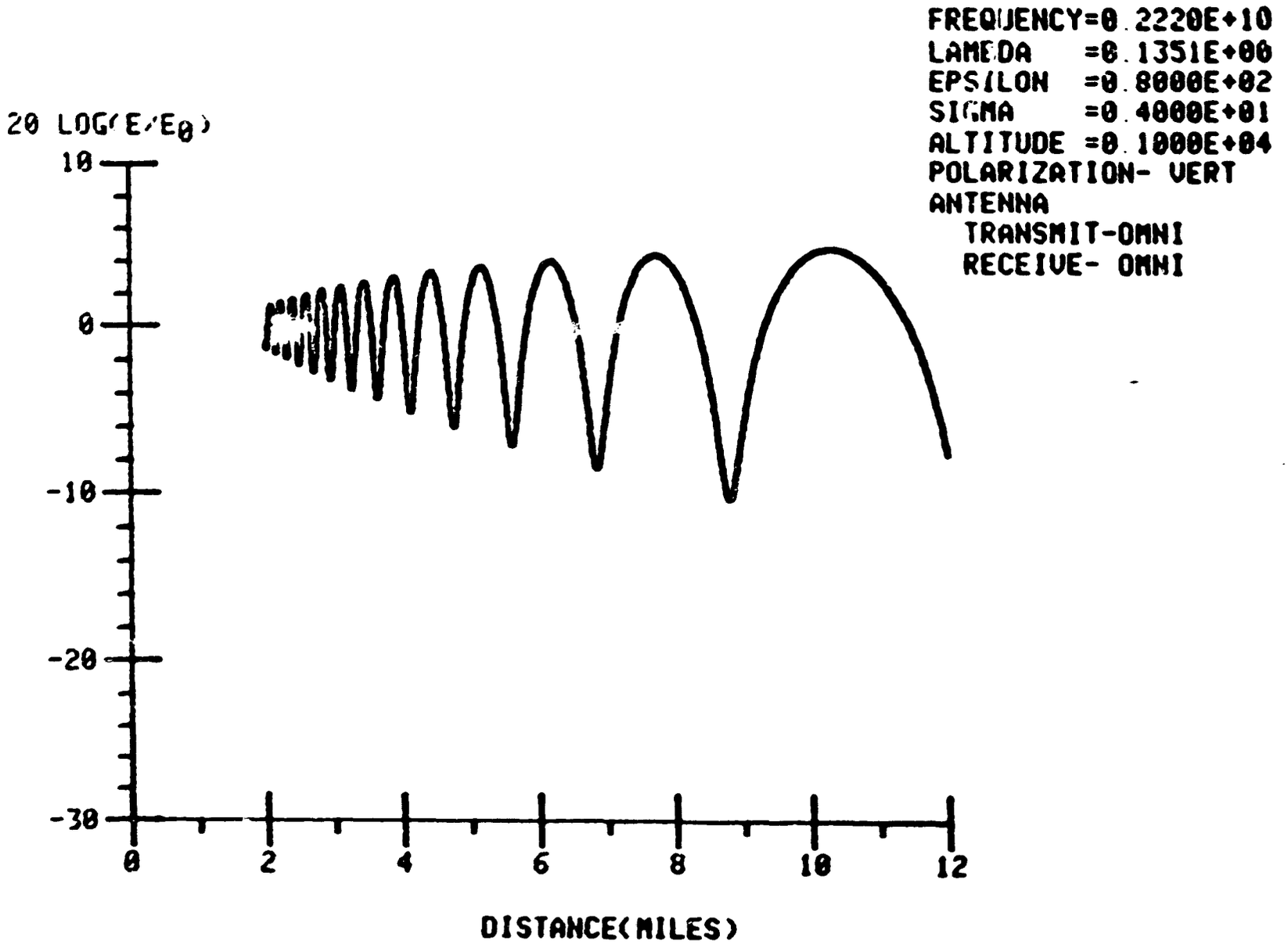
FREQUENCY=0.2220E+10
LAMBDA =0.1351E+00
EPSILON =0.8000E+02
SIGMA =0.4000E+01
ALTITUDE =0.1000E+04
POLARIZATION- VERT
ANTENNA
TRANSMIT-OMNI
RECEIVE- OMNI
20 LOG(E/E0)
10
0
-10
-20
-30
0
2
4
6
8
10
12
DISTANCE(MILES)

Figure C21

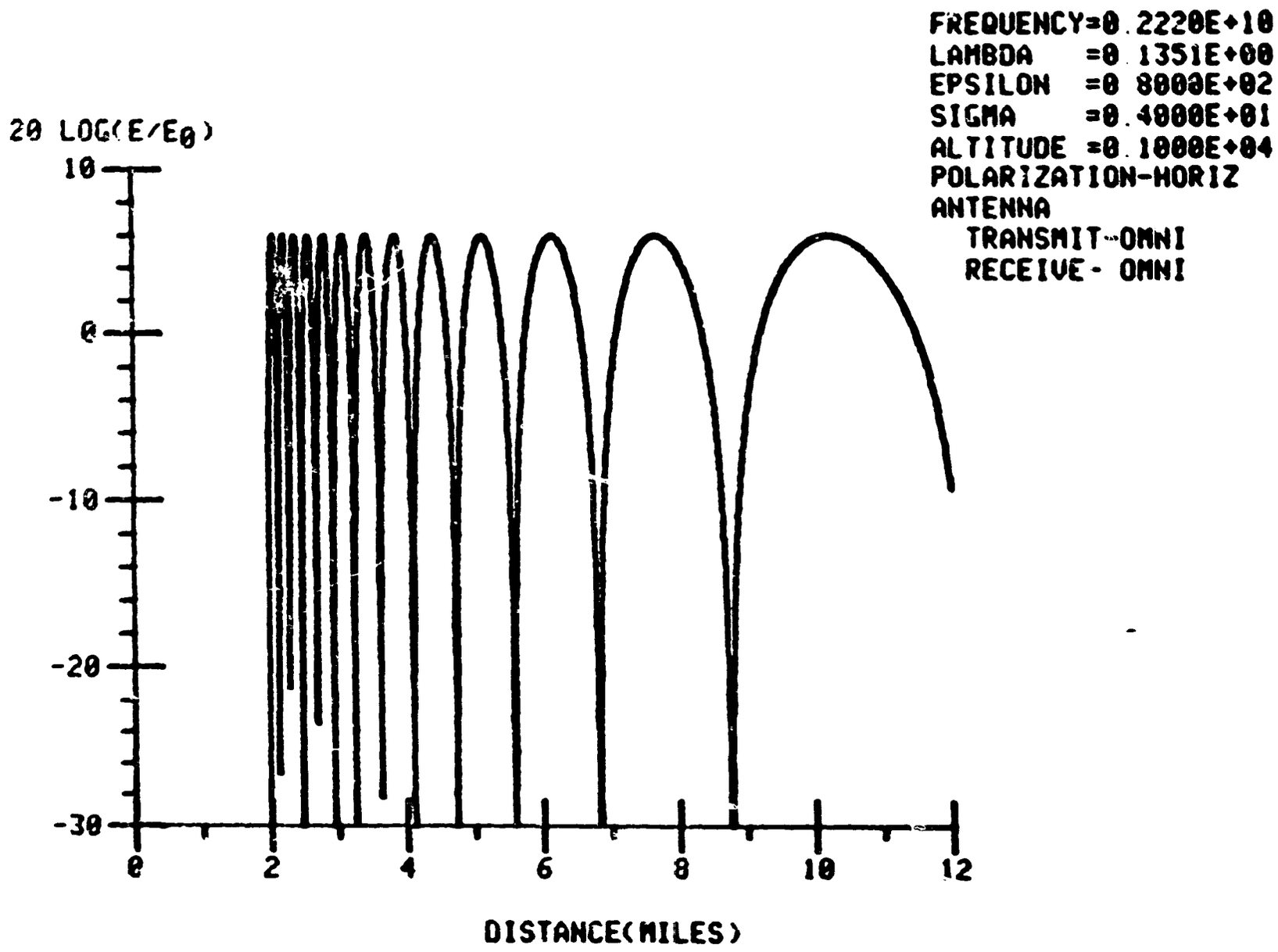
FREQUENCY=0.2220E+10
LAMBDA =0.1351E+00
EPSILON =0.8000E+02
SIGMA =0.4000E+01
ALTITUDE =0.1000E+04
POLARIZATION-HORIZ
ANTENNA
TRANSMIT-OMNI
RECEIVE- OMNI
20 LOG(E/E0)
10
0
-10
-20
-30
0
2
4
6
8
10
12
DISTANCE(MILES)

Figure C22

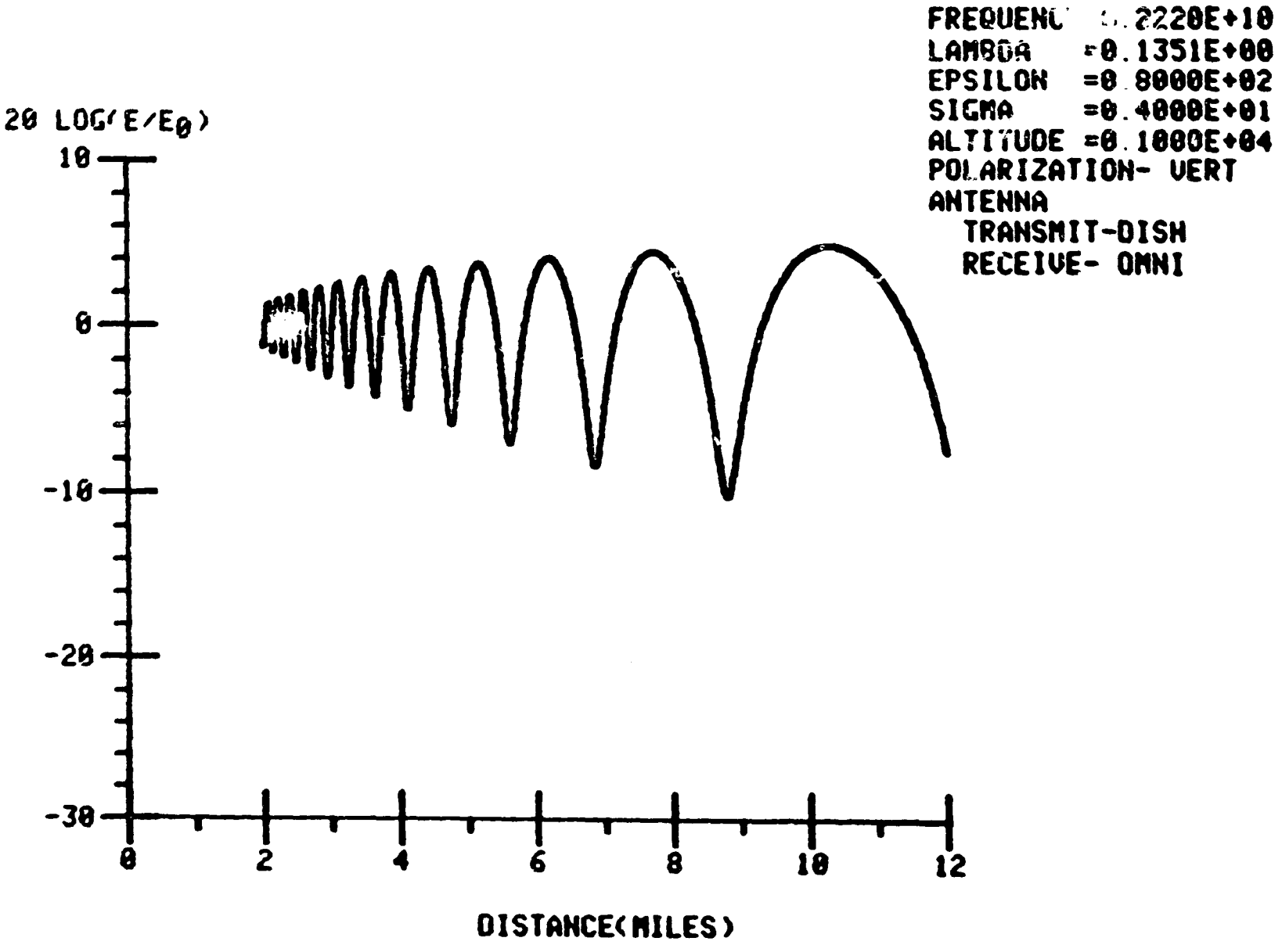
FREQUENC 0.2220E+10
LAMBDA =0.1351E+00
EPSILON =0.8000E+02
SIGMA =0.4000E+01
ALTITUDE =0.1000E+04
POLARIZATION- VERT
ANTENNA
TRANSMIT-DISH
RECEIVE- OMNI
20 LOG(E/E0)
10
0
-10
-20
-30
0
2
4
6
8
10
12
DISTANCE(MILES)

Figure C23

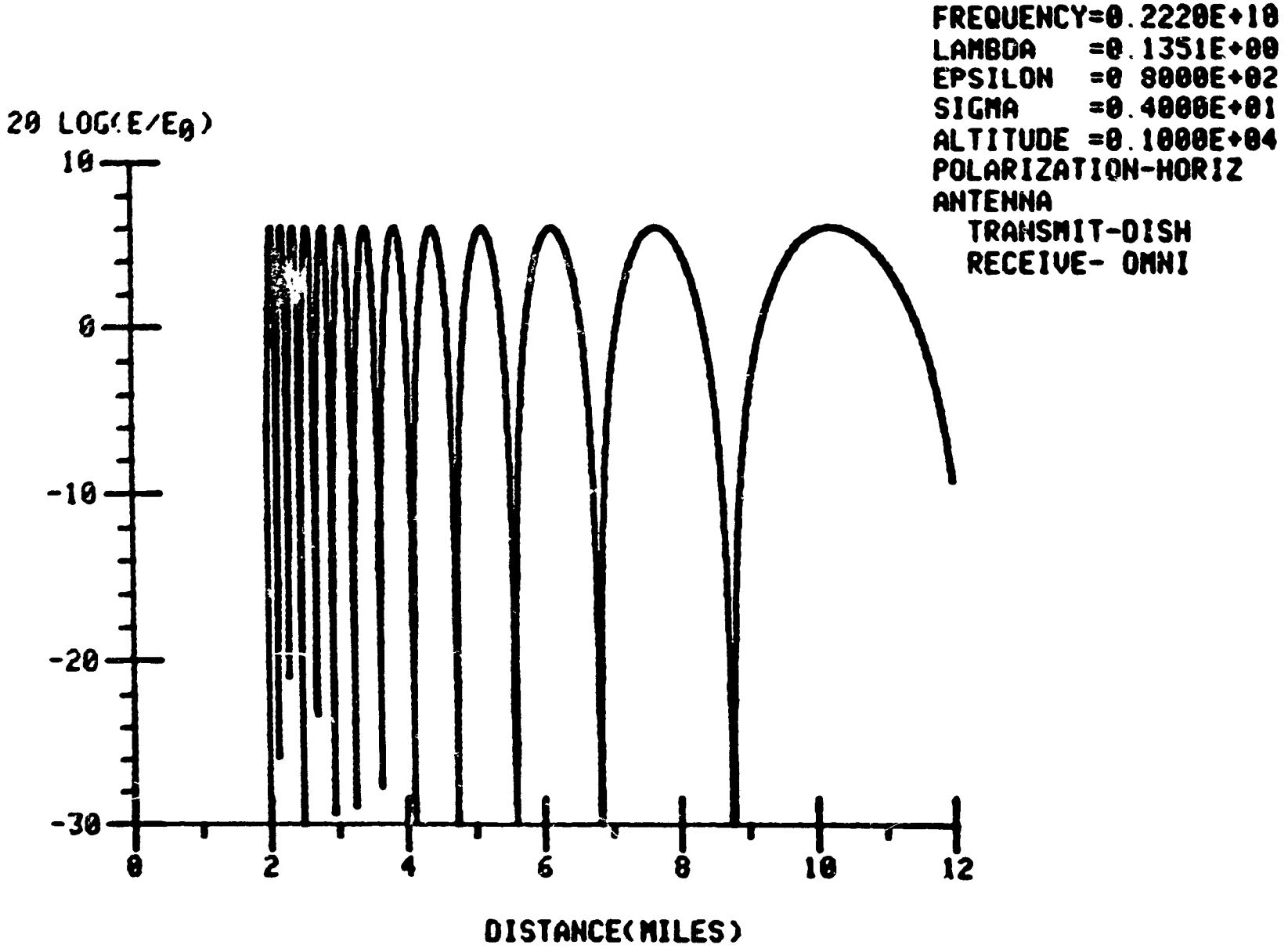
FREQUENCY=0.2220E+10
LAMBDA =0.1351E+00
EPSILON =0 8000E+02
SIGMA =0.4000E+01
ALTITUDE =0.1000E+04
POLARIZATION-HORIZ
ANTENNA
TRANSMIT-DISH
RECEIVE- OMNI
20 LOG(E/E0)
10
0
-10
-20
-30
0
2
4
6
8
10
12
DISTANCE(MILES)

Figure C24

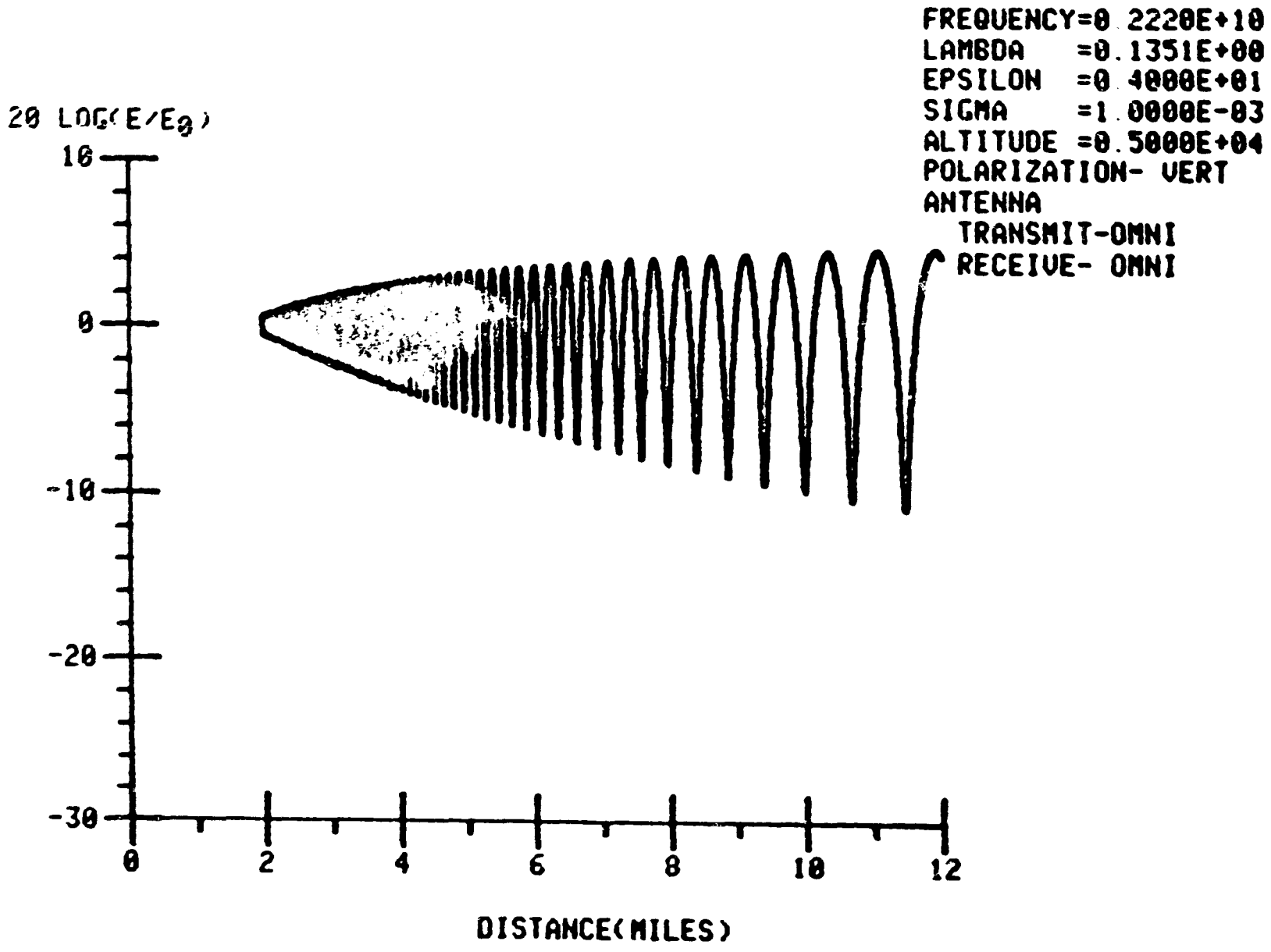
FREQUENCY=0.2220E+10
LAMBDA =0.1351E+00
EPSILON =0.4000E+01
SIGMA =1.0000E-03
ALTITUDE =0.5000E+04
POLARIZATION- VERT
ANTENNA
TRANSMIT-OMNI
RECEIVE- OMNI
20 LOG(E/E0)
10
0
-10
-20
-30
0
2
4
6
8
10
12
DISTANCE(MILES)

Figure C25

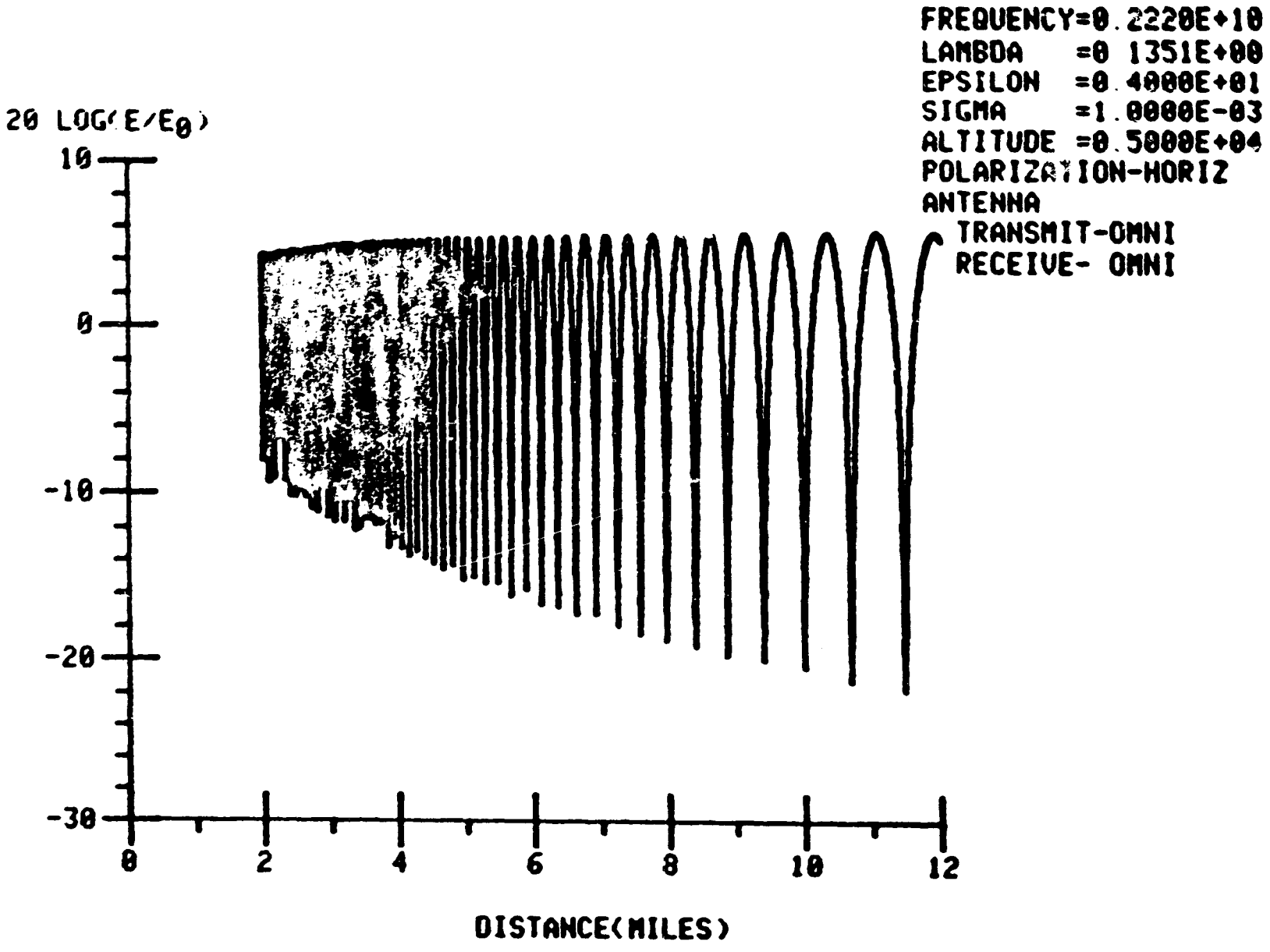
FREQUENCY=0.2220E+10
LAMBDA =0 1351E+00
EPSILON =0.4000E+01
SIGMA =1.0000E-03
ALTITUDE =0.5000E+04
POLARIZATION-HORIZ
ANTENNA
TRANSMIT-OMNI
RECEIVE- OMNI
20 LOG(E/E0)
10
0
-10
-20
-30
0
2
4
6
8
10
12
DISTANCE(MILES)

Figure C26

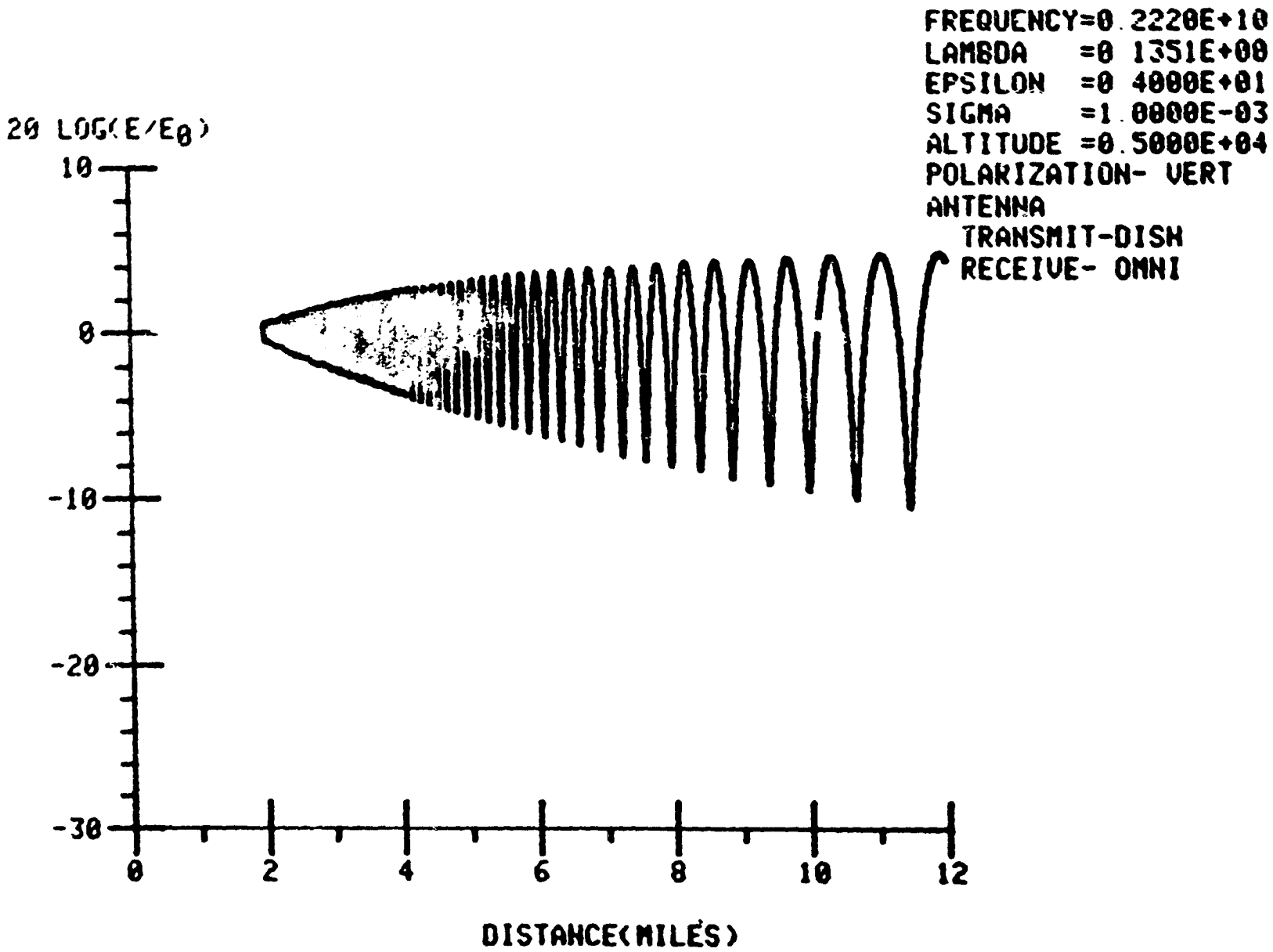
FREQUENCY=0.2220E+10
LAMBDA =0.1351E+00
EPSILON =0.4000E+01
SIGMA =1.0000E-03
ALTITUDE =0.5000E+04
POLARIZATION- VERT
ANTENNA
TRANSMIT-DISH
RECEIVE- OMNI
20 LOG(E/E0)
10
0
-10
-20
-30
0
2
4
6
8
10
12
DISTANCE(MILES)

Figure C27

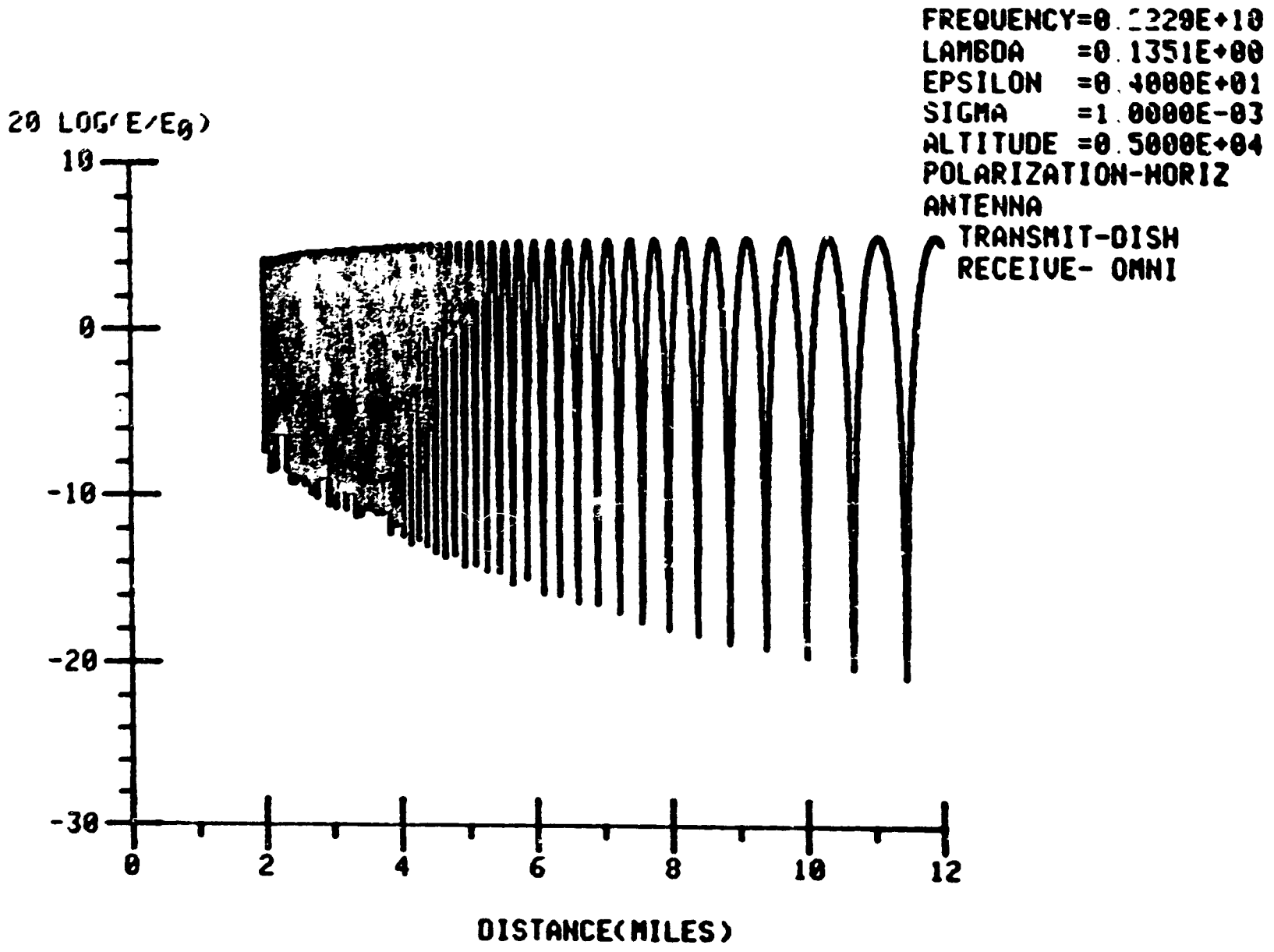
FREQUENCY=0.3220E+10
LAMBDA =0.1351E+00
EPSILON =0.4000E+01
SIGMA =1.0000E-03
ALTITUDE =0.5000E+04
POLARIZATION-HORIZ
ANTENNA
TRANSMIT-DISH
RECEIVE- OMNI
20 LOG(E/Eo)
10
0
-10
-20
-30
0
2
4
6
8
10
12
DISTANCE(MILES)

Figure C28

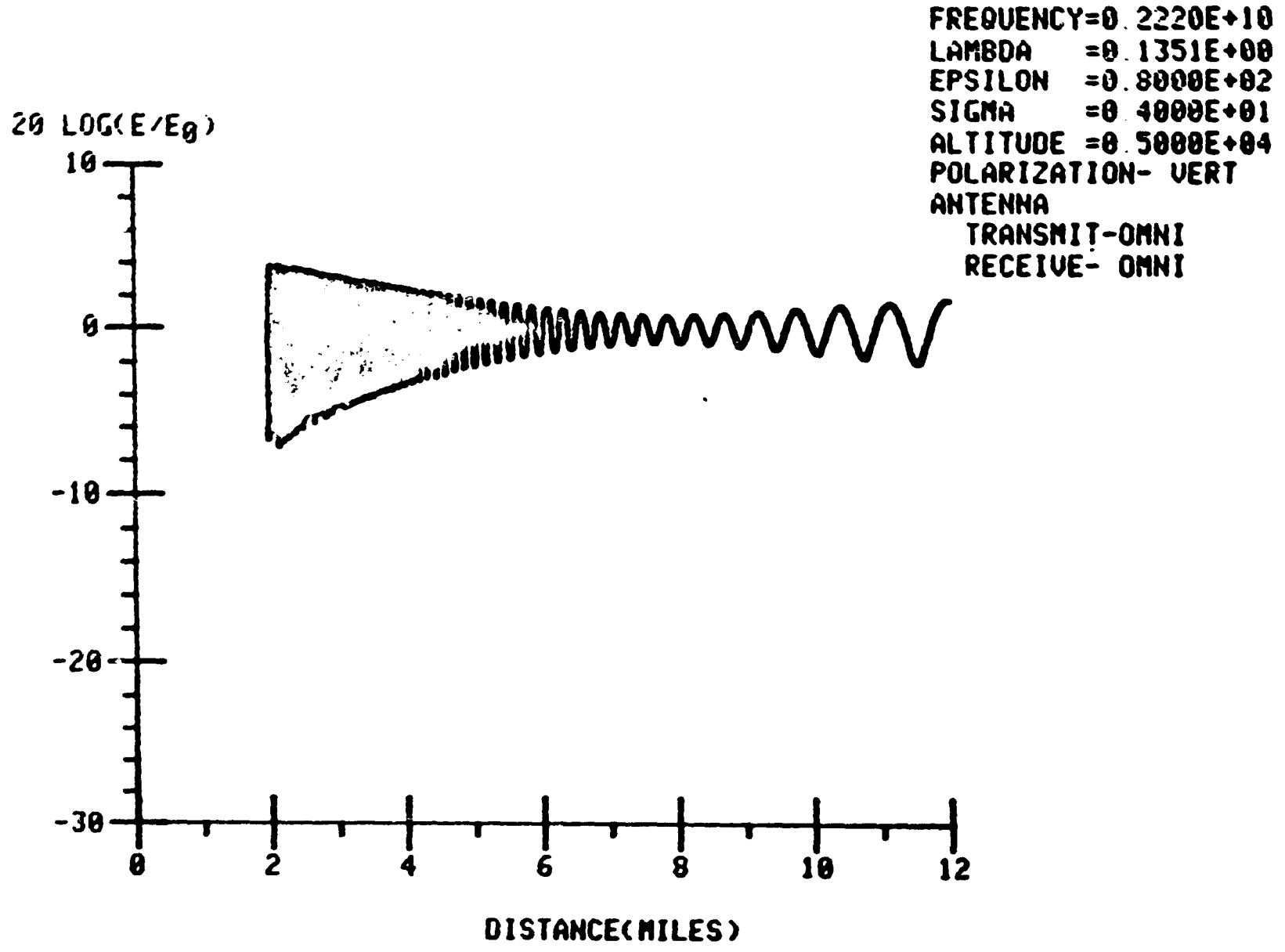
FREQUENCY=0.2220E+10
LAMBDA =0.1351E+00
EPSILON =0.8000E+02
SIGMA =0.4000E+01
ALTITUDE =0.5000E+04
POLARIZATION- VERT
ANTENNA
TRANSMIT-OMNI
RECEIVE- OMNI
20 LOG(E/Eo)
10
0
-10
-20
-30
0
2
4
6
8
10
12
DISTANCE(MILES)

Figure C29

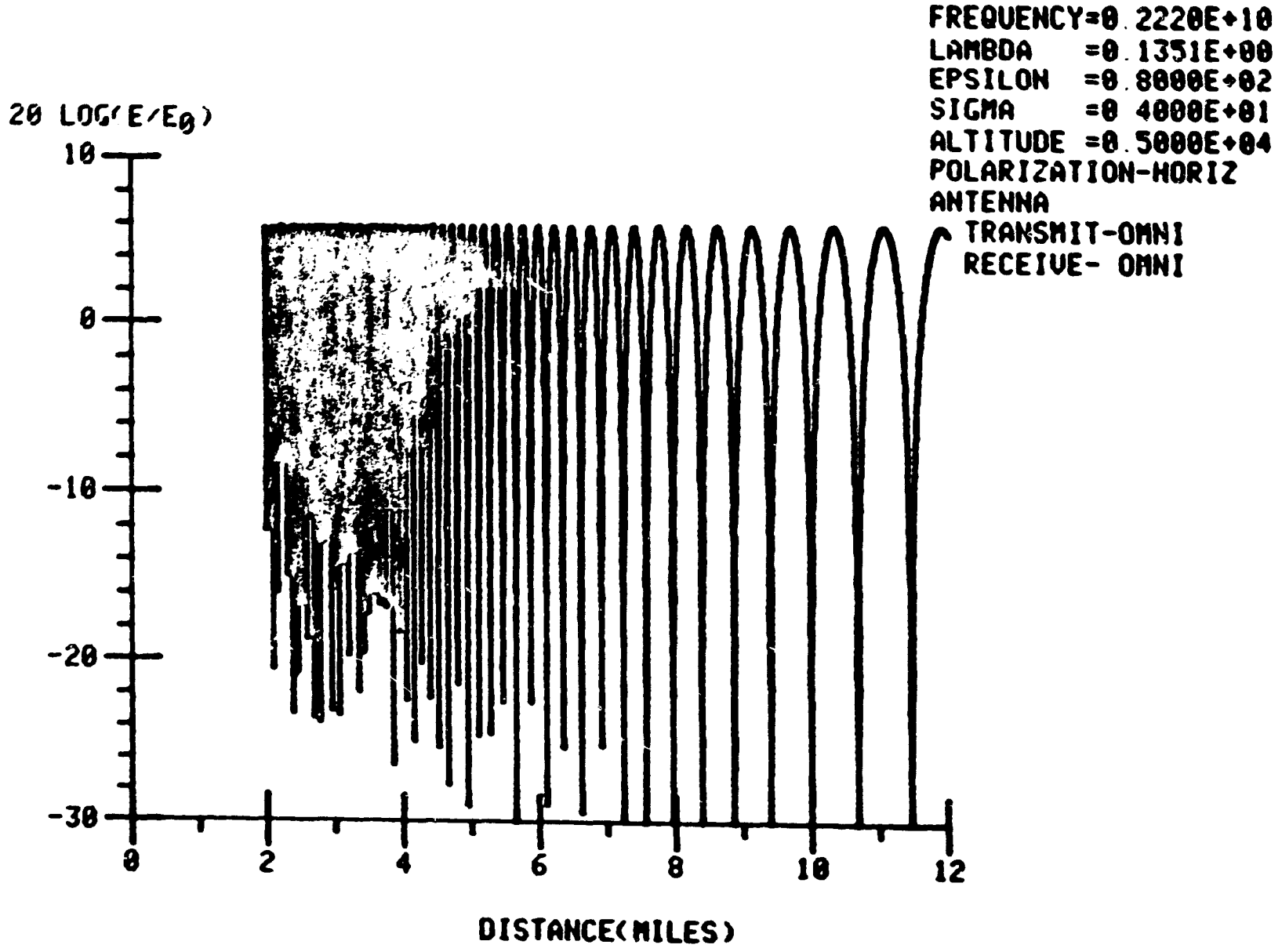
FREQUENCY=0.2220E+10
LAMBDA =0.1351E+00
EPSILON =0.8000E+02
SIGMA =0.4000E+01
ALTITUDE =0.5000E+04
POLARIZATION-HORIZ
ANTENNA
TRANSMIT-OMNI
RECEIVE- OMNI
20 LOG(E/E0)
10
0
-10
-20
-30
0
2
4
6
8
10
12
DISTANCE(MILES)

Figure C30

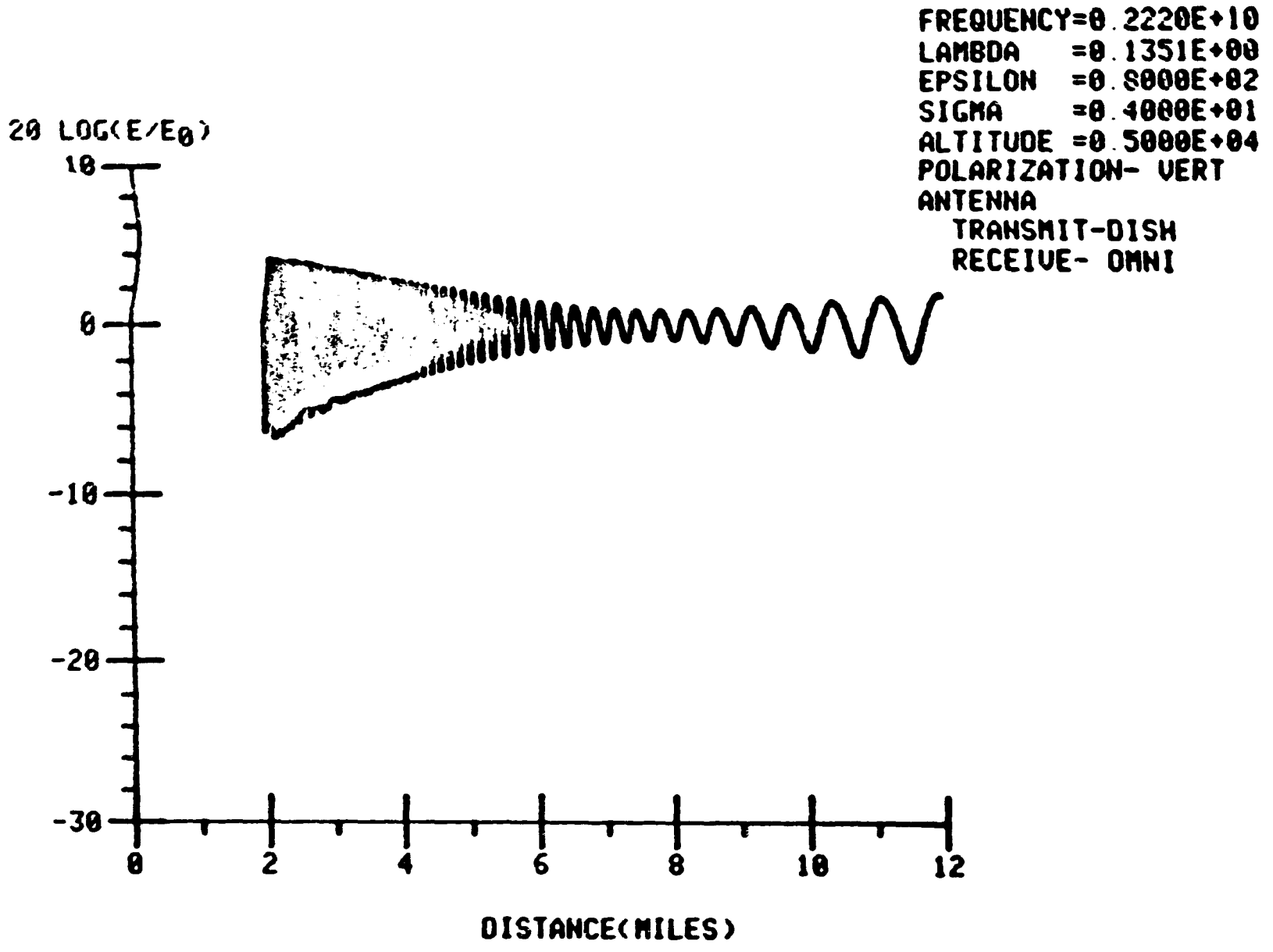
FREQUENCY=0.2220E+10
LAMBDA =0.1351E+00
EPSILON =0.8000E+02
SIGMA =0.4000E+01
ALTITUDE =0.5000E+04
POLARIZATION- VERT
ANTENNA
TRANSMIT-DISH
RECEIVE- OMNI
20 LOG(E/E0)
10
0
-10
-20
-30
0
2
4
6
8
10
12
DISTANCE(MILES)

Figure C31

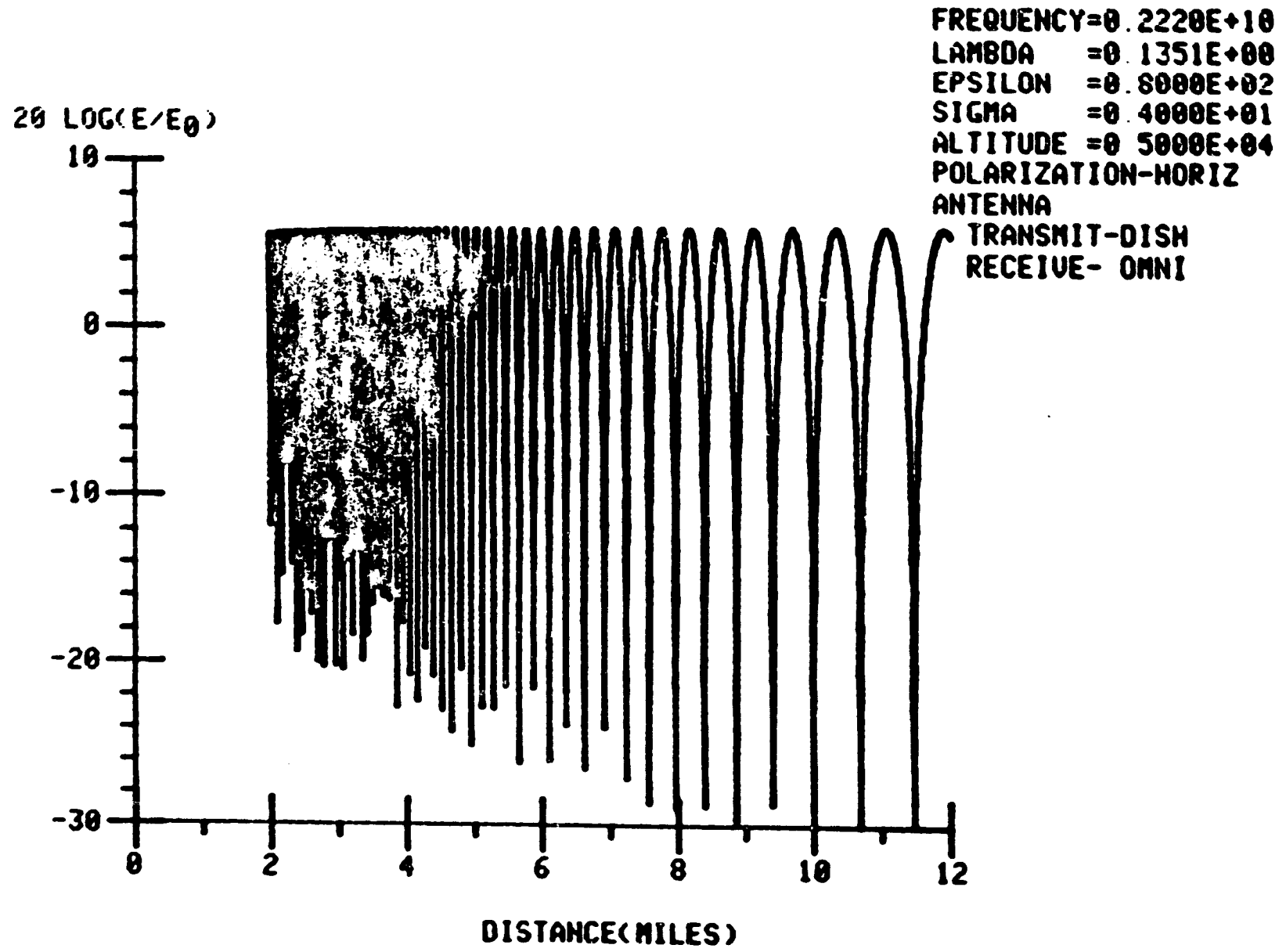

Figure C32

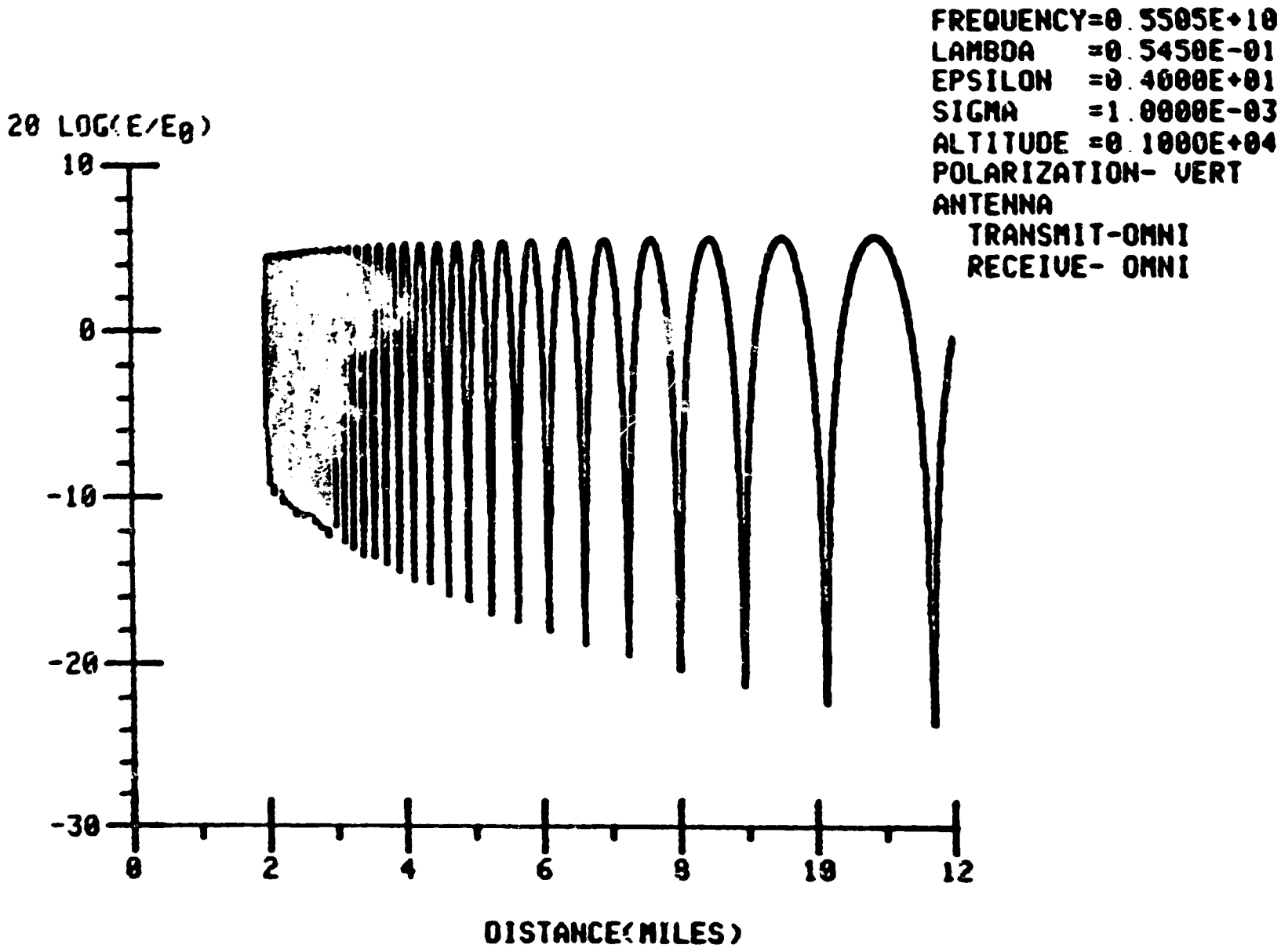
FREQUENCY=0.5505E+10
LAMBDA =0.5450E-01
EPSILON =0.4000E+01
SIGMA =1.0000E-03
ALTITUDE =0.1000E+04
POLARIZATION- VERT
ANTENNA
TRANSMIT-OMNI
RECEIVE- OMNI
20 LOG(E/E0)
10
0
-10
-20
-30
0
2
4
6
8
10
12
DISTANCE(MILES)

Figure C33

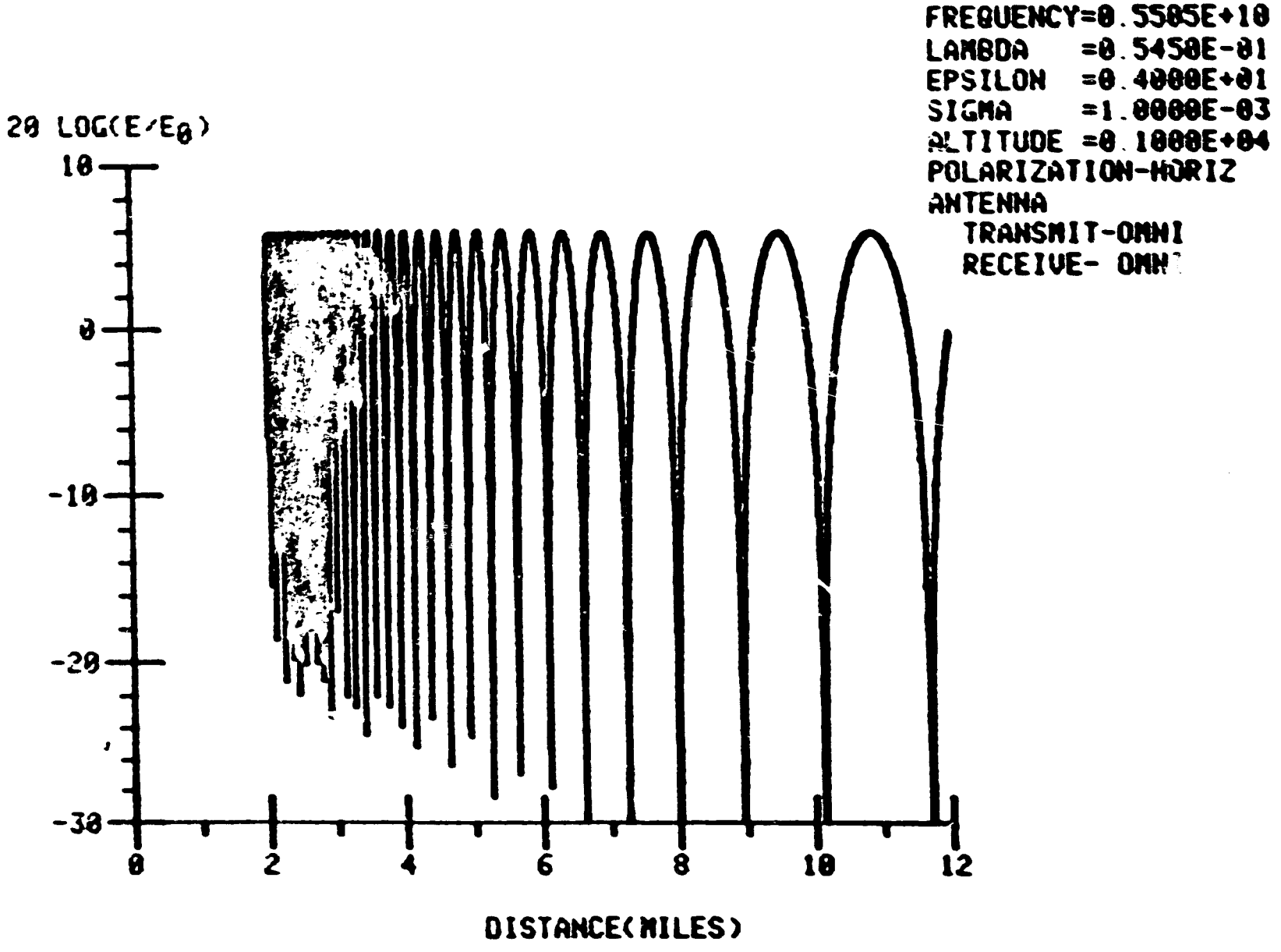
FREQUENCY=0.5585E+10
LAMBDA =0.5450E-01
EPSILON =0.4000E+01
SIGMA =1.0000E-03
ALTITUDE =0.1000E+04
POLARIZATION-HORIZ
ANTENNA
TRANSMIT-OMNI
RECEIVE- OMNI
20 LOG(E/E0)
10
0
-10
-20
-30
0
2
4
6
8
10
12
DISTANCE(MILES)

Figure C34

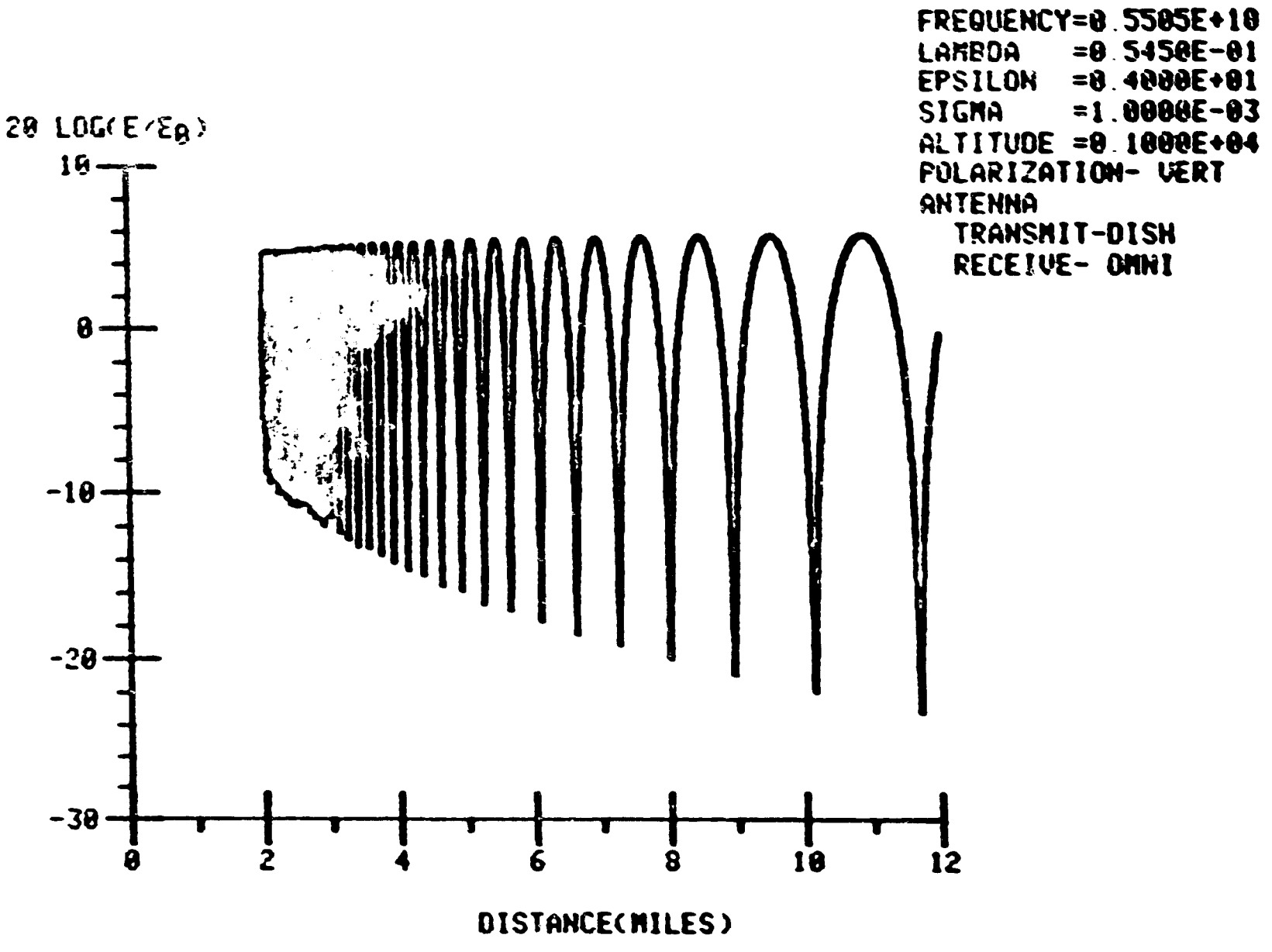
FREQUENCY=0.5585E+10
LAMBDA =0.5450E-01
EPSILON =0.4000E+01
SIGMA =1.0000E-03
ALTITUDE =0.1000E+04
POLARIZATION- VERT
ANTENNA
TRANSMIT-DISH
RECEIVE- OMNI
20 LOG(E/E0)
10
0
-10
-20
-30
0
2
4
6
8
10
12
DISTANCE(MILES)

Figure C35

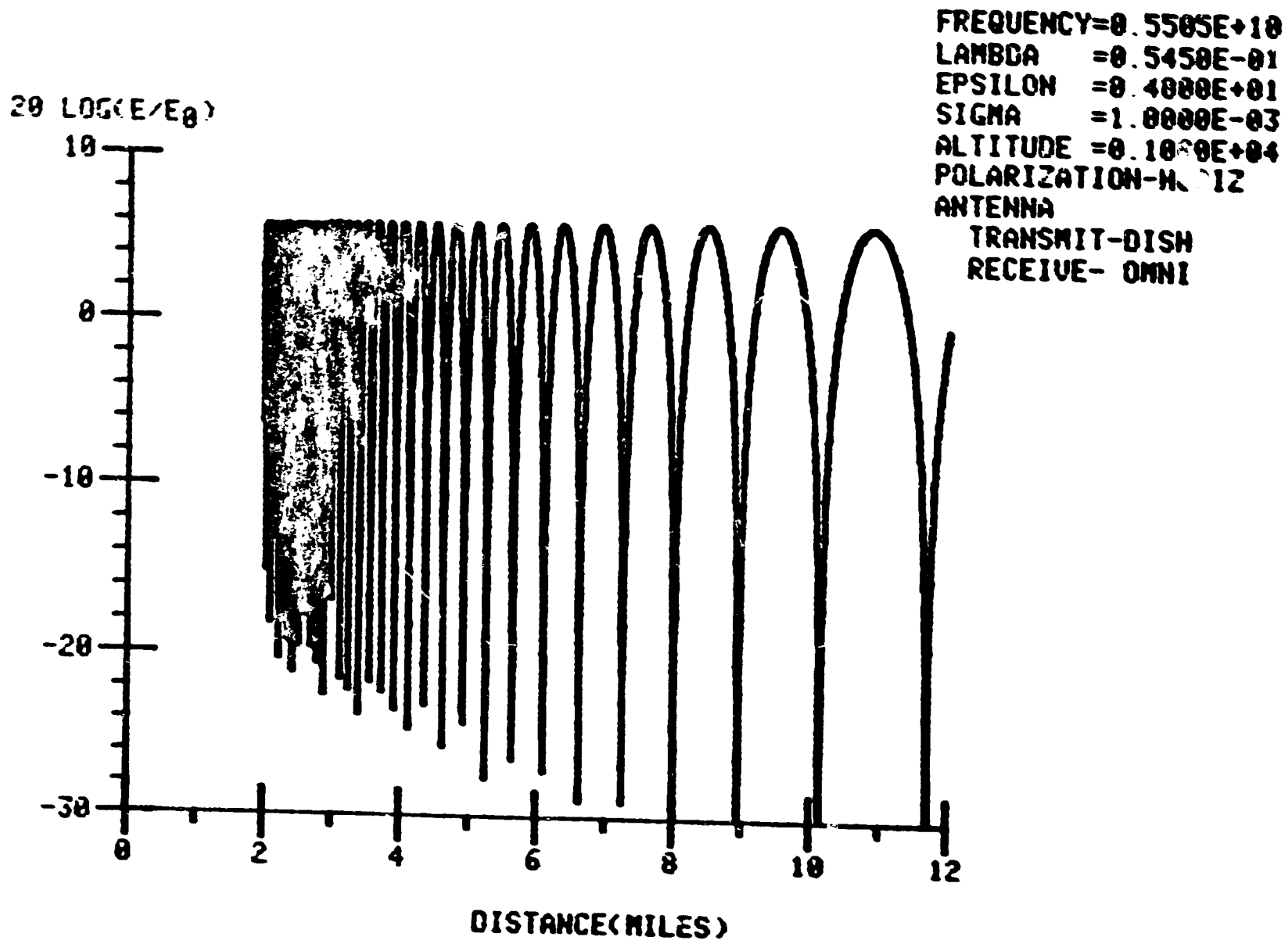
FREQUENCY=0.5505E+10
LAMBDA =0.5450E-01
EPSILON =0.4000E+01
SIGMA =1.0000E-03
ALTITUDE =0.10[illegible]0E+04
POLARIZATION-H[illegible]12
ANTENNA
TRANSMIT-DISH
RECEIVE- OMNI
20 LOG(E/E0)
10
0
-10
-20
-30
0
2
4
6
8
10
12
DISTANCE(MILES)

Figure C36

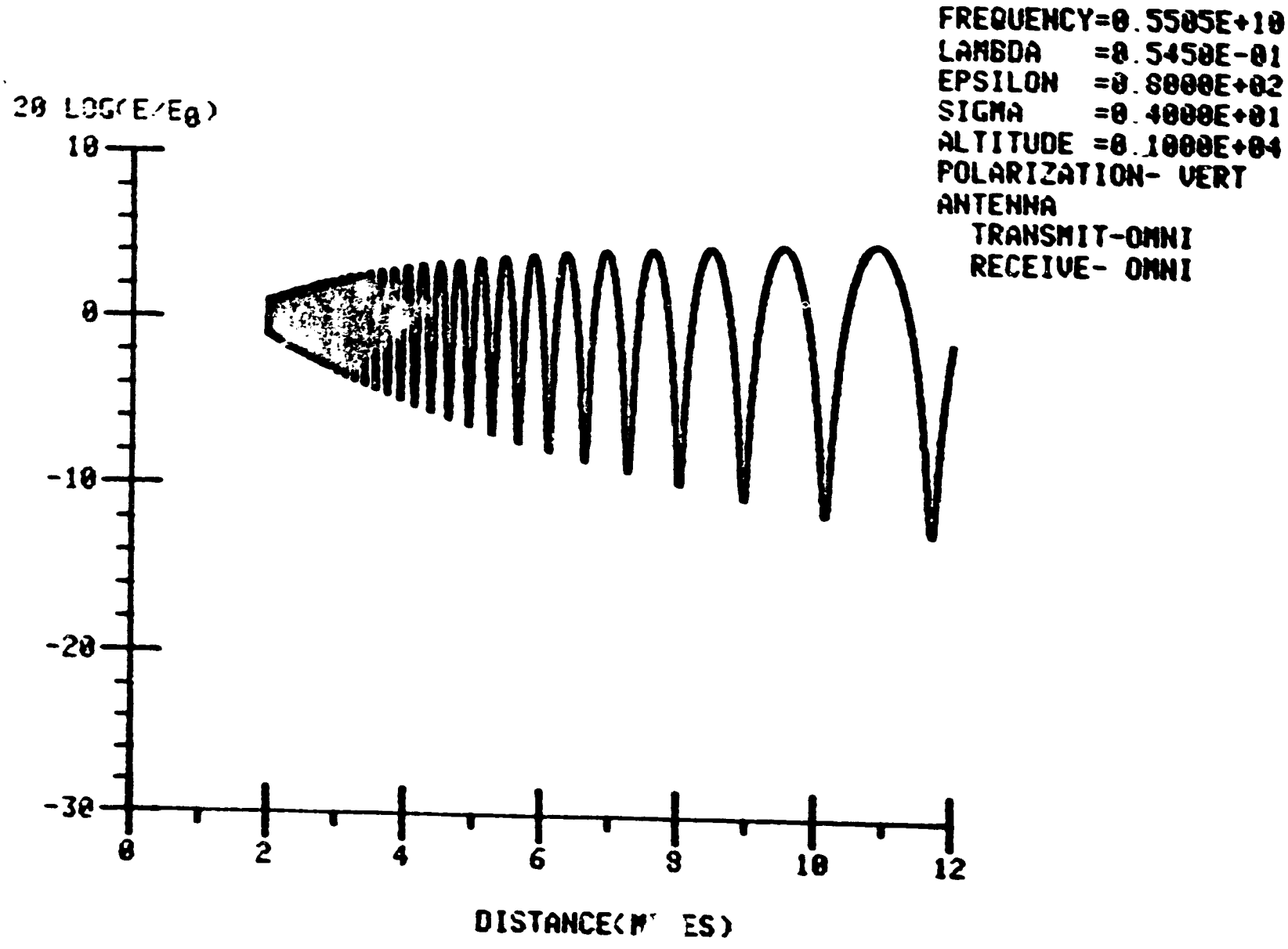
FREQUENCY=0.5505E+10
LAMBDA =0.5450E-01
EPSILON =0.8000E+02
SIGMA =0.4000E+01
ALTITUDE =0.1000E+04
POLARIZATION- VERT
ANTENNA
TRANSMIT-OMNI
RECEIVE- OMNI
20 LOG(E/E0)
10
0
-10
-20
-30
0
2
4
6
8
10
12
DISTANCE(M' ES)

Figure C37

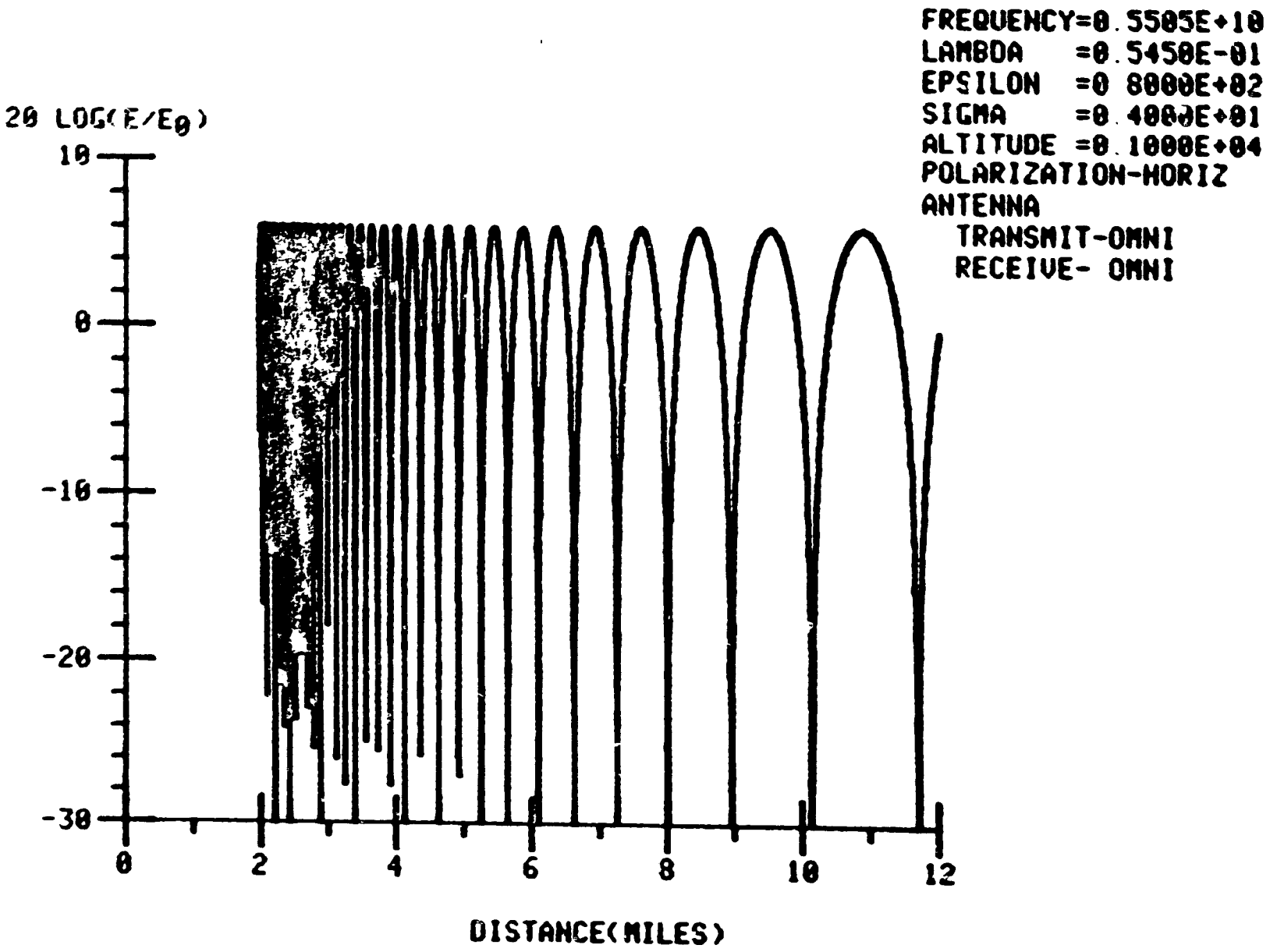
FREQUENCY=0.5585E+10
LAMBDA =0.5450E-01
EPSILON =0 8000E+02
SIGMA =0.4000E+01
ALTITUDE =0.1000E+04
POLARIZATION-HORIZ
ANTENNA
TRANSMIT-OMNI
RECEIVE- OMNI
20 LOG(E/E0)
10
0
-10
-20
-30
0
2
4
6
8
10
12
DISTANCE(MILES)

Figure C38

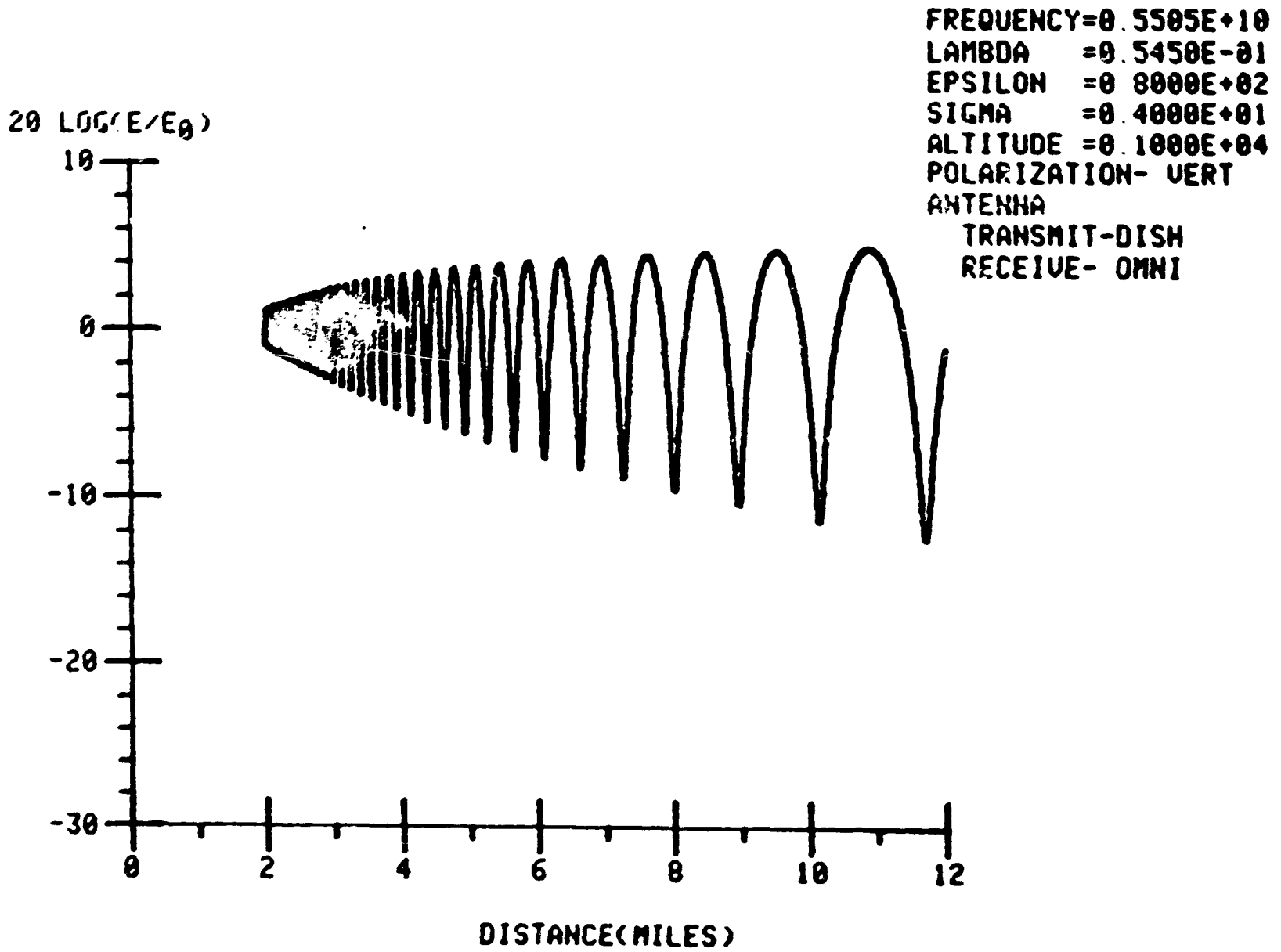
FREQUENCY=0.5585E+10
LAMBDA =0.5450E-01
EPSILON =0 8000E+02
SIGMA =0.4000E+01
ALTITUDE =0.1000E+04
POLARIZATION- VERT
ANTENNA
TRANSMIT-DISH
RECEIVE- OMNI
20 LOG(E/E0)
10
0
-10
-20
-30
0
2
4
6
8
10
12
DISTANCE(MILES)

Figure 630

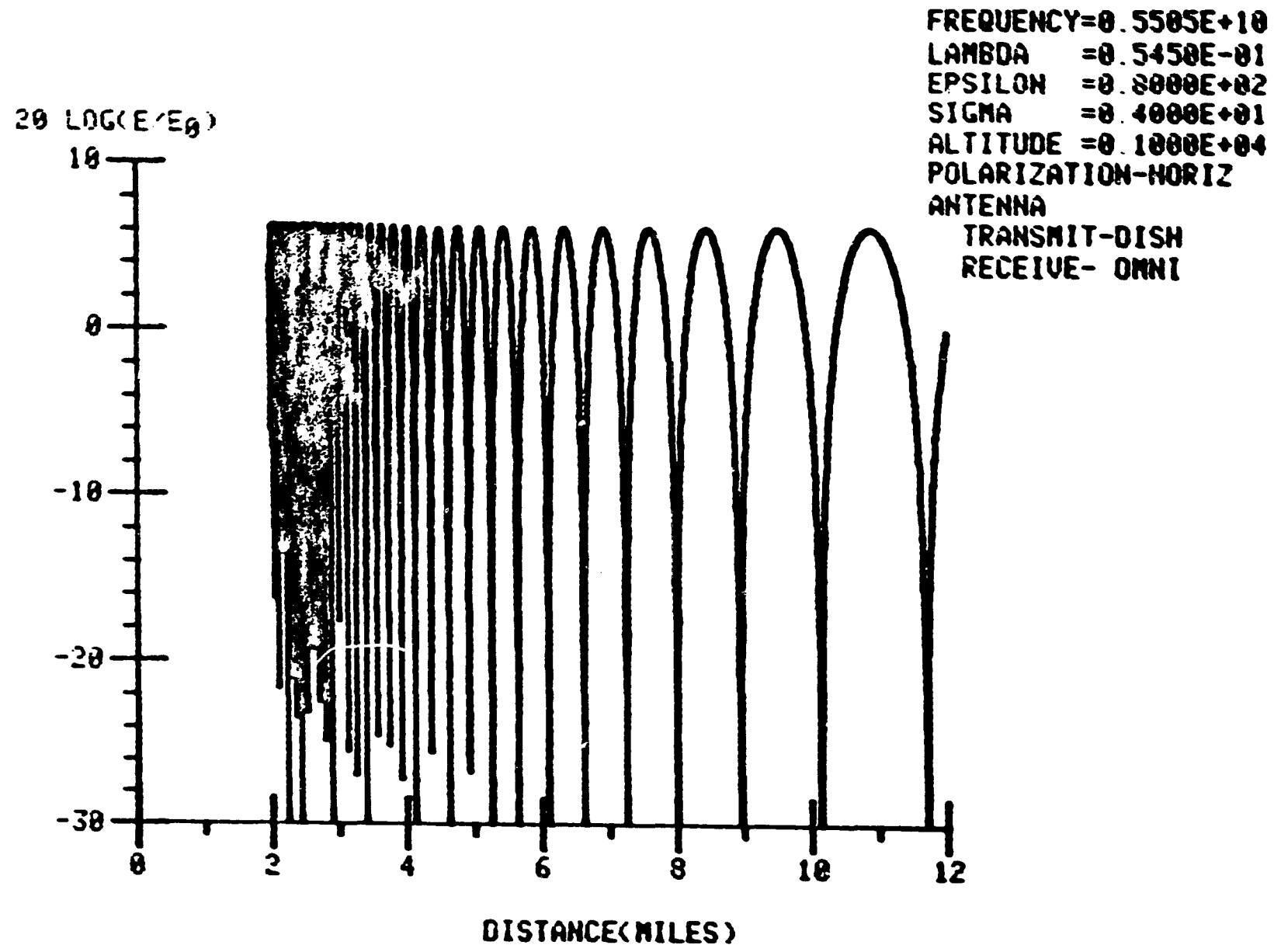
FREQUENCY=0.5585E+10
LAMBDA =0.5450E-01
EPSILON =0.8000E+02
SIGMA =0.4000E+01
ALTITUDE =0.1000E+04
POLARIZATION-HORIZ
ANTENNA
TRANSMIT-DISH
RECEIVE- OMNI
20 LOG(E/E0)
10
0
-10
-20
-30
0
2
4
6
8
10
12
DISTANCE(MILES)

Figure C40

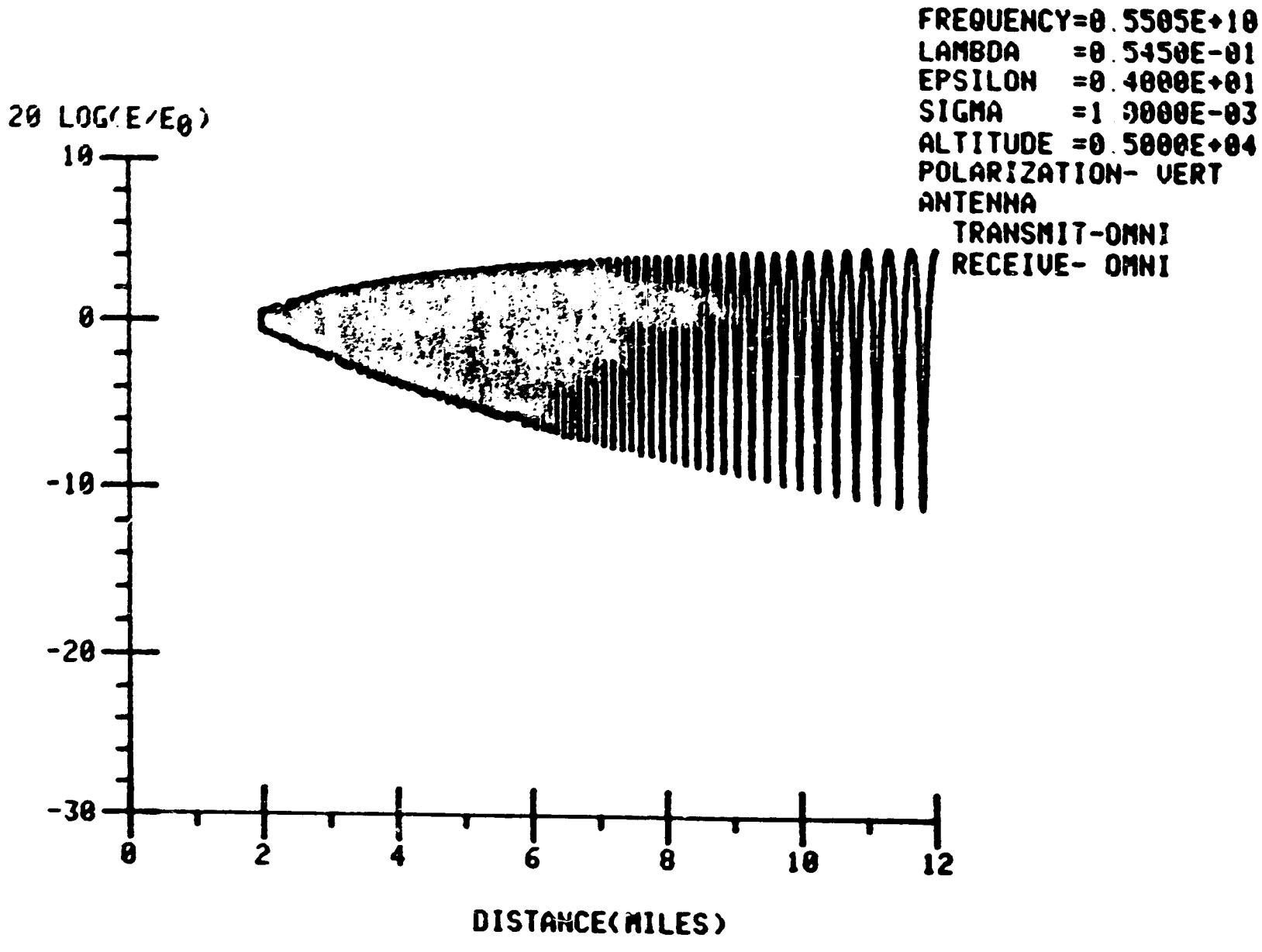
FREQUENCY=0.5505E+10
LAMBDA =0.5450E-01
EPSILON =0.4000E+01
SIGMA =1.0000E-03
ALTITUDE =0.5000E+04
POLARIZATION- VERT
ANTENNA
TRANSMIT-OMNI
RECEIVE- OMNI
20 LOG(E/E0)
10
0
-10
-20
-30
0
2
4
6
8
10
12
DISTANCE(MILES)

Figure C41

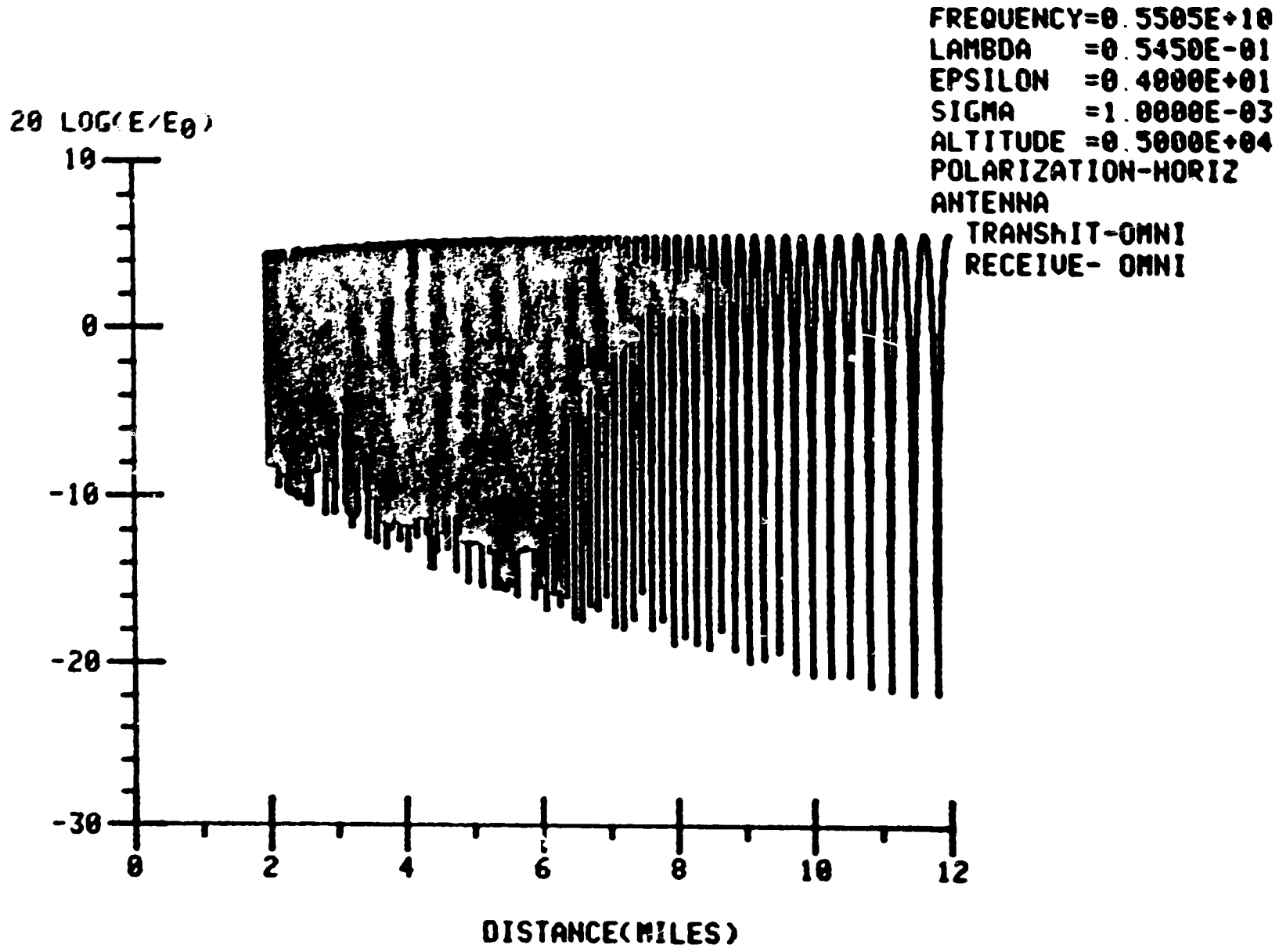
FREQUENCY=0.5505E+10
LAMBDA =0.5450E-01
EPSILON =0.4000E+01
SIGMA =1.0000E-03
ALTITUDE =0.5000E+04
POLARIZATION-HORIZ
ANTENNA
TRANSMIT-OMNI
RECEIVE- OMNI
20 LOG(E/E0)
10
0
-10
-20
-30
0
2
4
6
8
10
12
DISTANCE(MILES)

Figure C42

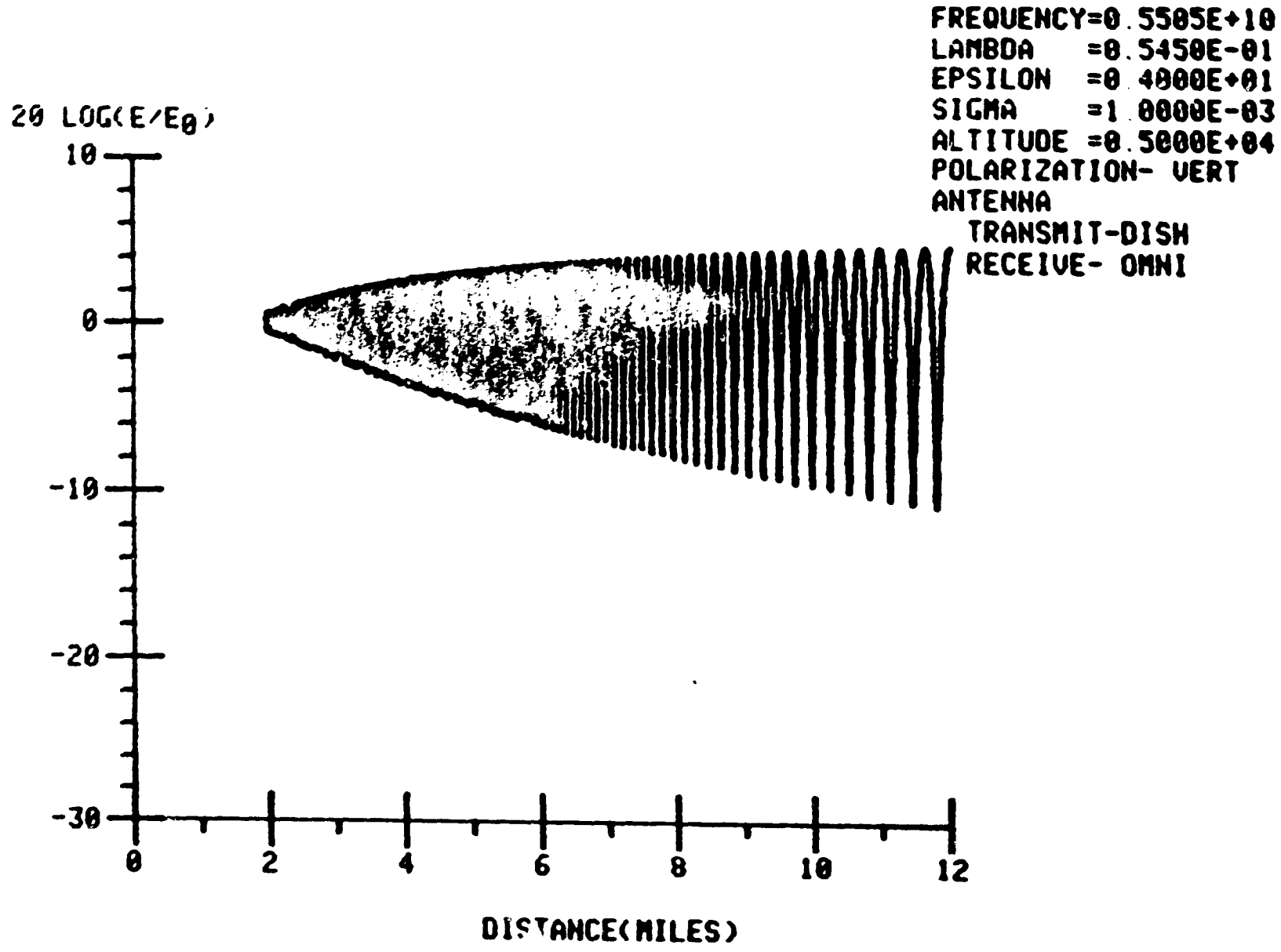

Figure C43

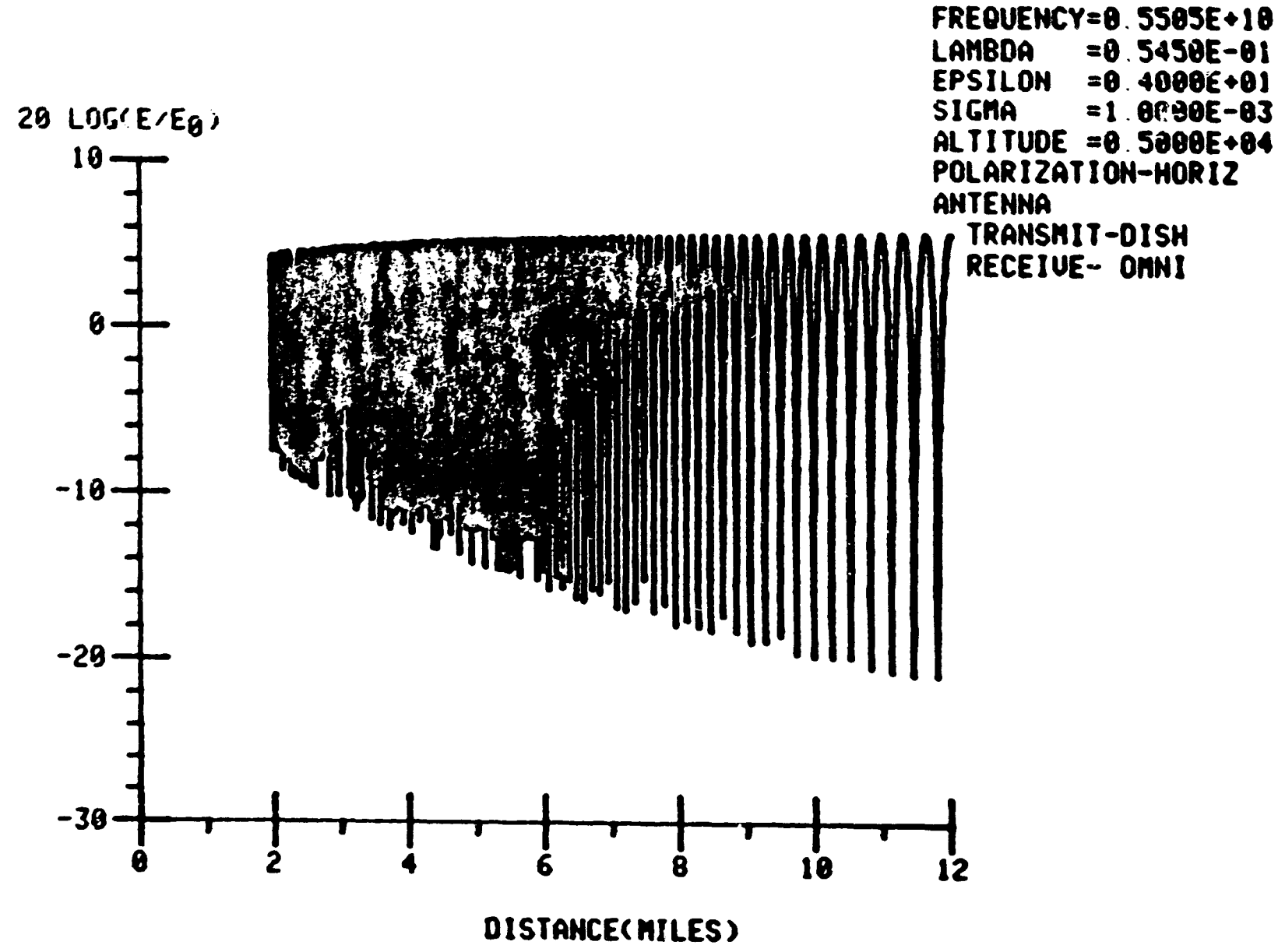

Figure C44

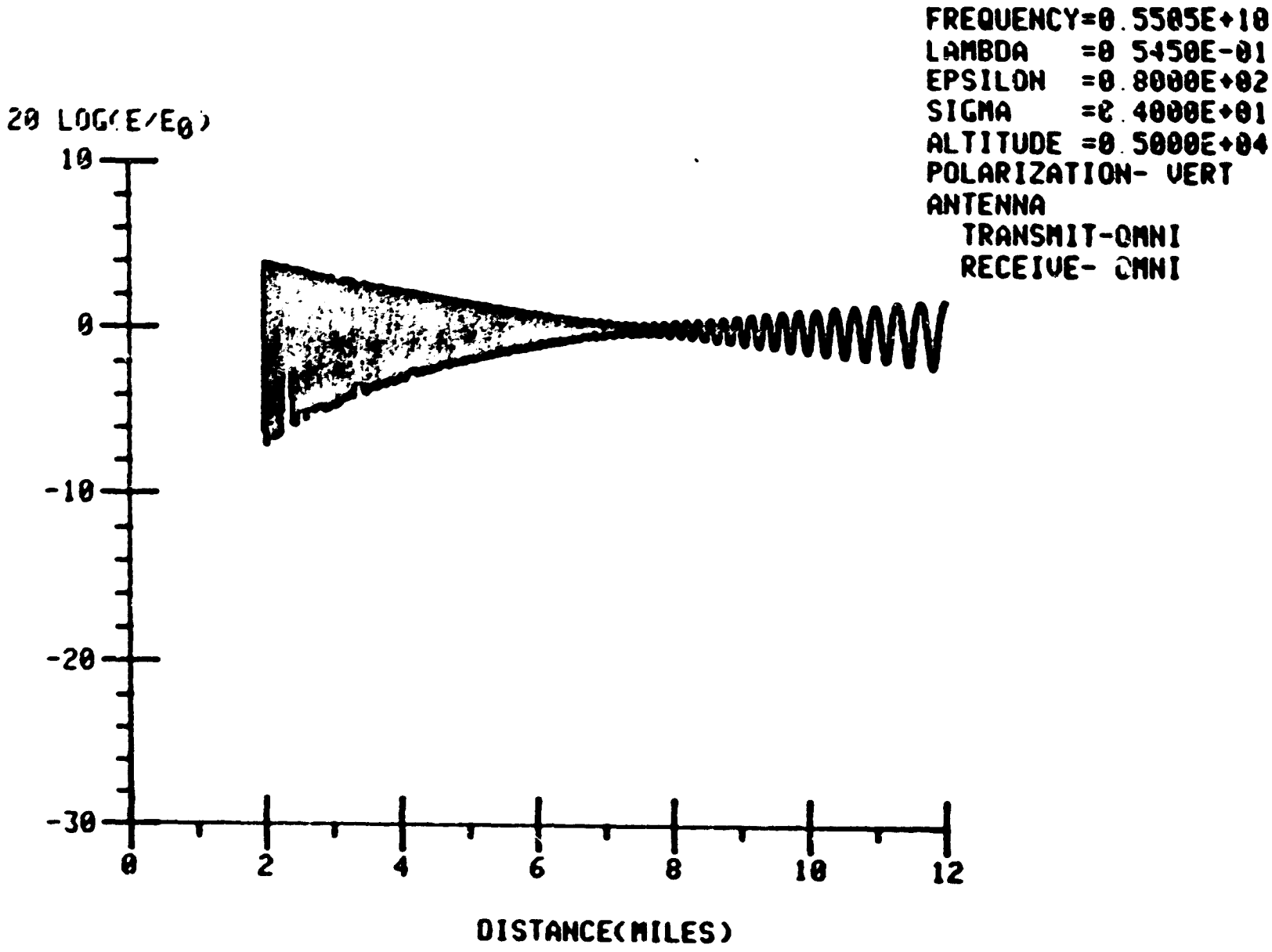
FREQUENCY=0.5585E+10
LAMBDA =0.5450E-01
EPSILON =0.8000E+02
SIGMA =0.4000E+01
ALTITUDE =0.5000E+04
POLARIZATION- VERT
ANTENNA
TRANSMIT-OMNI
RECEIVE- OMNI
20 LOG(E/E0)
10
0
-10
-20
-30
0
2
4
6
8
10
12
DISTANCE(MILES)

Figure C45

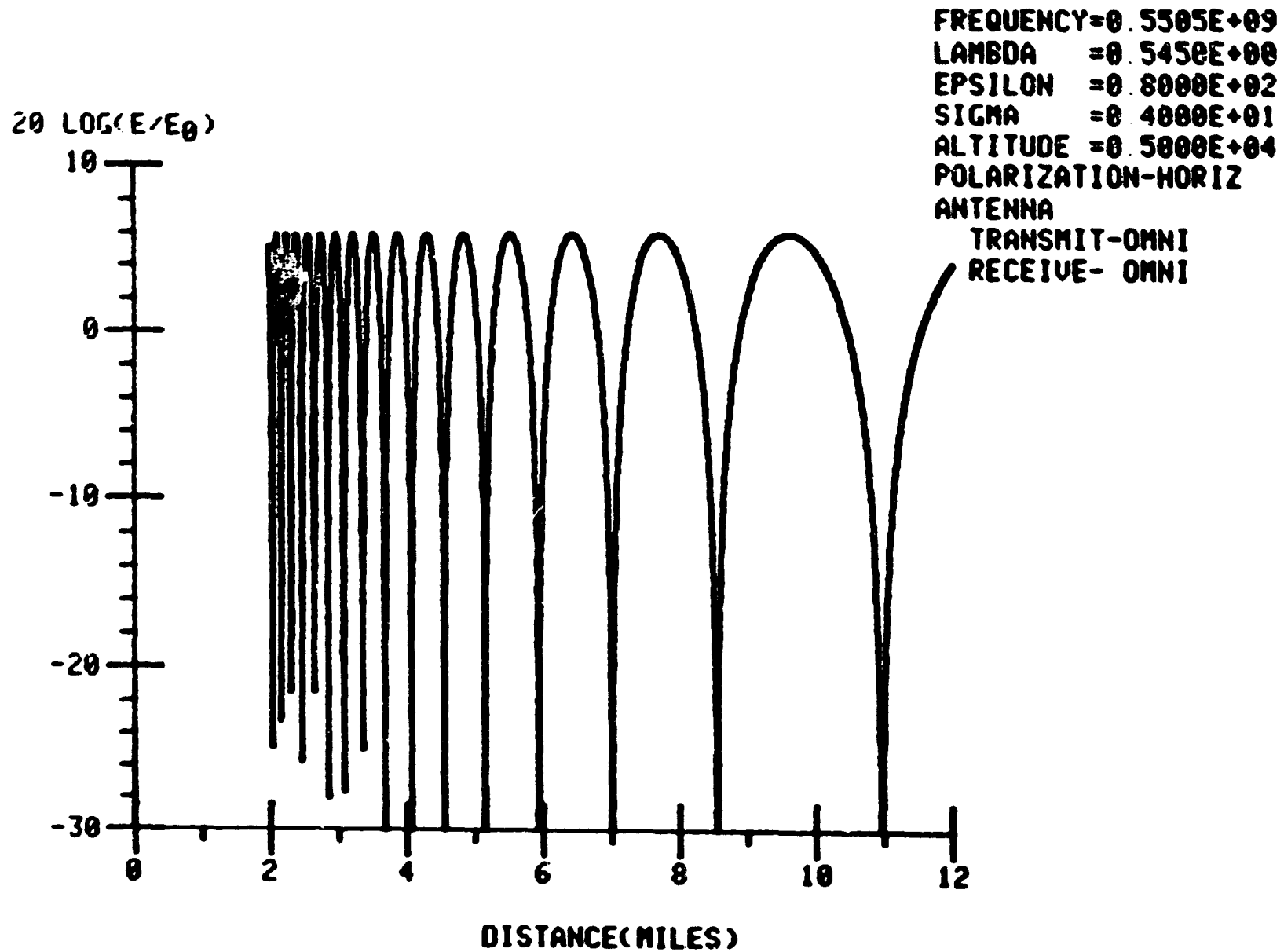
FREQUENCY=0.5505E+09
LAMBDA =0.5450E+00
EPSILON =0.8000E+02
SIGMA =0.4000E+01
ALTITUDE =0.5000E+04
POLARIZATION-HORIZ
ANTENNA
TRANSMIT-OMNI
RECEIVE- OMNI
20 LOG(E/E0)
10
0
-10
-20
-30
0
2
4
6
8
10
12
DISTANCE(MILES)

Figure C46

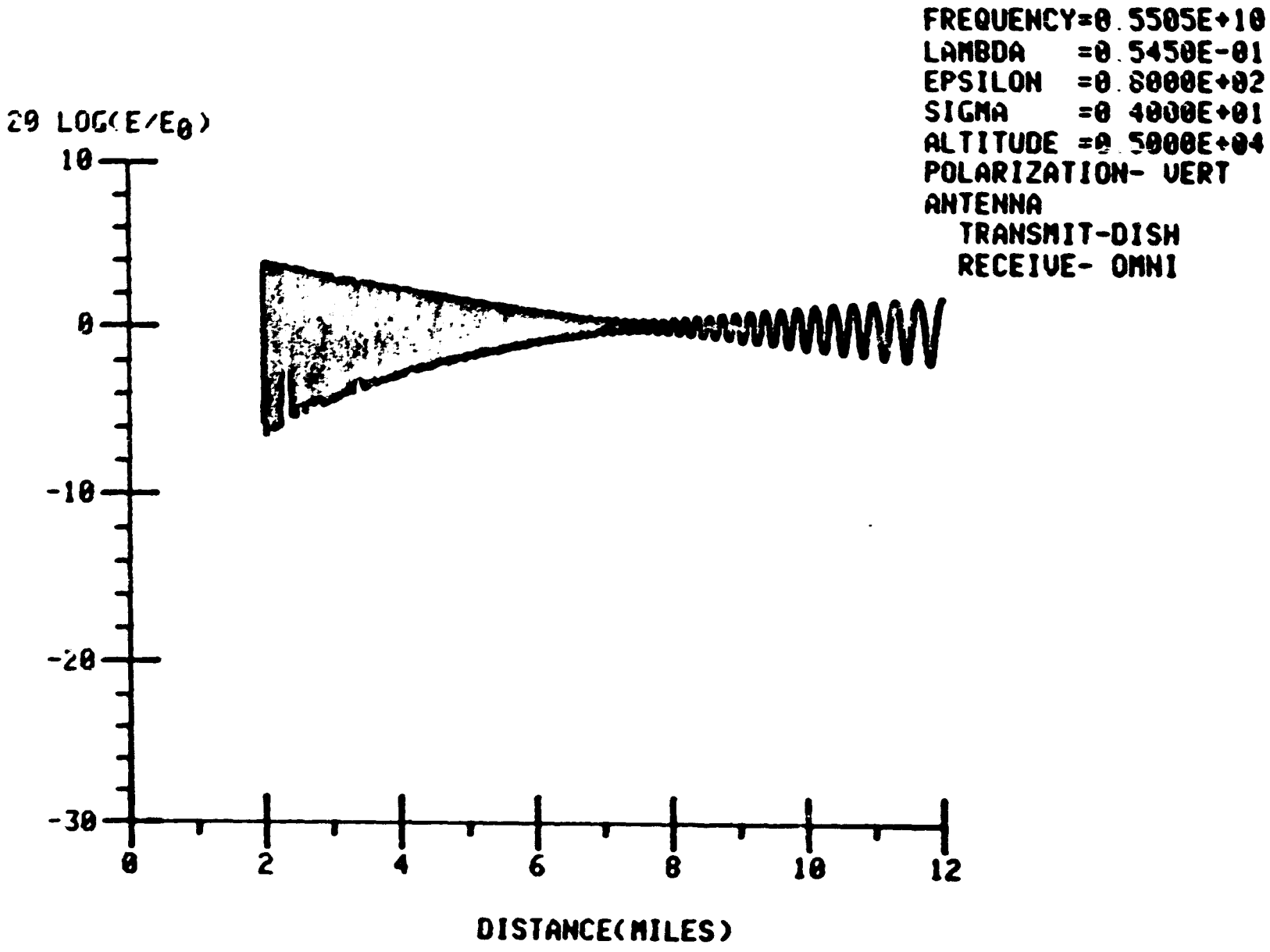
FREQUENCY=0.5505E+10
LAMBDA =0.5450E-01
EPSILON =0.8000E+02
SIGMA =0.4000E+01
ALTITUDE =0.5000E+04
POLARIZATION- VERT
ANTENNA
TRANSMIT-DISH
RECEIVE- OMNI
29 LOG(E/E0)
10
0
-10
-20
-30
0
2
4
6
8
10
12
DISTANCE(MILES)

Figure C47

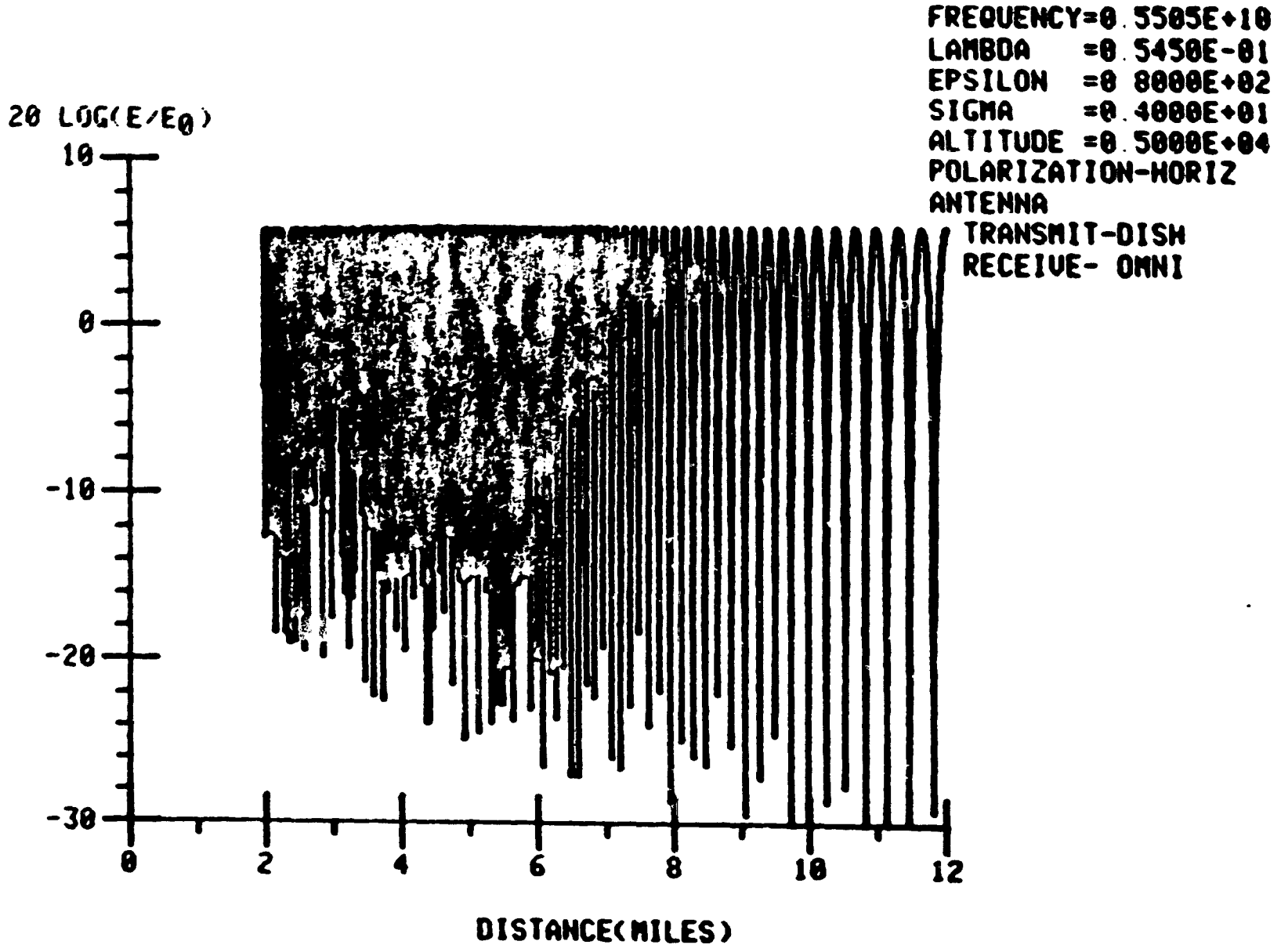
FREQUENCY=0.5505E+10
LAMBDA =0.5450E-01
EPSILON =0 8000E+02
SIGMA =0.4000E+01
ALTITUDE =0.5000E+04
POLARIZATION-HORIZ
ANTENNA
TRANSMIT-DISH
RECEIVE- OMNI
20 LOG(E/E0)
10
0
-10
-20
-30
0
2
4
6
8
10
12
DISTANCE(MILES)

Figure C48

APPENDIX D

SAMPLE SIGNALS FOR BOTH VERTICAL AND HORIZONTAL POLARIZATIONS IN THE 0.8 TO 3 KM RANGE

TABLE D

0.8 - 3 km Range

FIGURE	LAMBDA	ALTITUDE*	SIGMA	EPSILON	POLARIZATION	GAIN
D1	0.2000	1000 ft	0.001	4	V	no
D2	2000	1000 ft	4.000	80	V	no
D3	0.2000	2000 ft	0.001	4	V	no
D4	0.2000	2000 ft	4.000	80	V	no
D5	0.2000	5000 ft	0.001	4	V	no
D6	0.2000	5000 ft	4.000	80	V	no
D7	0.1351	1000 ft	0.001	4	V	no
D8	0.1351	1000 ft	4.000	80	V	no
D9	0.1351	2000 ft	0.001	4	V	no
D10	0.1351	2000 ft	4.000	80	V	no
D11	0.1351	5000 ft	0.001	4	V	no
D12	0.1351	5000 ft	4.000	80	V	no
D13	0.0545	1000 ft	0.001	4	V	no
D14	0.0545	1000 ft	4.000	80	V	no
D15	0.0545	2000 ft	0.001	4	V	no
D16	0.0545	2000 ft	4.000	80	V	no
D17	0.0545	5000 ft	0.001	4	V	no
D18	0.0545	5000 ft	4.000	80	V	no

* 1000 ft = 305 m, 2000 ft = 610 m, 5000 ft = 1524 m

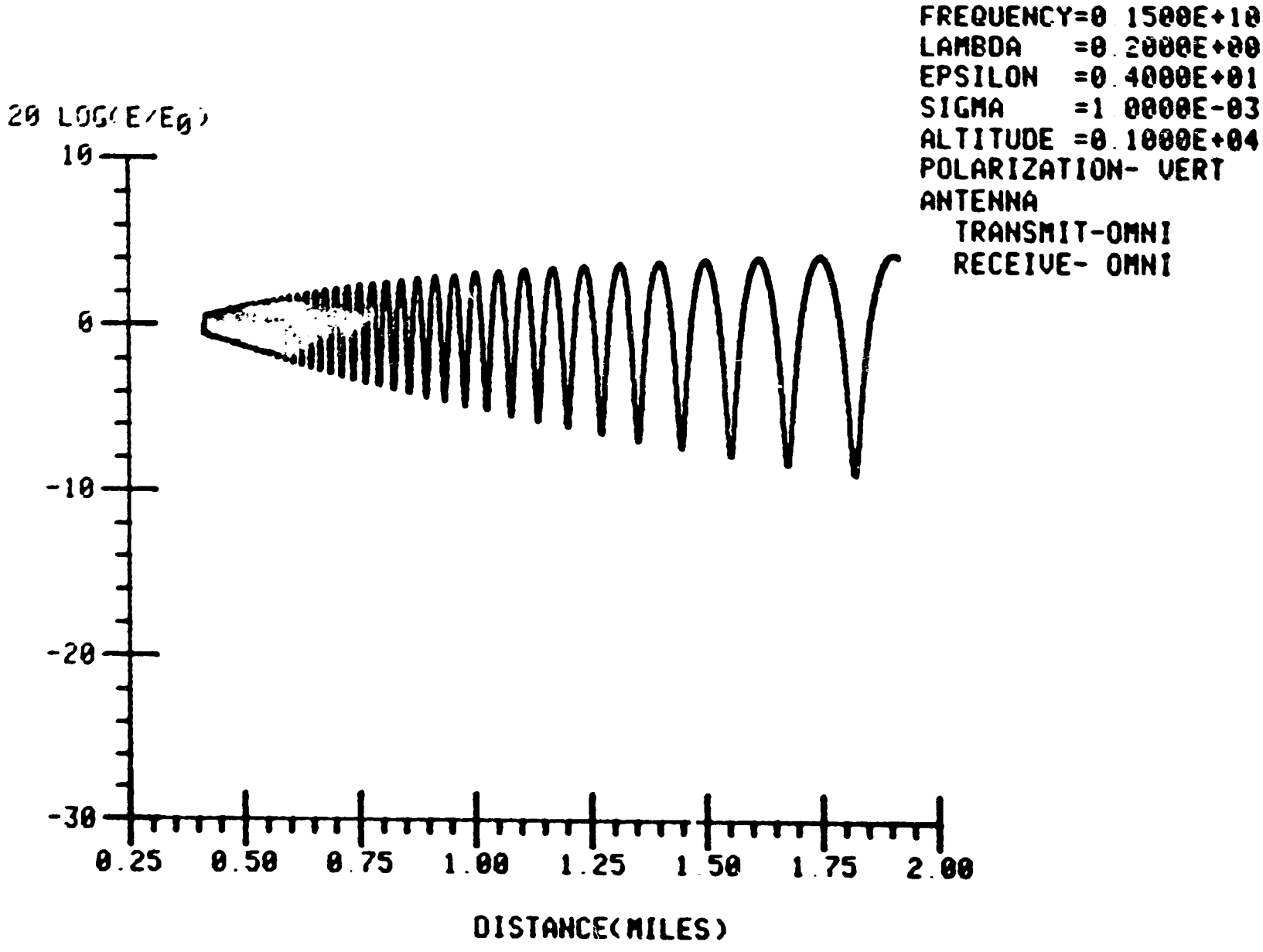
FREQUENCY=0 1500E+10
LAMBDA =0 2000E+00
EPSILON =0 4000E+01
SIGMA =1 0000E-03
ALTITUDE =0 1000E+04
POLARIZATION- VERT
ANTENNA
TRANSMIT-OMNI
RECEIVE- OMNI
20 LOG(E/E0)
10
0
-10
-20
-30
0.25
0.50
0.75
1.00
1.25
1.50
1.75
2.00
DISTANCE(MILES)

Figure D1

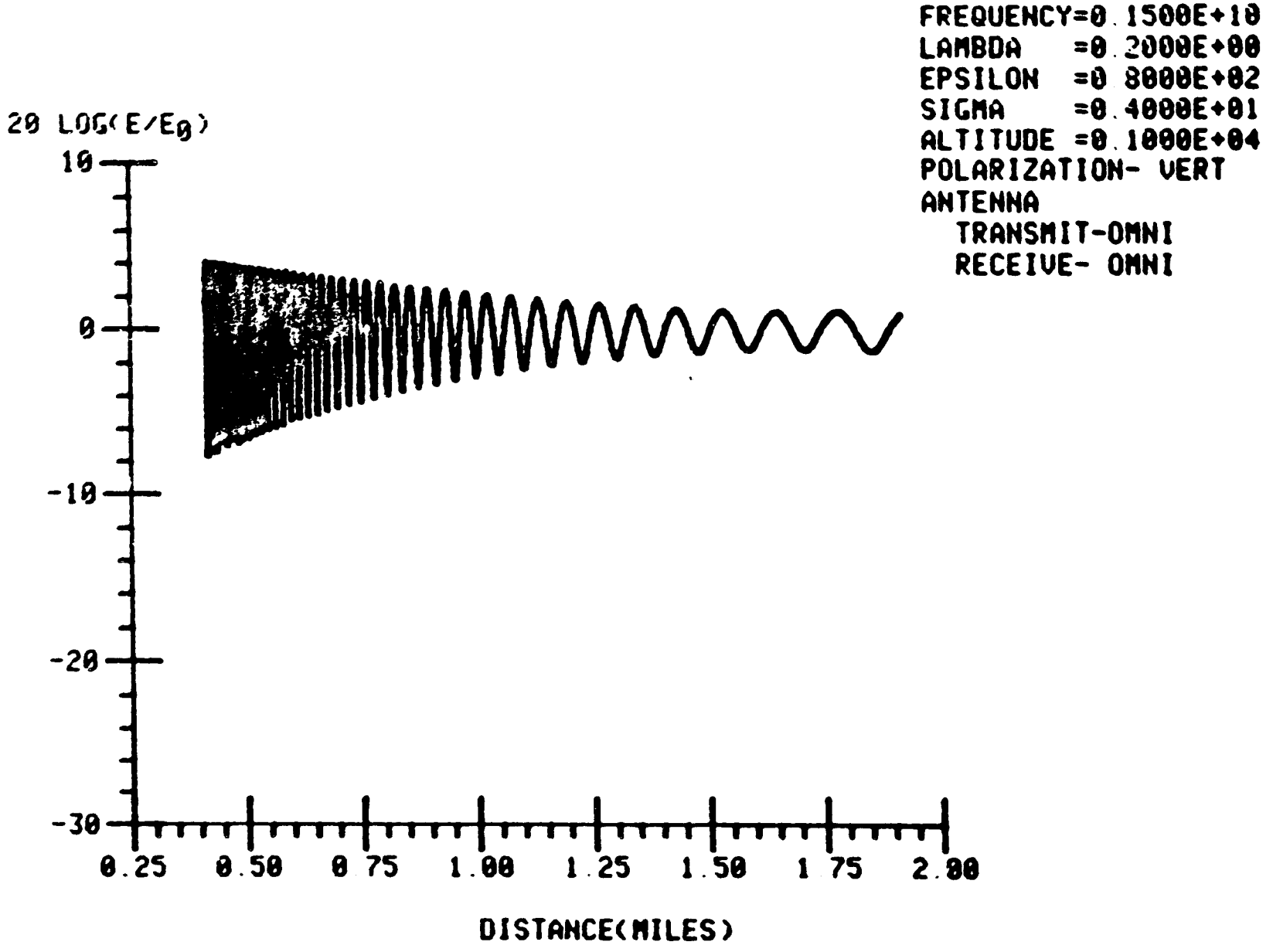
FREQUENCY=0.1500E+10
LAMBDA =0.2000E+00
EPSILON =0.8000E+02
SIGMA =0.4000E+01
ALTITUDE =0.1000E+04
POLARIZATION- VERT
ANTENNA
TRANSMIT-OMNI
RECEIVE- OMNI
20 LOG(E/E0)
10
0
-10
-20
-30
0.25
0.50
0.75
1.00
1.25
1.50
1.75
2.00
DISTANCE(MILES)

Figure D2

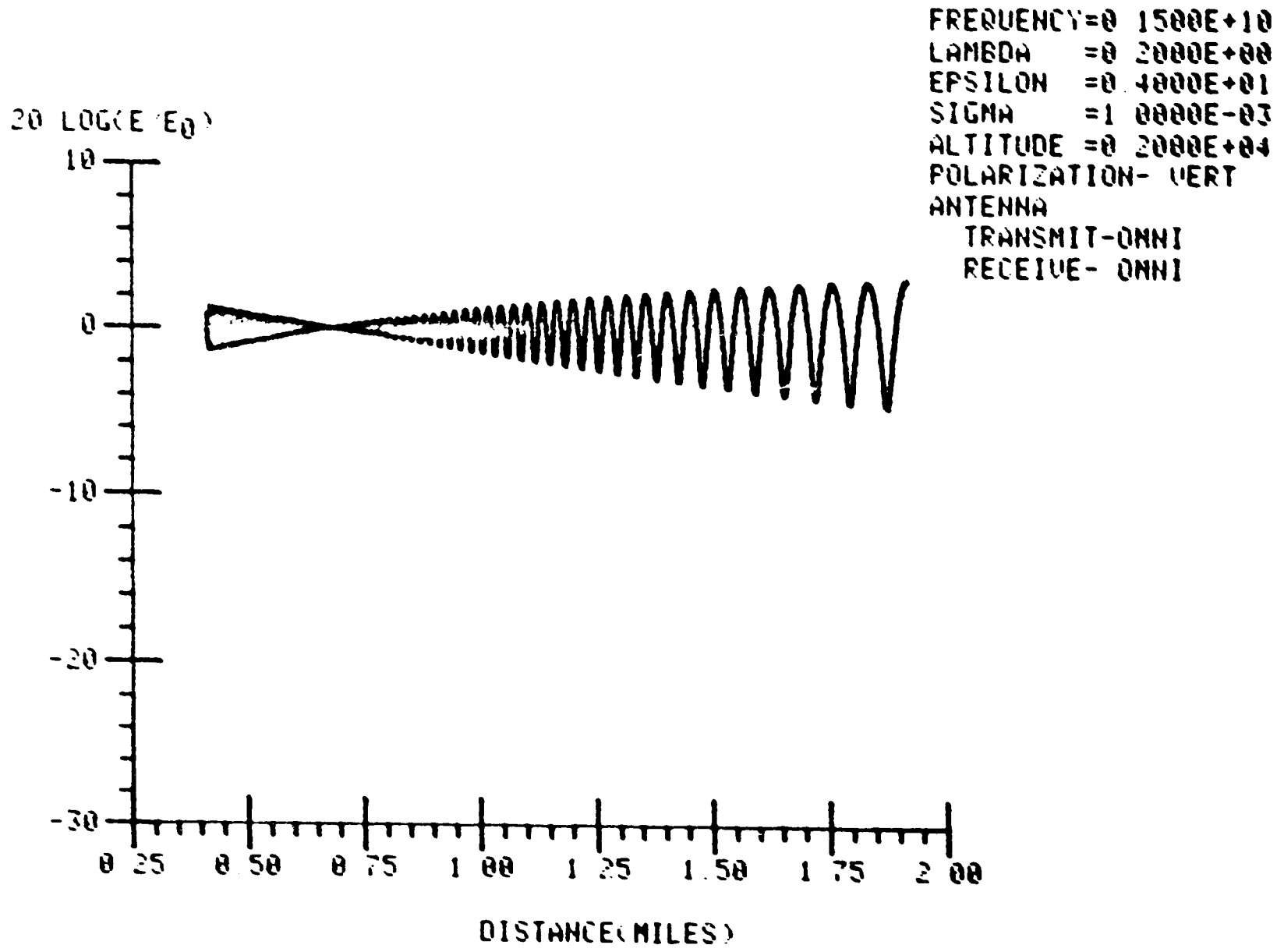
FREQUENCY=0 1500E+10
LAMBDA =0 2000E+00
EPSILON =0 4000E+01
SIGMA =1 0000E-03
ALTITUDE =0 3000E+04
POLARIZATION- VERT
ANTENNA
TRANSMIT-OMNI
RECEIVE- OMNI
20 LOG(E/E0)
10
0
-10
-20
-30
0 25
0 50
0 75
1 00
1 25
1 50
1 75
2 00
DISTANCE(MILES)

Figure D3

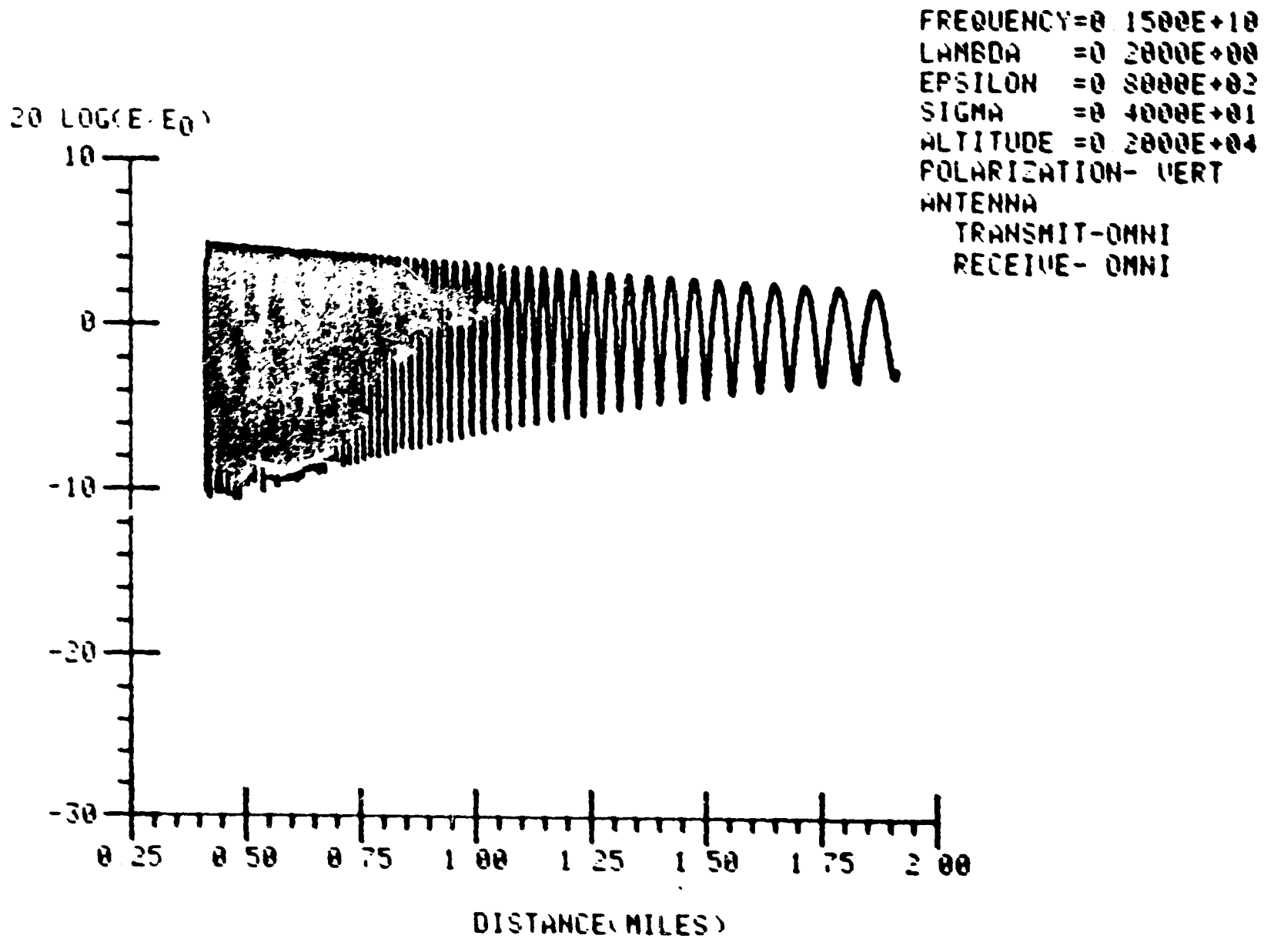
FREQUENCY=0 1500E+10
LAMBDA =0 2000E+00
EPSILON =0 8000E+02
SIGMA =0 4000E+01
ALTITUDE =0 2000E+04
POLARIZATION- VERT
ANTENNA
TRANSMIT-OMNI
RECEIVE- OMNI
20 LOG(E/E0)
10
0
-10
-20
-30
0 25
0 50
0 75
1 00
1 25
1 50
1 75
2 00
DISTANCE(MILES)

Figure D4

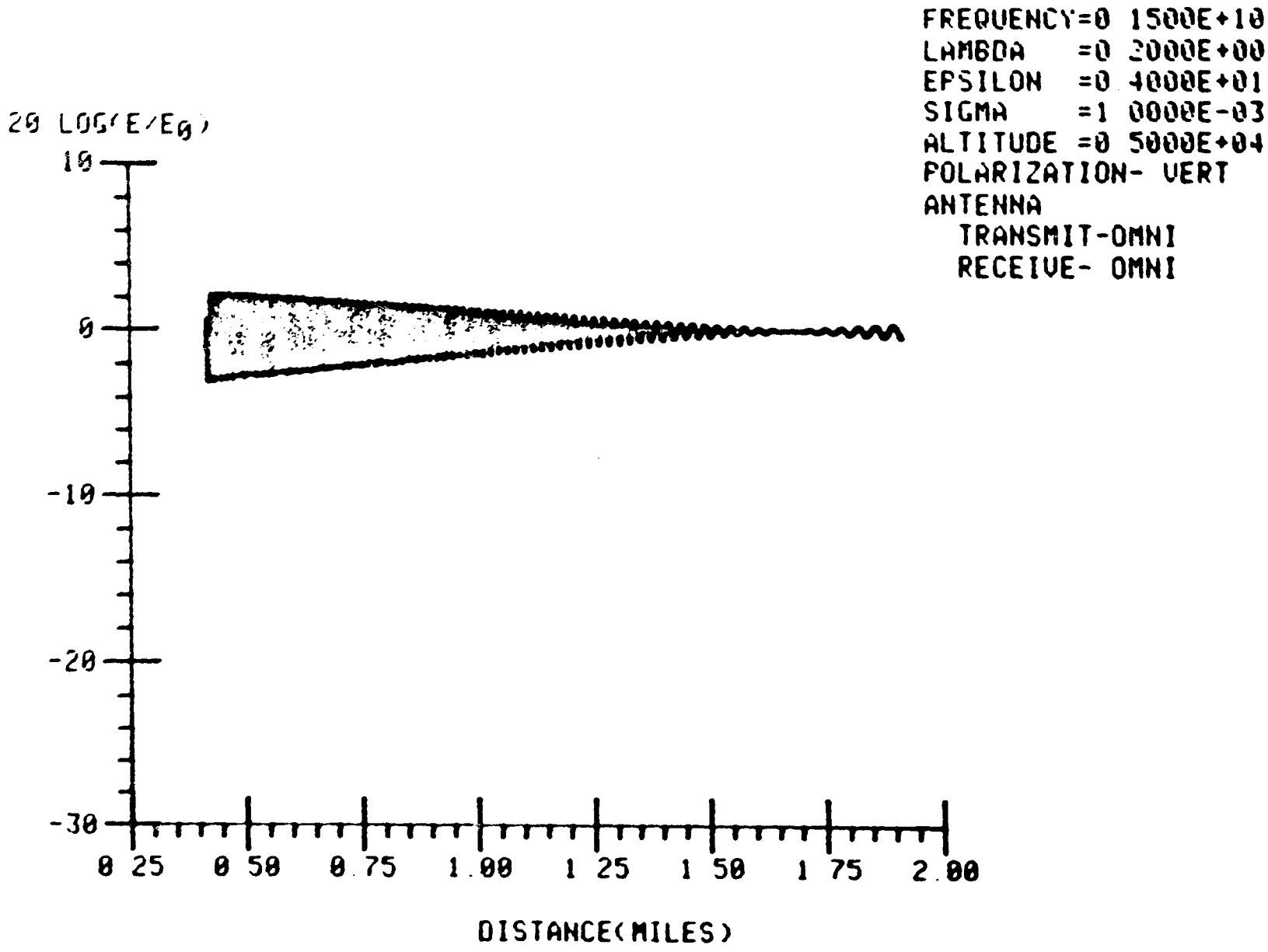
FREQUENCY=0 1500E+10
LAMBDA =0 2000E+00
EPSILON =0 4000E+01
SIGMA =1 0000E-03
ALTITUDE =0 5000E+04
POLARIZATION- VERT
ANTENNA
TRANSMIT-OMNI
RECEIVE- OMNI
20 LOG(E/E0)
10
0
-10
-20
-30
0 25
0 50
0 75
1 00
1 25
1 50
1 75
2 00
DISTANCE(MILES)

Figure D5

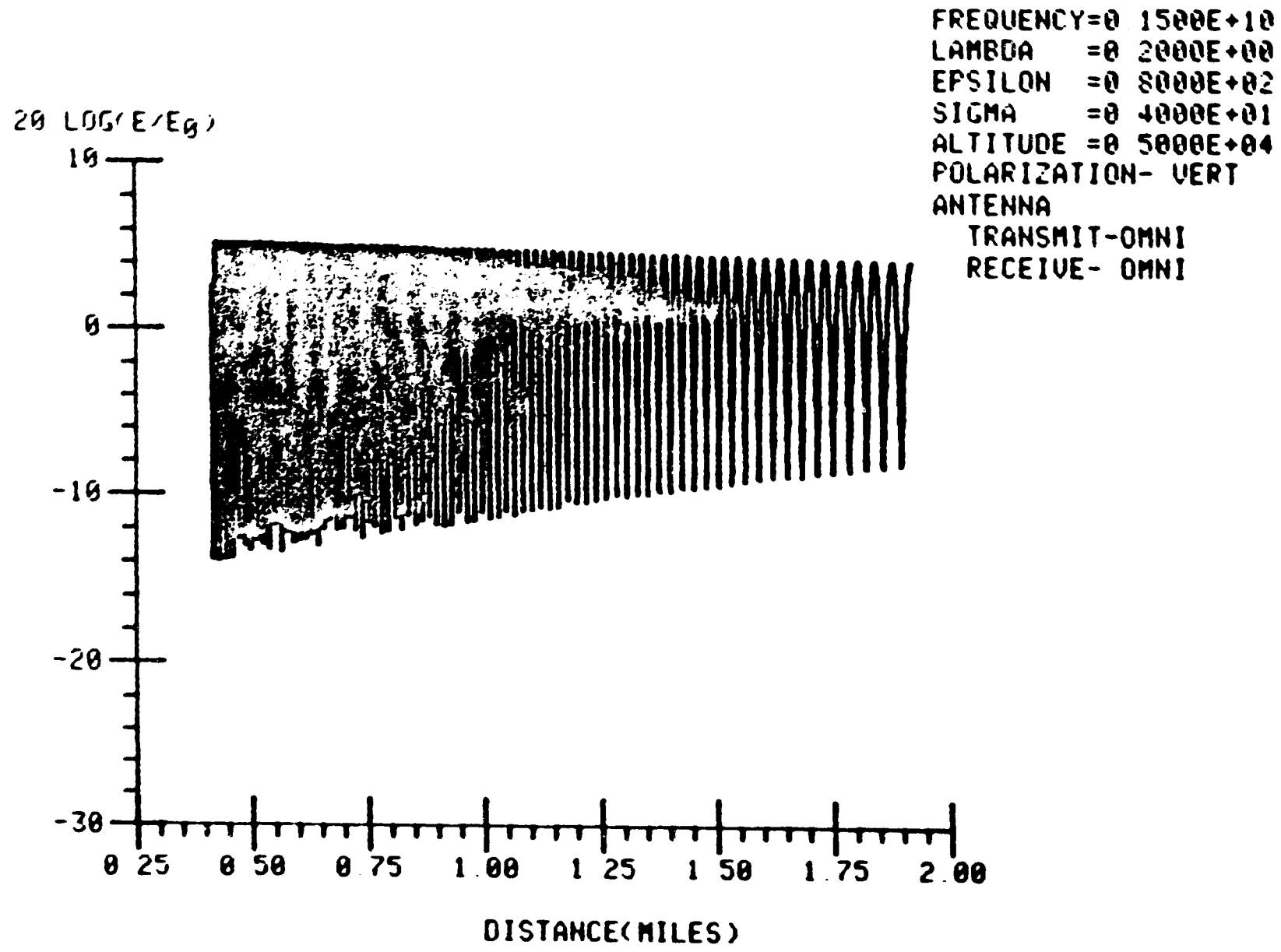
FREQUENCY=0 1500E+10
LAMBDA =0 2000E+00
EPSILON =0 8000E+02
SIGMA =0 4000E+01
ALTITUDE =0 5000E+04
POLARIZATION- VERT
ANTENNA
TRANSMIT-OMNI
RECEIVE- OMNI
20 LOG(E/Eo)
10
0
-10
-20
-30
0 25
0 50
0 75
1 00
1 25
1 50
1 75
2 00
DISTANCE(MILES)

Figure D6

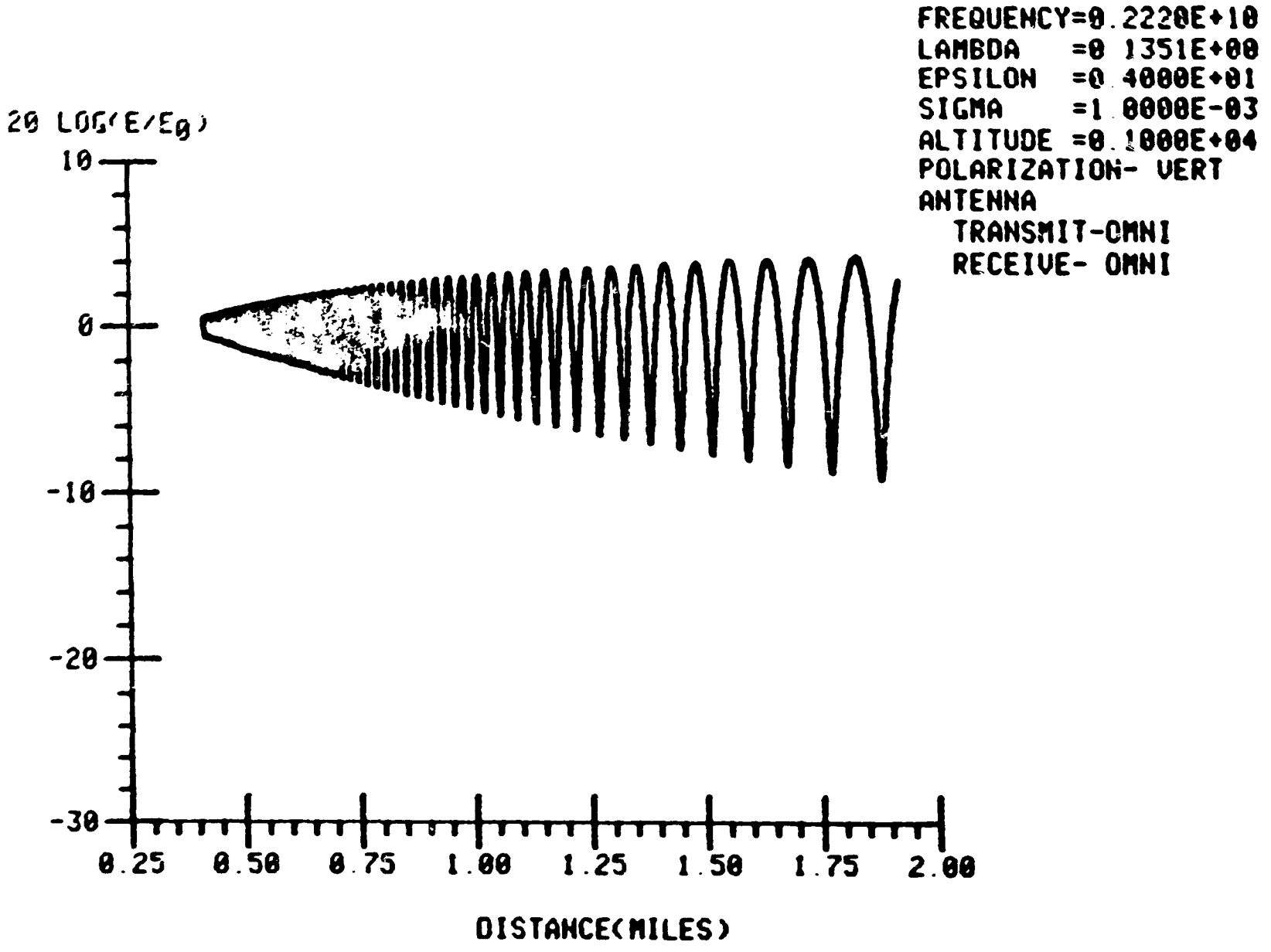
FREQUENCY=0.2220E+10
LAMBDA =0.1351E+00
EPSILON =0.4000E+01
SIGMA =1.0000E-03
ALTITUDE =0.1000E+04
POLARIZATION- VERT
ANTENNA
TRANSMIT-OMNI
RECEIVE- OMNI
20 LOG(E/Eo)
10
0
-10
-20
-30
0.25
0.50
0.75
1.00
1.25
1.50
1.75
2.00
DISTANCE(MILES)

Figure D7

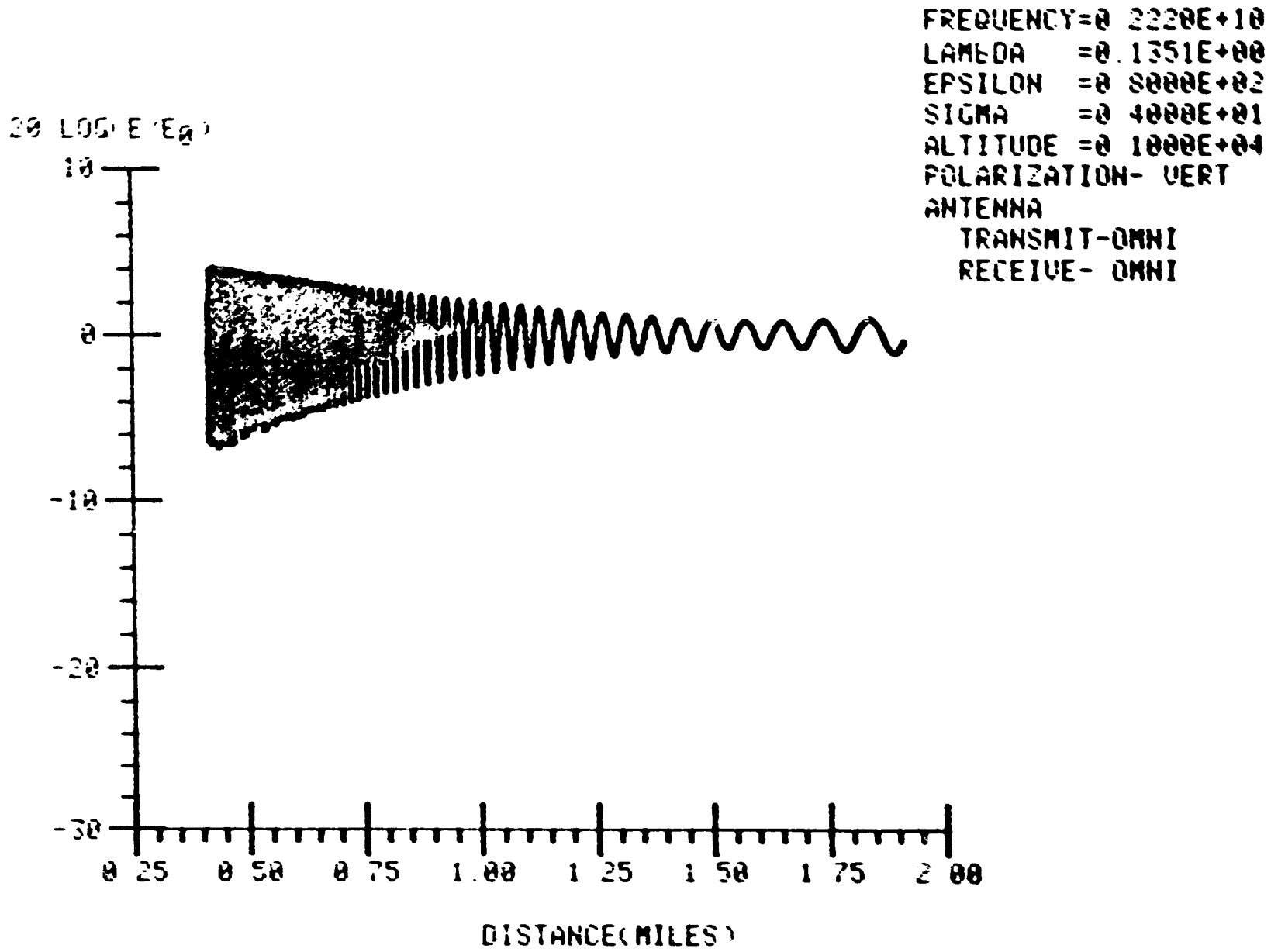
FREQUENCY=0 3220E+10
LAMBDA =0 1351E+00
EPSILON =0 5000E+02
SIGMA =0 4000E+01
ALTITUDE =0 1000E+04
POLARIZATION- VERT
ANTENNA
TRANSMIT-OMNI
RECEIVE- OMNI
20 LOG E (Eg)
10
0
-10
-20
-30
0 25
0 50
0 75
1 00
1 25
1 50
1 75
2 00
DISTANCE(MILES)

Figure D8

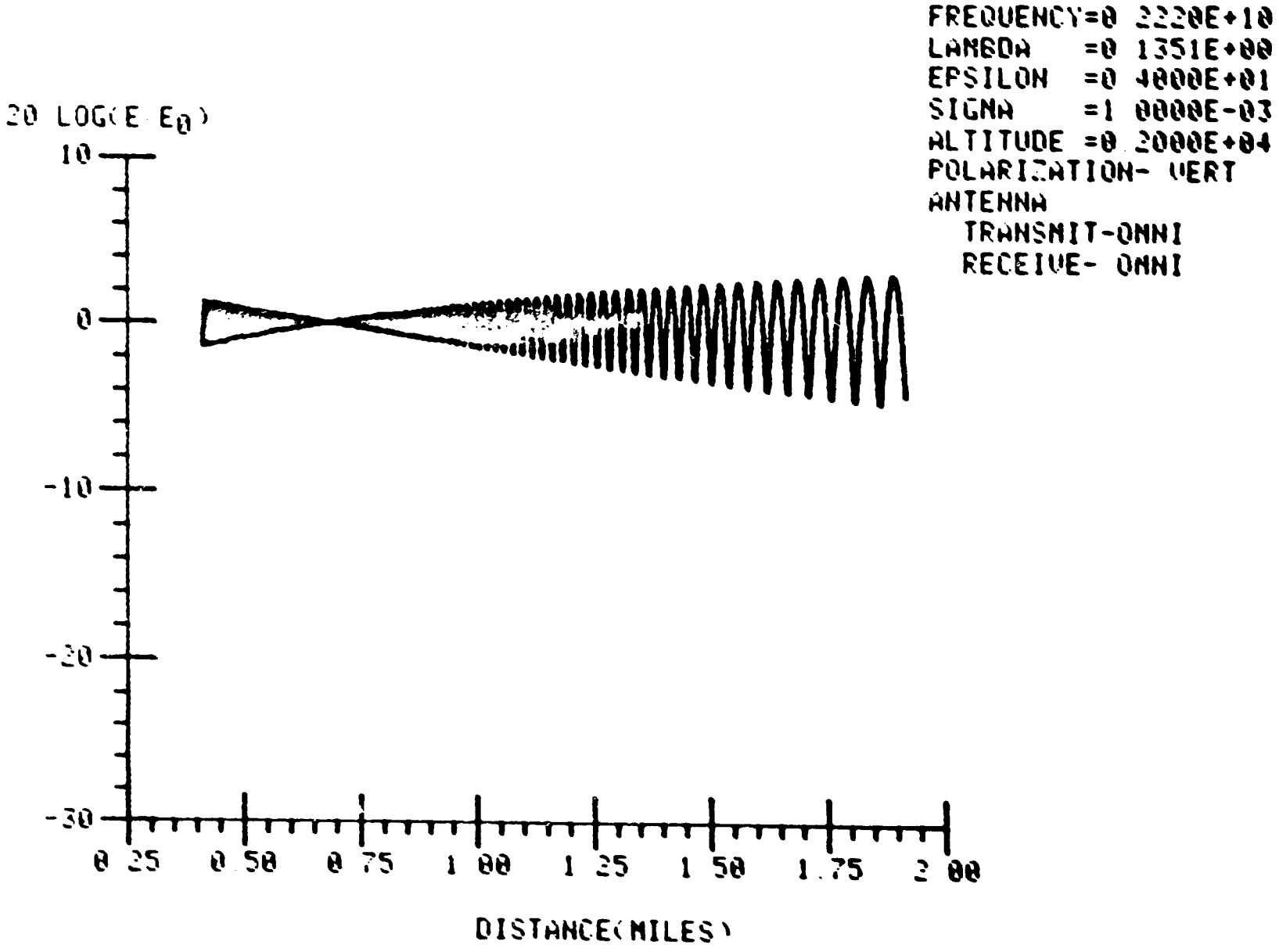
FREQUENCY=0 3330E+10
LAMBDA =0 1351E+00
EPSILON =0 4000E+01
SIGMA =1 0000E-03
ALTITUDE =0 2000E+04
POLARIZATION- VERT
ANTENNA
TRANSMIT-OMNI
RECEIVE- OMNI
20 LOG(E E0)
10
0
-10
-20
-30
0 25
0 50
0 75
1 00
1 25
1 50
1 75
2 00
DISTANCE(MILES)

Figure 09

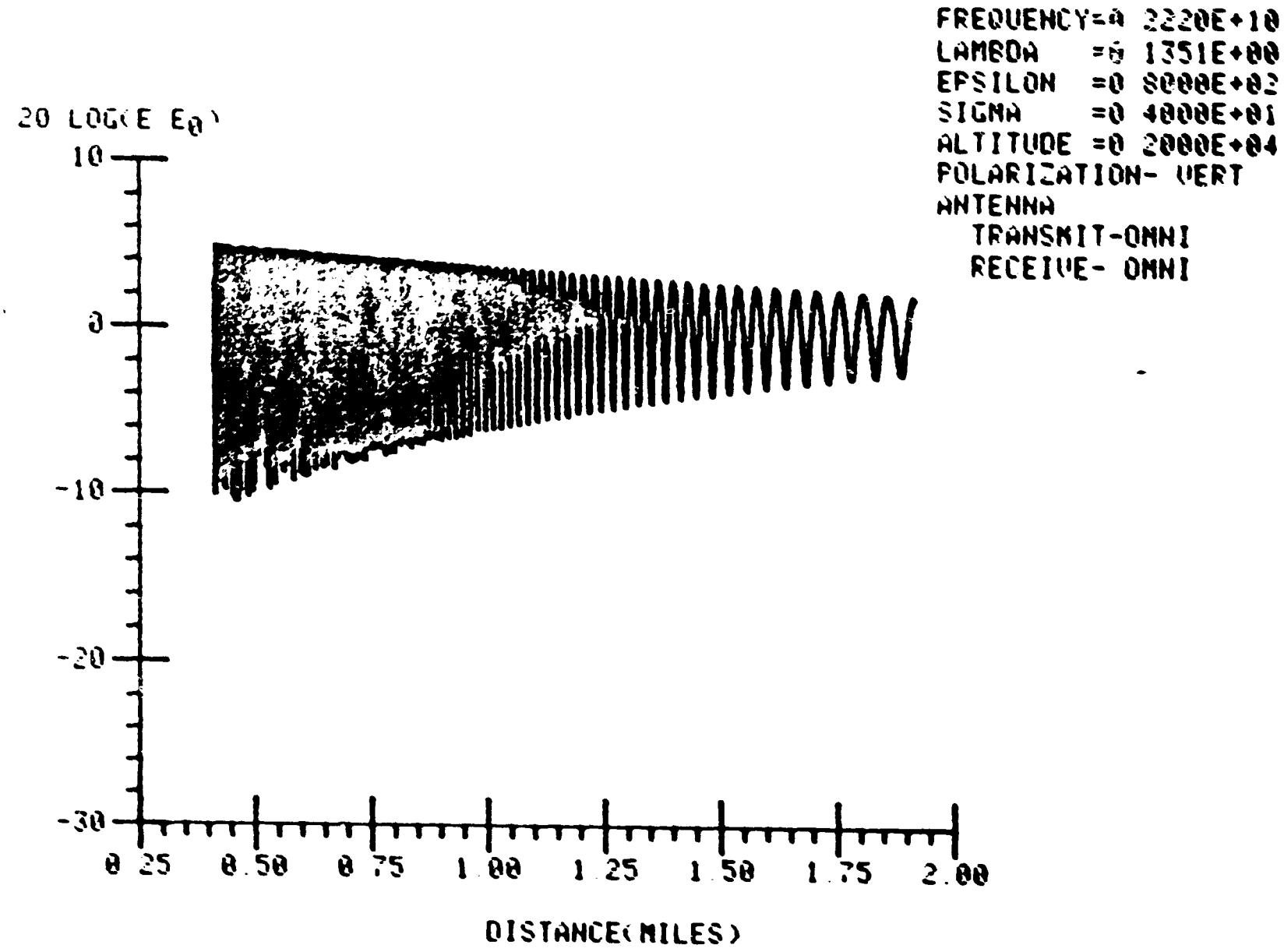
FREQUENCY=0 2220E+10
LAMBDA =0 1351E+00
EPSILON =0 8000E+02
SIGMA =0 4000E+01
ALTITUDE =0 2000E+04
POLARIZATION- VERT
ANTENNA
TRANSMIT-OMNI
RECEIVE- OMNI
20 LOG(E Eθ)
10
0
-10
-20
-30
0.25
0.50
0.75
1.00
1.25
1.50
1.75
2.00
DISTANCE(MILES)

Figure D10

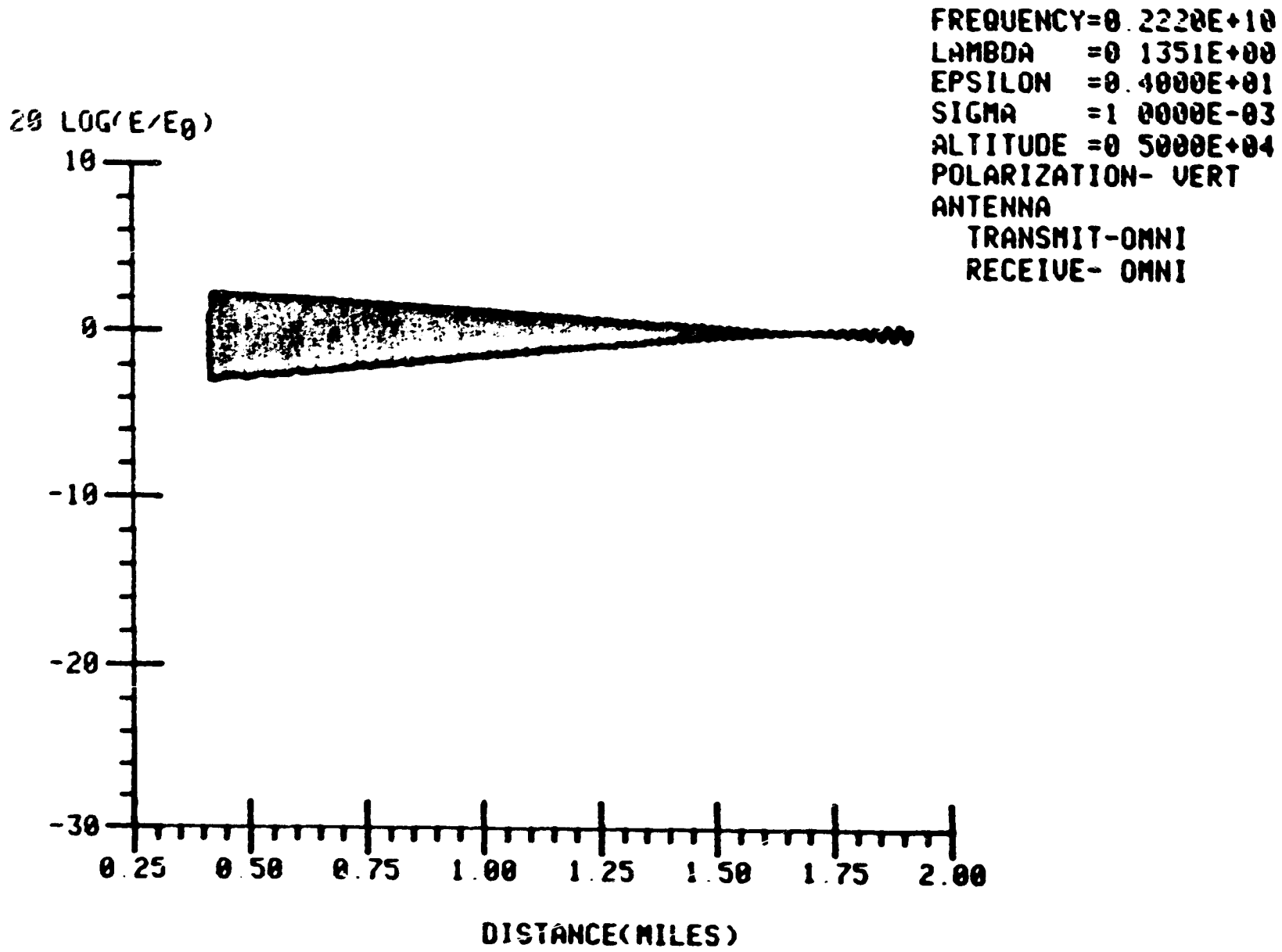
FREQUENCY=0.2220E+10
LAMBDA =0 1351E+00
EPSILON =0.4000E+01
SIGMA =1 0000E-03
ALTITUDE =0 5000E+04
POLARIZATION- VERT
ANTENNA
TRANSMIT-OMNI
RECEIVE- OMNI
20 LOG(E/E0)
10
0
-10
-20
-30
0.25
0.50
0.75
1.00
1.25
1.50
1.75
2.00
DISTANCE(MILES)

Figure D11

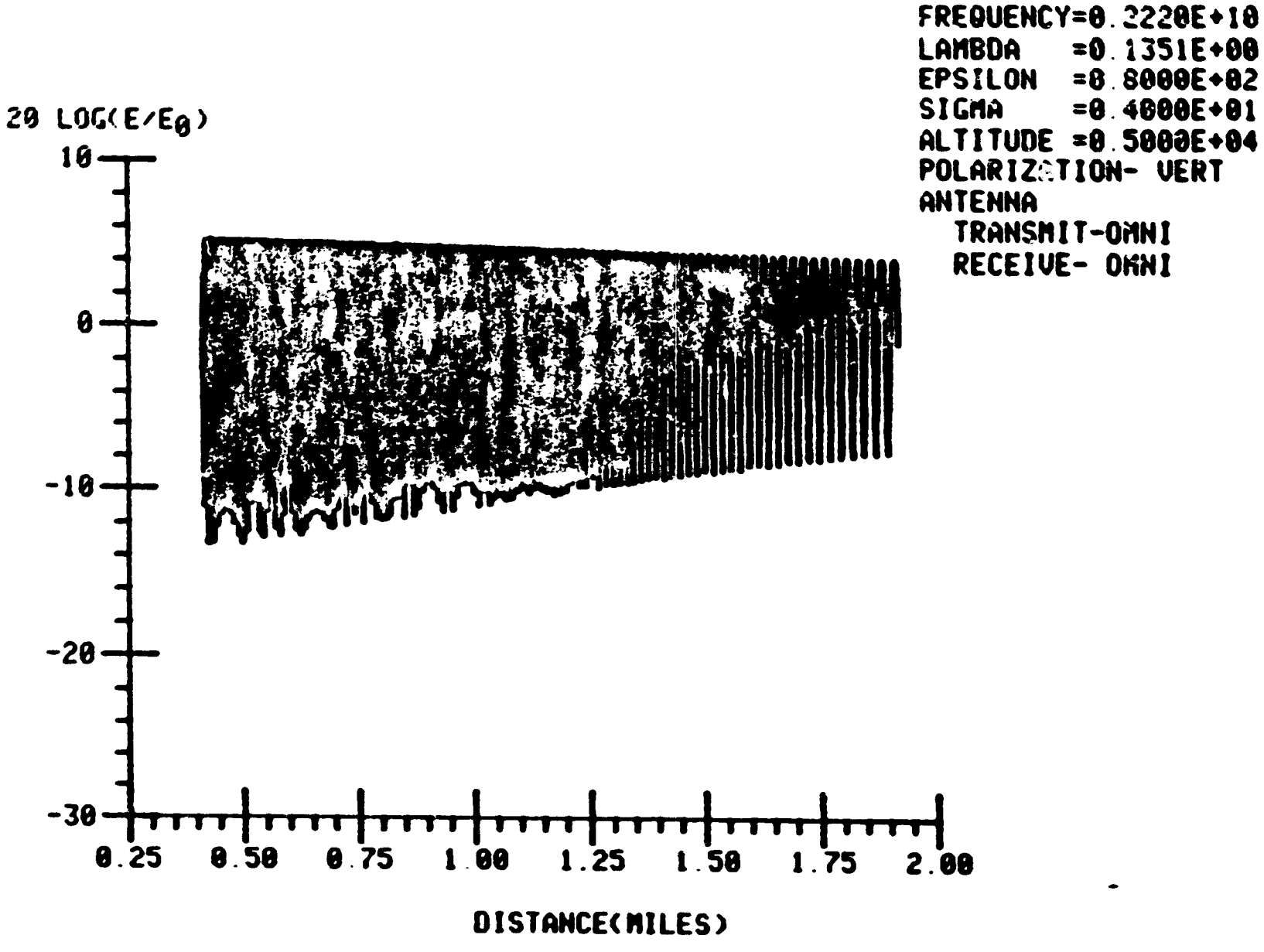
FREQUENCY=0.2220E+10
LAMBDA =0.1351E+00
EPSILON =0.8000E+02
SIGMA =0.4000E+01
ALTITUDE =0.5000E+04
POLARIZATION- VERT
ANTENNA
TRANSMIT-OMNI
RECEIVE- OMNI
20 LOG(E/E0)
10
0
-10
-20
-30
0.25
0.50
0.75
1.00
1.25
1.50
1.75
2.00
DISTANCE(MILES)

Figure D12

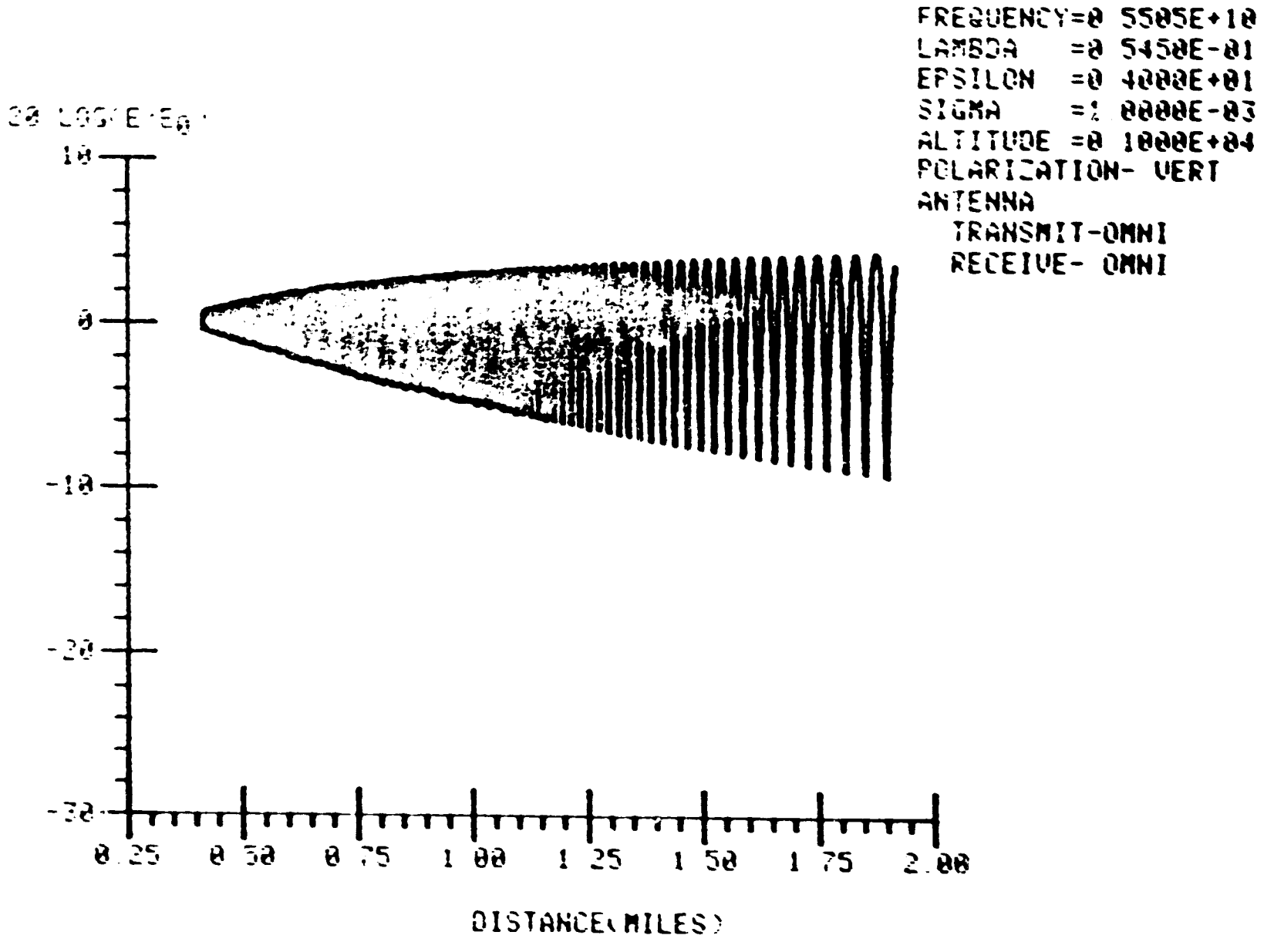
FREQUENCY=0 5505E+10
LAMBDA =0 5450E-01
EPSILON =0 4000E+01
SIGMA =1 0000E-03
ALTITUDE =0 1000E+04
POLARIZATION- VERT
ANTENNA
TRANSMIT-OMNI
RECEIVE- OMNI
10
0
-10
-20
-30
0 25
0 50
0 75
1 00
1 25
1 50
1 75
2.00
DISTANCE(MILES)

Figure 6.13

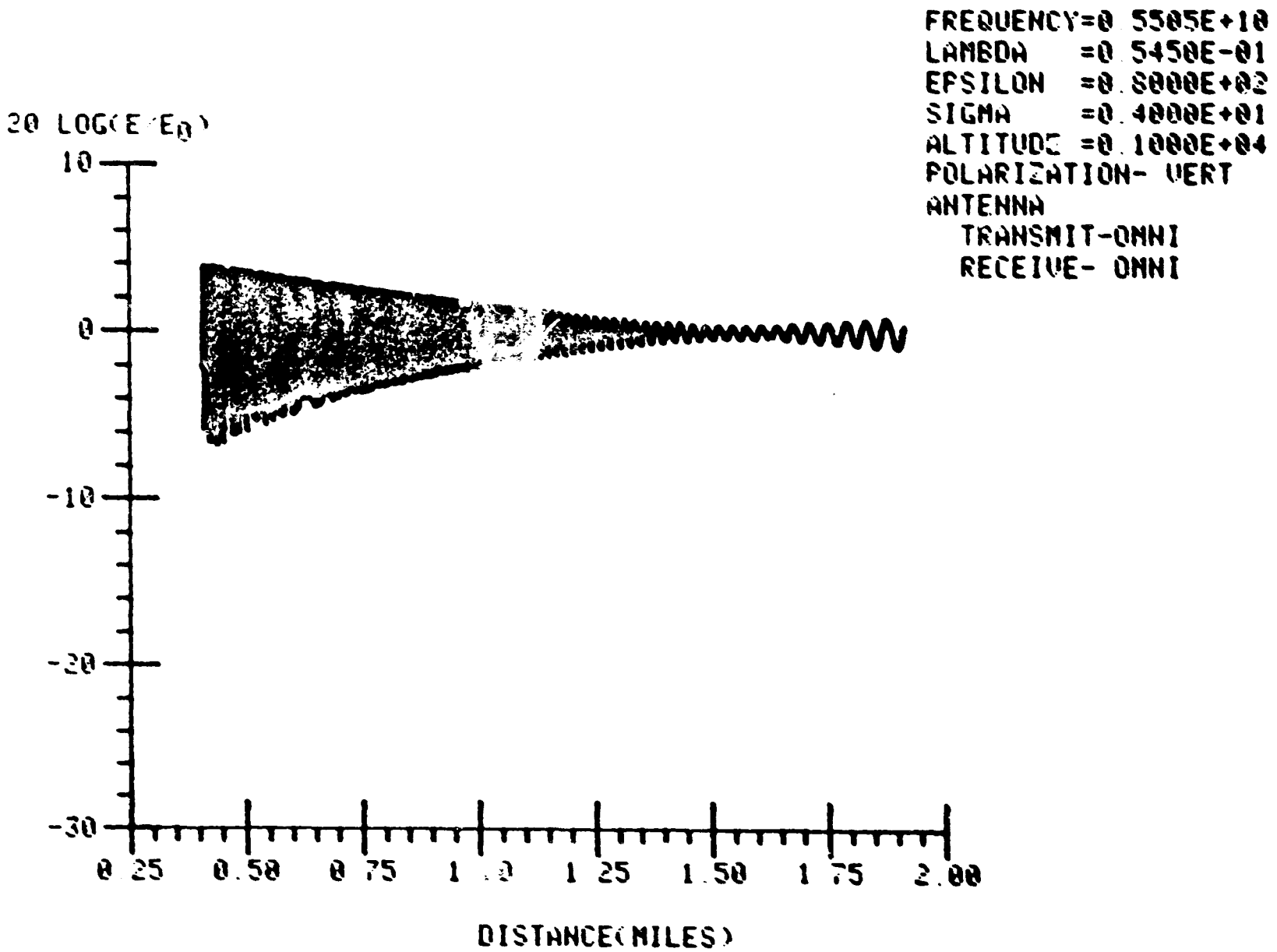
FREQUENCY=0.5505E+10
LAMBDA =0.5450E-01
EPSILON =0.8000E+02
SIGMA =0.4000E+01
ALTITUDE =0.1000E+04
POLARIZATION- VERT
ANTENNA
TRANSMIT-OMNI
RECEIVE- OMNI
20 LOG(E/E0)
10
0
-10
-20
-30
0.25
0.50
0.75
1.00
1.25
1.50
1.75
2.00
DISTANCE(MILES)

Figure D14

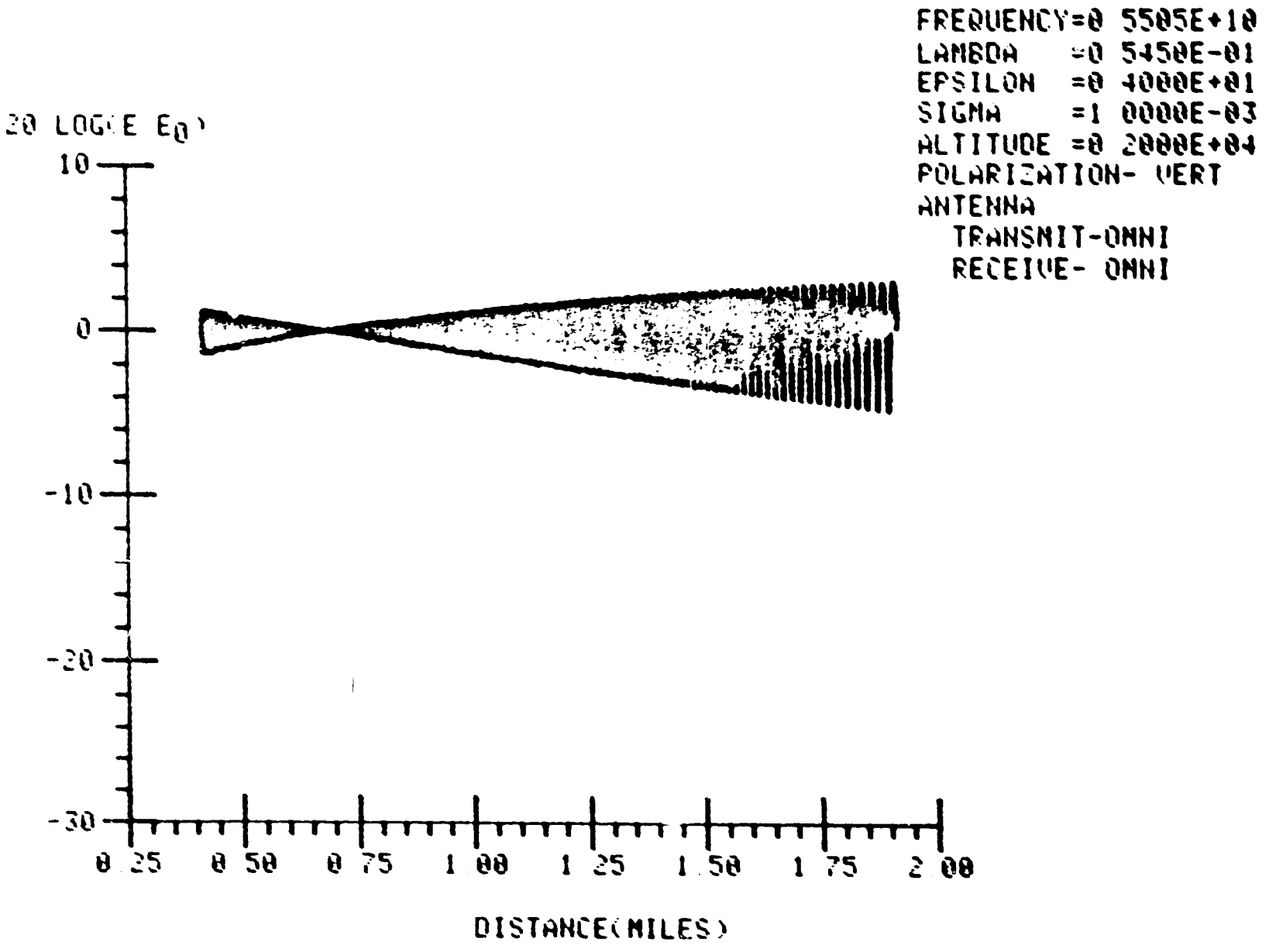
FREQUENCY=0 5505E+10
LAMBDA =0 5450E-01
EPSILON =0 4000E+01
SIGMA =1 0000E-03
ALTITUDE =0 2000E+04
POLARIZATION- VERT
ANTENNA
TRANSMIT-OMNI
RECEIVE- OMNI
20 LOG(E E0)
10
0
-10
-20
-30
0 25
0 50
0 75
1 00
1 25
1 50
1 75
2 00
DISTANCE(MILES)

Figure D15

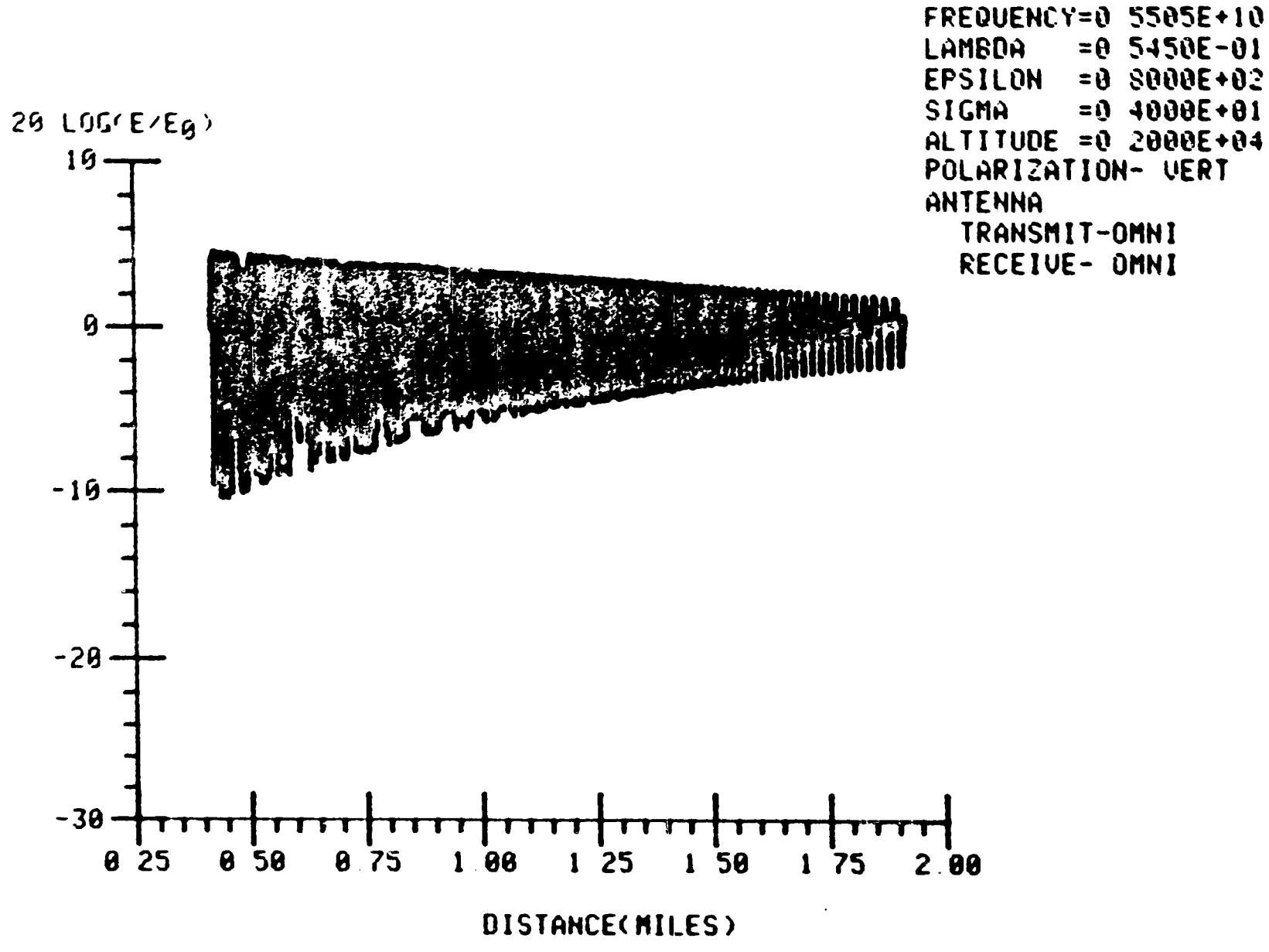
FREQUENCY=0 5505E+10
LAMBDA =0 5450E-01
EPSILON =0 8000E+02
SIGMA =0 4000E+01
ALTITUDE =0 2000E+04
POLARIZATION- VERT
ANTENNA
TRANSMIT-OMNI
RECEIVE- OMNI
20 LOG(E/Eo)
10
0
-10
-20
-30
0 25
0 50
0 75
1 00
1 25
1 50
1 75
2 00
DISTANCE(MILES)

Figure D16

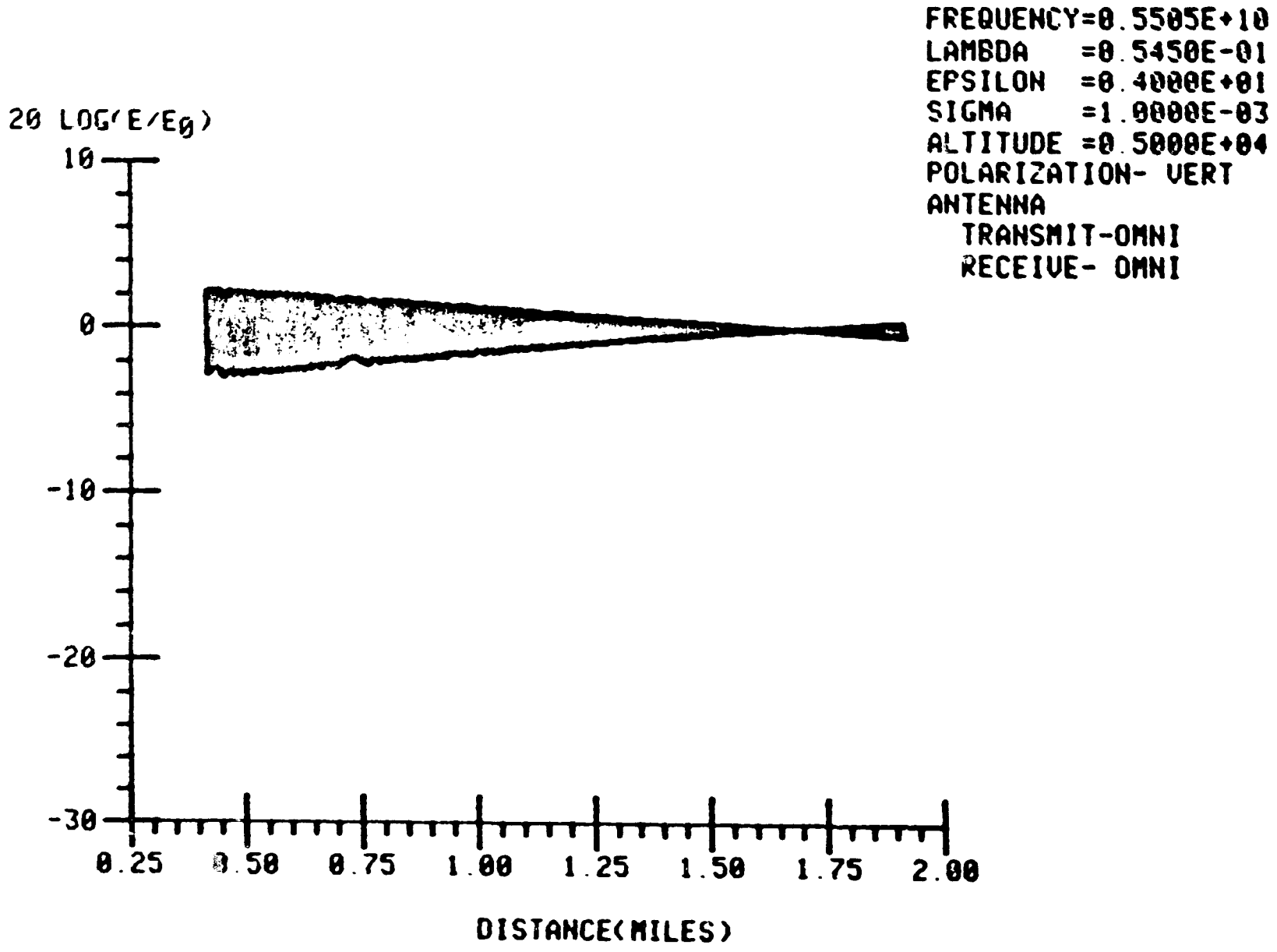
FREQUENCY=0.5505E+10
LAMBDA =0.5450E-01
EPSILON =0.4000E+01
SIGMA =1.0000E-03
ALTITUDE =0.5000E+04
POLARIZATION- VERT
ANTENNA
TRANSMIT-OMNI
RECEIVE- OMNI
20 LOG(E/Eo)
10
0
-10
-20
-30
0.25
0.50
0.75
1.00
1.25
1.50
1.75
2.00
DISTANCE(MILES)

Figure D17

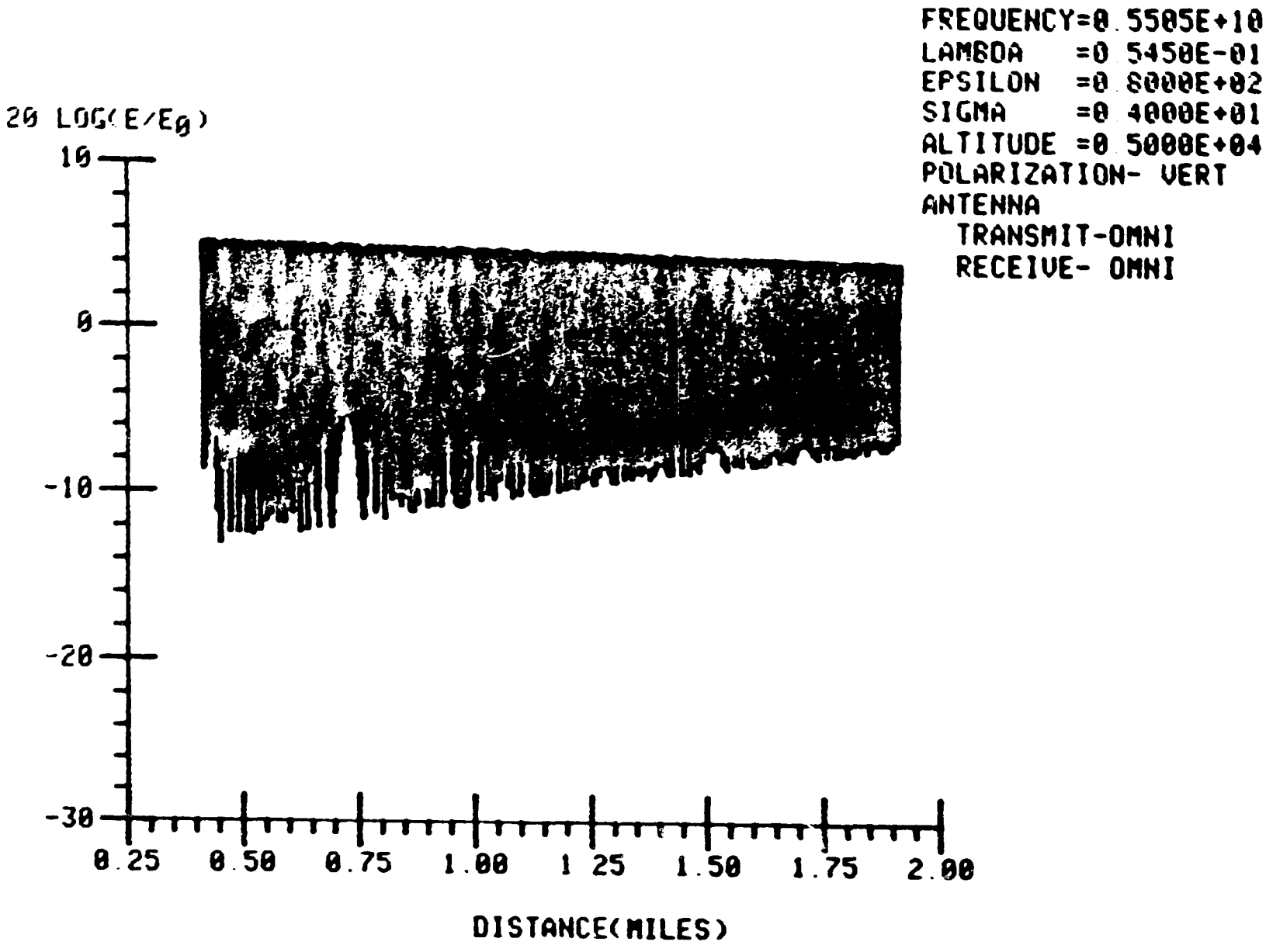
20 LOG(E/E0)
10
0
-10
-20
-30
0.25
0.50
0.75
1.00
1 25
1.50
1.75
2.00
DISTANCE(MILES)
FREQUENCY=0 5505E+10
LAMBDA =0 5450E-01
EPSILON =0 8000E+02
SIGMA =0 4000E+01
ALTITUDE =0 5000E+04
POLARIZATION- VERT
ANTENNA
TRANSMIT-OMNI
RECEIVE- OMNI

Figure D18

APPENDIX E

THE B-737 ANTENNA

The objectives of the designed antenna were to obtain omnidirectional coverages for each band without shadowing effects and with the minimum number of antenna locations. The studies indicated that the top of the vertical tail fin was the best suited. Stacked, vertical, stub antennas were selected due to geometrical restrictions (see fig. E1). The lower antennas consisted of two tiers of four vertical stubs spaced in the corners of a square whose diagonals equal half a wavelength. The top antenna was a single vertical stub. The final preflight patterns for L-band are found in figure E2, for S-band in figure E3, and for C-band in figure E4.

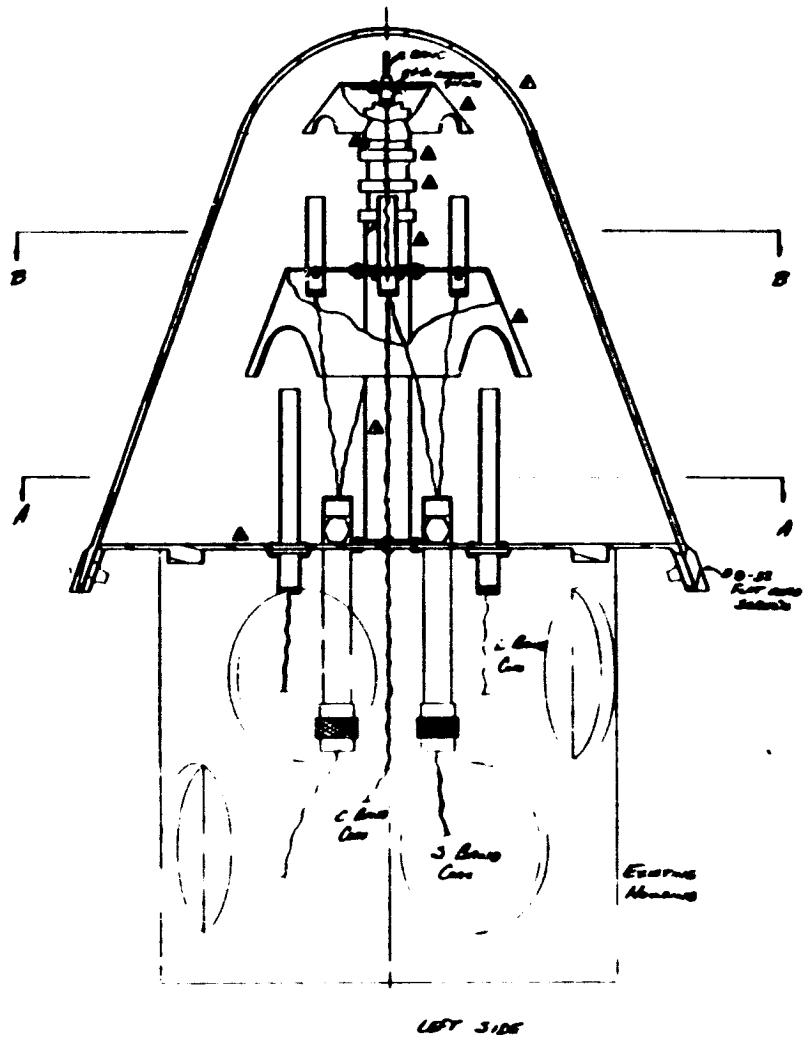

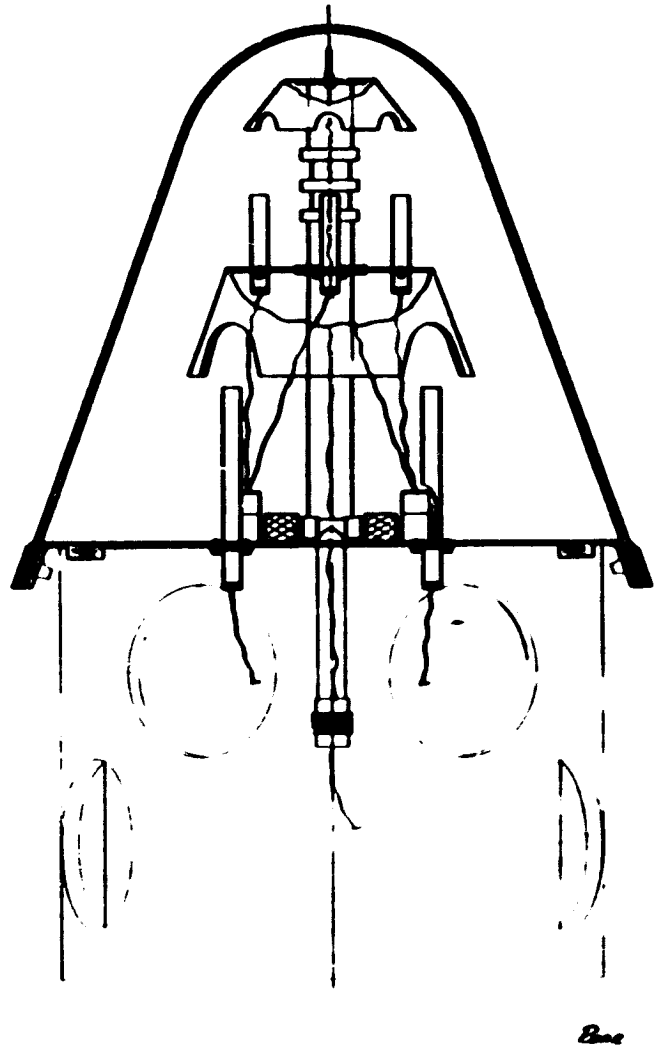

Figure El

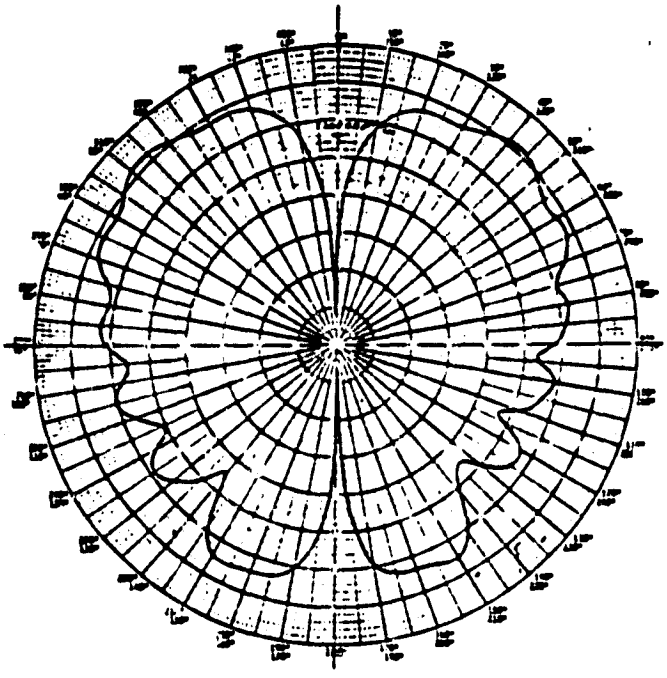

(a) 1015 MHz
Elevation Cut

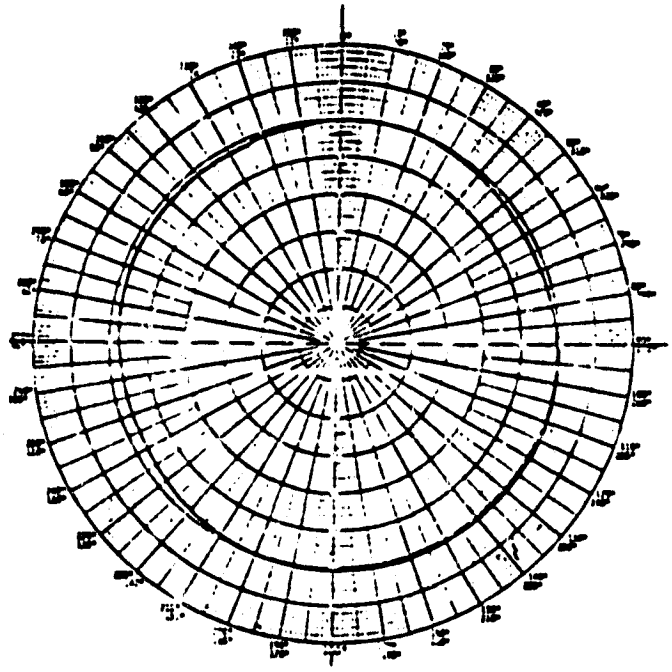

(b) 1015 MHz
Azimuthal Cut

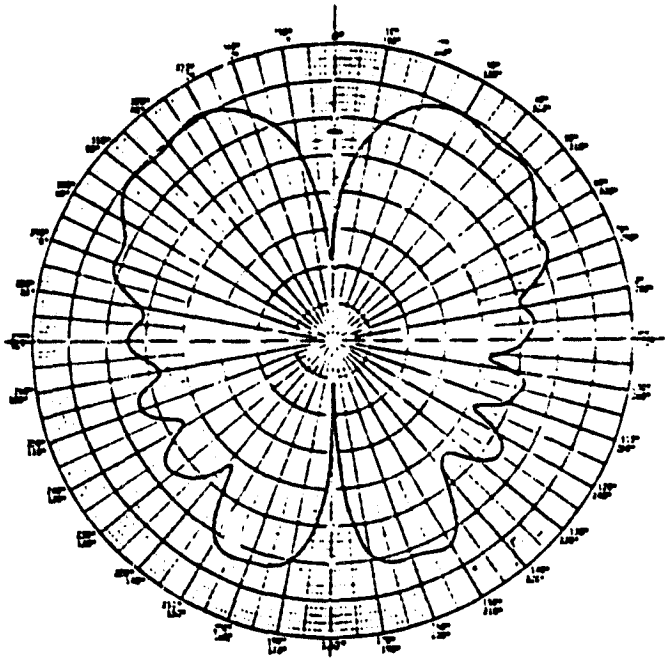

(c) 1078 MHz
Elevation Cut

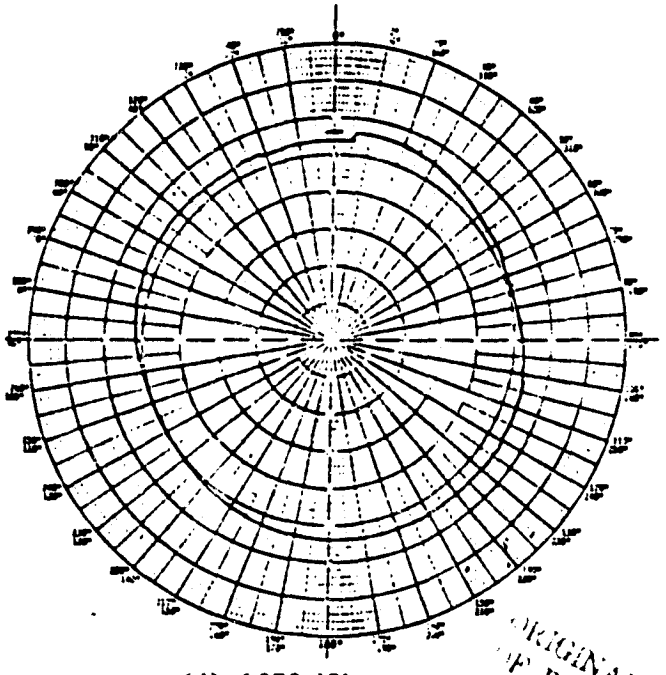

(d) 1078 MHz
Azimuthal Cut

Figure E2. L-band.

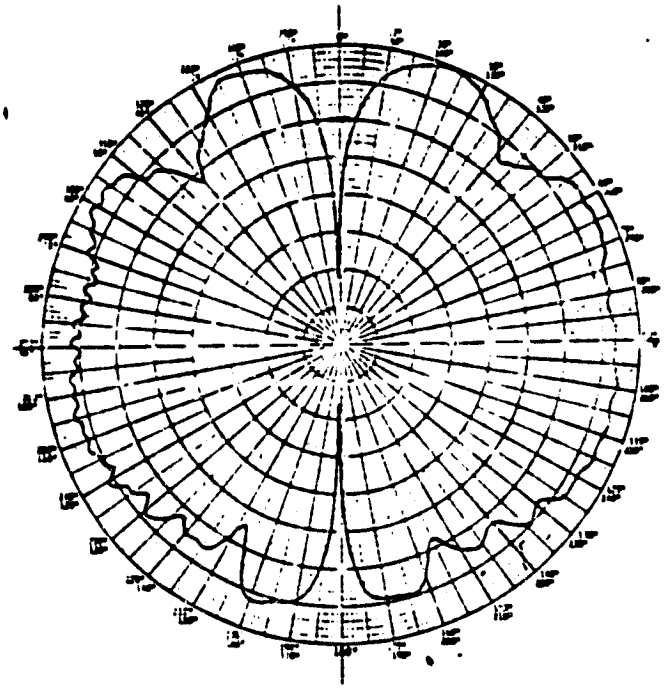

(a) 2220 MHz
Elevation Cut

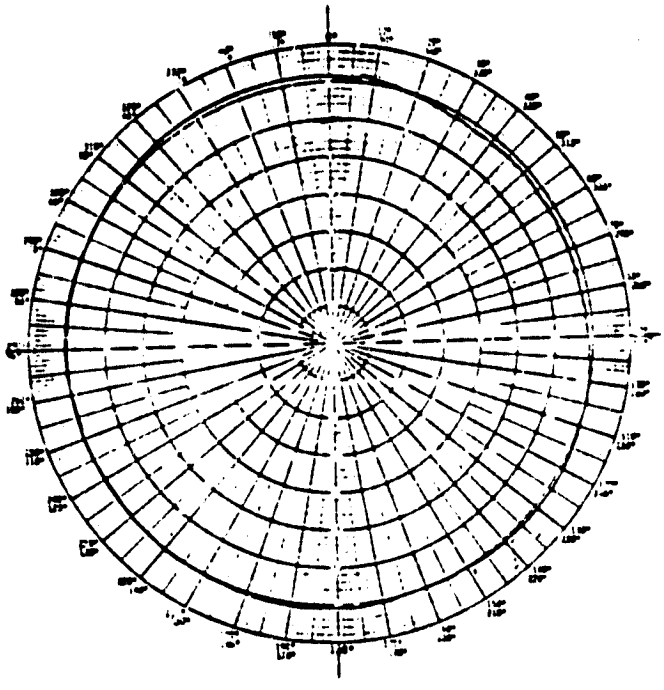

(b) 2220 MHz
Azimuthal Cut

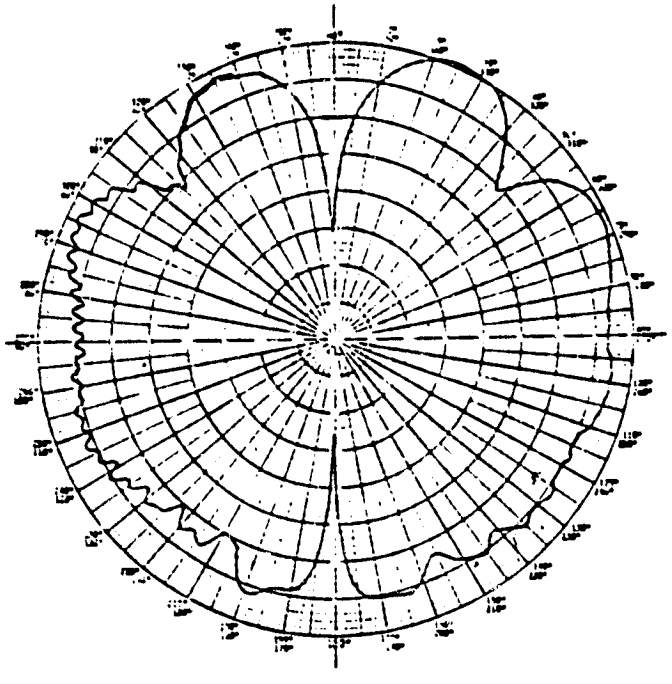

(c) 2320 MHz
Elevation Cut

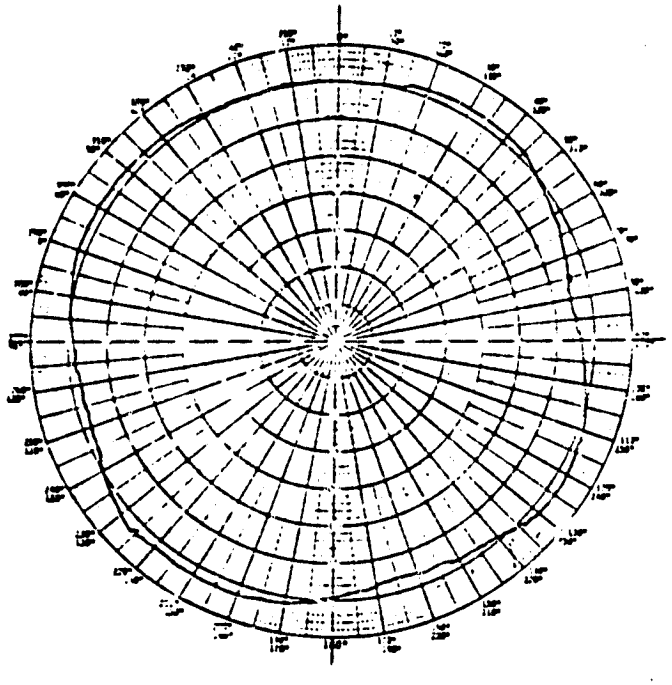

(d) 2320 MHz
Azimuthal Cut

Figure E5. S-band.

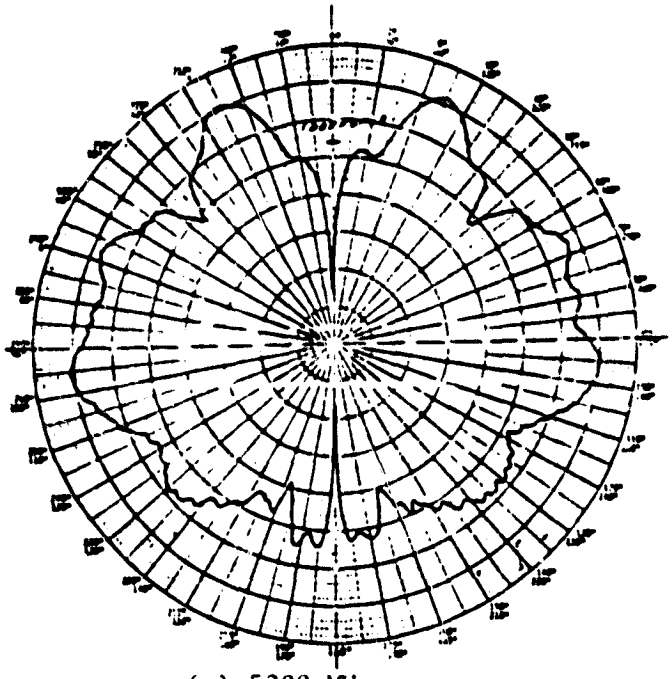

(a) 5200 MHz
Elevation Cut

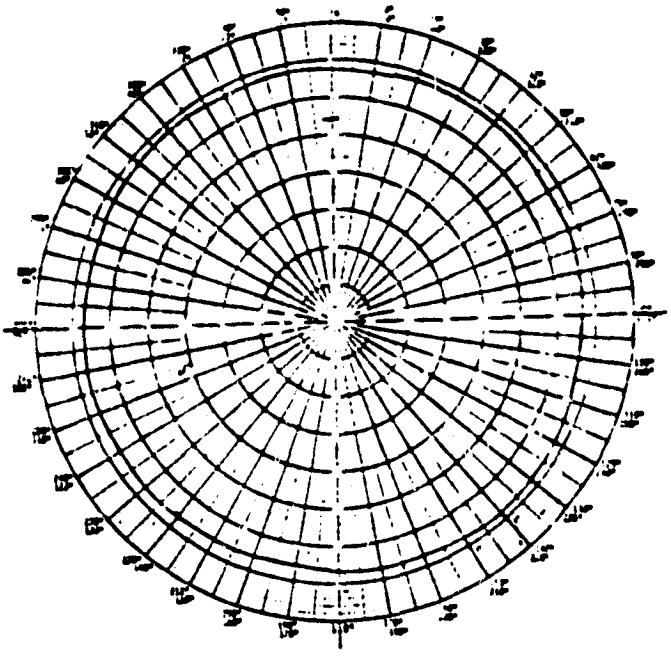

(b) 5200 MHz
Azimuthal Cut

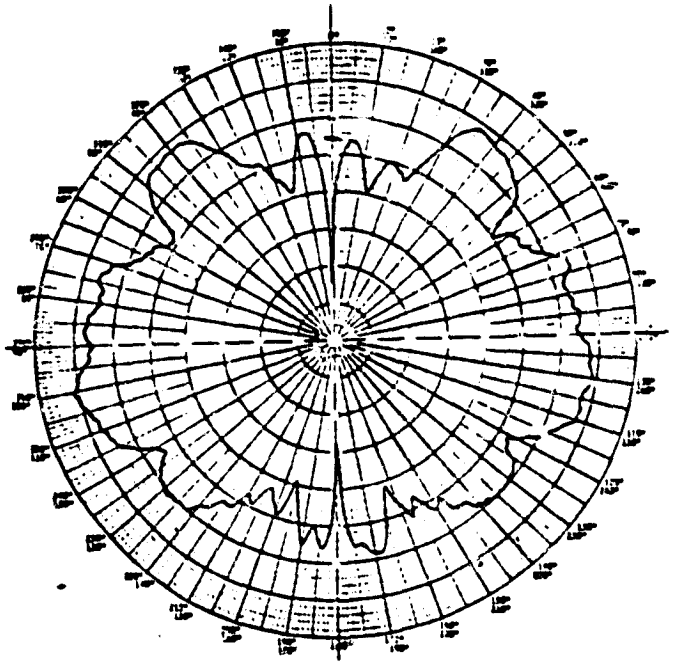

(c) 5700 MHz
Elevation Cut

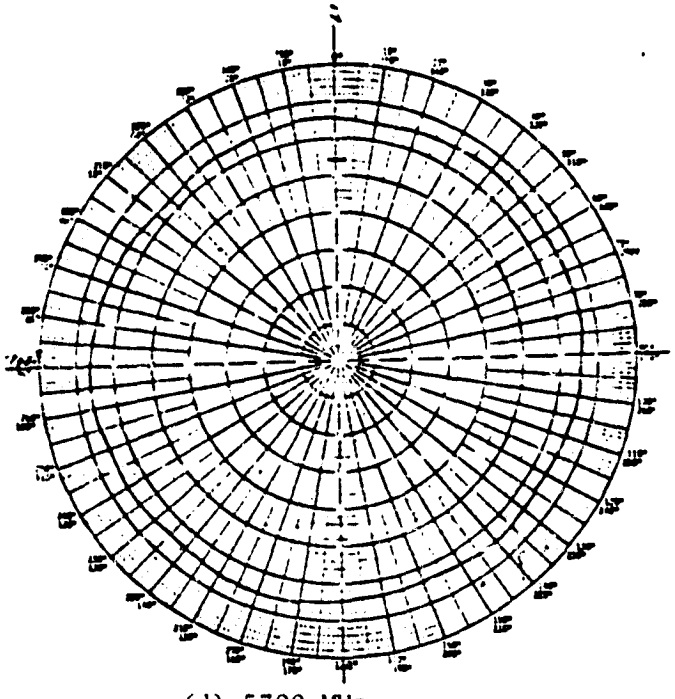

(d) 5700 MHz
Azimuthal Cut

Figure E4. C-band.

APPENDIX F

FDRS S-BAND ANTENNA SYSTEM

A high-gain S-band parabolic antenna system (which covers the range from 2150-2350 MHz) was installed on the FPS-16 C-band radar antenna mount at NASA/Wallops Flight Center, Wallops Island, Virginia. This antenna was intended to increase the communications distances previously provided by an omnidirectional antenna. Sufficient gain was achieved to improve the fade margin of the communications-television up-link capability.

The antenna system consists of a 36-in. parabolic reflector and a primary feed system of crossed dipoles backed by a flat plate reflector. It is mounted in the same plane as the 16-foot C-band antenna as shown in figure F1. The two antennas have parallel boresights. A remote-controlled polarizer, that provides horizontal and vertical linear and left-hand and right-hand circular polarizations, is located behind the S-band antenna. A three-channel azimuth rotary joint replaced the existing two-channel joint in the radio mount. For elevation and to allow for 180° motion, a semi-rigid coax except for a short run of RG 214 flexible cable was used. The AC control circuitry for the polarizer and the microwave circuits are shown in figures F2 and and F3.

Antenna gain, sidelobes, and beamwidth were checked in the E and H planes for horizontal and vertical polarizations, along with axial ratio and the left- and right-hand cases for circular polarization. The gain measurement included the insertion loss of the polarizer and its associated semi-rigid cable only. The requirements for antenna gain were +22 to 26 dB, first sidelobe level -16 dB, sidelobe level (±45° to ±175°) -25 dB, beamwidth 10° + 1°, and axial ratio 2.0 dB.

The on-site tests were conducted at NASA/Wallops Flight Center, Wallops Island, Virginia. These tests included VSWR and insertion loss for the antenna system and AC control to verify that the proper R.F. switches were being activated when switched to the required polarization. The requirements for this test were VSWR $\leq$ 1.4 and an insertion loss of < 4 dB. A block diagram of the system VSWR / insertion loss measurement test is found in figure F4 and the results in table F.

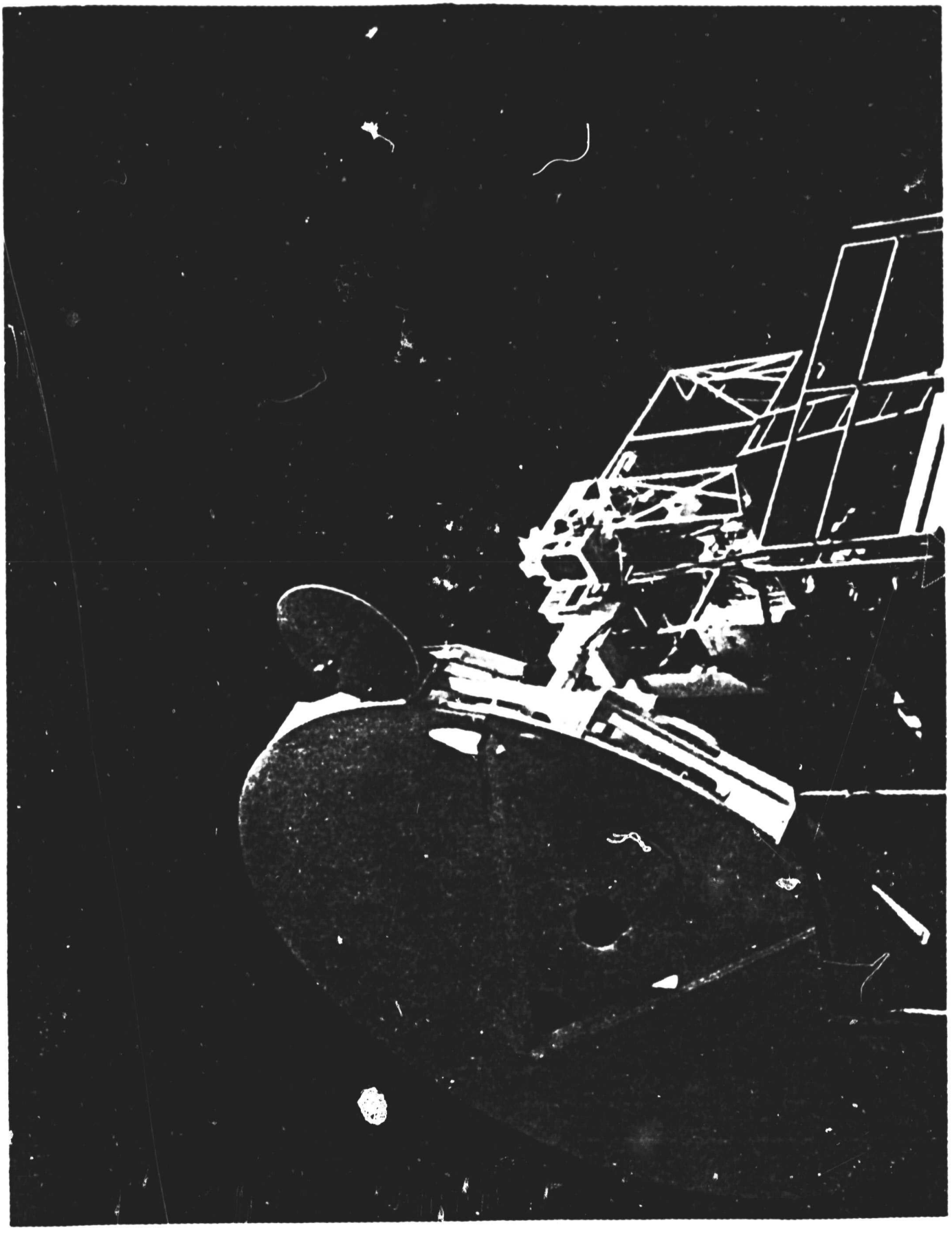

Figure F1

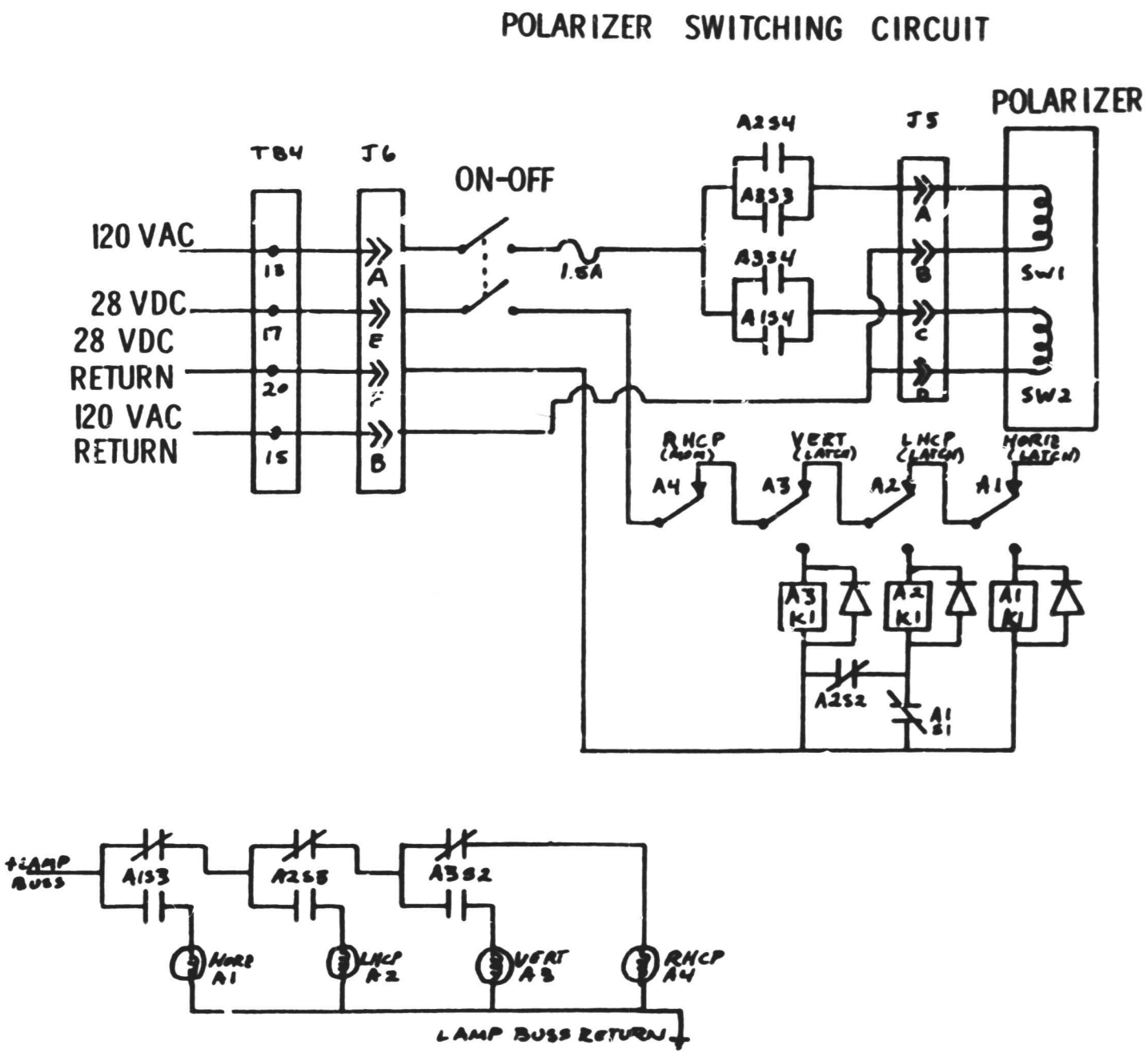
POLARIZER SWITCHING CIRCUIT
POLARIZER
TB4
J6
ON-OFF
A254
J5
120 VAC
28 VDC
28 VDC RETURN
120 VAC RETURN
18
17
20
15
A
E
B
1.5A
A253
A354
A154
A
B
C
D
SW1
SW2
RHCP (NORM)
VERT (LATCH)
LHCP (LATCH)
HORIZ (LATCH)
A4
A3
A2
A1
A3 K1
A2 K1
A1 K1
A252
A1 B1
+LAMP BUSS
A153
A258
A352
HORIZ A1
LHCP A2
VERT A3
RHCP A4
LAMP BUSS RETURN

Figure F2

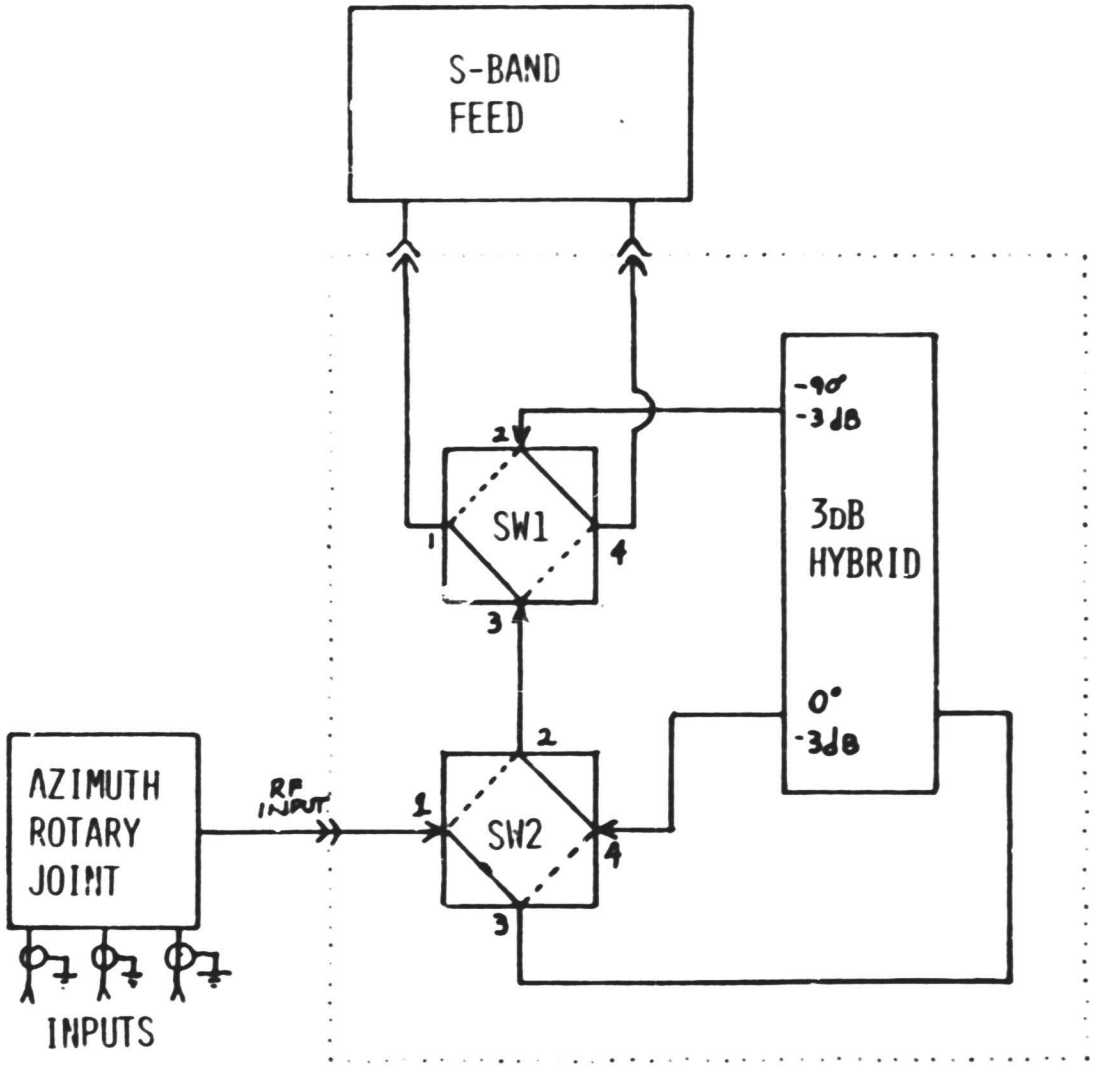

MICROWAVE CIRCUIT

Figure F3

SYSTEM VSWR / INSERTION LOSS MEASUREMENT

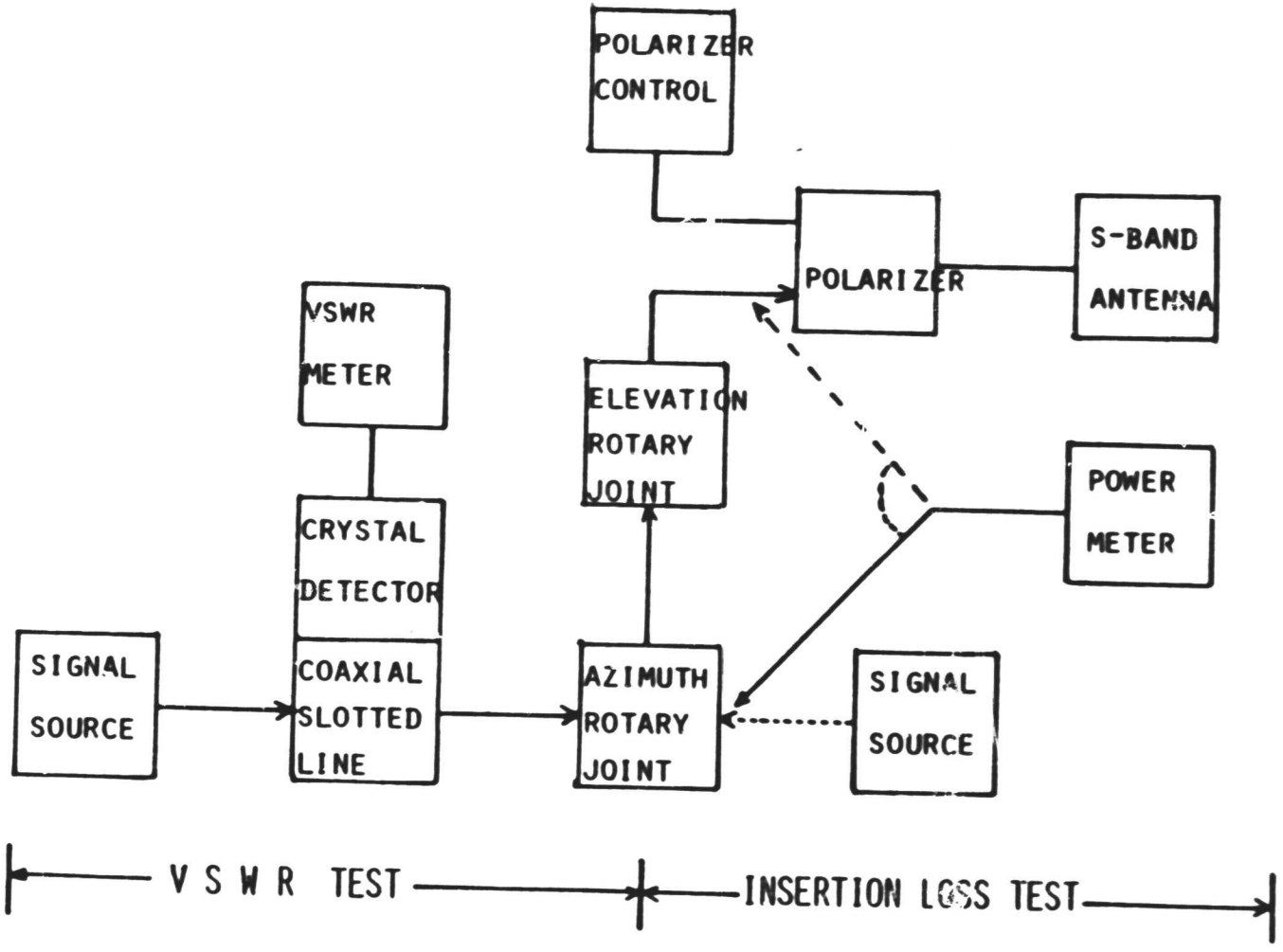

Figure F4

TABLE

SYSTEM GAIN

FREQUENCY	VERTICAL		HORIZONTAL		VSWR	INSERT. LOSS (DB)
	H	E	H	E		
2150	19.5	21.3	20.1	19.8	1.10	2.5
2220	22.5	23.0	22.4	22.5	1.15	2.1
2320	22.3	22.3	22.3	22.3	1.10	2.7
2350	23.1	22.9	22.0	21.9	1.26	2.5

REFERENCES

1. Burrows, C.R.: Radio Propagation over Plane Earth-Field Strength Curves. Bell System Tech. J., 1943, p. 45.

2. Osborn, J.D.; and Zuteck, M.D.: An Investigation of the Multipath Problems Associated with the Apollo CSM and SM S-Band High Gain Communication Antenna Tracking Systems. Communications and Sensor Systems Dept., Elec. Sys. Lab, NAS 9-8166, 1968.

3. Arens, V.R.: A Mathematical Model of Vertical Antennas of Finite Length over an Inhomogeneous Earth. Sylv. Elec. Svs. West, 1969, p. 225.

4. Deal, J.H.: Multipath Propagation Study for L-Band, Over-Ocean, Satellite-Aircraft Communication Link. Goddard Space Flight Center, 1972.

5. McGarty, T.P.: Antenna Performance in the Presence of Diffuse Multipath. Aerospace and Electronic Systems, Vol. 12, 1976, p. 42.

6. Breien, T.: Computer Analysis of MLS in Multipath Environment. Internat'l. Conf. on the Future of Aircraft All-Weather Operations. Proc. Inst. of Elec. Eng., 1976, p. 145.

7. McGarty, T.P.: The characterization of Diffuse Multipath for Satellite Communication Channels. Internat'l. Conf. on Communications, Vol. 1, 1975, p. 10-1.

8. Carver, K.R.: Surface Multipath Phenomena in Marine Environment. Internat'l. Conf. on Communications, Vol. 1, 1975, p. 10-6.

9. Fau-Tung Treng: Effective Spectrum Utilization in Satellite Communications by Improved Antenna Radiation Performance. Internat'l. Conf. on Communications, Vol. 1, 1975, p. 10-16.

10. Mizuno, T.; Mormaga, N.; Hirata, Y.; and Mamchawa, T.: Effects of Multipath Interference in Aeronautical and Marine Satellite Communications Links. Internat'l. Conf. on Communications, Vol. 1, 1975, p. 10-11.

11. Crane, K.C.: Bistatic Scatter from Ram. IEEE 22, No. 2, 1974, p. 312.

12. Otoshi, T.Y.: S-Band Zero-Delay Device Multipath Tests on the 64-Meter Antenna at DSS 43, DSS63, and DSS 14. JPL Deep Space Network Progress Report 42-29, 1975, p. 20.

13. Staras, H.: Rough Surface Scattering on a Communication Link. Radio Science, Vol. 3, 1968, p. 623.

14. Bullington, K.: Phase and Amplitude Variations in Multipath Fading of Microwave Signals. AT & T Co., Vol 50, 1971, p. 2040.

15. Nathanson, F.: Radar Design Principles. McGraw-Hill Book Co., 1977.